INTERACTIONS ENTRE COMPOSITION CHIMIQUE ET POPULATIONS MICROBIENNES DE LA NEIGE: QUELLES SONT LES CONSEQUENCES SUR LE CYCLE DU MERCURE EN ARCTIQUE ?

Catherine Larose

Interactions entre composition chimique et populations microbiennes de la neige : quelles sont les conséquences sur le cycle du mercure en Arctique ?

Catherine Larose

Manuscrit de thèse pour l'obtention du grade de docteur de l'Université Joseph-Fourier-Grenoble 1

Spécialité : Sciences de la Terre et de l'Univers

Composition du jury :

Mark Bailey	Professeur	Rapporteur
Martyn Tranter	Professeur	Rapporteur
Daniel Cossa	Directeur de recherche	Examinateur
Timothy M. Vogel	Professeur	Examinateur
Christophe Ferrari	Professeur	Directeur de thèse
Dominique Schneider	Professeur	Directeur de thèse

Université Joseph Fourier – Grenoble 1 / CNRS
Laboratoire de Glaciologie et Géophysique de l'Environnement
54, rue Molière – Domaine Universitaire BP 96
38402 Saint-Martin d'Hères Cedex FRANCE

ACKNOWLEDGEMENTS / REMERCIEMENTS

J'aimerais tout d'abord remercier les membres du jury ; Daniel, merci d'avoir accepté de présider, et merci aussi pour les nombreuses discussions tout au long de notre collaboration. I would like to thank Martyn Tranter and Mark Bailey for agreeing to evaluate my work and for the interesting discussions at the defense.

Le travail d'une thèse ne se fait pas tout seul ; pendant ces trois années, j'ai eu l'opportunité d'être entourée de nombreuses personnes. En premier lieu, merci à Christophe de m'avoir donné l'envie de venir en France lors d'une mémorable conférence à Madison; ainsi qu'à Dominique, qui a accepté d'accueillir une non microbiologiste dans son équipe ; merci pour votre soutien et votre confiance.

Ce travail a été mené sur trois labos, le LAPM, le LGGE, et le laboratoire AMPERE. Merci pour l'accueil chaleureux au LAPM : un grand merci à Evelyne pour sa patience, et pour avoir su m'aider dès le début ; et aussi à Elisabeth pour son amitié ; ainsi qu'à Mike, Iyad et tous les autres membres de l'équipe. Au LGGE, merci à Aurélien, le chef spirituel, pas seulement pour les discussions scientifiques, mais aussi pour les autres moments (WAMAS, Frozen Fox, les mots du jour…) ; si j'ai réussi à mener ma recherche à son terme, c'est en grande partie grâce à toi. Nico, le petit lapin blanc, merci pour les terrains, la pêche, le labo et tout le reste. Merci Martine, pour les discussions, et à toutes les personnes qui ont contribué à la bonne ambiance générale - Olivier, Julien, JC, Ludo, Christine. Je veux aussi remercier l'équipe du laboratoire AMPERE pour m'avoir accueillie, notamment Tim, qui dès le départ a cru à mon projet (thanks for the lengthy discussions, most of which may or may not have been work-related. I'm looking forward to the post-doc) ainsi que Pascal. Merci enfin aux étudiants, thésards et autres membres du labo qui sont devenus aujourd'hui des amis bien plus des collègues : Seb, Manu, JMM, Maude, Cédric, Aurélie, Marina, Barbara, Yo, Avi, Julie, Nico, Sandrine, Sam, Tom, Laure et tous les autres.

Je tiens à remercier en particulier Cédric pour son aide précieuse sur le terrain ; Nico et Alan qui m'ont vraiment appris ce qu'est le french flair, et ont permis d'assurer le bon déroulement du terrain. Xav, merci pour les performances, mas mas mas, WAMAS (la liste est trop longue). Sibel et Kévin, je vous remercie de m'avoir accueillie comme un membre de votre famille, notamment Sibel pour ta présence lors de ma formation ainsi que ton soutien lors des manipulations, et tout au long de la thèse. Thanks to Del and George for all the times spent in Lyon whether over dinner, on the make-shift dancefloor, or in the lab.

Merci à François, Max, Steph, Elise et Clara qui ont fait en sorte que je me sente chez moi à Grenoble, et pour tous ces bons moments, source de tellement de souvenirs… Big Up !

Je remercie tous les amis de Montréal & Toronto (Alex, Benoît, MC, JS, Kate, Roman, Stef, Tania, Farah, Peter, Ryan, Nico, Angela, Chantal, Alex) qui, même si j'étais plutôt absente lors des trois dernières années, étaient toujours prêts pour une bière ou une grosse poutine.

Vielen Dank Mama und Papa, ohne Eure Unterstützung hätte das ganze nicht möglich gewesen sein. Mir fehlen die Wörter. Chantal, Albert und Christian, ich habe auch von hier aus spüren können wie Ihr mir die Daumen gedrückt habt. Danke für alles.

Je garde le dernier merci pour Nico – tu sais pourquoi.

RESUME

L'objectif principal de cette thèse est de caractériser les interactions entre la composition chimique et la structure des communautés microbiennes dans un manteau neigeux arctique. Une attention toute particulière est portée au mercure, un polluant fortement toxique des régions polaires, dont le cycle biogéochimique complexe est encore mal connu.

Avant toute chose, les fractions biotiques et abiotiques d'un manteau neigeux saisonnier doivent être caractérisées. A partir d'échantillons de neige et d'eau de fonte prélevés au cours d'une étude de deux mois en 2007 à Ny-Ålesund (Svalbard, Norvège, 78°56'N, 11°52'E), nous avons montré que la diversité des séquences est élevée et que des espèces communes existent entre les différents environnements de la cryosphère. Dans ce manteau neigeux, nous avons également examiné le devenir du mercure, depuis son dépôt au cours des phénomènes de déplétions (atmospheric mercury depletion events, AMDEs) jusqu'à son transfert lors de la fonte des neiges, et nous avons constaté une augmentation des concentrations de méthylmercure dans le manteau neigeux à la fin du printemps. Les résultats de cette campagne ont souligné la nécessité d'améliorer nos connaissances sur la spéciation du mercure et ont conduit à l'élaboration d'un biocapteur *mer-lux* pour mesurer la fraction biodisponible de mercure, déployé lors d'une seconde campagne de deux mois au printemps 2008. Les résultats obtenus nous ont conduit à proposer un nouveau mécanisme de méthylation du mercure dans des environnements oxiques. En parallèle à l'analyse chimique, nous avons suivi les changements dans la structure des communautés microbiennes présentes dans les échantillons de neige et d'eau de fonte, en utilisant une puce à ADN. Une analyse statistique montre une évolution rapide et conjointe des paramètres chimiques et microbiologiques. Nous avons enfin exploré l'effet de la contamination au mercure sur la fonction de la communauté et démontré que le méthylmercure affecte la structure des communautés ainsi que sa fonction à des concentrations beaucoup plus faibles que précédemment rapportées. Bien que nos résultats soient spécifiques à une saison d'échantillonnage et ne peuvent être extrapolés à d'autres environnements, ils fournissent une base pour de nouvelles études sur l'interaction entre la composition chimique, la présence de contaminants anthropiques et la structure des communautés microbiennes.

ABSTRACT

The main objective of this thesis is to characterize the interactions between seasonal snow chemistry and microbial community structure in an arctic snowpack. However, in order to do so, the biotic and abiotic compartments of the snowpack must be first characterized. From snow and meltwater samples obtained during a two-month field study held in Ny-Ålesund (Svalbard, Norway, 78°56'N, 11°52'E) in 2007, we showed that the sequence diversity in arctic snow and meltwater libraries is elevated and that common species exist among different cryosphere environments. We also examined the fate of Hg in an arctic snowpack, from its deposition during atmospheric mercury depletion events (AMDEs) up until its transfer during snow melt and reported an increase in methylmercury concentrations in the snowpack during late spring. The results from this campaign highlighted the need to improve our knowledge on mercury speciation and led to the development of a *mer-lux* biosensor to measure the bioavailable fraction of mercury. We deployed the biosensor during a second two-month field campaign in Ny-Ålesund in spring 2008 and the results obtained led to a novel model for mercury methylation in oxic environments. In parallel to the chemical analyzes, we followed changes in microbial community structure in snow and meltwater samples using a 16S microarray. We modeled the interactions between snow chemistry and community structure and found a significant co-structure. We also explored functional community changes due to mercury contamination of snowpacks. Based on our results, methylmercury affects community structure and function at concentrations much lower than previously reported. While our results are specific to one particular field season and may not be extrapolated to other environments, they provide a basis for further studies on the interaction between chemistry and microbial community structure.

LIST OF ABBREVIATIONS

Ace+Glyc	Acetate glycolate
AMDEs	Atmospheric Mercury Depletion Events
AMSR-E	Advanced Microwave Scanning Radiometer
ANOVA	Analysis of variance
ASI	ARTISTSea Ice
BioHg	Bioavailable mercury
CIA	Co-inertia analysis
DGT	Diffusive Gradient in Thin Films
DHg	Dissolved total mercury
DiMeHg	Dimethylmercury
DIRB	Dissimilatory iron-reducing bacteria
DOC	Dissolved organic carbon
DSRB	Dissimilatory sulfate-reducing bacteria
EPS	Exopolysaccharides
FIAM	Free Ion Activity Model
Fl	Fluoride
F	Formate
FQRNT	le Fonds Québécois de la Recherche sur la Nature et les Technologies
Glut	Glutaric acid
GR	Glutathione reductase
GSH	Glutathione
GSSG	Glutathione disulfide
Hg	Mercury
Hg°	Gaseous elemental mercury
Hg^{2+}	Divalent mercury
HYSPLIT	HYbrid Single-Particle Lagrangian Integrated Trajectory
IPEV	French Polar Institute GC–ICP-MS
MerA	Mercuric reductase
MeHg	Methylmercury
MSA	Methanesulfonic acid
NOAA ARL	National Oceanic and Atmospheric Air Resources Laboratory
OTU	Operational Taxonomic Unit
Ox	Oxalic acid
PCA	Principal Component Analysis
PCR	Polymerase Chain Reaction
PM	Particulate mercury
Q-PCR	Quantitative Polymerase Chain Reaction
READY	Real-time Environmental Applications and Display system
RGM	Reactive gaseous mercury
THg	Total mercury

TABLE OF CONTENTS

FIGURE AND TABLE LEGEND

INTRODUCTION

The Arctic environment is undergoing changes due to climate shifts, long-range transportation of contaminants and increased human activity.The Arctic is polluted by industrial processes as recognized several decades ago, with observations by Aboriginals in the 1970s that visibility had been reduced (Schindler and Smol 2006). This observation served in part as a major impetus for funding Arctic research in Canada and highlighted the role of atmospheric transport in contaminating isolated environments with few local point sources of pollution.

A major component of the Arctic is seasonal snow. Snowpacks store nutrients, particles, contaminants, and microorganisms and are involved in the chemical cycling of trace gases and pollutants such as mercury. Seasonal snow has been shown to be a dynamic system that interacts with different environmental compartments such as the atmosphere, soil and aquatic systems. The concept of snow as a functional ecosystem able to sustain microorganisms is relatively new. The exploration of the cryobiosphere, the frozen part of the Earth in which organisms exist, has led to the discovery of diverse microbial communities that appear to be adapted to cold environments and are able to modify chemical processes. However, detailed knowledge about the interactions between the chemical composition of snow and microbial populations, especially in terms of contaminant cycling, is lacking. An overview of current research on snowpacks, polar-region bacteria and mercury is presented in Section I (Chapter 1) of this thesis.

The main objective of this thesis is to characterize the interactions between seasonal snow chemistry and microbial community structure in an Arctic snowpack. Among the different chemicals, we focused on mercury cycling in Arctic ecosystems, with emphasis on microbial transformations and metabolism. Mercury is one of the highest-profile metal contamination issues of recent decades for the Arctic and an estimated 200-300t are transported each year from various human (anthropogenic) and natural sources. Once deposited, it can undergo a variety of transformations that are biotically and abiotically mediated before contaminating the food chain. Snowpacks have been shown to be involved in mercury cycling and may impact its fate in Arctic systems. However, in order to elucidate potential interactions between biotic and abiotic compartments, the snowpack must be first characterized in terms of both its chemistry and microbial community structure.

In Section II of this thesis, the results of an initial field campaign held in spring 2007 in Ny-Ålesund, Norway are presented. In the first chapter of this section (Chapter 2), patterns of bacterial diversity, based on 16S ribosomal RNA-encoding gene clone libraries, are presented and the snow and meltwater clone libraries are compared using different statistical analyses. In the second chapter

(Chapter 3), the fate of mercury was examined in surface samples from an Arctic snowpack from its deposition during atmospheric mercury depletion events (AMDEs) up until its transfer during snow melt.

Based on the results presented in Section II, the necessity to improve current knowledge on mercury speciation in Arctic snowpacks was highlighted especially in terms of the bioavailable fraction, which is critical in determining potential ecotoxicological effects. In addition, the need for a more detailed chemical characterization of the snow was recognized. Section III contains two chapters that present data from a field campaign held in spring 2008 in Ny-Ålesund, Norway. The first chapter (Chapter 4) describes the development of a molecular tool able to quantify the bioavailable mercury fraction in environmental samples and the results obtained after its deployment in the field. The second chapter (Chapter 5) details the dynamics of snowpack chemistry from early spring up until snowmelt.

Section IV explores the relationships between snow/meltwater chemistry and microbial community structure. In the first chapter of this section (Chapter 6), changes in community population dynamics were evaluated in snow samples using 16S microarrays and linked to chemical parameters using multivariate statistical analyses. Changes in functional community structure due to mercury stress were also evaluated using Q-PCR. The second chapter (Chapter 7) further explores community function by looking at gene distributions within snow communities using a pyrosequencing approach.

Finally, Section V is a general conclusion of the results presented in this thesis and future research perspectives.

CHAPTER 1: GENERAL INTRODUCTION

1. AN INTRODUCTION TO THE ARCTIC

A large portion of the Earth is cold: about 14% of the biosphere is polar and 90% (by volume) is cold ocean (less than 5°C). About two thirds of global freshwater is contained in ice and roughly 20% of the soil ecosystem exists as permafrost (Priscu and Christner 2004). The Arctic is an important part of the cryosphere, which can be defined as the portion of the Earth where water is in solid form (Miteva 2008). Four million human residents of which approximately 10% are indigenous peoples inhabit many communities in 8 countries: Canada, the Kingdom of Denmark (including Greenland and the Faroe Islands), Finland, Iceland, Norway, Russia, Sweden, and the United States of America (Alaska) (AMAP 2009). The Arctic is a vast circumpolar area consisting mainly of seasonally ice-covered ocean surrounded by continental land masses and islands (Figure 1). It lies above 60°N and is characterized by a harsh climate, unique ecosystems and highly resilient biota (AMAP 2009).

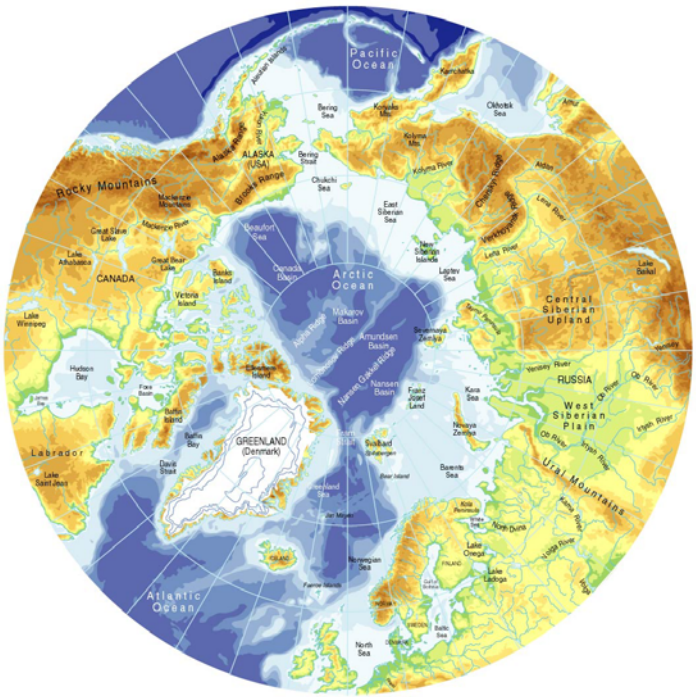

Figure 1: The Arctic (image modified from AMAP).

An important feature of the Arctic is seasonal snow-cover, which extends over a third of the Earth's land surface, covering up to 47 million km^2 (Hinkler et al. 2008). It can be considered as a dynamic habitat of limited duration (Jones 1999). Snow cover influences global energy and moisture budgets, thereby impacting climate (Hinkler et al. 2008). It is also be considered as a medium and a mediator that transmits and modifies interactions among microorganisms, plants, animals, nutrients, the atmosphere and soil (Pomeroy 2001). The influence of seasonal snow cover on soil temperature, soil

freeze-thaw processes, and permafrost has considerable impact on carbon exchange between the atmosphere and the ground and on the hydrological cycle in cold regions (Zhang 2005). Snow cover acts as both an energy bank by storing and releasing energy and a radiation shield due to its high radiative properties that reflect as much as 80-90% of the incoming radiation for fresh snow (Hinkler et al. 2008). This high surface albedo reduces absorbed solar energy and lowers snow surface temperature (Zhang 2005).

Snow, a porous media with elevated air content (Pomeroy 2001), also has a high latent heat of fusion and acts as a heat sink as well as a ground insulator, since heat transfer is poor (Hinkler et al. 2008). The extent and thickness of snow cover impacts subsurface soil temperature and soil metabolic activity (Larsen 2007) and its insulating properties protect soil surface organisms, such as vegetation, invertebrates and mammals against frost damage (Hinkler et al. 2008). Furthermore, snow acts as a reservoir and as a transport medium for liquid water that moves as a particulate flux and can be relocated by wind (Pomeroy 2001). Physical metamorphism, phase changes and chemical transformations, which are modulated by interactions with the atmosphere and soil systems, control both the dynamics and the duration of the snow cover (Jones 2001). Thus snow cover is an important factor in the functioning of the Arctic, and by extension, the global ecosystem.

2. THE CRYOSPHERE - A FUNCTIONAL ECOSYSTEM?

I. A BRIEF OVERVIEW OF SNOW STRUCTURE AND ITS FORMATION

Snow is formed in the atmosphere and consists of particles of ice that form in clouds. These crystals grow by vapor deposition and require atmospheric temperatures below 0°C and the presence of supercooled water (Libbrecht 2005). Because ice formation is not spontaneous at temperatures > -40°C, ice nucleation occurs mainly in the presence of substrates that act as catalysts. These substrates include dust, seasalt particles, sulfate, combustion products from industrial plants, volcanoes, forests and bacteria (Kuhn 2001; Pomeroy 2001). A recent report by Christner *et al.* (2008) found that biological particles such as proteins or proteinaceous compounds play a significant role in the initiation of ice formation, especially when cloud temperatures are warm. Once deposited, the snow cover forms as a result of snow crystal binding (Jordan 2008). Snow crystals are subject to temperature gradients that generate water vapor fluxes between crystals. This results in the sublimation of parts of crystals and condensation on other parts, thus changing crystal size and shape, and altering the physical properties of the snowpack. With each snowfall, the cover changes and the new layer may possess different properties than the preceding layer (Colbeck 1991). As snow ages, its physical properties, such as density, porosity, heat conductivity, hardness, specific surface

area and albedo, evolve in response to thermodynamic stress and weather conditions (Jordan 2008). Therefore, the composition of layered snow cover and ongoing changes in each of the layers' properties are not only due to the circumstances of formation, but also to changing conditions over time.

II. SNOW CHEMISTRY AND IMPURITY CYCLING

A) DEPOSITION AND INCORPORATION OF IMPURITIES WITHIN SNOWPACKS

The snowpack is a receptor surface and storage compartment for nutrients, soluble inorganic or organic matter and contaminants that may or may not be attached to insoluble particles that are delivered by wet and dry deposition (reviewed by (Kuhn 2001; Daly and Wania 2004). Their distribution within the snow is heterogeneous (Hodson et al. 2008) and depends upon different physical processes such as atmospheric loading, wind speed, and snow metamorphism (reviewed by Kuhn 2001). Nutrients exist in the atmosphere as trace gases such as SO_2, CO_2, NO_X, N_2O or HNO_3 and as aerosols such as pollen, sea salt particles, mineral dust and sulfates (reviewed by Kuhn 2001). Nutrients and contaminants can be delivered to the snowpack through wet and dry deposition (Figure 2). Wet deposition occurs when atmospheric components are scavenged and incorporated into growing or falling snow/rain as condensation or freezing nuclei, by either the impaction of particles, the solution of gases or by the collision of supercooled droplets with snow crystals (Kuhn 2001). Condensation or evaporation can alter the concentrations, resulting in the highly variable composition of individual snow crystals.

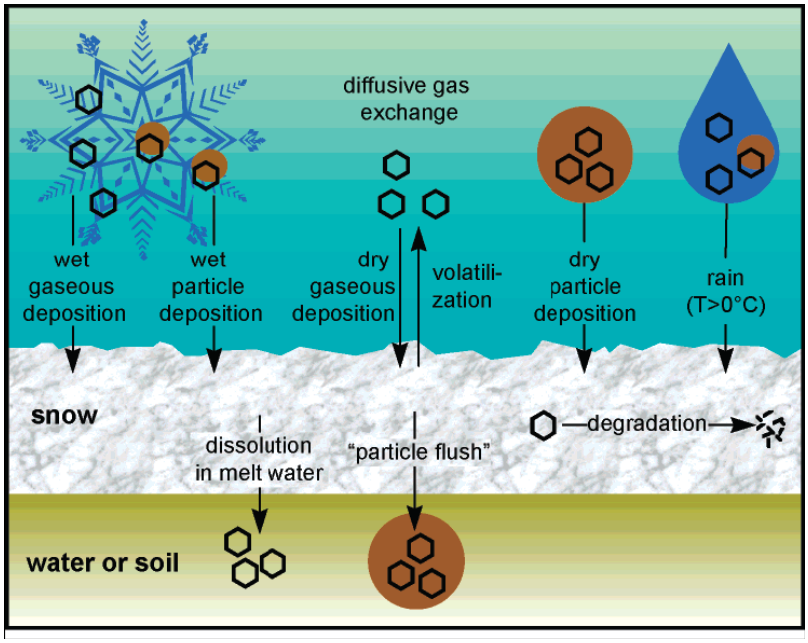

Figure 2: Processes involved in the delivery and loss of contaminants in a seasonal snow cover (reproduced from Daly and Wania 2004).

Atmospheric scavenging and condensation largely condition the presence of major ions in the snowpack, such as SO_4^{2-}, NH_4^+, NO_3^-, Ca^{2+}, Cl^- and Na^+ (reviewed by Kuhn 2001). Dry deposition occurs when gases and particulates are transferred directly to the snow surface without the intermediate scavenging by precipitation. This pathway is dependent upon the atmospheric concentration of the species, the stability or turbulence of the atmospheric boundary layer, as well as the capacity of the surface to retain the species (reviewed by Kuhn 2001). Once deposited, these species can be redistributed to the snowpack. Due to the permeability of the snowpack, gaseous diffusion occurs along a concentration gradient. Gases can also diffuse from the soil to the atmosphere (Jones 1999). Snow-air exchanges occur when the vapor diffuses through the air-filled pore space to the top of the snowpack and from there through a boundary layer to the atmosphere (Daly and Wania 2004). The penetration of gases and particles within the snowpack is dependent upon physical-chemical properties, the geometry of the pore space, vapor pressure gradients and wind pressure (reviewed by Kuhn 2001). Wind advection can accelerate solute transport within the snow pores, even after the resistance to molecular diffusive transport is too large to allow gas exchange (Daly and Wania 2004).

B) SNOW METAMORPHISM AND IMPURITY CYCLING

Physical processes of snow metamorphism also lead to the redistribution of chemical species (Figure 3). On a crystal, molecules diffuse from convex to concave sites, thus transforming crystals to small round snow grains that evaporate and distill onto larger grains once in close proximity. The grains grow rapidly by diffusion, which is initiated by temperature gradients within the snowpack and facilitated by the quasi-liquid surface layer of snow crystals that gives molecules high mobility. During this process, impurities are excluded from the crystals and concentrate at the grain boundaries and pore spaces of the snow (reviewed by Kuhn 2001). The layered nature of the snowpack, which is composed of a heterogeneous mixture of grains of various sizes, water saturation levels, densities, and ice layers that reduce the permeability to air and water (Colbeck 1991), is also important in the redistribution of solutes. Chemicals can be lost from the snow through degradation, volatilization and runoff with meltwater (Daly and Wania 2004). Impurities can be transformed within the snowpack and also returned to the atmosphere. Snow also transmits atmospherically derived impurities such as nutrients, microorganisms, particles and contaminants to meltwater-fed systems. Snow is thus a mediator favoring exchanges among different environmental compartments.

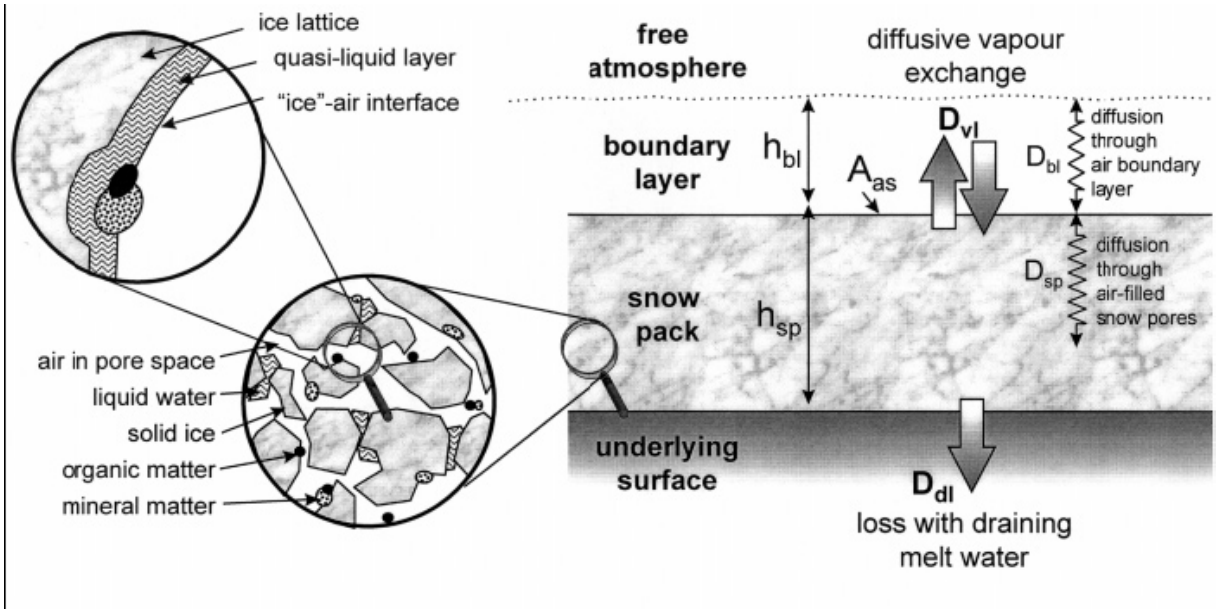

Figure 3: Chemical snowpack model representing volatilization loss and meltwater concentration (reproduced from Wania et al. 1999).

C) SNOW MELT AND ECOSYSTEM TRANSFER

Melting can occur at air temperatures below 0°C when solar radiation is intense enough and penetrates into the snowpack (Kuhn 1987). The top snow layers melt first and meltwater is drawn downward towards the base of the snowpack. Initially, meltwater is retained in the capillaries and pore walls where it fills 5-10% of the pore space before becoming more mobile (Colbeck 1978; Davis 1991). As melting progresses, the water mobilizes solutes and contaminants from the pore walls, thus becoming more concentrated. Preferential flow may develop due to the non-homogenous nature of the snow and lead to accelerated percolation and concentration of meltwater in certain areas (reviewed by Kuhn 2001). If the weather conditions prevent further melt, the highly concentrated meltwater may refreeze as a layer within the snowpack and becomes stationary. If multiple freeze/thaw cycles occur, each cycle will increase the solute concentrations of the meltwater, which becomes highly concentrated as it advances into deeper layers of the snowpack (Meyer and Wania 2008). Usually, meltwater reaches the ground, refreezes and develops into a solid layer (Figure 4). The first flush is highly concentrated, with preferential elution of certain solutes. The most soluble ions are removed first and ionic concentrations taper off as melting proceeds (Colbeck 1981; Goto-Azuma 1994). Based on laboratory and field studies, fractionation of solutes into meltwater has been shown to occur in all snowpacks, with variable concentration factors (e.g. Johannessen 1978; Colbeck 1981; Davies 1982). Roughly 80% of solutes are removed from the snowpack by the first 30% of meltwater (Brimblecombe 1986; reviewed by Kuhn 2001) and fractionation increases with the age of snow, by repeated melting and freezing and by slow

meltwater flow (Johannessen 1977; Colbeck 1981; Davis 1995). Soluble ions are removed first (Tranter et al. 1986; Meyer et al. 2008), followed by preferential elution of some ions (e.g. SO_4^{2-}, Ca^{2+}, Mg^{2+}, K^+, Na^+) over others (NO_3^-, NH_4^+, Cl^-, F^-) (Eichler 2001). Species such as non-polar organic molecules are also found in meltwater, but are less easily entrained by percolating water due to their weak water solubility (Meyer et al. 2006). Particulate material can also be removed by percolation, but usually remains in the snow until the final stages of melting (Hodgkins 1998; Lyons 2003; Meyer et al. 2006). Rain events during the snowmelt period may lead to increases in solute and contaminant load (Daly and Wania 2004).

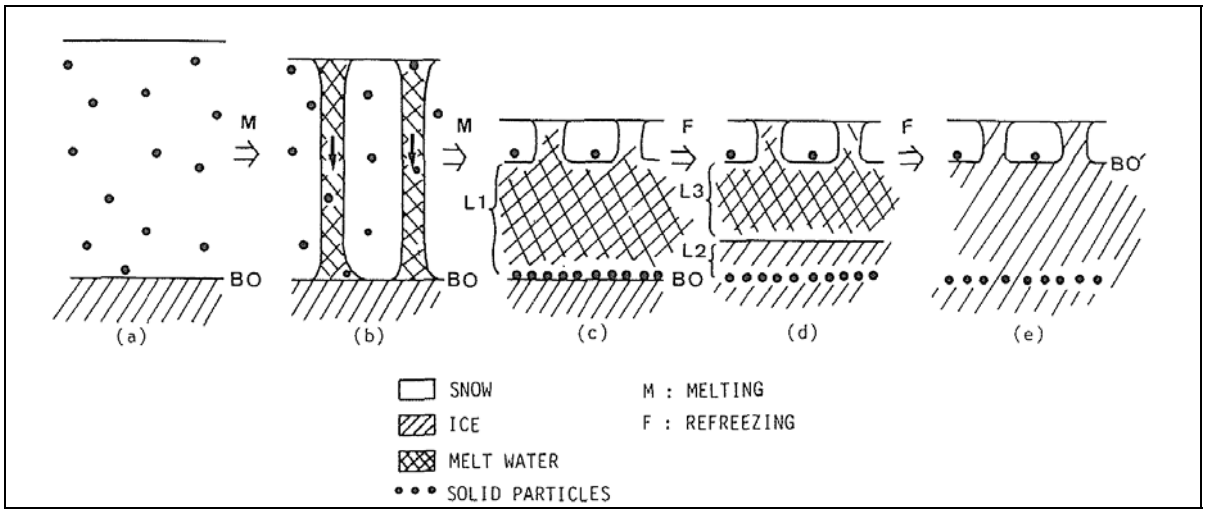

Figure 4: Formation of highly concentrated layers within a snowpack (reproduced from Goto-Azuma 1994).

Upon snowmelt, snow impurities are released to meltwater-fed catchments, soil and aquatic systems, potentially delivering a pulse of highly concentrated solutes and contaminants. Long melt periods have been shown to lead to increased evaporation of chemicals, thus reducing contaminant loading, while short melt periods deliver greater proportions of stored contaminants (Daly and Wania 2004). Since the melt period is short and the snow cover lasts several months in the Arctic, thereby leading to longer solute accumulation periods, arctic ecosystems are especially at risk for pulse exposure (Daly and Wania 2004).

III. BIOLOGY OF THE CRYOSPHERE

A) COLONIZATION AND ACTIVITY IN COLD ENVIRONMENTS

Microorganisms exist in several extreme cold environments such as glacial ice (Christner et al. 2000; Skidmore et al. 2000; Christner et al. 2001), sea ice (Brinkmeyer et al. 2003), Arctic biofilms (Poulain et al. 2007), supercooled clouds (Sattler et al. 2001) and Antarctic permafrost (Yergeau et al. 2007).

The colonization of the Arctic by microbes should be similar to that of Antarctica, where different colonization pathways have been described such as atmospheric circulation, ocean currents, birds, fishes, marine mammals and human vectors (Vincent 2000). Due to the cold conditions and the limited supply of liquid water, snow and ice have long been only considered as entrapment and storage systems for microorganisms that were thought to enter as vegetative and resting cells, transported by wind-blown particles, aerosols and ice crystals. These cells would then be buried by subsequent snowfall events before being transferred to other systems upon snowmelt (Cowan 2004). However, this view started to change with a number of studies that examined microbial diversity, ecology and function in the cryosphere. Whether the microorganisms found in cold environments are metabolically active and reproducing remains unclear, but it is assumed that certain species are at least able to survive (Miteva 2008).

The occurrence of related phylotypes from geographically-diverse cold environments has been reported (Brinkmeyer et al. 2003), suggesting that adaptation for survival, persistence and activity at low temperatures might be a common feature of these species and that they might possess common adaptive strategies (Priscu and Christner 2004). The bacterial genera most frequently reported are *Proteobacteria* (*Alphaproteobacteria*, *Betaproteobacteria* and *Gammaproteobacteria*), *Bacteroidetes* group, low and high G+C Gram-positive genera, and *Cyanobacteria* (Christner et al. 2001; Priscu and Christner 2004; Liu et al. 2006; Liu et al. 2009). Moreover, microorganisms might be metabolically active at low temperatures down to −20°C (Christner 2002; Junge 2004) and very low rates of metabolic activity might be sustained for up to 10^4 to 10^6 years and at temperatures as low as -40°C (Price and Sowers 2004).

However, these studies focused on characterizing bacteria in ice or permafrost and relatively little is known about life in snow, despite the extent and importance of seasonal snow. The snow cover might support a microbial community composed of snow algae, bacteria, yeasts and snow fungi (Jones 1999). While snow algae have been studied relatively extensively (Hoham 1975; Hoham and Duval 2001; Stibal et al. 2007), data on bacteria inhabiting seasonal snow cover are sparse, especially for polar snowpacks. Carpenter et al. (2000) reported low rates of DNA synthesis and the presence of *Thermus-Deinococcus*-like organisms in Antarctic snow, while Amato et al. (2007) used culture-based methods to isolate 10 bacterial strains belonging to *Proteobacteria*, *Firmicutes* and *Actinobacteria* from a snowpit dug on a polythermal glacier in Svalbard (Norway). Both studies focused on bacterial density and activity, but important questions about diversity, community structure, population dynamics and function remain unanswered.

B) LIFE IN THE COLD LANE

In order to colonize and survive in cold environments such as snowpacks, microorganisms must overcome a number of physiological stress parameters such as cold temperatures (less than 5°C), high levels of solar radiation, desiccation and freeze/thaw cycles (Priscu and Christner 2004). These harsh environmental conditions vary temporally as well as spatially and necessitate physiological acclimation. In the Arctic, because of the high latitudes, a pronounced seasonality causes gradual, yet extreme, changes in the photoperiod, irradiance, and temperature. During the springtime melt period, snow undergoes temperature shifts across the freezing point of water, leading to a more dynamic environment, but also to an increase in freeze/thaw cycles (Mueller et al. 2005).

Different survival strategies at low temperatures have been observed in bacteria: reduction of cell size and capsular polysaccharide coat thickness, changes in fatty acid and phospholipid membrane composition, decrease of the fractional volume of cellular water, increase of the fraction of ordered cellular water, energy synthesis by catalyzes of redox reactions of ions in aqueous veins in ice or in thin aqueous films in permafrost (Price and Sowers 2004). Moreover, many species that have been isolated form spores that provide high resistance levels, while others have thick cell walls or polysaccharide capsules that resist freeze/thaw cycles (Priscu and Christner 2004). Cold tolerance has been shown to involve down-regulation of enzymes involved in major metabolic processes such as glycolysis, anaerobic respiration, ATP synthesis, fermentation, electron transport, sugar metabolism as well as the metabolism of lipids, amino acids, nucleotides and nucleic acids (Qiu et al. 2009). However, up-regulation and overexpression of several enzymes and proteins (cold shock proteins, etc.) may enhance survivability during freeze-thaw cycles (Qiu et al. 2009). Other adaptive strategies include the production of pigments such as oligosaccharide mycosporine-like amino acids, scytonemins, carotenoids, phycobiliproteins and chlorophylls that offer a broad strategy to cope with high irradiance (Mueller et al. 2005).

Ability to attach to surfaces also provides bacteria with adaptive strategies. Junge et al. (2004) reported that particle-associated bacteria were more active than free-living cells as temperatures dropped and that they also produced exopolysaccharides (EPS). Bacteria growing in microbial mats were also shown to form EPS (Mueller et al. 2005). The EPS production favors attachment (Junge 2004) and protects against freezing, dessication, viral and bacterial attacks (Mueller et al. 2005). Moreover, it is likely that the presence of species with specialized mechanisms of stress resistance may provide a protective effect on other members of the community. For example, certain pigments

such as oligosaccharide mycosporine-like amino acids and scytonemin are located outside the cells and may benefit non-producing microorganisms against radiation damage (Mueller et al. 2005).

C) MICROORGANISMS - ACTIVE MEMBERS OF THE CRYOSPHERE?

Recent reports suggest that microorganisms impact nutrient dynamics, composition and abundance (Hodson et al. 2008), that they may shift surface albedo of snow and ice (Thomas and Duval 1995) and impact hydrochemistry (Tranter et al. 2002). Critical processes controlling biogenic trace gas (e.g. CO_2, CH_4, N_2O, and NO) fluxes are carried out by microorganisms (Schimel 1998). Within the snowpack, microbiological activities such as carbon fixation by algal communities may modify the nutrient cycle (Jones 1999). The importance of bacteria in governing redox conditions and their role in Fe, S, N and P cycling is now acknowledged (Hodson et al. 2008). In addition, they might be responsible for the metabolism and transformation of environmental contaminants such as mercury, a pollutant of arctic ecosystems (Barkay and Poulain 2007; Poulain et al. 2007).

3. MERCURY CONTAMINATION IN ARCTIC ECOSYSTEMS

I. HEALTH EFFECTS OF MERCURY IN ARCTIC POPULATIONS

The vulnerability of polar environments to contaminants transported from lower latitudes via long-range atmospheric processes has been the subject of numerous reports (e.g. Fitzgerald 1998; AMAP 2009). The Arctic is experiencing mercury (Hg) toxicity (Barkay and Poulain 2007) and Hg concentrations are increasing. Analyses of different soft and hard tissues, such as teeth, feathers and hair, demonstrated increases in Hg levels between the pre- and post-industrial periods over much of the Arctic with levels increasing exponentially since the 20th century (Dietz et al. 2009) (Figure 5). For example, hairs from mummified human remains from the 15-16th century found in Greenland revealed mercury levels 3 to 6-times lower than those found in contemporary Greenlanders (Dietz et al. 2009).

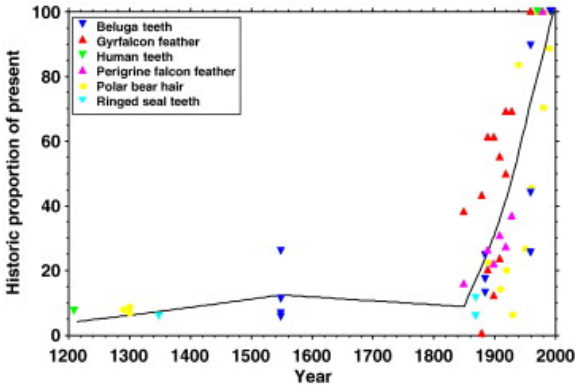

Figure 5: Historical trends of Hg concentrations in various animal hard tissues, expressed as percentage of present-day maximum annual average concentrations (reproduced from Dietz et al. 2009).

Mercury exists in several forms in the environment: elemental (Hg°), divalent form (Hg^{2+}) and an organo-metallic form of which methylmercury (MeHg) is the most important. The MeHg organic form is the most toxic of the three forms, even at very low exposure doses (Ullrich 2001). Since MeHg is highly neurotoxic (Yee 1994), it can cause damage to the visual cortex and the sensory system in humans. Symptoms of intoxication include constriction of the visual field, sensory impairment of extremities, hearing loss, muscle weakness, tremors, cardiovascular problems and mental deterioration (Harada 1995; Castoldi 2001; Yokoo 2003). The main source of MeHg in humans occurs by consumption of contaminated fish (Castoldi 2001; Daré 2001). In light of all these adverse effects, many countries developed consumer advisories which encourage people to limit their consumption of fish. Unlike inorganic mercury, MeHg easily accumulates in the foodweb (Berntssen et al. 2003).

Mercury levels, as well as the relative proportions of its organic and inorganic form, vary largely according to the trophic level, tissue studied and zoological group (Thompson 1990; Ancora et al. 2002). Species-dependent variations are also detected in the distribution of organic mercury (Nigro 1996). The concentrations of MeHg tend to increase with the trophic level in a foodweb, with top predators being the most contaminated (Schultz 1997). This phenomenon, known as MeHg biomagnification, is observed in most ecosystems regardless of the Hg source.

II. OVERVIEW OF THE MERCURY CYCLE: SOURCES, DEPOSITION AND TRANSFORMATION

Hg, a toxic element for all life forms, is found both naturally and as a human-introduced compound in the environment (Nriagu 1988; Nriagu 1989; Fitzgerald 1998). Historically, Hg has been used both as a pigment and for the extraction of gold and silver through mercury-amalgamation. Significant sources of Hg to the atmosphere include the combustion of coal and other fossil fuels associated with energy or heat production in power plants, small industrial or residential heating units or small-scale residential heating appliances (AMAP/UNEP 2008). Hg is also used in a variety of manufacturing industries such as chlor-alkali plants (production of chlorine and caustic soda) and pulp and paper mills (bleaching agents). Industrial use and subsequent release of Hg to the environment have contributed to increasing Hg levels in soil, sediments and aquatic ecosystems worldwide (Gray 2006). In the last century alone, anthropogenic emissions to the atmosphere have tripled atmospheric and oceanic Hg concentrations (Mason 1994). About 5000-6000 t of Hg are released each year, with about 50% linked to anthropogenic activity (Mason 1994; Lamborg 2002).

A) MERCURY TRANSPORT AND DEPOSITION ONTO SNOW SURFACES

Mercury is mainly emitted to the atmosphere in its gaseous form (Hg°), but also in the oxidized form (reactive gaseous mercury, RGM) or in the particle-bound form (particulate mercury, PM). Hg° has a relatively long atmospheric residence time (between 0.5 and 1.5 years) and average atmospheric concentrations have been estimated at 1.7 g/m^3 for the Northern Hemisphere (Lindberg et al. 2007). RGM and PM have shorter lifetimes and tend to be deposited near their sources (Lindberg et al. 2007).

Mercury reaches polar ecosystems mainly as Hg°; however due to the cyclical nature of Hg transformations (transport-deposition-re-emission), even mercury originally emitted as RGM and PM can be transported to the Arctic (Ariya et al. 2004). As for other contaminants, Hg can be deposited after atmospheric scavenging by precipitation and dry deposition. Once RGM is formed in the atmosphere, snow can act as an efficient surface for its sorption. In addition, active growth of snow and ice crystals from the vapor phase readily scavenges available RGM (Douglas et al. 2005).

In 1995 at Alert, Canada, Schroeder et al. (1998) measured the episodic near-total depletion of Hg° from the atmosphere during the spring (Schroeder et al. 1998). These events, termed Atmospheric Mercury Depletion Events (AMDEs), were observed in parallel to the depletion of ozone (Barrie et al. 1988) and led to intense field, laboratory and theoretical studies to determine which reactions were involved. In particular, mercury was shown to undergo rapid oxidation and deposition via photochemically-initiated reactions believed to involve reactive marine halogens, mainly Br and BrO (Lu et al. 2001; Lindberg et al. 2002; Skov et al. 2004). These reactions transform Hg° to PM and RGM species that can then be deposited onto the snow. It has been estimated that AMDEs enhance polar mercury deposition by 100 tonnes a year (Ariya et al. 2004), yet the post-depositional fate of this Hg remains uncertain. Hence, it can undergo a series of possible transformations once deposited (see Figure 6 for an overview of Hg cycling in the Arctic) (Steffen et al. 2008).

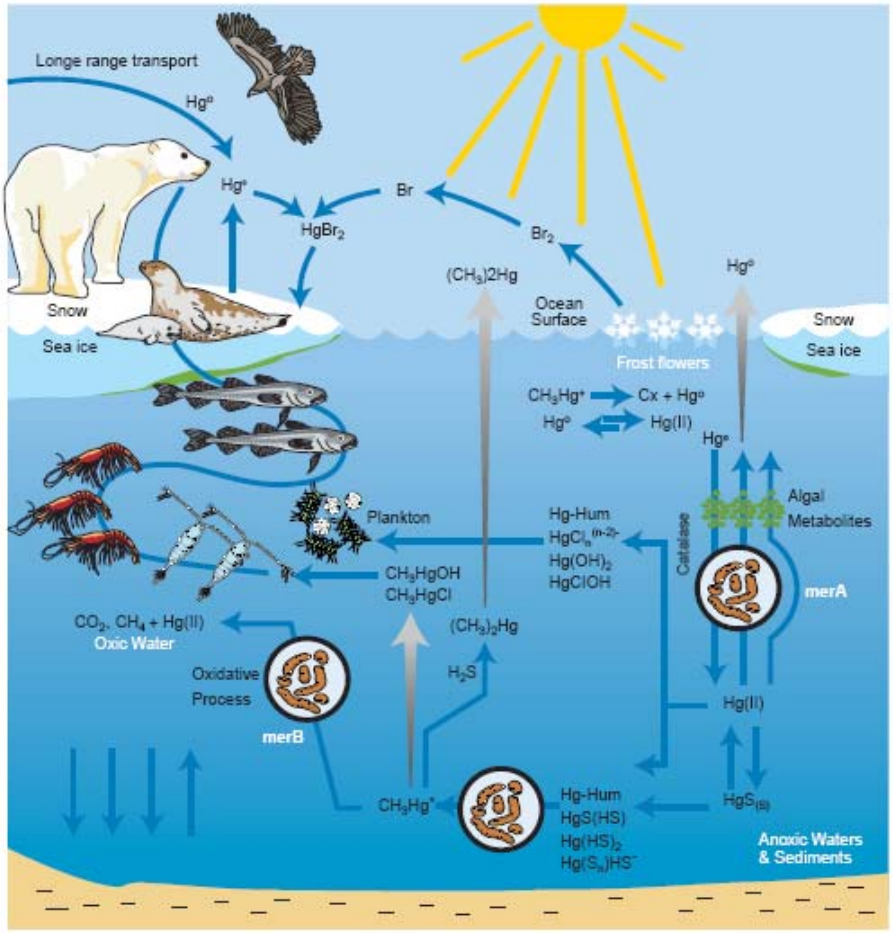

Figure 6: Atmospheric depletion events and possible uptake by biota (reproduced from AMAP/UNEP 2008).

B) BIOGEOCHEMICAL MERCURY TRANSFORMATIONS

Different simultaneous biotic and abiotic processes alter the chemical state of mercury and thereby its toxicity in the environment. Four different reactions control mercury speciation: methylation, demethylation, reduction and oxidation (Barkay et al. 2003). These reactions are summarized in Table I.

Table I: Summary of processes involved in Hg transformations

Process	Type	Mechanism
Methylation	Biotic	Enzymatic methyl transfer in sulfate reducers
	Abiotic	Methylation by organic compounds involving photochemical reactions. Determined in laboratory studies only
Demethylation	Biotic	Reductive methylation via MerAB
		Oxidative demethylation via unknown processes
	Abiotic	Photodegradation
Reduction	Biotic	Bacterial reduction via the *mer* operon
	Abiotic	Photochemical and chemical reactions
Oxidation	Biotic	Oxidation by hydroperoxidases
	Abiotic	Oxidation involving reactive halogens, and/or other oxidants (OH, O_3) Photo-oxidation and dark reactions involving Br

1) MERCURY METHYLATION

Methylmercury can be formed by two general pathways (Celo et al. 2006): microbial metabolism (biotic processes) and chemical methylation (abiotic processes). Microbial methylation has been considered as the dominant pathway, although the contribution of abiotic processes may have been overlooked.

Biotic environmental mercury methylation is an anaerobic process generally mediated by both dissimilatory sulfate-reducing bacteria (DSRB) and, as was shown more recently, dissimilatory iron-reducing bacteria (DIRB) (Fleming et al. 2006; Kerin et al. 2006). Although the exact mechanism is unknown, methylation appears to be related to the production of acetyl-CoA and methylcobalamin (B12) (Choi et al. 1994) and/or to a methyltransferase pathway, similar to the biological synthesis of methionine from homocysteine (Siciliano and Lean 2002) in DSRB. Biotic mercury methylation depends on microbial activity and the concentration of bioavailable mercury, both of which are influenced by temperature, pH, redox potential and the presence of inorganic and organic complexing agents (Barkay et al. 1997; Barkay et al. 2003; Barkay et al. 2005; Golding et al. 2007). Bacteria are also able to produce dimethylmercury (diMeHg), a highly volatile compound (Barkay et al. 2005). The production of diMeHg is suggested to be the result of the interaction of MeHg with H_2S in the water column (Rowland et al. 1977).

Chemical methylation of mercury is possible only if suitable methyl donors are present and, although available methyl donors may be products of biological processes, methylation of mercury by these compounds is considered to be abiotic (Craig 1986; Falter and Wilken 1998). The compounds involved in abiotic methylation include small organic molecules, such as methyl iodide and dimethylsulfide, and larger organic components of dissolved organic matter, such as fulvic and humic acids. Transmethylation reactions (the transfer of a methyl group from one compound to another) with organo-metallic complexes such as methylcobalamin, methyllead or methyltin compounds, may also be pathways for abiotic methylation of mercury. The rates and mechanisms of abiotic methylation are likewise expected to be affected by the parameters that influence mercury speciation such as pH, temperature, redox, nutrients and complexing agent availability (Ullrich 2001; Celo et al. 2006).

2) MERCURY DEMETHYLATION

Demethylation has been shown to occur via two microbial mechanisms that can be distinguished by their volatile carbon product: CH_4 is the sole product of reductive demethylation, whereas CO_2

prevails in oxidative demethylation, with only traces of CH_4 (Barkay et al. 2005). Each of these pathways lead to different mercurial end products: reductive demethylation generates Hg°, while oxidative demethylation leads to the formation of Hg^{2+}, which can subsequently be methylated again (Barkay et al. 2005). Reductive demethylation involves microorganisms that possess mercury resistance (*mer*) operons, while oxidative demethylation occurs via biochemical pathways, such as C1 metabolism (Oremland et al. 1991). The predominance of either pathway depends both on redox and mercury contamination levels, with reductive demethylation favored at high mercury concentrations and oxic conditions and oxidative demethylation at low mercury concentrations and anoxic conditions (Barkay et al. 2005).

The abiotic degradation of methylmercury can be catalyzed by light. UV irradiations with wavelengths of 185 and 254 nm have been shown to degrade methylmercury directly, while wavelengths between 280 and 800 nm can produce singlet oxygen and hydroxyl radicals that are then able to attack the C-Hg bond to form either Hg° or Hg^{2+} (Suda et al. 1993; Chen et al. 2003). This pathway appears to be dominant in surface waters (Sellers et al. 1996) but has little effect in sediments and bottom waters (Barkay et al. 2005).

3) MERCURY REDUCTION

Several mechanisms for inorganic mercury reduction have been discovered. Mercury resistant bacteria that possess the *mer* operon are able to enzymatically reduce Hg^{2+} to Hg° via MerA (an overview will follow, please see (Barkay et al. 2003) for a detailed review), while the others have been shown to reduce Hg^{2+} to Hg° by a Fe(II)-dependent activity (Iwahori et al. 2000) via cytochrome c oxidases (Sugio et al. 2001). In this last case however, the resistance levels are much lower. In the Fe-mediated reaction, cytochrome c is reduced by Fe(II) and the electrons are subsequently transported along the respiratory chain to Hg^{2+} (Sugio et al. 2003). In anaerobic bacteria, the reduction mechanism is thought to depend upon the respiratory electron-chain in the cell membrane that reduces Hg^{2+} before it enters the cytoplasm and becomes complexed to cytoplasmic thiols (Wiatrowski et al. 2006; Kritee et al. 2008).

The abiotic reduction of Hg^{2+} can occur photochemically following the generation of free radicals by photolysis of dissolved organic carbon (DOC) (Nriagu 1994), dissolved oxygen and ferric iron–organic acids coordination compounds in aquatic environments (Zhang and Lindberg 2001). The reduction reaction rates have been shown to slow down over time, possibly due to bleaching or ageing of organic matter leading to the loss of reductive capacity (Costa and Liss 1999). Hg^{2+} can also be reduced in the dark by fulvic and humic acid-associated free radicals (Skogerboe and Wilson 1981;

Allard and Arsenie 1991) and depends exclusively on the reducing capacity of the humic acids (Costa and Liss 1999).

In snowpacks, photochemical reactions are also believed to be involved in Hg^{2+} reduction. Field and laboratory studies demonstrated that UV-B wavelengths are the most effective at reducing Hg^{2+} in the snow (Dommergue et al. 2007), although the exact substrates (Hg species) remain to be characterized. Potential reductants have been proposed (e.g., HO_2), although their role has yet to be confirmed by thermodynamic experiments (Gardfeldt et al. 2003). Ferrari et al. (2005) suggested that the quasi-liquid layer surrounding snowflakes may be the main site of Hg redox transformations in snowpacks (Ferrari et al. 2005). Therefore, temperature may play an important role in dictating the occurrence and magnitude of these processes.

4) MERCURY OXIDATION

Mercury oxidation has been shown to occur in many different environmental compartments such as the atmosphere (Lindberg et al. 2002), aquatic environments (fresh and saltwater) (Amyot et al. 1997; Lalonde et al. 2001), soil (Thoming et al. 2000) and snow (Lalonde et al. 2002; Dommergue et al. 2003; Poulain et al. 2004). Mercury oxidation requires the presence of oxidants such as ozone or hydroxyl radicals (Munthe 1992; Seigneur et al. 1994) and halogen radicals such as bromine and bromine oxides (Ebinghaus et al. 2002; Lindberg et al. 2002). The halogen radicals are thought to be generated by a series of photochemical and heterogeneous reactions and therefore require light. Maron et al. (2008) recently reported that Br radicals are the only chemical species involved in the rapid oxidation of mercury and described a mechanism for mercury oxidation in the dark that is initiated by Br radicals (Maron et al. 2008).

Mercury oxidation has also been shown to occur in bacteria. Smith et al. (1998) demonstrated that Hg° could be oxidized to Hg^{2+} by bacterial hydroperoxidases that catalyze the transfer of two electrons from hydrogen peroxide to Hg°, similar to the mechanism observed in mammals and plants. The capacity to oxidize Hg appears to vary among bacterial strains and may involve other enzymes (Smith et al. 1998).

In terms of mercury toxicity, bioavailability is an important factor since several of the environmental biochemical transformations described above, such as methylation and reduction, are enzymatically catalyzed within the cytoplasm of the bacterial cell and are therefore dependent on Hg uptake (Golding et al. 2007). Uptake is complex and depends upon a variety of factors that are outlined in the following section.

4. MERCURY UPTAKE AND RESISTANCE IN MICROBIAL COMMUNITIES

I. GENERAL CONCEPTS OF METAL BIOAVAILABILITY

Metal bioavailability depends on highly complex and interdependent chemical, physical and biological factors. Bioavailability is related to the capacity of the metal to pass across biological barriers and can be predicted by the concentration or flux of the internalized metal (Worms 2006). Biouptake processes depend upon the internalization pathways and their specificity, in addition to the physico-chemistry of the medium and the size and nature of the organism. Processes that reduce interactions with binding sites on the organism's surface include complexation with organic and inorganic molecules or competition with other molecules (Buffle et al. 2009).

Different metal fluxes are involved in biouptake: mass transport, by which trace metals and their complexes diffuse from the environment to the surface of the cell; complexation/dissociation, since metal complexes are dynamic and able to dissociate and reassociate as they diffuse towards the cell; adsorption/desorption, since the metal must react with a binding site on the cell membrane; and internalization, during which the metal enters within the cell through passive or active transport (Figure 7) (Buffle et al. 2009). Any of the described fluxes may be rate-limiting and are affected by the chemical nature of the compound and physico-chemical conditions (pH, metal/ligand concentrations, membrane potentials). The cell response to the metal (efflux, pH changes, modifications in surface charge) may also alter the physico-chemistry of the metal in solution and at the interface, thus modifying internalization fluxes and concentrations (Worms 2006). In many cases, transport across the membrane is the rate limiting step. The process can be simplified into a thermodynamic equilibrium between metal species in the bulk solution and binding sites on the cell surface (with a number of limiting assumptions, especially chemical equilibrium in a dynamic natural medium) (Slaveykova and Wilkinson 2005). In an equilibrium model (pseudo-equilibrium conditions), the metal concentrations in the bulk solution are identical to those at the membrane-water interface and equilibrium is maintained throughout the solution. Therefore, uptake kinetics are best described by the concentration of the equilibrium species in the bulk medium (Worms 2006).

Biological membranes are active and can control internalization fluxes based on the requirements of the cell. Since biological membranes are hydrophobic, only neutral or non-polar molecules, such as organo-mercury and neutral silver chloride complexes, can enter into the cytoplasm by passive diffusion (depending on the concentration gradient between external and internal compartments and a partition coefficient between aqueous and lipid phases) (Worms 2006). However, the majority of environmentally relative trace metal species are hydrophilic and their transport has been shown to

be mediated by active transport systems involving specific proteins or transporters (Slaveykova and Wilkinson 2005). Certain metals use anionic transporters, whereby the metal is piggy-backed by transporters specific to low molecular weight ligands such as citrate, thiosulfate or phosphate. In this case, transport depends on metal speciation and cell nutrition (Worms 2006). Siderophores, which are highly specific ligands, can also be produced by the cell to facilitate the transport of essential cations (e.g. Fe^{2+}, Co^{+}) present at low concentrations in the environment (Worms 2006).

The majority of trace metals are thought to be transported as free aqueous ions. A toxic metal can bind to the uptake site of an essential metal (high affinity sites with low selectivity) with a similar ionic radius or coordination geometry: for example, Zn^{2+}, Cd^{2+}, Pb^{2+} enter using Ca^{2+} binding sites. The toxicity and uptake of trace metals depend on the concentration of major cations or competing trace metals. Under equilibrium conditions, a reduction in binding to the transport sites is predicted in the presence of competing ions (Worms 2006). Protons can also compete for the uptake of metals. Therefore, a decrease in pH may reduce uptake due to the protonation of the metal binding sites (only valid under equilibrium conditions). When a trace metal is internalized by multiple transport systems, uptake fluxes can no longer be represented as a function of metal concentration alone (Slaveykova and Wilkinson 2005).

The organism is able to regulate transport systems (e.g. transporter degradation/synthesis via feedback regulatory pathways) and this directly affects trace metal internalization fluxes (Buffle et al. 2009). However, once inside the cell, metals can induce cellular responses that influence bioavailability as well as exert toxic effects including the inactivation of proteins, the competitive interference on the uptake of other molecules and the induction of oxidative stress with subsequent cell damage (Worms 2006).

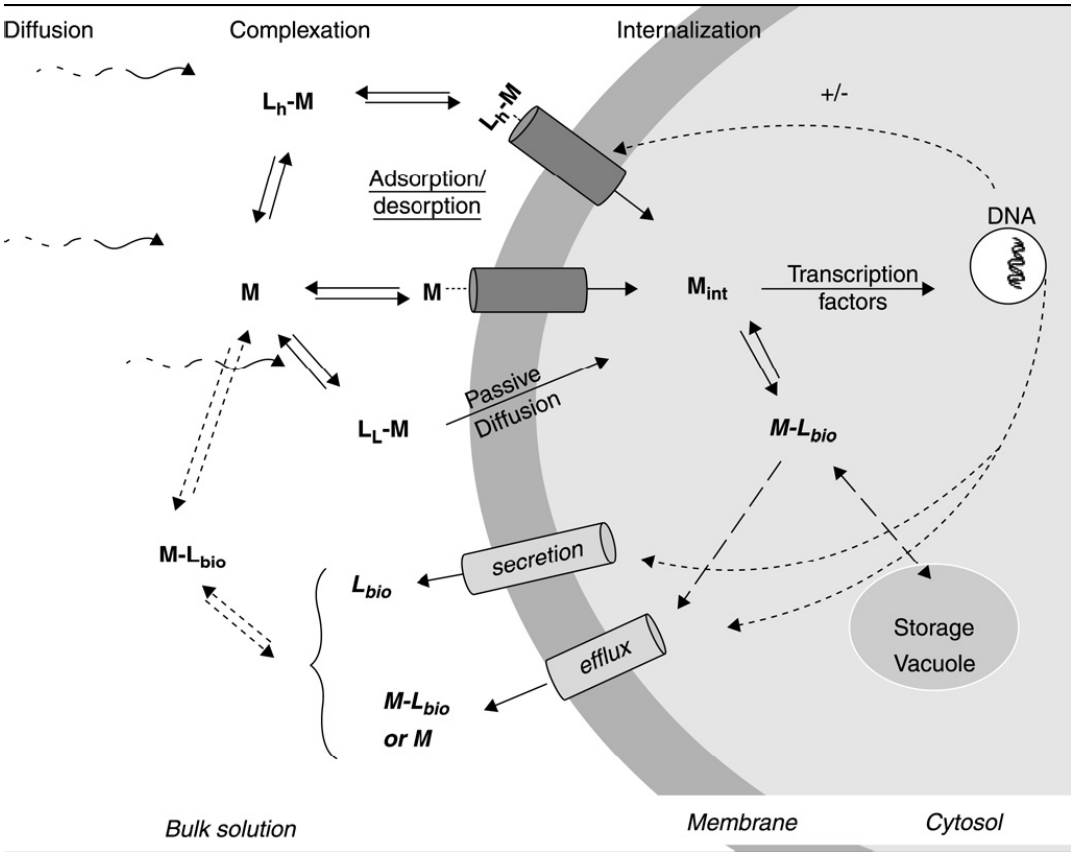

Figure 7: Conceptual model of some of the important physico-chemical processes leading to and after the uptake of a trace metal by an aquatic microorganism (reproduced from Worms 2006). L represents a ligand that can complex the metal M (subscripts: L, lipophilic; h, hydrophilic; bio, biological; int, internalized).

Microorganisms have developed several protective mechanisms: 1) intracellular binding or sequestration by metal-complexing agents, 2) compartmentalization and transport of metals to subcellular compartments and 3) efflux (Worms 2006).

Several classes of intracellular metal chelators, such as glutathione (GSH), amino acids, phytochelatins, metallothioneins, organic acids and thioredoxins (TRX), participate in cell protection (Bellion et al. 2006; Worms 2006). Metallothioneins are ubiquitous low molecular weight cysteine-rich proteins that bind metal ions in thiolate clusters. Physiological functions include storage and transport of essential metals in addition to the detoxification of non essential metal ions (Cd^{2+}, Hg^{2+}). Amino acids and organic acids, such as citrate, malate and oxalate, can complex metals in the cytoplasm (Worms 2006). Metal transport proteins may be involved in tolerance by extruding toxic metal ions out of the cell or by sequestering them into intracellular compartments such as vacuoles (Bellion et al. 2006).

II. MERCURY TRANSPORT AND FACTORS AFFECTING UPTAKE

Hg speciation in oxic aquatic environments is dominated by hydroxide and chloride complexes if organic complexation is not considered. Using laboratory-synthesized lipid bilayer membranes (lecithin-cholesterol-tetradecane), Gutknecht (1981) studied the permeability of mercuric salt complexes. Five major salt complexes were studied: $HgCl_2$, $HgCl_3^-$, $HgCl_4^{2-}$, HgOHCl and $Hg(OH)_2$, of which three are non-ionic and therefore more likely to pass across lipid bilayers and biological membranes (Gutknecht 1981). Since Hg^{2+} has only a small effect on membrane conductivity, it can probably pass across membranes in a non-ionic form *i.e.* $HgCl_2$, HgOHCl and $Hg(OH)_2$. Based on the results of this study, lipid membranes are highly permeable to $HgCl_2$ with a permeability estimated at $1.3x10^{-2}cm.sec^{-1}$, about 20 times higher than the permeability to water and more than a million times higher than the permeabilities to Na^+, K^+ and Cl^-. However, the permeability to CH_3HgCl is expected to be even higher (Lakowicz and Anderson 1980). Barkay et al. (1997) obtained similar results with uncharged $HgCl_2$ being more bioavailable than anionic forms of mercuric chloride. However, they also reported permeability at significant rates for other non ionic forms of Hg, such as $Hg(OH)_2$ and HgClOH, in contrast with the findings of Gutknecht (1981). This difference is attributed to differential transfer efficiency of mercurial compounds since the bacterial cell membrane also contains other components in addition to lipids (Barkay et al. 1997).

Toxicity has often been shown to decrease after the addition of ligands able to complex the metal (Kong et al. 1995). However, in a study using a mercury biosensor, uptake was not affected by ligand predominance, but rather by total Hg concentration under both aerobic and anaerobic conditions (Golding et al. 2007). In addition, uptake was not altered when the predominant ligand was changed from Cl^- to OH^- and to NH_3, suggesting that the bioavailable form of Hg is the free ion form, in agreement with the free ion activity model (FIAM) (Golding et al. 2007).

However, the uptake pattern appears to be different in anaerobic bacteria. When Hg is bound to either histidine or H^+ concentrations increase, uptake is enhanced. This is inconsistent both with the FIAM model and to what is seen with other metals, where competition of H^+ with uptake of the positively-charged free ion leads to a decrease in bioavailability (Golding et al. 2007). Another molecule that has been shown to interact with Hg is dissolved organic carbon (DOC). At neutral pH, DOC was shown to inhibit Hg^{2+} bioavailability, but the inhibition was less severe at pH 5, which suggests that free H^+ ions may compete with Hg^{2+} for binding sites in DOC (Barkay et al. 1997). These studies suggest that there may be a facilitated uptake mechanism for mercury. There is a growing body of evidence, based on studies using biosensors (Golding et al. 2002; Scott 2003) and bacterial

cultures (Najera et al. 2005), that passive diffusion is not the only transport mechanism and that facilitated uptake of species such as $Hg(NH_3)^{2+}$ may play an important role in toxicity.

III. MERCURY TOXICITY IN BACTERIA

Mercury ions can interact with a variety of reactive sites in both the cell membrane and the cytoplasm. Hg ions have been shown to cause irreversible membrane damage (Passou and Rothstein 1960), leading to potassium (K^+) leakage. Brunker (1976) found that Hg ions inhibited catabolic metabolism and cell respiration thereby provoking the cellular depletion of endogenous ATP (Brunker 1976). The inhibition of membrane ATPases due to the lack of intracellular substrates (i.e. after depletion of ATP) was suggested to be responsible for the uncontrolled release of K^+ previously observed (Passou and Rothstein 1960). Mercury has also been reported to induce oxidative stress by inhibiting glutathione reductase (GR), which catalyzes the reduction of GSSG (glutathione disulfide) to two molecules of glutathione (Gueldry et al. 2003).

Hg toxicity appears to be dependent on speciation. If Hg ions remain uncomplexed, the intracellular concentrations of mercury should remain low and the toxic effect of Hg^{2+} would mainly involve interactions with the cell membrane (Gueldry et al. 2003). However, if Hg ions form complexes with other molecules, these complexes may be actively absorbed and internalized. Once in the cell, Hg ions can undergo ligand exchange. For instance, complexes containing two molecules of glutathione and one mercuric ion might act as mimics of oxidized glutathione molecules and be recognized by glutathione transporters (Gueldry et al. 2003).

Recently, bacterial real-time gene expression profiles were realized to assess Hg toxicity in *Escherichia coli* by using a cell-array library of 93 *E. coli* K12 strains that carried transcriptional green-fluorescent protein fusions with most of the known stress response genes (Onnis-Hayden et al. 2009). Mercury either up-regulated or down-regulated several genes in a time- and concentration-dependent manner. Of the 22 overexpressed genes, eight belonged to the drug resistance/sensitivity and detoxification category including *zntA*, a gene encoding an ATPase involved in the transport of divalent soft metals (Onnis-Hayden et al. 2009); two genes belonged to the MerR family, *cueR*, a mercury-resistance gene regulator, and *ycgE*, a MerR homolog (Peng and Chuan 2004); the others belonging to the SOS response and the energy and oxidative stress regulons. Other genes from the SOS regulon were also repressed. These results suggest that mercury induces oxidative stress caused by the formation of superoxide compounds that lead to redox stress and DNA damage in bacteria (Onnis-Hayden et al. 2009).

IV. MOLECULAR MECHANISM OF RESISTANCE

A) THE MER SYSTEM

The most well documented mechanism of specific microbial mercury resistance involves the *mer* operon, a genetic system encoding transporters, regulators and the mercuric reductase (MerA) enzyme that catalyzes the reduction of Hg^{2+} to Hg°, which then diffuses outside the cell (Wiatrowski et al. 2006). This system is described in detail in an elegant review (Barkay et al. 2003). Although identified in both Gram-positive and negative bacteria, the *mer* operon is best described in the last group (figure 8). The reducing enzyme, MerA, is a cytosolic flavin disulfide oxidoreductase that uses NAD(P)H as a reductant. The MerA enzyme was found to contain a flexible amino-terminal domain that is homologous to MerP, a periplasmic mercury-binding protein that uses two cysteine residues to bind Hg^{2+}, in all but one genus of Gram-positive bacteria. MerP transfers Hg^{2+} onto two cysteine residues in the first of three transmembrane helices of MerT, a cytosolic membrane protein. The subsequent transfer of Hg^{2+} into the cytosol has yet to be fully understood, but within the cytosol, millimolar concentrations of thiol redox buffers (i.e. glutathione, cysteine) compete with MerT to remove Hg^{2+} as a dithiol derivate. This form is the substrate for MerA. Alternatively, MerA may also directly remove Hg^{2+} from MerT (Figure 8) (Barkay et al. 2003). Biochemical and structural analyses of MerA have shown that each monomer contains four cysteine residues that are important in the reduction of Hg^{2+} and that two tyrosine residues confer optimal functionality (Schiering et al. 1991). In order to improve resistance against oxidized mercury, some MerA proteins have an Hg^{2+}-binding N-terminal domain (Ledwidge et al. 2005).

In most loci, the expression of these proteins is controlled by MerR, a metal specific activator-repressor of the operon that encodes the MerT, MerP and MerA structural genes (Hamlett et al. 1992). The *mer* operon has also been found to encode other proteins such as MerC, MerF, MerE, MerB , MerD, MerG (Barkay et al. 2003) and the recently discovered MerH transport protein in mycobacteria (Schue et al. 2009). MerC is a membrane-bound protein with four transmembrane helices that is able to transport Hg^{2+} across the bacterial membrane (Sasaki et al. 2005).

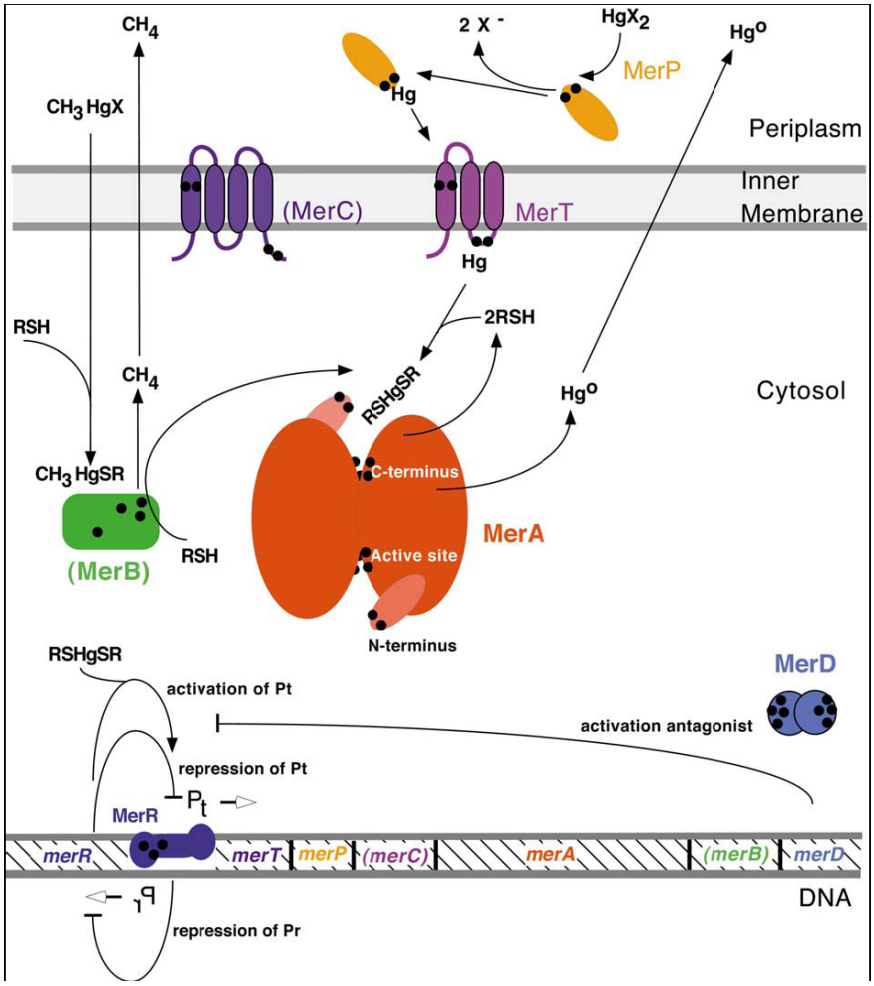

Figure 8: Model of a Gram-negative mercury resistance (*mer*) operon (reproduced from Barkay et al. 2003). The symbol "•" indicates a cysteine residue. X refers to a generic solvent nucleophile. RSH is the low-molecular-mass, cytosolic thiol redox buffer such as glutathione. Parentheses around gene or protein designations indicate proteins/genes that do not occur in all examples of the operon.

MerF is predicted to be a membrane-bound protein with two transmembrane helices involved in Hg^{2+} uptake, but its activity is not enhanced by MerP (Barkay et al. 2003). MerE is a membrane-bound broad mercury transporter that mediates the transport of both CH_3Hg^+ and Hg^{2+} across the bacterial membrane (Kiyono et al. 2009). Some bacteria are able to transform both inorganic and organic mercury compounds, while others (even of the same genus) are only able to transform inorganic mercury compounds. This resistance to organic mercury is conferred via MerB, an organomercurial lyase enzyme that transfers a proton to the C-Hg bond in alkyl and aryl mercurials yielding Hg^{2+}, which can then be reduced to Hg° by MerA. A periplasmic protein, MerG, found in Gram-negative bacteria, is thought to increase resistance to organomercurials in bacteria lacking MerB (Barkay et al. 2003).

MerR belongs to a family of transcriptional activator-repressors that act as negative autoregulators. In the absence of mercury, MerR binds the *mer* operator (*merO*) as a dimer and represses the

transcription of both *merR* and the other genes (Lund and Brown 1987). MerR forms a stable non-transcribing pre-initiation complex by attracting RNA polymerase to the Pt promoter in the absence of the metal ion inducer and by bending the promoter DNA away from the polymerase. This pre-initiation complex allows for an instantaneous response to the presence of cytosolic Hg^{2+}, although induction requires Hg^{2+} in the nmol · liter^{-1} range (Barkay et al. 2003). Once Hg^{2+} binds to MerR, the operator DNA unwinds, allowing RNA polymerase to access the transcriptional start site (Barkay et al. 2003). MerD is a co-regulator that represses the induction of the *mer* operon by displacing the Hg-bound MerR from the *mer* operator to allow new synthesis of metal-free MerR able to switch off the induction of the *mer* genes when the external mercury is exhausted (Champier et al. 2004). This system is purported to be less effective in anaerobic conditions.

Genes encoding MerA have been isolated from diverse environments, including soil (Oregaard and Sorensen 2007), Siberian permafrost (Mindlin et al. 2005) and Arctic biofilms (Poulain et al. 2007), and have been described in bacteria (Barkay et al. 2003) and archaea (Schelert et al. 2004). The MerA sequences are highly diverse, with differences in protein length, depending on the presence of zero, one or two Hg-binding domains at the N-terminus. The MerA protein has been found in *Firmicutes*, *Actinobacteria*, α-,β/γ-, and δ-*Proteobacteria*, *Bacteroidetes*, *Deinococcus-Thermus* and Archaea (Oregaard and Sorensen 2007).

B) **Effects of mercury on microbial community structure and function**

Microbial adaptation to environmental stress can occur via three different mechanisms: enrichment of populations that carry the required resistance/tolerance traits, induction of expression of genes involved in the detoxification or resistance mechanisms, and genetic adaptation by horizontal gene transfer (Sørensen et al. 2002). Mercury has been shown to alter microbial community structure in laboratory studies. After the addition of 25 µg $Hg^{2+}.g^{-1}$ to soil microcosms, culturable heterotrophic and genetic diversity decreased immediately, but then slowly increased again. This change in diversity was linked to a shift in community structure that contained Hg-resistant bacteria (Rasmussen and Sørensen 2001). Maron et al. (2007) also demonstrated that Hg was able to induce significant changes in both community functional structure and community genetic structure in a study using freshwater microcosms. However, these results were obtained after the addition of 8 mg $Hg.L^{1}$ (Maron et al. 2007), far above values found in natural environments that are typically in the $ng.L^{-1}$ range. To date, it is unclear how microbial communities respond to mercury contamination in the environment, especially in Arctic snowpacks that are subject to transient, yet non-negligible deposition of Hg during AMDEs.

REFERENCES

Allard B, Arsenie I (1991) Abiotic reduction of mercury by humic substances in aquatic system — an important process for the mercury cycle Water, Air and Soil Pollution 56:457–464

AMAP (2009) AMAP Assessment 2009: Human Health in the Arctic. Arctic Monitoring and Assessment Programme (AMAP). Oslo, Norway

AMAP/UNEP (2008) Technical Background Report to the Global Atmospheric Mercury Assessment. Arctic Monitoring and Assessment Programme/UNEP Chemicals Branch. Oslo, p 159

Amato P et al. (2007) Bacterial characterization of the snow cover at Spitzberg, Svalbard. Fems Microbiology Ecology 59:255-264

Amyot M, Gill GA, Morel FMM (1997) Production and Loss of Dissolved Gaseous Mercury in Coastal Seawater. Environmental Science and Technology 31:3606–3611

Ancora S, Rossi R, Di Simplicio P, Lusini L, Leonzio C (2002) In Vitro Study of Methylmercury in Blood of Bottlenose Dolphins (Tursiops truncatus) Archives of Environmental Contamination and Toxicology:348-353

Ariya PA et al. (2004) The Arctic: a sink for mercury. Tellus Series B-Chemical and Physical Meteorology 56:397-403

Barkay T, Gillman M, Turner RR (1997) Effects of dissolved organic carbon and salinity on bioavailability of mercury. Applied and Environmental Microbiology 63:4267-4271

Barkay T, Miller SM, Summers AO (2003) Bacterial mercury resistance from atoms to ecosystems. FEMS Microbiology Reviews 27:355-384

Barkay T, Poulain AJ (2007) Mercury (micro)biogeochemistry in polar environments. FEMS Microbiology Ecology 59:232-241

Barkay T, Wagner-Döbler I, Laskin AI, Bennett JW, M. GG (2005) Microbial Transformations of Mercury: Potentials, Challenges, and Achievements in Controlling Mercury Toxicity in the Environment. In: Advances in Applied Microbiology. Academic Press, pp 1-52

Barrie LA, Bottenheim JW, Schnell RC, Crutzen PJ, Rasmussen RA (1988) Ozone destruction and photochemical reactions at polar sunrise in the lower Arctic atmosphere. Nature 334:138–141

Bellion M, Courbot M, Jacob C, Blaudez D, Chalot M (2006) Extracellular and cellular mechanisms sustaining metal tolerance in ectomycorrhizal fungi. FEMS Microbiology Letters 254:173–181

Berntssen MHG, Aatland A, Handy RD (2003) Chronic dietary mercury exposure causes oxidative stress, brain lesions, and altered behaviour in Atlantic salmon (Salmo salar) paar Aquatic Toxicology 65:55-72

Brimblecombe P, Tranter, M., Tsiouris, S., Davies, T. D. and Vincent, C. E. (1986) The chemical evolution of snow and meltwater. Modelling Snowmelt-Induced Processes (Proceedings of the Budapest Symposium July 1986) IAHS Publ 155:283-295

Brinkmeyer R, Knittel K, Jurgens J, Weyland H, Amann R, Helmke E (2003) Diversity and structure of bacterial communities in Arctic versus Antarctic pack ice. Applied and Environmental Microbiology 69:6610-6619

Brunker RL (1976) Mercurial Toxicity in Yeast: Evidence for Catabolic Pathway Inhibition. Applied and Environmental Microbiology 32:498-504

Buffle J, Wilkinson KJ, van Leeuwen HP (2009) Chemodynamics and Bioavailability in Natural Waters. Environmental Science and Technology 43:7170-7174

Carpenter EJ, Lin S, Capone DG (2000) Bacterial activity in South Pole snow. Applied and Environmental Microbiology 66:4514-4517

Castoldi AF, Coccini, Teresa, Ceccatelli, Sandra, Manzo, Luigi (2001) Neurotoxicity and molecular effects of methylmercury. Brain Research Bulletin 55:197-203

Celo V, Lean DR, Scott SL (2006) Abiotic methylation of mercury in the aquatic environment. Science of the Total Environment 368:126-137

Champier L, Duarte V, Michaud-Soret I, Coves J (2004) Characterization of the MerD protein from *Ralstonia metallidurans CH34*: a possible role in bacterial mercury resistance by switching off the induction of the *mer* operon. Molecular Microbiology 52:1475-1485

Chen J, Pehkonen SO, Lin C-J (2003) Degradation of monomethylmercury chloride by hydroxyl radicals in simulated natural waters. Water Research 37:2496-2504

Choi SC, Chase Jr. T, Bartha R (1994) Enzymatic catalysis of mercury methylation by Desulfovibrio desulfuricans LS. . Applied and Environmental Microbiology 60 1342-1346

Christner BC (2002) Incorporation of DNA and protein precursors into macromolecules by bacteria at -15 degrees C. Applied and Environmental Microbiology 68:6435-6438

Christner BC, Morris CE, Foreman CM, Cai R, Sands DC (2008) Ubiquity of biological ice nucleators in snowfall. Science 319:1214

Christner BC, Mosley-Thompson E, Thompson LG, Reeve JN (2001) Isolation of bacteria and 16S rDNAs from Lake Vostok accretion ice. Environmental Microbiology 3:570-577

Christner BC, Mosley-Thompson E, Thompson LG, Zagorodnov VS, Sandman K, Reeve JN (2000) Recovery and Identification of Viable Bacteria Immured in Glacial Ice. Icarus 144:479-485

Colbeck SC (1978) The physical aspects of water flow through snow. Advances in Hydrosciences 11:165-206

Colbeck SC (1981) A simulation of the enrichment of atmospheric pollutants in snow cover runoff. Water Resources Research 17 1383–1388

Colbeck SC (1991) The layered character of snow covers. Reviews of Geophysics 29:81-96

Costa M, Liss PS (1999) Photoreduction of mercury in sea water and its possible implications for Hg 0 air–sea fluxes. Marine Chemistry 68:87–95

Cowan DA, Tow, LA (2004) Endangered Antacrctic Environments. Annual Reviews of Microbiology 58:649-690

Craig PJ (1986) Organometallic compounds in the environment. Longman, London

Daly GL, Wania F (2004) Simulating the Influence of Snow on the Fate of Organic Compounds. Environmental Science and Technology 38:4176-4186

Daré E, Li, W., Zhivotovsky, B., Yuan, X., Ceccatelli, S. (2001) Methylmercury and H2O2 provoke lysosomal damage in human astrocytoma D384 cells followed by apoptosis Free Radical Biology & Medicine 30:1347-1356

Davies TD, Vincent, C.E., Brimblecombe, P. (1982) Preferential elution of strong acids from a Norwegian ice cap. Nature 300:161-163

Davis RE (1991) Links between snowpack physics and snowpack chemistry. In: T.D. Davies MT, H.G. Jones (ed) Seasonal Snowpacks NATO ASI Series G. Springer-Verlag, Berlin, pp 115-138

Davis RE, Petersen, C.E., Bales, R.C. (1995) Ion flux through a shallow snowpack: effects of initial conditions and melt sequences. IAHS Publication 228:115–126

Dietz R, Outridge PM, Hobson KA (2009) Anthropogenic contributions to mercury levels in present-day Arctic animals--A review. Science of The Total Environment 407:6120-6131

Dommergue A, Bahlmann E, Ebinghaus R, Ferrari C, Boutron C (2007) Laboratory simulation of Hg0 emissions from a snowpack. Analytical and Bioanalytical Chemistry 388:319-327

Dommergue A, Ferrari CP, Poissant L, Gauchard PA, Boutron CF (2003) Diurnal cycles of gaseous mercury within the snowpack at Kuujjuarapik/Whapmagoostui, Quebec, Canada. Environmental Science and Technology 37:3289-3297

Douglas TA, Sturm M, Simpson WR, Brooks S, Lindberg SE, Perovich DK (2005) Elevated mercury measured in snow and frost flowers near Arctic sea ice leads. Geophysical Research Letters 32:-

Ebinghaus R et al. (2002) Antarctic Springtime Depletion of Atmospheric Mercury. Environmental Science and Technology 36:1238 –1244

Eichler A, Schwikowski, M., Gäggeler, H.W., 2001. (2001) Meltwater induced relocation of chemical species in Alpine firn. Tellus 53B:192–203

Falter R, Wilken R-D (1998) Isotope experiments for the determination of the abiotic mercury methylation potential of a River Rhine sediment. Vom Wasser 90:217-231

Ferrari C et al. (2005) Snow-to-air exchanges of mercury in an Arctic seasonal snow pack in Ny-Alesund, Svalbard. Atmospheric Environment 39:7633-7645

Fitzgerald WF, Engstrom, D. R., Mason, R. P., Nater, E. A. (1998) The case for atmospheric mercury contamination in remote areas. Environmental Science and Technology 32:1-7

Fleming EJ, Mack EE, Green PG, Nelson DC (2006) Mercury Methylation from Unexpected Sources: Molybdate-Inhibited Freshwater Sediments and an Iron-Reducing Bacterium. Applied and Environmental Microbiology 72:457-464

Gardfeldt K, Munthe J, Stromberg D, Lindqvist O (2003) A kinetic study on the abiotic methylation of divalent mercury in the aqueous phase. Science of the Total Environment 304:127-136

Golding GR, Kelly CA, Sparling R, Loewen PC, Barkay T (2007) Evaluation of mercury toxicity as a predictor of mercury bioavailability. Environmental Science and Technology 41:5685-5692

Golding GR, Kelly CA, Sparling R, Loewen PC, Rudd JWM, Barkay T (2002) Evidence for facilitated uptake of Hg(II) by Vibrio anguillarum and Escherichia coli under anaerobic and aerobic conditions. Limnology and Oceanography 47:967–975

Goto-Azuma K, Nakawo, M., Han, J., Watanabe,O., Azuma, N. (1994) Melt-induced relocation of ions in glaciers and in a seasonal snowpack IAHS Publication 223 287–298

Gray JE, Hines, M. E. (2006) Mercury: Distribution, Transport, and Geochemical and Microbial Transformations from Natural and Anthropogenic Sources. Applied Geochemistry 21:1819-1820

Gueldry O et al. (2003) Ycf1p-dependent Hg(II) detoxification in *Saccharomyces cerecisiae*. European Journal of Biochemistry 270:2486-2496

Gutknecht J (1981) Inorganic mercury (Hg^{2+}) transport through lipid bilayer membranes. Journal of Membrane Biology 61:61–66

Hamlett NV, Landale EC, Davis BH, Summers AO (1992) Roles of the Tn21 *merT*, *merP*, and *merC* gene products in mercury resistance and mercury binding. Journal of Bacteriology 174:6377-6385

Harada M (1995) Minamata disease: methylmercury poisoning in Japan caused by environmental pollution. Critical Reviews in Toxicology 25:1-24

Hinkler J, Hansen BU, Tamstorf MP, Sigsgaard C, Petersen D (2008) Snow and Snow-Cover in Central Northeast Greenland. Advances in Ecological Research 40:175-195

Hodgkins R, Tranter, M., and Dowdeswell, J. A. (1998) The hydrochemistry of runoff from a 'coldbased' glacier in the High Arctic (Scott Turnerbreen, Svalbard) Hydrological Processes 12:87–103

Hodson A et al. (2008) Glacial Ecosystems. Ecological Monographs 78:41-67

Hoham RW (1975) Optimal temperatures and temperature ranges for growth of snow algae. Arctic, Alpine Research 7:13-24

Hoham RW, Duval B (2001) Microbial ecology of snow and freshwater ice with emphasis on snow algae In: Jones HG, Pomeroy JW, Walker DA, Hoham RW (eds) Snow ecology: an interdisciplinary examination of snow-covered ecosystems. Cambridge University Press, Cambridge, pp 168–228

Iwahori K, Takeuchi F, Kamimura K, Sugio T (2000) Ferrous Iron-Dependent Volatilization of Mercury by the Plasma Membrane of Thiobacillus ferrooxidans. Applied and Environmental Microbiology 66:3823-3827

Johannessen M, Dale, T., Gjessing, E.T., Henriksen, A., Wright, R.F. (1977) Acid precipitation in Norway: the regional distribution of contaminants in snow and the chemical concentration processes during snow melt. IAHS Publication 118:116–120

Johannessen M, Henriksen, A. (1978) Chemistry of snow melt water: changes in concentration during melting Water Resources Research 14:615-619

Jones HG (1999) The ecology of snow-covered systems: a brief overview of nutrient cycling and life in the cold. Hydrological Processes 13:2135–2147

Jones HG, Pomeroy, J. W., Walker, D. A., Hoham, R. W. (ed) (2001) Snow Ecology. Cambridge University Press, Cambridge, UK

Jordan RE, Albert, M.R., Brun, E. (2008) Physical Processes within Snow and Their Parameterization. In: Armstrong RL, Brun, E. (ed) Snow and Climate. Cambridge University Press, Cambridge, pp 12-69

Junge K, Eicken,Hajo, Deming, Jody W. (2004) Bacterial Activity at -2 to -20°C in Arctic Wintertime Sea Ice. Applied and Environmental Microbiology 70:550-557

Kerin EJ, Gilmour CC, Roden E, Suzuki MT, Coates JD, Mason RP (2006) Mercury Methylation by Dissimilatory Iron-Reducing Bacteria. Applied and Environmental Microbiology 72:7919-7921

Kiyono M, Sone Y, Nakamura R, Pan-Hou H, Sakabe K (2009) The MerE protein encoded by transposon Tn21 is a broad mercury transporter in Escherichia coli. FEBS Letters 583:1127-1131

Kong IC, Bitton G, Koopman B, Jung KH (1995) Heavy metal toxicity testing in environmental samples Reviews of Environmental Contamination & Toxicology 142:119−147

Kritee K, Blum JD, Barkay T (2008) Mercury stable isotope fractionation during reduction of Hg(II) by different microbial pathways. Environmental Science and Technology 42:9171-9177

Kuhn M (1987) Micro-meteorological conditions for snow melt Journal of Glaciology 33:24-26

Kuhn M (2001) The nutrient cycle through snow and ice, a review. Aquatic Science 63:150-167

Lakowicz JR, Anderson CJ (1980) Permeability of lipid bilayers to methylmercuric chloride: Quantification by fluorescence quenching of a carbazole-labeled phospholipid. Chemico-Biological Interactions 30:309-323

Lalonde JD, Amyot M, Kraepiel AML, Morel FMM (2001) Photooxidation of Hg(0) in artificial and natural waters. Environmental Science and Technology 35:1367–1372

Lalonde JD, Poulain AJ, Amyot M (2002) The role of mercury redox reactions in snow on snow–to–air mercury transfer. Environmental Science and Technology 36:174–178

Lamborg CH, Fitzgerald, W.F., O'Donnell, J., Torgersen,T. (2002) A non-steady-state compartmental model of global-scale mercury biogeochemistry with interhemispheric atmospheric gradients Geochimica et Cosmochimica Acta 66:1105-1118

Larsen KS, Grogan, Paul, Jonasson, Sven, Michelsen, Anders (2007) Respiration and Microbial Dynamics in Two Subarctic Ecosystems during Winter and Spring Thaw: Effects of Increased Snow Depth Arctic, Antarctic, and Alpine Research 39:268-276

Ledwidge R et al. (2005) NmerA, the metal binding domain of mercuric ion reductase, removes Hg^{2+} from proteins, delivers it to the catalytic core, and protects cells under glutathione-depleted conditions. Biochemistry 44:11402–11416

Libbrecht KG (2005) The physics of snow crystals. Reports on Progress in Physics 68:855-895

Lindberg S et al. (2007) A synthesis of progress and uncertainties in attributing the sources of mercury in deposition. Ambio 36:19-32

Lindberg SE et al. (2002) Dynamic Oxidation of Gaseous Mercury in the Arctic Troposphere at Polar Sunrise. Environmental Science and Technology 36:1245–1256

Liu Y et al. (2009) Bacterial diversity in the snow over Tibetan Plateau Glaciers. Extremophiles 13:89-99

Liu Y, Yao T, Jiao N, Kang S, Zeng Y, Huang S (2006) Microbial community structure in moraine lakes and glacial meltwaters, Mount Everest. FEMS Microbiology Letters 265:98-105

Lu JY et al. (2001) Magnification of atmospheric mercury deposition to polar regions in springtime: the link to tropospheric ozone depletion chemistry. Geophysical Research Letters 28:3219–3222

Lund PA, Brown NL (1987) Role of the merT and merP gene products of transposon Tn501 in the induction and expression of resistance to mercuric ions. Gene 52:207-214

Lyons WB, Welch K. A., Fountain A. G., Dana G. L., Vaughn B. H., McKnight D. M. (2003) Surface glaciochemistry of Taylor Valley, southern Victoria Land, Antarctica, and its relation to stream chemistry. Hydrological Processes 17 115–130

Maron L, Dommergue A, Ferrari C, Delacour-Larose M, Fain X (2008) How elementary mercury reacts in the presence of halogen radicals and/or halogen anions: a DFT investigation. Chemistry 14:8322-8329

Maron P-A, Mougel C, Siblot S, Abbas H, Lemanceau P, Ranjard L (2007) Protein Extraction and Fingerprinting Optimization of Bacterial Communities in Natural Environment. Microbial Ecology 53:426–434

Mason RP, Fitzgerald, W. F., Morel, F.M.M. (1994) The biogeochemistry of elemental mercury−anthropogenic influences. Geochimica et Cosmochimica Acta 58:3191-3198

Meyer T, Lei YD, Muradi I, Wania F (2008) Organic Contaminant Release from Melting Snow. 2. Influence of Snow Pack and Melt Characteristics. Environmental Science and Technology 43:663-668

Meyer T, Lei YD, Wania F (2006) Measuring the release of organic contaminants from melting snow under controlled conditions. Environmental Science and Technology 40:3320–3326

Meyer T, Wania F (2008) Organic contaminant amplification during snowmelt. Water Research 42:1847-1865

Mindlin S et al. (2005) Present-day mercury resistance transposons are common in bacteria preserved in permafrost grounds since the Upper Pleistocene. Research in Microbiology 156:994-1004

Miteva V (2008) Bacteria in Snow and Glacier Ice. In: Margesin Rea (ed) Psychrophiles: from Biodiversity to Biotechnology Springer-Verlag, Berlin Heidelberg, pp 31-47

Mueller DR, Vincent WF, Bonilla S, Laurion I (2005) Extremotrophs, extremophiles and broadband pigmentation strategies in a high arctic ice shelf ecosystem. FEMS Microbiology Ecology 53:73–87

Munthe J (1992) The aqueous oxidation of elemental mercury by ozone. Atmospheric Environment 26A:1461–1468

Najera I, Lin CC, Kohbodi GA, Jay JA (2005) Effect of chemical speciation on toxicity of mercury of Escherichia coli biofilms and planktonic cells. Environmental Science and Technology 39:3116−3120

Nigro M, Leonzio,C. (1996) Intracellular storage of mercury and selenium in different marine vertebrates. Marine Ecology Progress Series 135:137-143

Nriagu JO (1989) A global assessment of natural sources of atmospheric trace metals. Nature 338:47–49

Nriagu JO (1994) Mechanistic steps in the photoreduction of mercury in natural waters. The Science of the Total Environment 154:1-8

Nriagu JO, Pacyna, J.M. (1988) Quantitative assessment of worldwide contamination of air, water and soils with trace metals. Nature 333:134-139

Onnis-Hayden A et al. (2009) Prokaryotic real-time gene expression profiling for toxicity assessment. Environmental Science and Technology 43:4574-4581

Oregaard G, Sorensen SJ (2007) High diversity of bacterial mercuric reductase genes from surface and sub-surface floodplain soil (Oak Ridge, USA). Isme J 1:453-467

Oremland RS, Culbertson CW, Winfrey MR (1991) Methylmercury Decomposition in Sediments and Bacterial Cultures: Involvement of Methanogens and Sulfate Reducers in Oxidative Demethylation. Applied and Environmental Microbiology 57:130-137

Passou H, Rothstein A (1960) The binding of mercury by the yeast cell in relation to changes in permeability. The Journal of General Physiology 43:621-633

Peng C, Chuan H (2004) A General Strategy to Convert the MerR Family Proteins into Highly Sensitive and Selective Fluorescent Biosensors for Metal Ions. Journal of the American Chemical Society 126:728-729

Pomeroy JW, Brun, E. (2001) Physical properties of snow. In: H.G. Jones JWP, D.A. Walker and R.W. Hoham (ed) Snow Ecology. An Interdisciplinary Examination of Snow-Covered Ecosystems. Cambridge University Press, Cambridge, pp 45–126

Poulain AJ, Lalonde JD, Amyot M, Shead JA, Raofie F, Ariya PA (2004) Redox transformations of mercury in an Arctic snowpack at springtime. Atmospheric Environment 38:6763-6774

Poulain AJ et al. (2007) Potential for mercury reduction by microbes in the high arctic. Applied and Environmental Microbiology 73:2230-2238

Price PB, Sowers T (2004) Temperature dependence of metabolic rates for microbial growth, survival and maintenance. Proc Natl Acad Sci USA 101 4631–4636

Priscu JC, Christner BC (2004) Earth's icy biosphere. In: Bull AT (ed) Microbial Diversity and Bioprospecting. American Society for Microbiology, Washington, D.C. , pp 130-145

Qiu Y, Vishnivetskaya TA, Lubman DM (2009) Proteomic Insights: Cryoadaptation of Permafrost Bacteria. In: Permafrost Soils, pp 169-181

Rasmussen LD, Sørensen SJ (2001) Effects of mercury contamination on the culturable heterotrophic, functional and genetic diversity of the bacterial community in soil. FEMS Microbiology Ecology 36:1-9

Rowland IR, Davies MJ, Grasso P (1977) Volatilization of methylmercuric chloride by hydrogen sulphide. Nature 265 718-719

Sasaki Y, Minakawa T, Miyazaki A, Silver S, Kusano T (2005) Functional dissection of a mercuric ion transporter MerC from *Acidithiobacillus ferrooxidans.* Bioscience, Biotechnology, and Biochemistry 69:1394–1402

Sattler B, Puxbaum H, Psenner R (2001) Bacterial growth in super cooled cloud droplets. Geophysical Research Letters 28:239–242

Schelert J, Dixit V, Hoang V, Simbahan J, Drozda M, Blum P (2004) Occurrence and Characterization of Mercury Resistance in the Hyperthermophilic Archaeon Sulfolobus solfataricus by Use of Gene Disruption. The Journal of Bacteriology 186:427-437

Schiering N, Kabsch W, Moore MJ, Distefano MD, Walsh CT, Pai EF (1991) Structure of the detoxification catalyst mercuric ion reductase from Bacillus sp. strain RC607. Nature 352:168-172

Schimel JP, Gulledge, J. (1998) Microbial community structure and global trace gases. Global Change Biology 4:745–758

Schindler DW, Smol JP (2006) Cumulative Effects of Climate Warming and Other Human Activities on Freshwaters of Arctic and Subarctic North America. AMBIO: A Journal of the Human Environment 35:160-168

Schroeder WH et al. (1998) Arctic springtime depletion of mercury. Nature 394:331–332

Schue M, Dover LG, Besra GS, Parkhill J, Brown NL (2009) Sequence and analysis of a plasmid-encoded mercury resistance operon from Mycobacterium marinum identifies MerH, a new mercuric ion transporter. The Journal of Bacteriology 191:439-444

Schultz IR, Newman, M. C. (1997) Methyl mercury toxicokinetics in channel catfish (Ictalurus punctatus) and largemouth bass (Micropterus salmoides) after intravascular administration. Environmental Toxicology and Chemistry 16:990-996

Scott KJ (2003) Development and Use of a mer-lux Bioreporter for the Measurement and Characterization of Bioavailable Hg(II) in Defined Media and Aquatic Environmental Samples. In: Department of Microbiology. University of Manitoba, Winnepeg, p 172

Seigneur C, Wrobel J, Constantinou E (1994) A chemical kinetic mechanism for atmospheric inorganic mercury. Environmental Science and Technology 28:1589–1597

Sellers P, Kelly CA, Rudd JWM, MacHutchon AR (1996) Photodegradation of methylmercury in lakes. Nature 380:694-697

Siciliano SD, Lean DR (2002) Methyltransferase: an enzyme assay for microbial methylmercury formation in acidic soils and sediments. Environmental Toxicology and Chemistry 21:1184-1190

Skidmore ML, Foght JM, Sharp MJ (2000) Microbial life beneath a high arctic glacier. Applied and Environmental Microbiology 66:3214-3220

Skogerboe RK, Wilson SA (1981) Reduction of ionic species by fulvic acid Analytical Chemistry 53:228–232

Skov H et al. (2004) Fate of elemental mercury in the arctic during atmospheric mercury depletion episodes and the load of atmospheric mercury to the arctic. Environmental Science and Technology 38:2373-2382

Slaveykova VI, Wilkinson KJ (2005) Predicting the bioavailability of metals and metal complexes: critical review of the biotic ligand model. Environmental Chemistry 2 9–24

Smith T, Pitts K, McGarvey JA, Summers AO (1998) Bacterial Oxidation of Mercury Metal Vapor, Hg(0). Applied and Environmental Microbiology 64:1328-1332

Sørensen SJ, de Lipthay JR, K. MA, T B, Hansen LH, Rasmussen LD (eds) (2002) Molecular methods for assessing and manipulating the diversity of microbial populations and processes. Marcel Dekker Inc., New York

Steffen A et al. (2008) A synthesis of atmospheric mercury depletion event chemistry in the atmosphere and snow. Atmospheric Chemistry and Physics 8:1445-1482

Stibal M, Elster J, Sabacka M, Kastovska K (2007) Seasonal and diel changes in photosynthetic activity of the snow alga *Chlamydomonas nivalis* (*Chlorophyceae*) from Svalbard determined by pulse amplitude modulation fluorometry. FEMS Microbiology Ecology 59:265-273

Suda I, Suda M, Hirayama K (1993) Degradation of methyl and ethyl mercury by singlet oxygen generated from sea water exposed to sunlight or ultraviolet light. Archives of Toxicology 67:365-368

Sugio T, Fujii M, Takeuchi F, Negishi A, Maeda T, Kamimura K (2003) Volatilization of mercury by an iron oxidation enzyme system in a highly mercury-resistant Acidithiobacillus ferrooxidans strain MON-1. Bioscience, Biotechnology, and Biochemistry 67:1537-1544

Sugio T, Iwahori K, Takeuchi F, Negishi A, Maeda T, Kamimura K (2001) Cytochrome c oxidase purified from mercury-resistant strain of Acidithiobacillus ferroxidans volatilizes mercury. Journal of Bioscience and Bioengineering 92:44-49

Thomas WH, Duval B (1995) Sierra Nevada, California, USA, snow algae: snow albedo changes, algal-bacterial interrelationships, and ultraviolet radiation effects. Arctic, Antarctic, and Alpine Research 27:389–399

Thoming J, Kliem BK, Ottosen LM (2000) Electrochemically enhanced oxidation reactions in sandy soil polluted with mercury. The Science of the Total Environment 261:137-147

Thompson DR (1990) Metal levels in marine vertebrates. In: Furness RW, Rainbow, P. S. (ed) Heavy metals in the marine environment. CRC Press, Boca Raton

Tranter M, Brimblecombe, P., Davies, T.D., Vincent, C.E., Abrahams, P.W. (1986) A composition of snowfall, snowpack and meltwater in the Scottish Highlands—evidence for preferential elution Atmospheric Environment 20:517–525

Tranter M, Sharp MJ, Lamb HR, Brown GH, Hubbard BP, Willis IC (2002) Geochemical weathering at the bed of Haut Glacier d'Arolla, Switzerland—a new model. Hydrological Processes 16:959-993

Ullrich SM, Tanton, T.W., Abdrashitova, S.A. (2001) Mercury in the aquatic environment: a review of factors affecting methylation. Critical Reviews in Environmental Science and Technology 31:241-293

Vincent WF (2000) Evolutionary origins of Antarctic microbiota: invasion, selection and endemism. Antarctic Science 12:374-385

Wania F, Semkin R, Hoff JT, Mackay D (1999) Modelling the fate of non-polar organic chemicals during the melting of an Arctic snowpack. Hydrological Processes 13:2245-2256

Wiatrowski HA, Ward PM, Barkay T (2006) Novel reduction of mercury (II) by mercury-sensitive dissimilatory metal reducing bacteria. Environmental Science and Technology 40:6690-6696

Worms I, Simon, D. F., Hassler,C.S., Wilkinson,K.J. (2006) Bioavailability of trace metals to aquatic microorganisms: importance of chemical, biological and physical processes on biouptake. Biochimie 88:1721-1731

Yee S, Choi, B. H. (1994) Methylmercury Poisoning Induces Oxidative Stress in the Mouse Brain. Experimental and Molecular Pathology 60:188-196

Yergeau E, Newsham KK, Pearce DA, Kowalchuk GA (2007) Patterns of bacterial diversity across a range of Antarctic terrestrial habitats. Environmental Microbiology 9:2670-2682

Yokoo EM, Valente, J. G., Grattan, L., Schmidt, S. L., Platt, I., Silbergeld, E. K. (2003) Low level methylmercury exposure affects neurophysiological function in adults. Environmental Health, A Global Access Science Source 2:8

Zhang H, Lindberg SE (2001) Sunlight and iron(III)–induced photochemical production of dissolved gaseous mercury in freshwater. Environmental Science and Technology 35:928–935

Zhang T (2005) Influence of the seasonal snow cover on the ground thermal regime: An overview Rev. Geophys. 43:RG4002, doi:4010.1029/2004RG000157

SECTION II

Determining whether snow chemistry and mercury contamination has an effect on microbial community structure in cold environments requires detailed information on both microbial communities present in the snow and its chemistry. In order to improve our understanding of arctic snowpacks, we carried out a two-month preliminary field study in Ny-Ålesund (Svalbard, Norway, 78°56'N, 11°52'E) in spring 2007. The first objective was to gain insight into the organisms present in snow and meltwater. Therefore, using culture-independent techniques, we constructed two snow and two meltwater 16S (*rrs*) clone libraries and explored their biodiversity using a variety of indicators. A total of 19 different microbial classes were observed in our clone libraries, of which many had been identified in other cold environments, thus supporting the hypothesis for globally uniform characteristics among microbial communities of the cryosphere. These results are presented in more detail in Chapter 2.

In Chapter 3, we examined the fate of Hg in an Arctic snowpack, from its deposition during atmospheric mercury depletion events (AMDEs) up until its transfer during snow melt. During AMDEs, concentrations of up to 373 $ng.L^{-1}$ of Hg are deposited onto snow surfaces. Although most of the Hg is re-emitted to the atmosphere via photochemical reactions, a fraction is stored in the snow and is transferred to meltwater-fed systems. Spring melt was estimated to contribute for 8 to 21% of the fjord's Hg content. We also monitored methylmercury (MeHg) concentrations in the snow throughout the field study. During the snow melt period, MeHg concentrations increase. Possible sources include wet deposition and *in situ* methylation.

CHAPTER 2: MICROBIAL SEQUENCES RETRIEVED FROM ENVIRONMENTAL SAMPLES FROM SEASONAL ARCTIC SNOW AND MELTWATER FROM SVALBARD, NORWAY

Manuscript accepted for publication in *Extremophiles*

Catherine Larose[1,2,3], Sibel Berger[4], Christophe Ferrari[1], Elisabeth Navarro[4], Aurélien Dommergue[1], Dominique Schneider[2,3] and Timothy M. Vogel*[4]*

[1]Laboratoire de Glaciologie et Géophysique de l'Environnement (LGGE), UMR (CNRS/UJF) 5183, Université Joseph Fourier, 54 rue Molière, 38402 Saint Martin d'Hères cedex, France

[2]Laboratoire Adaptation et Pathogénie des Microorganismes, Université Joseph Fourier, Grenoble 1, BP 170, F-38042 Grenoble cedex 9, France

[3] CNRS UMR 5163

[4]Environmental Microbial Genomics Group, Laboratoire AMPERE, UMR CNRS 5005, Ecole Centrale de Lyon, Université de Lyon, 36 avenue Guy de Collongue, 69134 Ecully, France

*Contributed equally

Abstract

16S rRNA gene (*rrs*) clone libraries were constructed from two snow samples (May 11th, 2007 and June 7th, 2007) and two meltwater samples collected during the spring of 2007 in Svalbard, Norway (79°N). The libraries covered 19 different microbial classes, including *Betaproteobacteria* (21.3%), *Sphingobacteria* (16.4%), *Flavobacteria* (9.0%), *Acidobacteria* (7.7%) and *Alphaproteobacteria* (6.5%). Significant differences were detected between the two sets of sample libraries. First, the meltwater libraries had the highest community richness (Chao1: 103.2 and 152.2) and Shannon biodiversity indices (between 3.38 and 3.59), as compared to the snow libraries (Chao1: 14.8 and 59.7; Shannon index: 1.93 and 3.01). Second, ∫-LIBSHUFF analyses determined that the bacterial communities in the snow libraries were significantly different from those of the meltwater libraries. Despite these differences, our data also support the theory that a common core group of microbial populations exist within a variety of cryohabitats.

Keywords: Arctic, snow bacteria, biodiversity, environmental samples, meltwater

Introduction

A large portion of the Earth is cold: about 14% of the biosphere is polar and 90% (by volume) is cold ocean, with temperatures less than 5°C (Priscu and Christner 2004). Due to the strong feedback mechanisms between snow, ice and the atmosphere, the cryosphere influences the entire biosphere (Jones 1999). The seasonal snow cover is an important component of the cryosphere (Jones 1999), which can at times cover about 35% of the Earth's surface (Miteva 2008). Despite the importance of the cryosphere, the microbiological analysis of this environment is a relatively recent field of research. Microorganisms have been described in several extreme environments such as glacial ice (Christner et al. 2000; Skidmore et al. 2000; Christner et al. 2001), sea ice (Brinkmeyer et al. 2003) and polar snow (Carpenter et al. 2000; Amato et al. 2007), but their importance in cryosphere ecology has only begun to be recognized. Recent reports suggest that microorganisms impact the dynamics, composition and abundance of nutrients (Hodson et al. 2008), that they may shift surface albedo of snow and ice (Thomas and Duval 1995) and impact the hydrochemistry (Tranter et al. 2002). The importance of bacteria in governing redox conditions and their role in Fe, S, N and P cycling is becoming apparent (Hodson et al. 2008). In addition, they are probably responsible for the metabolism and transformation of environmental contaminants such as mercury (Barkay and Poulain 2007; Poulain et al. 2007). While snow algae have been studied relatively extensively (Hoham 1975; Hoham and Duval 2001; Stibal et al. 2007), little is known about the bacteria inhabiting seasonal snow cover, especially polar snowpacks. Carpenter et al. (2000) reported low rates of DNA synthesis and the presence of *Thermus-Deinococcus*-like organisms in Antarctic snow. Amato et al. (2007) used culture-based methods to isolate 10 bacterial strains belonging to *Proteobacteria*, *Firmicutes* and *Actinobacteria* from a snowpit dug on a polythermal glacier in Svalbard (Norway). Unfortunately, culture-based techniques will not recover the full diversity of species present and might not even recover the dominant population (Ward et al. 1990). A metagenomic approach, which extracts and analyzes nearly all the microbial community DNA, should provide more detailed insight into polar snow microbial diversity. Such an approach was used to reveal relatively high microbial diversity in the snow of glaciers of the Tibetan Plateau around Mount Everest (Liu et al. 2009). Whether the snow in other environments is equally diverse has yet to be determined.

Here, we present the results of an exploratory study on microbial sequences retrieved from surface snow and meltwater samples from a high Arctic site, Svalbard, Norway (79°N), using culture-independent techniques. We hypothesize that the snow is a highly diverse ecosystem that might have some globally uniform characteristics in terms of microbial populations in cryohabitats.

Materials and Methods

Samples for microbial analysis were taken during a 2007 springtime field campaign in Ny-Ålesund (Svalbard, Norway, 78°56'N, 11°52'E). A total of four samples were collected: an early spring (sample date May 11th, 2007) snow sample (ESS), a late spring (sample date June 7th, 2007) snow sample (LSS), a meltwater river (sample date June 11th, 2007) sample (MWR) and a snow-soil interface meltwater (sample date June 10th, 2007) sample (SSIM). Surface snow (3 cm depth) and meltwater samples were collected in 3 L sterile sampling bags using a Teflon shovel sterilized for microbial analyzes. To avoid contamination, Tyvex® body suits and latex gloves were worn during sampling and gloves were worn during all subsequent handling of samples. In the ESS sample, pH was slightly acidic (5.3) and the snowpack temperature was around freezing (< 0°C), whereas in LSS, pH was circumneutral (6.4) and the temperature was positive (around 1°C), indicating spring melt and the presence of liquid water within the snowpack. Meltwater samples were circumneutral, with a value of 6.8 for SSIM and 7.3 for MWR.

Microbial sample processing

Samples were processed immediately after collection in the field laboratory. Surface snow samples were left to melt at room temperature prior to being filtered onto sterile 0.22 µM 47 mm filters (Millipore) using a sterile filtration unit (Nalge Nunc International Corporation), while meltwater samples were filtered immediately. Filters were stored in sterile collection tubes at -20°C until further analysis. Procedural blanks were carried out by filtering Nanopure water (Siemens) using the same procedure.

DNA extraction

DNA was extracted using the protocol outlined in David *et al*. (2009). Briefly, filters were chopped and placed in a Fastprep® bead-beating tube (Lysing matrix E, MP Biomedicals) to which 1 mL of DNA extraction buffer (David et al. 2009) and 20 mg ml^{-1} lysing enzyme (*Trichoderma harzianum*, Sigma L1412) were added. Tubes were left at room temperature for 1 hour and then frozen at -20°C overnight. The frozen tubes were incubated at 65°C for 30 minutes and placed in a Fastprep® bead-beater (MP Biomedicals) set at speed 5.5 for 30 seconds. DNA was extracted from the water phase with an equal volume of chloroform:isoamyl alcohol (24:1) and precipitated with isopropanol.

DNA amplification

Since DNA yield was low (between 0.1 and 8 ng µl^{-1}), the DNA extracted from each sample was amplified using multiple displacement amplification with the illustra™ GenomiPhi™ V2 DNA

Amplification Kit (GE Healthcare). Amplification was carried out according to the manufacturer's instructions, except that twice the amount of DNA was used.

Clone library construction

Using universal 16S rRNA gene (*rrs*) primers pA (5'AGAGTTTGATCCTGGCTGAG3') and pH (5'AAGGAGGTGATCCAGCCGCA3') and the illustra Hot Start Mix RTG (GE Healthcare) PCR kit, four bacterial clone libraries were constructed: ESS, LSS, MWR and SSIM. The 25 µL volume PCR reaction mix contained 0.6 µM of each primer, 5 µl Genomiphi-amplified DNA or 5 µl sterile water for the negative control. The PCR conditions used were 5 minutes at 95°C, followed by 45 cycles of 45 seconds of denaturation at 95°C, 45 seconds of annealing at 56°C, and 45 seconds of elongation at 72°C. After a final 10-min extension at 72°C, PCR products were separated by 1%-agarose gel electrophoresis and purified using the NucleoSpin® Extract II kit (Clonetech). Amplicons were cloned into pCR4-TOPO using a TOPO-TA cloning kit (Invitrogen) as per the manufacturer's instructions. Ninety-six clones from each library were screened for the correct-sized insert (1.5 kb) by PCR amplification using M13F (5'GTAAAACGACGGCCAG3') and M13R (5'CAGGAAACAGCTATGA3') primers and the same protocol outlined above. Of these clones, a total of 192 PCR amplicons had the correct-sized insert and were sequenced in both directions (GATC Biotech). The sequencing run returned 155 sequences. Sequences were assembled using DNASTAR (DNASTAR®, Inc.) and average base pair coverage was 200. In the rare cases of base pair mismatch, chromatograms were consulted and the nucleotide was determined by two independent readers.

Clone library analysis

Sequences were aligned using the Clustal W alignment function in the BioEdit software package (http://www.mbio.ncsu.edu/BioEdit/bioedit.html). Distance matrices of the aligned sequences were generated for each library with the model F84 for nucleotide substitution using the DNADIST program in PHYLIP (version 3.6; Department of Genomic Sciences, University of Washington, Seattle, WA; http://evolution.genetics.washington.edu/phylip.html). Biodiversity indices for clone libraries were generated by running the outfiles through the DOTUR 1.53 program (Schloss and Handelsman 2005). Rarefaction curves (Hughes et al. 2001) were drawn for all libraries and the Shannon biodiversity index (Magurran 1988), Chao1 species richness index (Chao 1984), as well as clone library coverage based on Good's coverage for an OTU definition (Good 1953) were determined using 97% identity level. The phylogenetic diversity of all four libraries was compared using the ∫-LIBSHUFF (http://schloss.micro.umass.edu/software/slibshuff.html) (Schloss et al. 2004). The program uses the Cramér-von Mises test (Pettitt 1982) to determine significant differences (p<0.05 after applying the

Bonferroni correction) among libraries independent of arbitrary OTU similarity percentage cut-off values and is designed to compare undersampled 16S rRNA gene libraries.

Phylogenetic analysis

Sequences were checked for chimera with the CHIMERA detection program (http://rdp8.cme.msu.edu/cgis/chimera.cgi) (Cole et al. 2003). Database sequences with the highest degree of similarity were obtained with the NCBI BLAST-N program (http://www.ncbi.nih.gov/blast). The Ribosomal Database Project 10.0 Classifier tool (RDP, http://rdp.cme.msu.edu) was used to assign genus level groupings with 80% confidence (Cole et al. 2009). Phylogenetic trees were then generated using Clustal X (Thompson et al. 1997) to align sequences and run bootstrapping analysis (1000 repetitions) with the Jukes-Cantor distance correction (Jukes and Cantor 1969) and the Neighbour-Joining method (Saitou and Nei 1987). The trees were visualized with NjPLOT (Perrière and Gouy 1996).

Results

16S rRNA gene (rrs) clone libraries

Four 16S rRNA gene (*rrs*) clone libraries were constructed from the ESS, LSS, SSIM and MWR samples from which a total of 155 independent sequences were obtained. All PCR amplification controls performed in parallel to the assays were negative. Based on the coverage estimates (Table 1), about 50% and 80% of the diversity in the clone libraries for snow samples was sampled (ESS and LSS, respectively), whereas meltwater clone libraries had lower values (around 30%).

Table 1: Biodiversity indices and statistics among the snow and meltwater libraries.[a]

Library	Sample date	Individuals	OTUs	Chao1 (95% CI)	% coverage	H' (95%CI)
ESS	May 11th, 2007	40	29	59.67 (38.40-124.45)	50	3.01 (2.73-3.29)
LSS	June 7th, 2007	29	11	14.75 (11.64-33.02)	80	1.93 (1.54-2.30)
SSIM	June 10th, 2007	40	32	103.20 (57.71-232.43)	33	3.38 (3.15-3.62)
MWR	June 11th, 2007	46	39	152.20 (81.72-341.74)	26	3.59 (3.36-3.81)

[a] Individuals, number of clones sequenced; OTUs, number of operational taxonomic units observed; Chao1, Chao1 nonparametric richness estimate with 95% confidence interval in parentheses; % coverage, percent library coverage based on Good's estimate; H', Shannon-Weaver diversity index with 95% confidence interval in parentheses. ESS, LSS, SSIM and MWR correspond to the early spring snow library, the late spring snow library, the snow-soil interface meltwater library and the meltwater river library, respectively.

This is reflected in the rarefaction curves that begin to plateau for snow, but not for the meltwater libraries, which suggests that meltwater libraries were relatively undersampled (Figure 1). The MWR library had the highest community richness (Chao1, Table 1), followed by SSIM, ESS and LSS. The 95% confidence interval of the Chao1 estimator overlapped between the ESS and meltwater samples. The meltwater libraries also had the highest Shannon biodiversity indices, followed by the two snow-derived libraries (ESS and LSS). Based on the ∫-LIBSHUFF analyses, the ESS clone library is significantly different from the LSS clone library ($p<0.0001$). There was no significant difference between meltwater clone libraries ($p=0.6826$), however, the snow libraries differed significantly from the meltwater libraries ($p<0.0001$ for each pairwise comparison).

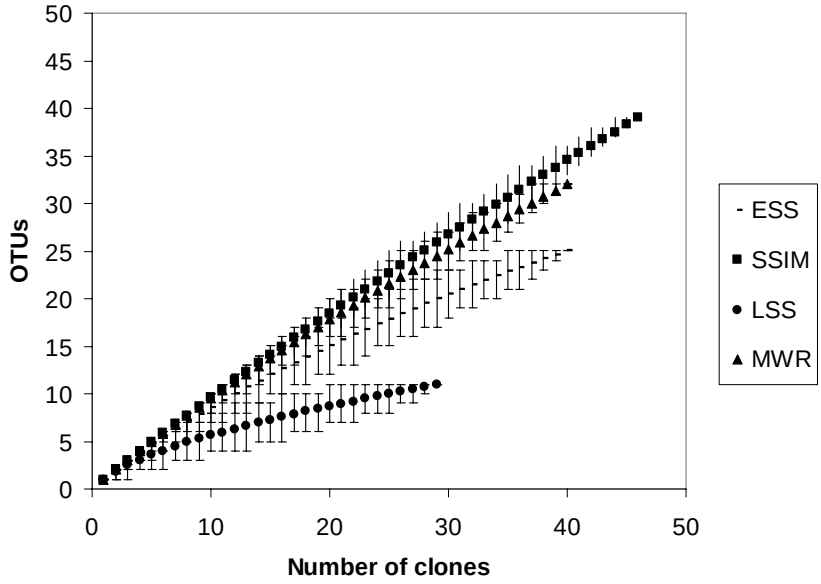

Figure 1: Rarefaction curves for each clone library showing the number of clones sampled versus the number of operational taxonomic units (OTUs) within each library. Error bars represent the 95% CI. ESS, LSS, SSIM and MWR correspond to the early spring snow library, the late spring snow library, the snow-soil interface meltwater library and the meltwater river library, respectively.

Sequence Analysis

The combined four clone libraries covered 19 different microbial classes, with *Betaproteobacteria* (21.3%) and *Sphingobacteria* (16.4%) dominating. *Flavobacteria* (9.0%), *Acidobacteria* (7.7%) and *Alphaproteobacteria* (6.5%) were the next most-represented classes, with the remaining classes each representing less than 5% of the total. The genus for almost half of the sequences could not be determined with 80% confidence using the classifier tool, however, common genera existed for ESS and MWR (*Curvibacter*), ESS and LSS (*Xiphinematobacteriaceae_genera_incertae_sedis*), MWR and SSIM (*Clostridium*, *Pedobacter*, *Niastella*, *Gp4*, *Gp6*) and for LSS and SSIM (*Flavobacterium*, *Polaromas*) (Figure 2 a, b, c).

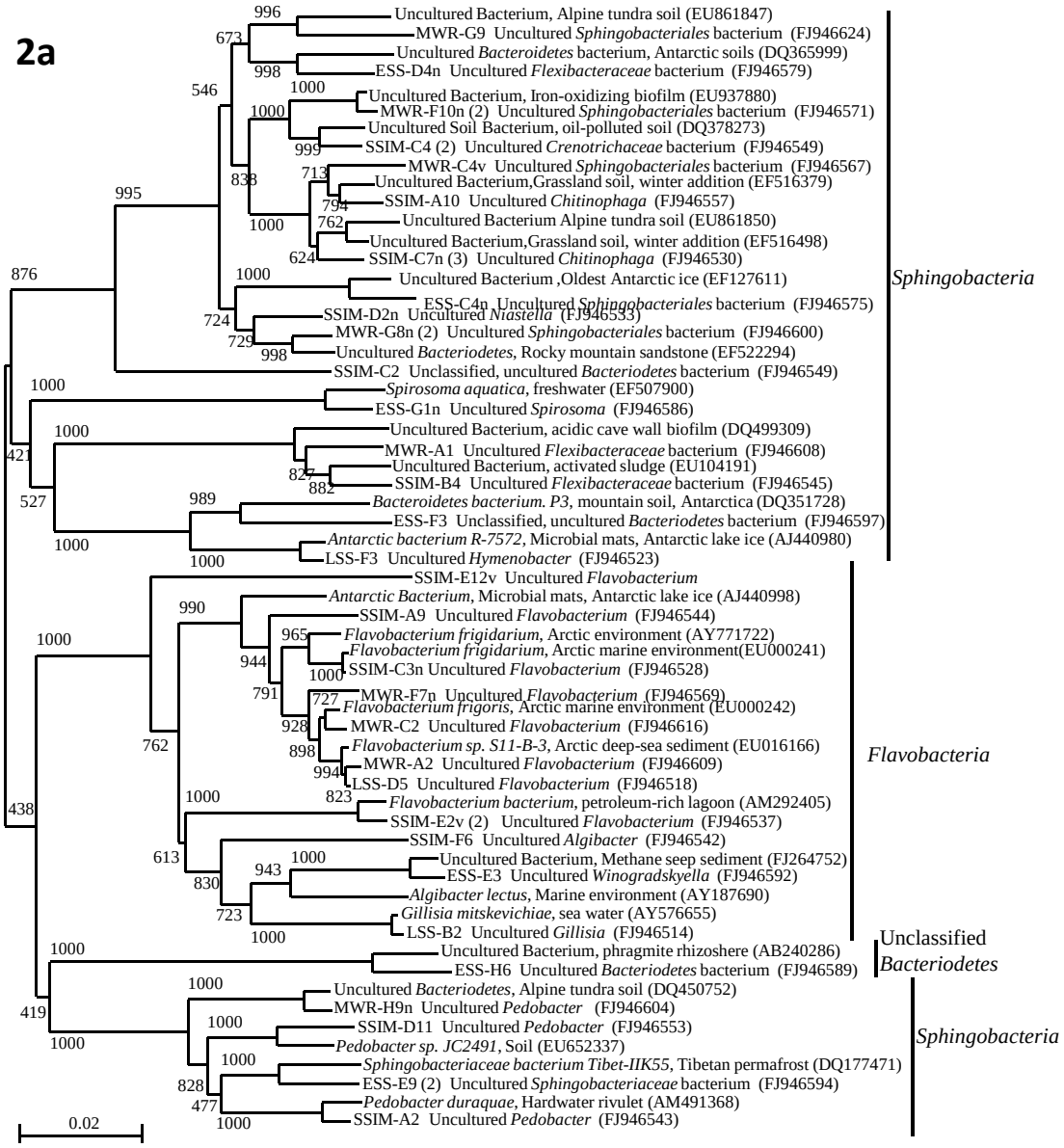

Figure 2: Neighbour-joining tree showing phylogenetic relationships among 16S rRNA gene (*rrs*) sequences from snow and meltwater libraries and their nearest neighbours in the GenBank database. One representative clone from each OTU is shown with the number of clones per OTU per library in parentheses followed by the taxonomic affiliation as determined using the RDP Classifier tool. The associated GenBank accession number is shown in parentheses. 2A is the first subtree showing *Bacteriodetes* (*Sphingobacteria* and *Flavobacteria*); 2B is the subtree showing Proteobacteria (*Alpha*, *Beta*, *Delta*, *Gamma*), *Nitrospira*, *Acidobacteria*, and *Chloroflexi*; 2C is the subtree showing *Cyanobacteria*, Chloroplast, *Firmicutes*, *Planctomycetes*, *Actinobacteria*, *Epsilonproteobacteria* and *Verrucomicrobia*, as well as other classes.

2b

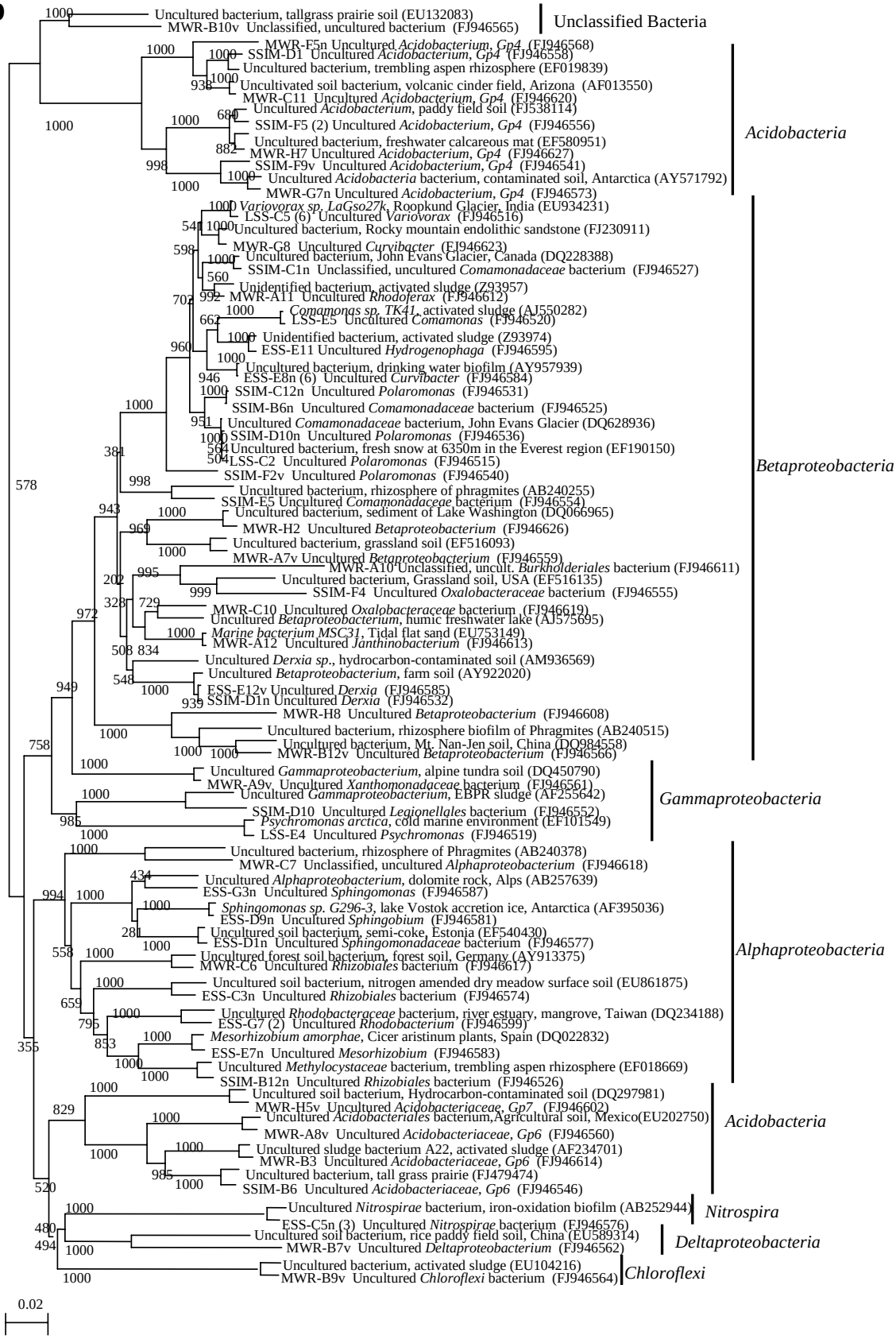
Uncultured bacterium, tallgrass prairie soil (EU132083)
MWR-B10v Unclassified, uncultured bacterium (FJ946565)
Unclassified Bacteria
MWR-F5n Uncultured Acidobacterium, Gp4 (FJ946568)
SSIM-D1 Uncultured Acidobacterium, Gp4 (FJ946558)
Uncultured bacterium, trembling aspen rhizosphere (EF019839)
Uncultivated soil bacterium, volcanic cinder field, Arizona (AF013550)
MWR-C11 Uncultured Acidobacterium, Gp4 (FJ946620)
Uncultured Acidobacterium, paddy field soil (FJ538114)
SSIM-F5 (2) Uncultured Acidobacterium, Gp4 (FJ946556)
Uncultured bacterium, freshwater calcareous mat (EF580951)
MWR-H7 Uncultured Acidobacterium, Gp4 (FJ946627)
SSIM-F9v Uncultured Acidobacterium, Gp4 (FJ946541)
Uncultured Acidobacteria bacterium, contaminated soil, Antarctica (AY571792)
MWR-G7n Uncultured Acidobacterium, Gp4 (FJ946573)
Acidobacteria
Variovorax sp. LaGso27k, Roopkund Glacier, India (EU934231)
LSS-C5 (6) Uncultured Variovorax (FJ946516)
Uncultured bacterium, Rocky mountain endolithic sandstone (FJ230911)
MWR-G8 Uncultured Curvibacter (FJ946623)
Uncultured bacterium, John Evans Glacier, Canada (DQ228388)
SSIM-C1n Unclassified, uncultured Comamonadaceae bacterium (FJ946527)
Unidentified bacterium, activated sludge (Z93957)
MWR-A11 Uncultured Rhodoferax (FJ946612)
Comamonas sp. TK41, activated sludge (AJ550282)
LSS-E5 Uncultured Comamonas (FJ946520)
Unidentified bacterium, activated sludge (Z93974)
ESS-E11 Uncultured Hydrogenophaga (FJ946595)
Uncultured bacterium, drinking water biofilm (AY957939)
ESS-E8n (6) Uncultured Curvibacter (FJ946584)
SSIM-C12n Uncultured Polaromonas (FJ946531)
SSIM-B6n Uncultured Comamonadaceae bacterium (FJ946525)
Uncultured Comamonadaceae bacterium, John Evans Glacier (DQ628936)
SSIM-D10n Uncultured Polaromonas (FJ946536)
Uncultured bacterium, fresh snow at 6350m in the Everest region (EF190150)
LSS-C2 Uncultured Polaromonas (FJ946515)
SSIM-F2v Uncultured Polaromonas (FJ946540)
Uncultured bacterium, rhizosphere of phragmites (AB240255)
SSIM-E5 Uncultured Comamonadaceae bacterium (FJ946554)
Uncultured bacterium, sediment of Lake Washington (DQ066965)
MWR-H2 Uncultured Betaproteobacterium (FJ946626)
Uncultured bacterium, grassland soil (EF516093)
MWR-A7v Uncultured Betaproteobacterium (FJ946559)
MWR-A10 Unclassified, uncult. Burkholderiales bacterium (FJ946611)
Uncultured bacterium, Grassland soil, USA (EF516135)
SSIM-F4 Uncultured Oxalobacteraceae bacterium (FJ946555)
MWR-C10 Uncultured Oxalobacteraceae bacterium (FJ946619)
Uncultured Betaproteobacterium, humic freshwater lake (AJ575695)
Marine bacterium MSC31, Tidal flat sand (EU753149)
MWR-A12 Uncultured Janthinobacterium (FJ946613)
Uncultured Derxia sp., hydrocarbon-contaminated soil (AM936569)
Uncultured Betaproteobacterium, farm soil (AY922020)
ESS-E12v Uncultured Derxia (FJ946585)
SSIM-D1n Uncultured Derxia (FJ946532)
MWR-H8 Uncultured Betaproteobacterium (FJ946608)
Uncultured bacterium, rhizosphere biofilm of Phragmites (AB240515)
Uncultured bacterium, Mt. Nan-Jen soil, China (DQ984558)
MWR-B12v Uncultured Betaproteobacterium (FJ946566)
Betaproteobacteria
Uncultured Gammaproteobacterium, alpine tundra soil (DQ450790)
MWR-A9v Uncultured Xanthomonadaceae bacterium (FJ946561)
Uncultured Gammaproteobacterium, EBPR sludge (AF255642)
SSIM-D10 Uncultured Legionellales bacterium (FJ946552)
Psychromonas arctica, cold marine environment (EF101549)
LSS-E4 Uncultured Psychromonas (FJ946519)
Gammaproteobacteria
Uncultured bacterium, rhizosphere of Phragmites (AB240378)
MWR-C7 Unclassified, uncultured Alphaproteobacterium (FJ946618)
Uncultured Alphaproteobacterium, dolomite rock, Alps (AB257639)
ESS-G3n Uncultured Sphingomonas (FJ946587)
Sphingomonas sp. G296-3, lake Vostok accretion ice, Antarctica (AF395036)
ESS-D9n Uncultured Sphingobium (FJ946581)
Uncultured soil bacterium, semi-coke, Estonia (EF540430)
ESS-D1n Uncultured Sphingomonadaceae bacterium (FJ946577)
Uncultured forest soil bacterium, forest soil, Germany (AY913375)
MWR-C6 Uncultured Rhizobiales bacterium (FJ946617)
Uncultured soil bacterium, nitrogen amended dry meadow surface soil (EU861875)
ESS-C3n Uncultured Rhizobiales bacterium (FJ946574)
Uncultured Rhodobacteraceae bacterium, river estuary, mangrove, Taiwan (DQ234188)
ESS-G7 (2) Uncultured Rhodobacterium (FJ946599)
Mesorhizobium amorphae, Cicer aristinum plants, Spain (DQ022832)
ESS-E7n Uncultured Mesorhizobium (FJ946583)
Uncultured Methylocystaceae bacterium, trembling aspen rhizosphere (EF018669)
SSIM-B12n Uncultured Rhizobiales bacterium (FJ946526)
Alphaproteobacteria
Uncultured soil bacterium, Hydrocarbon-contaminated soil (DQ297981)
MWR-H5v Uncultured Acidobacteriaceae, Gp7 (FJ946602)
Uncultured Acidobacteriales bacterium,Agricultural soil, Mexico(EU202750)
MWR-A8v Uncultured Acidobacteriaceae, Gp6 (FJ946560)
Uncultured sludge bacterium A22, activated sludge (AF234701)
MWR-B3 Uncultured Acidobacteriaceae, Gp6 (FJ946614)
Uncultured bacterium, tall grass prairie (FJ479474)
SSIM-B6 Uncultured Acidobacteriaceae, Gp6 (FJ946546)
Acidobacteria
Uncultured Nitrospirae bacterium, iron-oxidation biofilm (AB252944)
ESS-C5n (3) Uncultured Nitrospirae bacterium (FJ946576)
Nitrospira
Uncultured soil bacterium, rice paddy field soil, China (EU589314)
MWR-B7v Uncultured Deltaproteobacterium (FJ946562)
Deltaproteobacteria
Uncultured bacterium, activated sludge (EU104216)
MWR-B9v Uncultured Chloroflexi bacterium (FJ946564)
Chloroflexi
0.02

2c

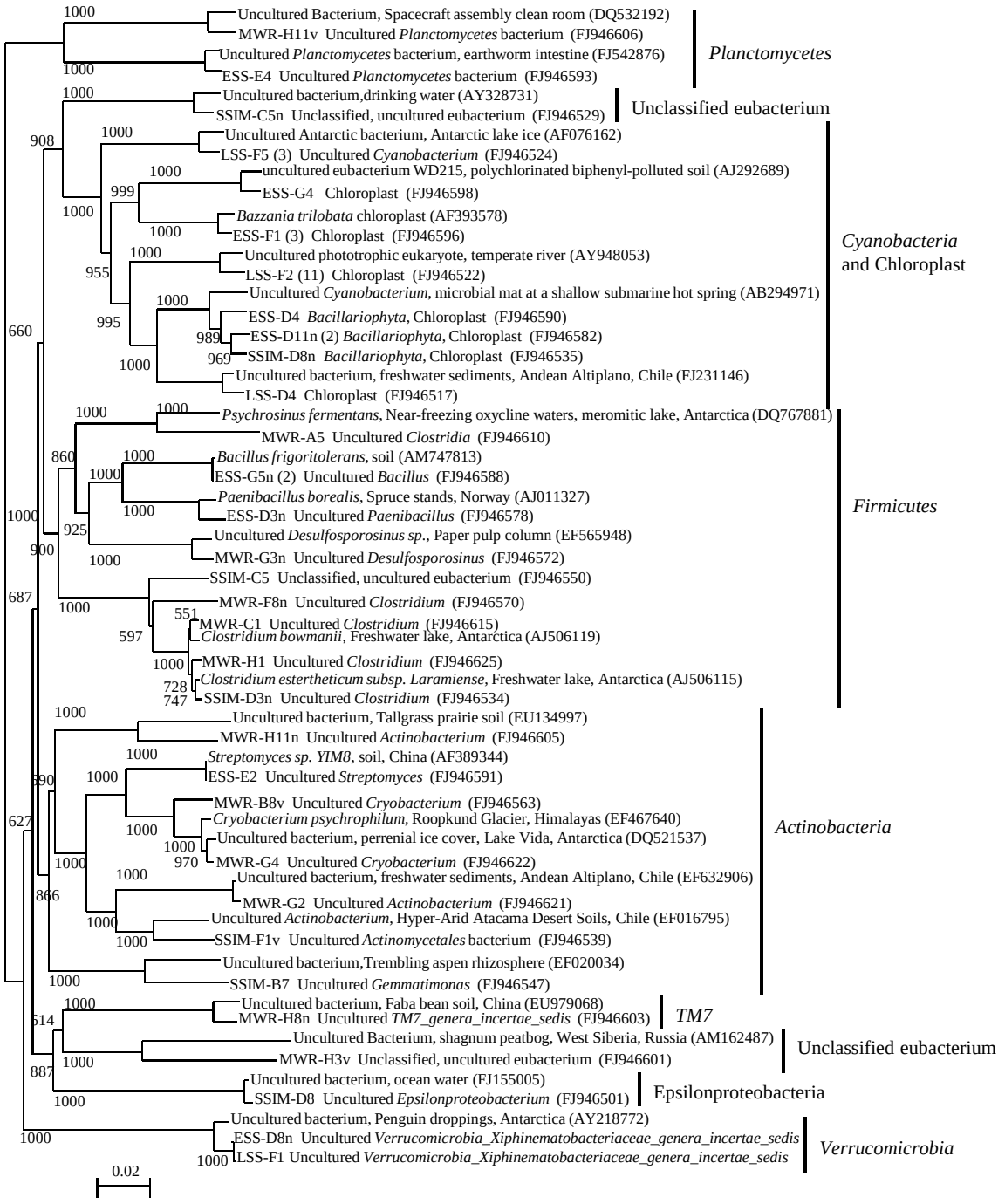

The ESS library sequences contained 12 bacteria classes and one unclassified sequence. It was dominated by *Betaproteobacteria* (20.0%), *Alphaproteobacteria* (17.5%), *Sphingobacteria* (15.0%) and *Bacilli* (7.5%). *Flavobacteria* and *Cyanobacteria* comprised only a small percentage of the library (5.0% each) and some sequences related to eukaryote chloroplasts were also identified (Figure 2). Most members of *Alphaproteobacteria*, *Bacilli* and *Sphingobacteria* are closely related to

environmental clone sequences from alpine/polar environments. The LSS library was dominated by clones related to phototrophic eukaryotes (37.9%). A total of six different bacterial classes were represented, with *Betaproteobacteria* (27.6%) dominating, followed by *Cyanobacteria* (13.8%) and *Flavobacteria* (10.3%) (Figure 2). A total of 12 classes were represented in the SSIM library, which was dominated by *Sphingobacteria* (25.0%), *Betaproteobacteria* (20.0%), *Flavobacteria* (15.0%) and *Acidobacteria* (12.5%). Half of the *Betaproteobacteria* had members with sequences nearest to environmental clone sequences retrieved from polar environments and snow (Figure 2) and 60% of the *Flavobacteria* clustered with clone sequences from Arctic marine environments. The MWR library was dominated by *Betaproteobacteria* (19.6%), followed by *Sphingobacteria* (17.4%), *Acidobacteria* (15.2%) and *Clostridia* (10.9%). All *Flavobacteria* sequences had nearest neighbours that originated from Arctic marine environments, while 75% of *Clostridia* sequences were nearest to environmental clone sequences from alpine/polar environments (Figure 2).

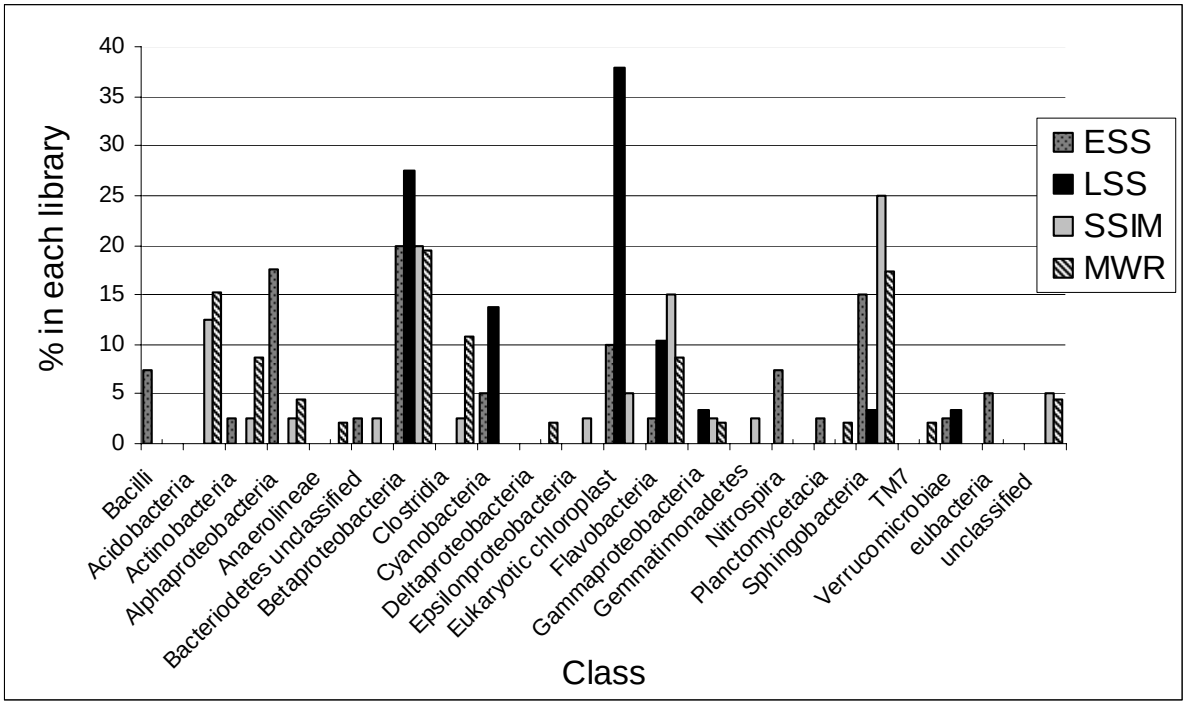

Figure 3: Class distribution in each of the four clone libraries. The bars represent the percentage of each class in each library. ESS, LSS, SSIM and MWR correspond to the early spring snow library, the late spring snow library, the snow-soil interface meltwater library and the meltwater river library, respectively.

Common classes among all clone libraries were *Betaproteobacteria*, *Sphingobacteria* and *Flavobacteria*. Classes exclusive to snow libraries were *Verrucomicrobia* and *Cyanobacteria*, while *Acidobacteria* and *Clostridia* were limited to meltwater clone libraries (Figure 3). *Bacilli* and *Nitrospira* were only found in the ESS library, which also had the highest proportion of

Alphaproteobacteria amongst all libraries. The LSS library contained no *Alphaproteobacteria* or *Actinobacteria*, unlike the other three libraries. The MWR library had a higher proportion of clones that were from the *Clostridia* class than the other libraries and no phototrophic organisms were present, while the SSIM library had the highest proportion of *Flavobacteria* (Figure 3).

Clone sequences were also grouped based on the geographical origin of their nearest neighbour using the NCBI BLAST-N results. Sequences with nearest neighbours that were retrieved from alpine/polar environments (Antarctica/Arctic –soil, water, sediments and non-polar high altitude sites) represented 34.2% of all sequences, followed by sequences similar to isolates from soil (21.9%), aquatic (29.0%) and contaminated (11.0%) environments (Table 2). In the ESS library, sequences with nearest neighbours from aquatic sites accounted for 47.5% of the library, followed by alpine/polar sites (25.0%), soil (12.5%) and contaminated environments (10.0%). Almost all LSS sequences had nearest neighbours that were from alpine/polar (55.2%) or aquatic (41.4%) sites. The SSIM library was dominated by sequences with nearest neighbours from soil (32.5%) followed by alpine/polar and aquatic (25.0% and 22.5% respectively) and contaminated environments (20.0%). The nearest neighbours of the sequences in the MWR library were mainly from alpine/polar regions (37.0%) and soil (32.6%) followed by aquatic environments (10.9%) (Table 2).

Table 2: Distribution of clones in each of the four libraries based on nearest-neighbour isolation environment.[a]

Nearest neighbour environment	Total clones	ESS clones	LSS clones	SSIM clones	MWR clones
Alpine/Polar	34.2	25.0	55.2	25.0	37.0
Aquatic	29.0	47.5	41.4	22.5	10.9
Contaminated	11.0	10.0	3.4	20.0	8.7
Other	3.9	5.0	0.0	0.0	10.9
Soil	21.9	12.5	0.0	32.5	32.6

[a] Values are in percent of total. ESS, LSS, SSIM and MWR correspond to the early spring snow library, the late spring snow library, the snow-soil interface meltwater library and the meltwater river library, respectively.

Discussion

Clone library analysis

Arctic snow and meltwater are highly diverse systems. The fact that the rarefaction curves fail to plateau for meltwater libraries and only begin to plateau for early spring snow, suggests that further sampling or clone selection would reveal even higher diversity at the species level (Figure 1) and that a large amount of the bacterial diversity still remains to be sampled from these environments. Based on the ∫-LIBSHUFF analyses, designed to analyze undersampled libraries, snow bacterial communities (ESS and LSS) were significantly different (p<0.0001) and snow and meltwater communities also differed significantly (p<0.0001). Another estimator, the Chao1 nonparametric richness estimator, can be used as an alternative to the ∫-LIBSHUFF for comparing undersampled libraries since it approaches a stable maximum before rarefaction curves plateau (Kemp and Aller 2004). Although there is some overlap in the 95% confidence interval of the Chao1 estimator between the ESS and meltwater libraries (Table 1), no overlap is observed with the LSS library, further supporting the significance of the difference.

The observed differences in the retrieved sequences from the different libraries could be due to the seasonal changes in the respective microbial communities at the time of sampling, since the snow environment at the time of sampling differed in terms of temperature and pH. Another factor may also be atmospheric deposition. The relatively large percentage of cloned sequences with nearest neighbours isolated from the soil (12.5%) and contaminated environments (10.0%) in the ESS library might implicate atmospheric deposition of pollutants and/or microbes. Liu et al. (2006) also reported the presence of bacteria related to isolates from activated sludge in snow from glaciers in the Tibetan Plateau at altitudes above 5000 m that they suggested originated from atmospheric deposition since bacteria attached to aeolian dust can be transported to glaciers (Yao et al. 2006) and microbial concentrations have been correlated to mineral particle density in the snow (Segawa et al. 2005). Whether these bacteria are then able to colonize and multiply in the snow depends on their ability to survive the harsh surface conditions, i.e. high UV radiation, temperature extremes, variable wind ventilation and variable (low) organic matter deposition (Jones 1999; Kuhn 2001; Hodson et al. 2008). The *Sphingobacteria* in the ESS library cluster with bacteria isolated from either Antarctica or tundra soils and are probably able to grow in the snow, since certain members are psychrotrophic and produce pigments that may protect them from solar radiation (Chauhan and Shivaji 1994).

We observed a decrease in biodiversity in the LSS library as compared to the ESS library and an increase in clones with nearest neighbours from polar/alpine environments and with DNA belonging to algae and *Cyanobacteria*. While it is possible that the proximity of the fjord to the sampling site

may have influenced species composition in the LSS library due to sea spray, it is unlikely since most of the sequences clustered with sequences retrieved from freshwater sources (lakes or glaciers, Figure 2). The observed decrease in biodiversity in the LSS clone library may be due to meltwater washout. A decrease in microbial biomass and mineral particle concentration in mid-latitude mountain summer snow (June and July) due to meltwater washout was reported by Segawa et al. (2005), and meltwater has also been shown to washout nutrients (Kuhn 2001). Since meltwater integrates what is washed out of the snow, it would be expected to incorporate most species/classes found within the seasonal snowpack, with the exception of those able to attach themselves or form biofilms, thus reducing their mobility. The meltwater libraries sequenced contained all of the bacterial classes found in the ESS and LSS libraries with the exception of *Bacilli*, *Nitrospira*, *Verrucomicrobia* and *Cyanobacteria*.

Since meltwater also drains the soil, it would be expected that its community structure reflects this influence. For both meltwater libraries, over a third of the sequences had nearest neighbours isolated from the soil. Certain classes, such as *Acidobacteria* and *Clostridia*, were found in meltwater, but not snow, libraries. *Acidobacteria* are commonly isolated from soils (Jones et al. 2009), while *Clostridia* are anaerobic bacteria commonly isolated from Antarctic soils and anaerobic microbial mats (Miwa 1975; Spring et al. 2003; Stackebrandt et al. 2004).

Snow and meltwater diversity

Meltwater clone libraries were more diverse than snow libraries, with Shannon biodiversity indices between 3.38 and 3.59. These values are higher than those reported for meltwater libraries collected on the northern slope of Mount Everest: between 0.6199 and 2.398 (Liu et al. 2006). Bacteria in the Everest region were probably exposed to lower oxygen concentrations, stronger radiation and less nutrients than those from the Svalbard region, thus, the increased stress might have limited biodiversity. In the Everest meltwater clone libraries, the dominant groups were the *Bacteroidetes* group and *Betaproteobacteria*, similar to those found in this study. We also identified several *Actinobacteria* strains, which were absent in the Everest libraries. Cheng and Foght (2007) reported higher biodiversity indices (3.143-3.713) for libraries constructed from subglacial environments in the high Arctic, with *Bacteriodetes*, *Betaproteobacteria* and *Actinobacteria* dominating, and Skidmore et al. (2005) found mainly *Betaproteobacteria* and some CFB in Canadian subglacial environments (Skidmore et al. 2005; Cheng and Foght 2007).

In contrast, clone libraries from snow samples from four different sites around Mount Everest had relatively high Shannon biodiversity indices, between 2.2 and 4 (Liu et al. 2009). Our snow libraries fell within this range (ESS: 3.01, LSS: 1.93). In Everest snow libraries, *Gammaproteobacteria* were

dominant, followed by *Alphaproteobacteria* and *Actinobacteria*, unlike in our snow libraries where *Betaproteobacteria* dominated (Figure 3). *Actinobacteria* and *Alphaproteobacteria* were only present in the ESS library, while only one *Gammaproteobacteria* clone was sequenced in the LSS library. In a study on the seasonal shifts in microbial populations in mid-altitude snowpacks, Segawa et al. (2005) reported that a large portion of their library was composed of *Betaproteobacteria* (Segawa et al. 2005). They also found a higher percentage of *Actinobacteria*, *Bacillus* and *Alphaproteobacteria* in the early spring (March) library than in the summer (June and August) libraries, similar to the shift we observed in our snow libraries. The biodiversity indices of our snow libraries are comprised between those of Arctic pack ice and Arctic microbial mats (0.812-1.291 and 3.50– 4.41, respectively, (Brinkmeyer et al. 2003).

Conclusion

The snowpack is a diverse habitat that remains largely unexplored as research efforts have focused on glacier systems and ice. Many studies report the occurrence of related phylotypes from geographically diverse, but predominantly cold environments, and the community structure has common populations in different cryohabitats. However, the seasonal evolution of the microbial community and the physiological state of the organisms within the snowpack are topics that remain to be addressed. Our understanding of the microbial community needs to be expanded and functional analyses will determine both the effect of season on microbial activity as well as the extent that these communities influence snowpack dynamics – such as nutrient cycling, gas transfer and environmental contaminant cycling and downstream ecosystem transfer.

Acknowledgements

The authors would like to acknowledge the contribution of Cédric Couret and the entire AWIPEV staff, Xavier Faïn and Jean Philippe Balestrieri. This research was supported by grants from EC2CO/CYTRIX (Programme National INSU), LEFE, IPEV CHIMERPOL program (399) and CL would like to acknowledge the FQRNT (le Fonds Québécois de la Recherche sur la Nature et les Technologies) for a PhD research fellowship.

References

Amato P et al. (2007) Bacterial characterization of the snow cover at Spitzberg, Svalbard. Fems Microbiology Ecology 59:255-264

Barkay T, Poulain AJ (2007) Mercury (micro)biogeochemistry in polar environments. FEMS Microbiology Ecology 59:232-241

Brinkmeyer R, Knittel K, Jurgens J, Weyland H, Amann R, Helmke E (2003) Diversity and structure of bacterial communities in Arctic versus Antarctic pack ice. Applied and Environmental Microbiology 69:6610-6619

Carpenter EJ, Lin S, Capone DG (2000) Bacterial activity in South Pole snow. Applied and Environmental Microbiology 66:4514-4517

Chao A (1984) Non-parametric estimation of the number of classes in apopulation. Scandinavian Journal of Statistics 11:265-270

Chauhan S, Shivaji S (1994) Growth and pigmentation in Sphingobacterium antarcticus, a psychrotrophic bacterium from Antarctica. Polar Biology 14:31-36

Cheng SM, Foght JM (2007) Cultivation-independent and -dependent characterization of Bacteria resident beneath John Evans Glacier. FEMS Microbiology Ecology 59:318-330

Christner BC, Mosley-Thompson E, Thompson LG, Reeve JN (2001) Isolation of bacteria and 16S rDNAs from Lake Vostok accretion ice. Environmental Microbiology 3:570-577

Christner BC, Mosley-Thompson E, Thompson LG, Zagorodnov VS, Sandman K, Reeve JN (2000) Recovery and Identification of Viable Bacteria Immured in Glacial Ice. Icarus 144:479-485

Cole JR et al. (2003) The Ribosomal Database Project (RDP-II): previewing a new autoaligner that allows regular updates and the new prokaryotic taxonomy. Nucleic Acids Res 31:442-443

Cole JR et al. (2009) The Ribosomal Database Project: improved alignments and new tools for rRNA analysis. Nucleic Acids Research 37, :Database Issue D141–D145 doi:110.1093/nar/gkn1879

David MM, Mesle M, Malandain C, Cohen D, Vogel TM (2009) Molecular Biology-based strategy for site remediation. Environmental Science and Technology Submitted

Good IL (1953) The population frequencies of species and the estimation of population parameters. Biometrika 40:237-264

Hodson A et al. (2008) Glacial Ecosystems. Ecological Monographs 78:41-67

Hoham RW (1975) Optimal temperatures and temperature ranges for growth of snow algae. Arct. Alp. Res. 7:13-24

Hoham RW, Duval B (2001) Microbial ecology of snow and freshwater ice with emphasis on snow algae In: Jones HG, Pomeroy JW, Walker DA, Hoham RW (eds) Snow ecology: an interdisciplinary examination of snow-covered ecosystems. Cambridge University Press, Cambridge, pp 168–228

Hughes JB, Hellmann JJ, Ricketts TH, Bohannan BJM (2001) Counting the uncountable: statistical approaches to estimating microbial diversity. Applied and Environmental Microbiology 67:4399–4406

Jones HG (1999) The ecology of snow-covered systems: a brief overview of nutrient cycling and life in the cold. Hydrological Processes 13:2135–2147

Jones RT, Robeson MS, Lauber CL, Hamady M, Knight R, Fierer N (2009) A comprehensive survey of soil acidobacterial diversity using pyrosequencing and clone library analyses. Isme J 3:442-453

Jukes TH, Cantor CR (1969) Evolution of protein molecules. In: Munro HN (ed) Mammalian protein metabolism. Academic Press, New York, pp 21-132

Kemp PF, Aller JY (2004) Bacterial diversity in aquatic and other environments: what 16S rDNA libraries can tell us. FEMS Microbiology Ecology 47:161-177

Kuhn M (2001) The nutrient cycle through snow and ice, a review. Aquatic Science 63:150-167

Liu Y et al. (2009) Bacterial diversity in the snow over Tibetan Plateau Glaciers. Extremophiles 13:89-99

Liu Y, Yao T, Jiao N, Kang S, Zeng Y, Huang S (2006) Microbial community structure in moraine lakes and glacial meltwaters, Mount Everest. FEMS Microbiology Letters 265:98-105

Magurran AE (1988) Ecological diversity and its measurement. Princeton University Press, Princeton, N.J.

Miteva V (2008) Bacteria in Snow and Glacier Ice. In: Margesin Rea (ed) Psychrophiles: from Biodiversity to Biotechnology Springer-Verlag, Berlin Heidelberg, pp 31-47

Miwa T (1975) Clostridia in soil of the Antarctica. Japanese Journal of Medical Science & Biology 28:201-213

Perrière G, Gouy M (1996) WWW-Query: An on-line retrieval system for biological sequence banks. Biochimie 78:364-369

Pettitt AN (1982) Cramér-von Mises statistic. In: Kotz S, Johnson NL, Read CB (eds) Encyclopedia of statistical sciences. Wiley, New York, pp 220-221

Poulain AJ et al. (2007) Potential for mercury reduction by microbes in the high arctic. Applied and Environmental Microbiology 73:2230-2238

Priscu JC, Christner BC (2004) Earth's icy biosphere. In: Bull AT (ed) Microbial Diversity and Bioprospecting. American Society for Microbiology, Washington, D.C., pp 130-145

Saitou N, Nei M (1987) The neighbor-joining method: a new method for reconstructing phylogenetic trees. Molecular Biology and Evolution 4:406-425

Schloss PD, Handelsman J (2005) Introducing DOTUR, a computer program for defining operational taxonomic units and estimating species richness. Applied and Environmental Microbiology 71:1501-1506

Schloss PD, Larget BR, Handelsman J (2004) Integration of microbial ecology and statistics: a test to compare gene libraries. Applied and Environmental Microbiology 70:5485-5492

Segawa T, Miyamoto K, Ushida K, Agata K, Okada N, Kohshima S (2005) Seasonal change in bacterial flora and biomass in mountain snow from the Tateyama Mountains, Japan, analyzed by 16S rRNA gene sequencing and real-time PCR. Applied and Environmental Microbiology 71:123-130

Skidmore M, Anderson SP, Sharp M, Foght J, Lanoil BD (2005) Comparison of microbial community compositions of two subglacial environments reveals a possible role for microbes in chemical weathering processes. Applied and Environmental Microbiology 71:6986-6997

Skidmore ML, Foght JM, Sharp MJ (2000) Microbial life beneath a high arctic glacier. Applied and Environmental Microbiology 66:3214-3220

Spring S, Merkhoffer B, Weiss N, Kroppenstedt RM, Hippe H, Stackebrandt E (2003) Characterization of novel psychrophilic clostridia from an Antarctic microbial mat: description of *Clostridium frigoris* sp. nov., *Clostridium lacusfryxellense* sp. nov., *Clostridium bowmanii* sp. nov. and *Clostridium psychrophilum* sp. nov. and reclassification of *Clostridium laramiense* as *Clostridium estertheticum subsp. laramiense subsp. nov*. International Journal of Systematic and Evolutionary Microbiology 53:1019-1029

Stackebrandt E, Brambilla E, Cousin S, Dirks W, Pukall R (2004) Culture-independent analysis of bacterial species from an anaerobic mat from Lake Fryxell, Antarctica: prokaryotic diversity revisited. Cellular and Molecular Biology (Noisy-le-grand) 50:517-524

Stibal M, Elster J, Sabacka M, Kastovska K (2007) Seasonal and diel changes in photosynthetic activity of the snow alga *Chlamydomonas nivalis* (*Chlorophyceae*) from Svalbard determined by pulse amplitude modulation fluorometry. FEMS Microbiology Ecology 59:265-273

Thomas WH, Duval B (1995) Sierra Nevada, California, USA, snow algae: snow albedo changes, algal-bacterial interrelationships, and ultraviolet radiation effects. Arctic, Antarctic, and Alpine Research 27:389–399

Thompson JD, Gibson TJ, Plewniak F, Jeanmougin F, Higgins DG (1997) The ClustalX windows interface: flexible strategies for multiple sequence alignment aided by quality analysis tools. Nucleic Acids Research 24:4876-4882

Tranter M, Sharp MJ, Lamb HR, Brown GH, Hubbard BP, Willis IC (2002) Geochemical weathering at the bed of Haut Glacier d'Arolla, Switzerland—a new model. Hydrological Processes 16:959-993

Ward DM, Weller R, Bateson MM (1990) 16S rRNA sequences reveal numerous uncultured microorganisms in a natural community. Nature 345:63-65

Yao TD, Xiang SR, Zhang XJ, Wang NL, Wang YQ (2006) Microorganisms in the Malan ice core and their relation to climatic and environmental changes. Global Biogeochemical Cycles 20:GB1004. doi:1010.1029/2004GB002424

CHAPTER 3: DEPOSITION OF MERCURY SPECIES IN THE NY-ÅLESUND AREA (79°N) AND THEIR TRANSFER DURING SNOWMELT

Manuscript accepted for publication in Environmental Science and Technology

Aurélien Dommergue[1], Catherine Larose[1,2], Xavier Faïn[3], Olivier Clarisse[4,5], Delphine Foucher[4], Holger Hintelmann[4], Dominique Schneider[2] and Christophe P Ferrari[1]

[1] Université Joseph Fourier – Grenoble 1 / CNRS, LGGE
54 rue Molière BP56
38402 Saint Martin d'Hères – France

[2]Laboratoire Adaptation et Pathogénie des Micro-organismes, Université Joseph Fourier – Grenoble 1,
BP 170, F-38042 Grenoble cedex – France

[3]Division of Atmospheric Sciences, Desert Research Institute, 2215 Raggio Parkway, Reno, NV, USA

[4]Department of Chemistry- Trent University
1600 West Bank Drive
Peterborough ON K9J 7B8 – Canada

[5]Now at Département de chimie et biochimie- Université de Moncton
Moncton, N.-B. E1A 3E9 – Canada

[6] CNRS UMR 5163

Abstract

Arctic snowpacks are often considered as temporary reservoirs for atmospheric mercury deposited during springtime events. The fate of deposited species is of utmost importance since melt leads to the transfer of contaminants to snowmelt-fed ecosystems. Here we examined the deposition, fate and transfer of mercury (Hg) species (Total Hg (THg) and methylmercury) in an arctic environment from the beginning of mass-deposition of Hg during atmospheric mercury depletion events (AMDEs) up until full snowmelt. We estimated that AMDEs deposited important amounts of THg onto the snow surface with concentrations up to 373 ng/L and estimated deposition fluxes of 200-2160 ng/m². Most of the deposited Hg is re-emitted to the atmosphere via photochemical reactions. However, a fraction remained stored in the snow and we estimated that the spring melt contributed to an input of 1.5-3.6 kg/year of THg to the fjord (*i.e.* 8-21% of the fjord's THg content). A monitoring of methylmercury in snow using DGT sensors showed that atmospheric sources of methylmercury and in situ production may exist.

Introduction

Mercury (Hg) is a toxic metal that can be transported far from its emission sources and contaminate remote areas. Anthropogenic sources of mercury (combustion, chemical industry and mining) have significantly decreased since the 1970s in the western countries of the northern hemisphere, but

these declines are today certainly offset by increases in Asia (1). Whether the variations of sources have affected background concentrations of gaseous elemental mercury (Hg°), the predominant form of Hg in the atmosphere, is under discussion (2-4). Nowadays Hg° averages 1.5-1.7 ng/m^3 in the northern hemisphere. Despite the effort made to reduce anthropogenic emissions, levels of oxidized species in environmental matrixes remain elevated. Some studies even reveal an increase in Hg levels that can be seen in many species all over the planet including some arctic animals (5, 6). Of particular concern is the exposure to methylmercury (MeHg), a powerful neurotoxin that biomagnifies in the food chain and constitutes the majority of the Hg burden in fish and marine mammal tissues (7).

The Hg issue in the Arctic generates interest in scientific communities (*e.g.* (8)) due in part to wildlife and human health implications. Additionally, the reasons for elevated Hg levels in the Arctic have yet to be elucidated. Historically, the discovery made in Alert (Canada) in 1995 (9) that revealed that Hg° is oxidized and deposited onto polar environmental surfaces more rapidly than anywhere else due to a phenomenon called Atmospheric Mercury Depletion Events (AMDEs) sparked considerable interest. Numerous studies suggest that sea-salt is involved in a photochemically-initiated and autocatalytic release of reactive halogen (Br and BrO radicals). The conversion of Hg° by bromine radicals is certainly fast, even if the kinetics are poorly understood, and leads to the formation of divalent species of Hg. These species are more water-soluble and reactive and can thus be deposited by wet and dry processes onto surfaces. Significant increases in oxidized levels of Hg have been measured in the snow following AMDEs and a fraction of Hg has been reported as bioavailable (10). Yet the link to the methylation of Hg in this system is still unknown.

The AMDEs were thought to be a dominant source of contamination to arctic ecosystems. Yet, an increasing number of studies seem to suggest that their contribution is not as important as previously reported. Among these, several studies since 2002 have shown that a part of deposited mercury can be reemitted back to the atmosphere by photo-mediated reduction processes (*e.g.*11) thus adding uncertainty to the net deposition. A recent report (12) related to the Hg mass balance in the Arctic even argues that the atmospheric input might not be as high as expected. Besides the ambiguous role of AMDEs in the contamination of the Arctic, the mechanisms that produce MeHg in these cold environments are to date unresolved although many pathways have been suggested (13).

In order to fill some of the gaps highlighted in the literature and the still open questions, longer data sets, as well as new analytical tools are required. The objective of the following study is to better constrain the fate of Hg once in the snowpack and its transfer to other reservoirs. For this purpose, we monitored mercury changes in the snow reservoir at a high temporal resolution, together with measurements in surrounding glaciers and in many meltwater streams. Along with THg,

methylmercury concentrations are reported. The study took place at the onset of AMDEs to the snowmelt of a seasonal snowpack in an arctic coastal location near Ny-Ålesund, Svalbard (Norway).

Material and Methods

Field campaign and study site

The spring research campaign was held between April 16th, 2007 and June 20th, 2007 at Ny-Ålesund in the Spitsbergen Island of Svalbard, Norway (78°56'N, 11°52'E). The field site, a 50 m^2 perimeter with restricted access (to reduce contamination from human sources), is located along the south coast of the Kongsfjorden, which is oriented SE-NW and open to the sea on the west side (Figure S1 in Supporting Information). The Kongsfjorden was free of sea ice throughout the campaign.

Atmospheric Hg° measurements

Atmospheric Hg° was measured two meters above snow surface using a Tekran model 2537A vapor-phase Hg analyzer. Due to logistical problems, measurements were available at our field site from April 26th. Data from the 16th to the 26th (courtesy of NILU) were at Zeppelin air monitoring station (474 meters above sea level). An international study has already compared both measurement sites (14). Snow-to-air fluxes of Hg° were also continuously measured from April 26 in 10 min intervals using a dynamic flux chamber (15). Detailed characteristics and testing are available in the Supporting Information.

Snow and seawater sampling

Snow was sampled daily using clean sampling techniques and was collected in acid-washed 250 mL borosilicate glass bottles. Snow samples were also collected from pits dug in the surrounding glaciers (Figure S1 in Supporting Information), Kongsvegen (N78°45.29, E13°20.20, 670 m) Austre Lovénbreen (N78°51.79, E12°08.03, 472 m) and Holtedahlfonna (N79°08.17 E13°16.12, 1173 m). All snow samples were maintained frozen in the dark until analysis. Surface seawater was sampled at 200 m from the snow field site every 5 days. The sampling point was identified with a buoy and was at a distance of 50 m from the shore.

Meltwater sampling

Meltwater was sampled using two different methods. The first consisted of a Teflon-coated v-shaped sampler that was placed at about 10 cm under the surface of the snow pack. This surface meltwater runoff was collected in clean 250 mL borosilicate glass bottles. Snowpack meltwater was collected in sterile sampling bags at the snow-soil interface as small rivers formed. Both collection methods were

tested by multiple blanks measurements. THg concentration was measured constantly below detection limit in MQ water sampled on our Teflon-coated v-shaped sampler as well as in sterile sampling bags.

Analytical Techniques

THg determination

THg was measured in the field with a Tekran model 2600 using USEPA method 1631 revision E. All samples were analyzed in triplicate. THg concentrations are presented as mean ± 1 stdv. The limit of quantification calculated as 10 times the standard deviation of a set of 10 blanks was 0.3 ng L^{-1}. Detection Limit (DL) is about 0.1 ng L^{-1}. Analytical information is available in Supporting Information.

Methylmercury determination using DGT (Diffusive Gradient in Thin Films)

Developed initially as a monitoring tool for MeHg in the water column (16, 17) or in sediment pore water DGT technique was used for the first time in the snow and melting snow. 3 DGT units were deployed every five days in the snow pack below the surface. DGTs were also deployed in triplicate for 5 days at a depth of 1 m in the nearby fjord.

DGT principle is based on the diffusion of the dissolved species through a gel and their subsequent accumulation on an ion exchange resin. After extraction and elution in the lab, MeHg was ethylated and analysed by GC–ICP-MS. DGT blanks, collected on a regular basis in the field assessed the absence of contamination of this new monitoring tool. Details on the technique and its limitation are available in Supporting Information.

Results

Atmospheric Hg° concentrations and flux measurements over time

AMDEs, defined when hourly averages of Hg° concentrations fall below 1 ng.m^{-3}, were complex and of short duration (Figure 1a). Two long AMDEs occurred: from April 18 to April 20 and from May 26 to May 28. Additional short and shallow AMDEs were recorded on April 21, April 22, April 24, April 27, May 1, May 4, and May 8. During this extended period (April 18 to May 8), Hg° concentrations oscillated between 0.6-1.0 ng m^{-3} and background concentrations (*i.e.* ~1.5 ng m^{-3}).

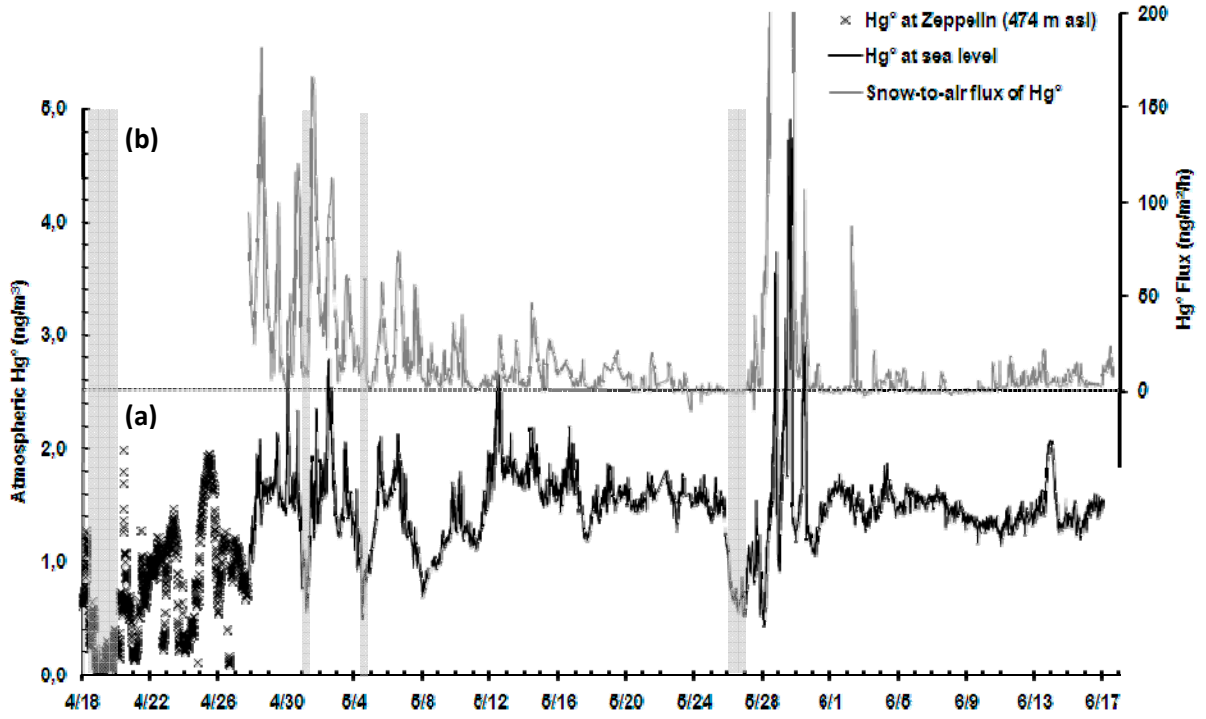

Figure 1 (a) Atmospheric Hg° concentrations at sea level (black line) are shown on the left axis. Atmospheric Hg° data from the 16th to the 26th of April (cross) are the courtesy of NILU and were obtained at Zeppelin air monitoring station (474 meters above sea level). (b) Hg° fluxes recorded from the snowpack (grey line) are shown on the right axis. Grey rectangles represent AMDEs. For clarity, AMDEs occurring between April 21st and April 27th are not shown

The beginning of the 1st AMDE (April 18-April 20) corresponded to a snowfall event as well as an episode of strong wind coming from the Arctic Ocean on the west side of Spitsbergen. Based on HYSPLIT results, air masses originated from North-East Greenland, where high BrO concentrations in the atmospheric column were detected. The sea ice map shows that the air mass had passed over sea ice and open ocean areas (Figure S2a in Supporting Information). The AMDE was at its maximum amplitude (*i.e.* lowest Hg° values) on the 19th, when the wind speed dropped (1-2 m/s). Finally, Hg° concentrations returned to background levels (above 1 ng m^{-3}) on the 20th when wind from inland Spitsbergen swept away the depleted air and local reactants to replace it with air containing background Hg° concentrations. The second long AMDE (May 26-May 28) occurred simultaneously with a temperature drop and during a snow fall. In fact, it started with the contribution of a cooler air masses coming down from the Kongsvegen glacier and a high wind speed (7-8 m/s). During this period, north eastern and eastern regions from Spitsbergen presented higher BrO concentrations. Backward trajectories show a contribution of air masses coming from the North Pole (Figure S2b in Supporting Information).

Hg° trends and flux measurements

Atmospheric Hg° concentrations were influenced by emissions from the snowpack. In the absence of AMDEs, a diel pattern of Hg° values with higher variability and higher values was observed during the day, with values reaching 2.5 ng.m^{-3} periodically. Hourly-averaged Hg° concentration even stayed above 3 ng m^{-3} for 6 hours (peaking at more than 4 ng m^{-3}) on May 29 after the last AMDE (Figure 1a). Flux measurements confirmed the importance of Hg° emission from the snowpack (Figure 1b). They revealed a clear diel pattern with daily hourly maximum averaging more than 20 ng.m^{-2}.h^{-1} (average of the whole campaign). Large emission events were observed following both AMDEs. Following the second AMDE, atmospheric Hg° concentration was influenced by snow reemission up to a height of 7 meters (data not shown) and fluxes reached 1000 ng.m^{-2}.h^{-1}. Forced ventilation of interstitial snow air, however, may have led to an overestimation of Hg° fluxes during this event. Excluding the high reemission event mean Hg° fluxes was around 12.5 ng.m^{-2}.h^{-1} for the whole campaign.

Speciation of Hg in the surface snow

THg concentrations ranged from below detection limit to 373.1 ng.L^{-1} (Figure 2). THg increased as Hg° concentrations decreased, indicating Hg° oxidation and deposition. From the beginning to April 24, THg averaged 191 ng.L^{-1}, due to deposition of oxidized species of mercury (Hg(II)) through AMDEs. Hg deposition was enhanced by the occurrence of snow precipitation.

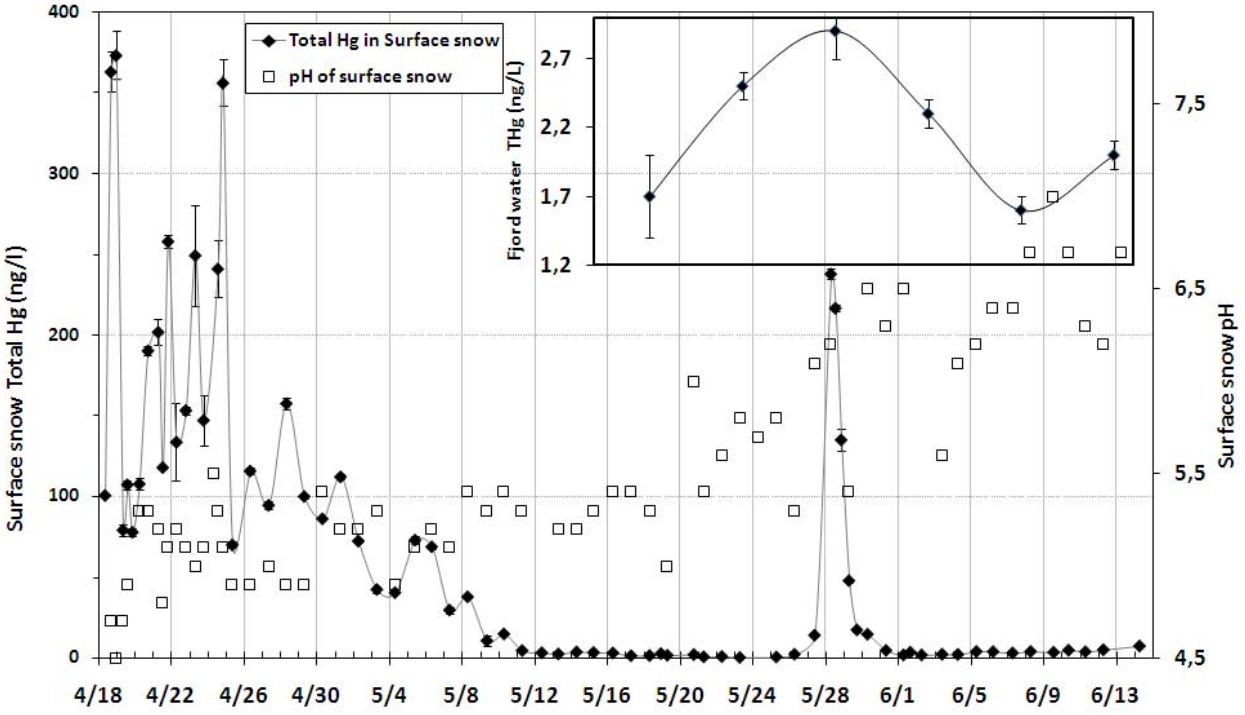

Figure 2: THg concentration (black diamonds, left axis) in surface snow samples as a function of the day of the year. Samples were analyzed in triplicate. The error bars show the standard deviation of the 3 triplicates. Errors bars are most of the time small than 0.2 ng/L and are thus not visible with the present scale. pH (squares, right axis) of melted snow sample is as well shown. A few triplicate measurements of THg in the nearby surface fjord water are also presented in the insert panel.

Between the evening of the 24th and the morning of the 25th, surface THg fell from 356 to 70 ng.L^{-1} due to an important snow fall. Since almost 20 cm of snow covered the previous layers and because an AMDE had just terminated, the THg value of 70 ng.L^{-1} reflected a measurement of wet deposition of Hg(II). In the absence of Hg deposition events, the THg content in surface snow slowly decreased to values below 2 ng.L^{-1}. The last AMDE at the end of May increased THg levels from 2.1 to 237.7 ng.L^{-1}. Photoreduction of deposited mercury and evasion of Hg° occurred immediately after (Figure 1b). After 3 days, surface THg concentration had returned to "normal values", *i.e.* that 99% of deposited Hg has been transformed, transferred or reemitted.

Methylmercury species (MeHg), as integrated over 5-day periods by DGT probes in surface snow, showed increasing levels throughout the campaign (Figure 3 and Table S1 in Supporting Information). A first period showed low levels averaging around 0.049±0.022 ng.L^{-1}. Then, after May 10, higher values and higher variability were observed (0.117±0.050 ng.L^{-1}). A maximum of 0.259±0.015 ng.L^{-1} was recorded on June 3 to 8.

Speciation of Hg in the seawater

THg in the surface seawater close to the snow sampling area was quite elevated around 1.5 ng.L^{-1} (Figure 2). A net increase occurred on May 29 with a measured value of 2.9 ng L^{-1}. DGT probes recorded MeHg values from 0.007 to 0.158 ng.L^{-1} (Figure 3 and Table S1 in Supporting Information). The highest values were recorded on samples of May 19-24 and May 29-June 3 (respectively 0.158 and 0.131 ng.L^{-1}).

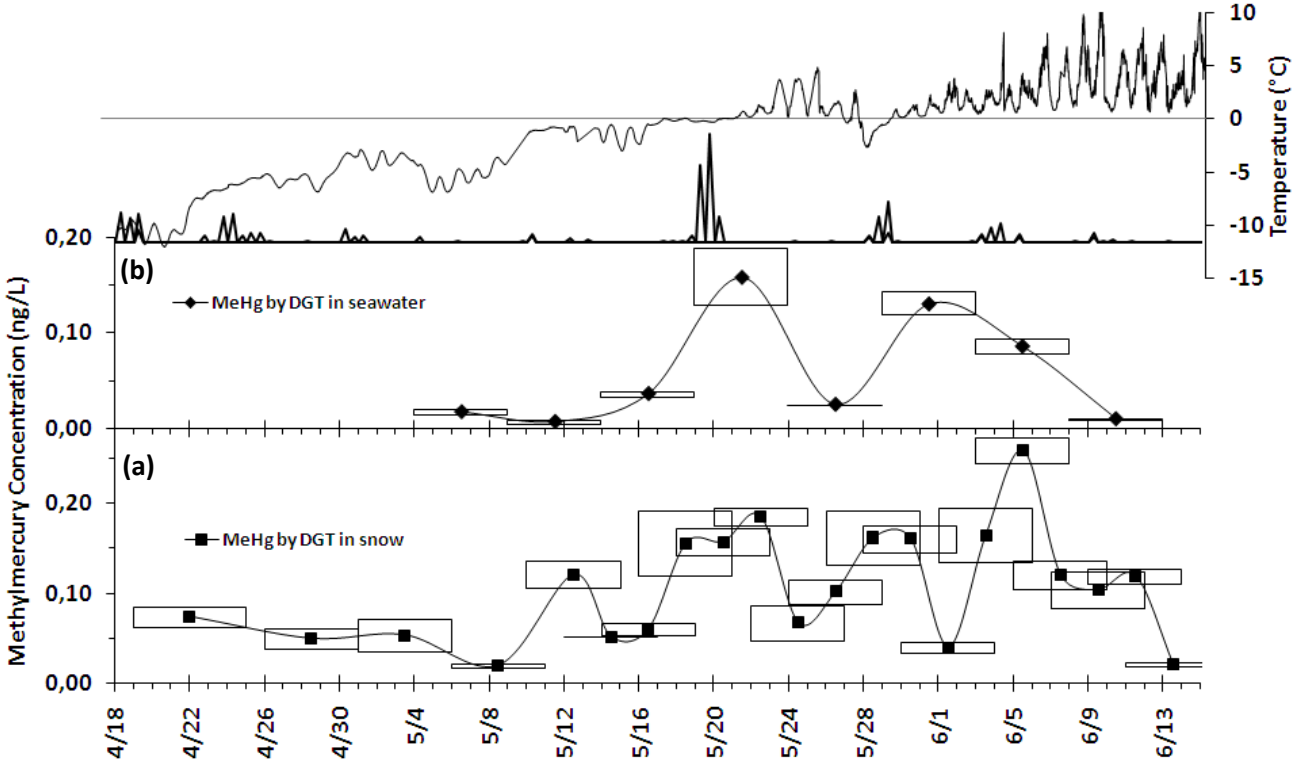

Figure 3**:** MeHg concentrations in (a) surface snow and (b) seawater over 5 days as measured by the DGT technique (see Material and Methods and Supporting Information). The central dot represents the mean value of 3 DGT deployed at the same time and at the same place. The rectangle height shows the standard deviation of the 3 DGT, and the rectangle length the duration of the MeHg collection by the DGT. The DGT do not show a point value of MeHg but rather an integration of 5 days of MeHg presence in the snow. Precipitation events are represented by bold black spikes (no scale). The snow temperature (15 cm below the surface) is shown on the right vertical axis.

THg on surrounding glaciers

The 3 pits were dug at different locations (Figure S1 in Supporting Information) and different periods. As shown in Table 1, the Kongsvegen pit (April 20) had elevated surface THg concentrations (30.3 ng.L^{-1}), however below this depth, THg was comprised between 0.5 and 7.0 ng.L^{-1}. High values were found at the bottom of the pit on the icy layer which corresponded to the refrozen layer of the

summer melt. The pit dug in Austre Lovénbreen is closer to the snow sampling site and was dug later in the season on May 18. The samples collected around 25 and 50 cm depths showed high THg values of 57.4 and 15.2 ng.L^{-1} respectively. The Holtedahlfonna pit (May 05) is situated farther from the fjord and THg values between 0.3 and 4.7 ng.L^{-1} were recorded, with the highest concentrations found in the surface layers.

Table 1: THg concentration measured in pit dug on three different glaciers (Figure S1 in Supporting Information) representing the snow accumulation as of last summer. Mean value (triplicate measurements) and standard deviations are shown.

Glacier / Date	Kongsvegen April 20	Austre Lovénbreen May 18	Holtedahlfonna May 15
Depth (cm)	**THg (ng.L^{-1})**		
Surface	31.0 ± 0.3	1.2 ± 0.1	4.1 ± 0.2
25 ± 10	5.5 ± 0.1	57.4 ± 0.3	4.7 ± 0.2
50 ± 10	2.4 ± 0.1	15.2 ± 0.1	3.0 ± 0.2
75 ± 10	1.6 ± 0.1	0.4 ± 0.2	1.7 ± 0.2
100 ± 10	0.7 ± 0.1	0.6 ± 0.4	1.9 ± 0.3
125 ± 10	0.5 ± 0.1	2.4 ± 0.1	0.3 ± 0.1
150 ± 10	3.7 ± 0.1	0.2 ± 0.1	2.6 ± 0.4
175 ± 10	2.9 ± 0.1	<DL	
200 ± 10	3.5 ± 0.1	<DL	
225 ± 10	7.0 ± 0.1		

THg in meltwater

Meltwater samples were collected as of May 24 even though some partial melting occurred inside the snowpack as of May 20 attested by temperature sensors. The surface meltwater (see Material and Methods) had relatively high THg (up to 24.0 ng.L^{-1}) that lowered progressively to almost undetectable values over time, whereas snowpack meltwater THg remained relatively constant (mean value of 4.8±1.7 ng.L^{-1}) (Figure 4). There appears to be a change in snowpack characteristics as the season progressed. The snowpack data can be divided into two distinct groups based on pH

values, an early spring group and a late spring group. The early spring group is characterized by slightly acidic pH values (around 5.5). As temperatures increased, the snowpack became less and less acidic, with mean values around 6.2. The turning point appears to coincide with snowmelt around the 20th of May.

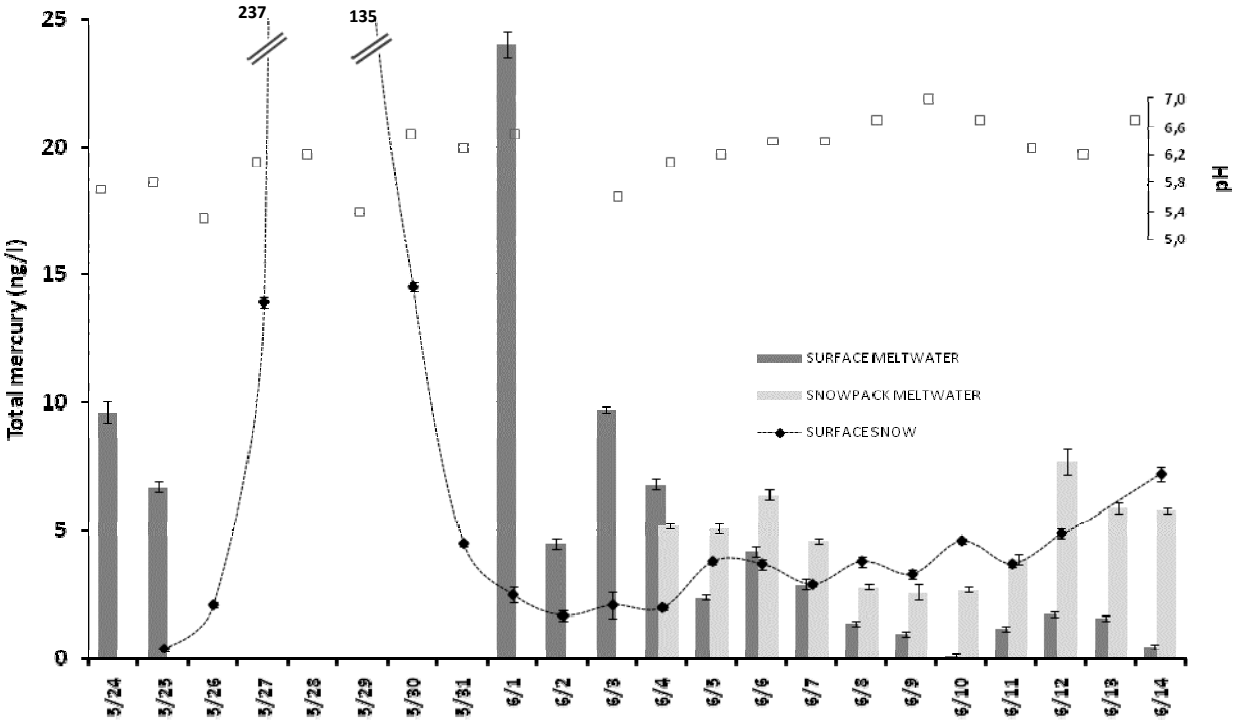

Figure 4: THg concentrations in surface meltwater (dark grey bars) and snowpack meltwater (light grey bars) as defined in the method section. The standard deviation of the triplicate analysis of each sample is represented with error bars. Data of pH and THg of surface snow already shown in Figure 3 are also plotted. The first snowmelt sample was taken on May 24. From May 26 to May 31, a cooler period interrupted the meltwater collection.

Discussion

AMDEs sources and chemistry

The occurrence of AMDEs in polar environments has been reported since 1995 (9). Following this discovery, intensive springtime campaigns were carried out since 2000 in Ny-Ålesund (14, 18-22). The chemistry that causes AMDEs is probably connected to what drives the ozone depletion events (23). Reactive halogens species – generated from open water regions or refreezing sea ice – rapidly oxidize Hg° into oxidized mercury as gaseous Hg(II) or particulate Hg [for more details, see (8)]. According to meteorological (*i.e.* wind direction and back-trajectories) and chemical data (*i.e.* calculation of ozone destruction rates and BrO maps), the AMDEs observed in Ny-Ålesund in 2007 result from an influx of air masses (24) that were previously depleted in Hg° rather than a local chemistry, a phenomenon that has been described elsewhere (25, 26). However the sole influence of a transport of depleted air

masses is not always sufficient to explain the several short-time AMDEs observed in April. On occasions, local chemistry may explain a reactivity of Hg° that may have been initiated by a transport of reactive species. For instance, we recently proposed a theoretical mechanism by which products of Hg° depletion such as $HgBr_4^{2^\circ}$/$HgCl_4^{2^\circ}$ could interact at a sea/air interface with chloride or bromide (27). These pathways could generate a source of reactive bromine that could then oxidize in situ Hg°. A similar process could exist at an air/snow interface if a source of chlorine or bromine is available. However, the capacity of analytical instruments to accurately determine oxidized Hg products is currently inadequate, thus limiting our comprehension of these mechanisms. Another factor that may influence the magnitude and origin of AMDEs in Ny-Ålesund is the more complex topography (presence of mountainous areas, glaciers, and fjords) than for other sites of study (19).

Atmospheric inputs to environmental surfaces

The daily monitoring of THg in surface snow shows that AMDEs deposit an important quantity of mercury. These high values are similar to those reported for Barrow (AK, US) (10, 26), where a local production of Hg(II) usually exists. Elevated THg values in Ny-Ålesund may result in an enhanced deposition of Hg(II) by the scavenging by snow precipitation, which was usually associated to AMDEs. The resulting calculated deposition fluxes to the upper snow layer (assuming a snow density of 0.3 and a collection depth of 1-3 cm) range from 200-650 $ng.m^{-2}$ to 720-2160 $ng.m^{-2}$ for the first and the last AMDEs respectively. Deposition fluxes are comparable to those (320-700 $ng.m^{-2}$) calculated by Johnson *et al.* (26) at Barrow.

Enhanced deposition of Hg(II) following the AMDEs probably occurs on the surrounding glaciers up to a distance of 35-40 km from our surface sampling site and up to an elevation of 670 m. Calculations (26) and vertical measurements (28) showed that AMDEs can occur in the first 200-450 m and 100 m of the troposphere respectively. Previous studies in Ny-Ålesund have shown that AMDEs can be detected at two elevation points (12 m and 474 m) and that Hg° concentrations were comparable (14). No evident influence was observed on our highest sampling site Holtedahlfonna (1173 m), but the elevated surface THg concentrations measured in the surface layers of the Kongsvegen glacier (670 m) sampled during the first AMDE suggest enhanced deposition. In addition, the samples collected later in the season in Austre Lovénbreen, which is closer to the snow sampling site also appear to reflect increased THg deposition. The samples collected at 25 and 50 cm depths (Table I) showed elevated THg values (57.4 and 15.2 $ng.L^{-1}$ respectively) while surface concentrations were low. These values may represent a signature of Hg deposition during the first AMDE that subsequently buried by the snowfall (~20 cm) occurring 2 days after. From these data, we conclude that Hg deposition by AMDEs can impact inland regions of Spitsbergen.

Although the THg levels reported here appear alarming, it seems that most of the deposited Hg on snow is reduced back to Hg° and returns to the atmosphere, as evidenced by the high Hg° fluxes and the drop in surface snow THg concentrations (Figure 1 and Figure 2). Based on these observations, most of the Hg deposited by AMDEs on surface snow is photochemically active. The photoreduction of oxidized Hg has been demonstrated in other laboratory or incubation experiments (11, 29, 30). Even though most of deposited Hg is reemitted, there is still a fraction which is not active as evidenced by the presence of a THg background level of a few $ng.L^{-1}$ and values above detection limit in the snowmelt water. Future research is needed to assess the bioavailability of the deposited Hg in the snow, *i.e.* its ability to cross cellular membranes and interact with organisms.

Impact of snowmelt

Change in pH suggests that increase in temperature leads to an evolution of both physical and ionic composition of snow. The Hg-concentration factor, *i.e.* the ratio of THg concentration in the surface meltwater (collected as of May 24) to that in the parent snow, is highest immediately at the onset of the snowmelt. This suggests that meltwater appears to concentrate THg because most Hg(II) species are rapidly expulsed from the snow matrixes and eluted with the meltwater in the snowpack (*e.g.* (31)). This expulsion of Hg(II) species is associated with an increase of the pH in the snow samples. It could be explained by an initial pulse of acidic ion-rich melt water due to the loss of strong acid at the beginning of the thaw (32, 33) which thus increases the pH of the snow. At the end of the season, most of the Hg(II) has been liberated from the snow matrix. The remaining fraction of Hg (~ 4 $ng.L^{-1}$) present in the snow is probably poorly soluble. The slight increase in snow surface THg concentrations towards the end of the sampling campaign may be due to an increased input from soils, which had begun to thaw, but also due to the loss of water from the snow.

From June 10 to the end of the campaign, the snowmelt accelerated draining run-off water to the fjord. Many run-off stream samples were analysed and values averaged 3.5±1.9 $ng.L^{-1}$ (n=13). The run-off waters originating from the Austre Lovénbreen glacier averaged 2.2±1.1 $ng.L^{-1}$ (n=7). Based on mass balance studies, run-off measurements and meteorological data, run-off water input to the fjord is estimated at 0.83 $km^3.year^{-1}$ (± 30% due to year-to-year changes) excluding glacier calving and run-off from rainfall (34). Based on our THg measurements in different meltwater streams, and assuming that the fjord has a THg load of 17.6 kg (volume of 29.4 km^3 and mean THg in the water column of 0.6 $ng.L^{-1}$ extrapolated from (12)), we estimate that spring melt represents an input of 1.5-3.6 $kg.year^{-1}$ of THg to the fjord (*i.e.* 8-21% of the fjord's THg content). Although a large fraction of Hg deposited during AMDEs is re-emitted back to the atmosphere, the snowpack seems to play an important role as a temporary reservoir in the Hg transfer from the atmosphere to the fjord.

The origin of methylmercury species

Current concerns with mercury toxicity are based on the neurotoxin methylmercury. An important question today is the identification of pathways for methylation in polar areas, which are for the most part linked to microbiological activities (13). A popular mechanism described in recent papers suggests that monomethylmercury is deposited onto snow following its transformation (oxidation or photodegration) from dimethylmercury evasion produced by phytoplankton in the water column (35). However other pathways such as methylation in the snowpack, abiotic processes (36) or aqueous phase methylation in the atmosphere (37) remain likely.

We observed an increase in both THg and MeHg concentrations (Figure 2 and Figure 3) in the fjord that began around the 22nd of May, a date which appears to coincide with the beginning of snow melt (20-24 May). Whether or not this increase can be attributed to direct Hg(II) and MeHg deposition, Hg(II) or MeHg inputs from the snowpack, or to an increase in primary production and subsequent Hg methylation in the fjord due to an increase in nutrient availability following spring melt is debatable. A phytoplankton accumulation began around May 5 at about 25 m depth and sank with a later maximum around 80 m on May 15 (38). Our sampling site is situated in shallow water close to snow sampling site, and we do not know if phytoplankton data are applicable even though organisms were visible on our sampling equipment. As demonstrated for other sites, high-resolution MeHg vertical profiles in addition to nutrient measurements have to be undertaken to clearly verify the hypothesis of an in situ production of methylmercury (39). High levels of MeHg were observed in the snow and these peaks appear to coincide with snow/rain events (Figure 3). While this suggests wet deposition of MeHg from either the fjord or the atmosphere, other sources may also contribute. These peaks could be due to freeze-thaw cycles that generate a MeHg pulse, as has been observed for ions and nutrients, or to in situ mercury methylation by bacteria. Another possibility is that the increased presence of liquid water within the snowpack may facilitate MeHg transport to the DGTs. Regardless, spring melt appears to be an important period in terms of Hg chemistry and requires more research.

Acknowledgments

This study is funded by INSU/CNRS, program EC2CO (CYTRIX) and by the French Polar Institute IPEV (program #399 CHIMERPOL). We gratefully thank Cédric Couret and Nicolas Le Viavant for field support. We acknowledge the AWIPEV station, and especially Rainer Vockenroth. We also thank NILU for providing Hg° data at Zeppelin station.

References

(1) Pacyna, E. G.; Pacyna, J. M.; Steenhuisen, F.; Wilson, S. Global anthropogenic mercury emission inventory for 2000. Atmos. Environ. **2006,** 40 (22), 4048-4063.

(2) Slemr, F.; Brunke, E. G.; Ebinghaus, R.; Temme, C.; Munthe, J.; Wangberg, I.; Schroeder, W.; Steffen, A.; Berg, T. Worldwide trend of atmospheric mercury since 1977. Geophys. Res. Lett. **2003,** 30 (10).

(3) Lindberg, S.; Bullock, R.; Ebinghaus, R.; Engstrom, D.; Feng, X. B.; Fitzgerald, W.; Pirrone, N.; Prestbo, E.; Seigneur, C. A synthesis of progress and uncertainties in attributing the sources of mercury in deposition. Ambio **2007,** 36 (1), 19-32.

(4) Faïn, X.; Ferrari, C. P.; Dommergue, A.; Albert, M. R.; Battle, M.; Severinghaus, J.; Arnaud, L.; Barnola, J.-M.; Cairns, W.; Barbante, C.; Boutron, C. Polar firn air reveals large-scale impact of anthropogenic mercury emissions during the 1970s. Proc. Natl. Acad. Sci. U. S. A. **2009**, 10.1073/pnas.0905117106.

(5) Riget, F.; Dietz, R.; Born, E. W.; Sonne, C.; Hobson, K. A. Temporal trends of mercury in marine biota of west and northwest Greenland. Mar. Pollut. Bull. **2007,** 54 (1), 72-80.

(6) Dietz, R.; Riget, F.; Born, E. W.; Sonne, C.; Grandjean, P.; Kirkegaard, M.; Olsen, M. T.; Asmund, G.; Renzoni, A.; Baagoe, H.; Andreasen, C. Trends in mercury in hair of greenlandic polar bears (Ursus maritimus) during 1892-2001. Environ. Sci. Technol. **2006,** 40 (4), 1120-1125.

(7) Wagemann, R.; Trebacz, E.; Boila, G.; Lockhart, W. L. Methylmercury and total mercury in tissues of arctic marine mammals. Sci. Total Environ. **1998,** 218 (1), 19-31.

(8) Steffen, A.; Douglas, T.; Amyot, M.; Ariya, P.; Aspmo, K.; Berg, T.; Bottenheim, J.; Brooks, S.; Cobbett, F.; Dastoor, A.; Dommergue, A.; Ebinghaus, R.; Ferrari, C.; Gardfeldt, K.; Goodsite, M. E.; Lean, D.; Poulain, A. J.; Scherz, C.; Skov, H.; Sommar, J.; Temme, C. A synthesis of atmospheric mercury depletion event chemistry in the atmosphere and snow. Atmos. Chem. Phys. **2008,** 8 (6), 1445-1482.

(9) Schroeder, W. H.; Anlauf, K. G.; Barrie, L. A.; Lu, J. Y.; Steffen, A.; Schneeberger, D. R.; Berg, T. Arctic springtime depletion of mercury. Nature **1998,** 394 (6691), 331–332.

(10) Lindberg, S. E.; Brooks, S.; Lin, C. J.; Scott, K. J.; Landis, M. S.; Stevens, R. K.; Goodsite, M.; Richter, A. Dynamic Oxidation of Gaseous Mercury in the Arctic Troposphere at Polar Sunrise. Environ. Sci. Technol. **2002,** 36 (6), 1245–256.

(11) Lalonde, J. D.; Poulain, A. J.; Amyot, M. The role of mercury redox reactions in snow on snow–to–air mercury transfer. Environ. Sci. Technol. **2002,** 36 (2), 174–178.

(12) Outridge, P. M.; Macdonald, R. W.; Wang, F.; Stern, G. A.; Dastoor, A. P. A mass balance inventory of mercury in the Arctic Ocean. Environ. Chem. **2008,** 5 (2), 89–111.

(13) Barkay, T.; Poulain, A. J. Mercury (micro)biogeochemistry in polar environments. FEMS Microbiol. Ecol. **2007,** 59 (2), 232-241.

(14) Aspmo, K.; Gauchard, P. A.; Steffen, A.; Temme, C.; Berg, T.; Bahlmann, E.; Banic, C.; Dommergue, A.; Ebinghaus, R.; Ferrari, C.; Pirrone, N.; Sprovieri, F.; Wibetoe, G. Measurements of atmospheric mercury species during an international study of mercury depletion events at Ny-Alesund, Svalbard, spring 2003. How reproducible are our present methods? Atmos. Environ. **2005,** 39 (39), 7607-7619.

(15) Faïn, X.; Grangeon, S.; Bahlmann, E.; Fritsche, J.; Obrist, D.; Dommergue, A.; Ferrari, C. P.; Cairns, W.; Ebinghaus, R.; Barbante, C.; Cescon, P.; Boutron, C. Diurnal production of gaseous mercury in the alpine snowpack before snowmelt. J. Geophys. Res. **2007,** 112 (D21), doi:10.1029/2007JD008520.

(16) Clarisse, O.; Foucher, D.; Hintelmann, H. Methylmercury speciation in the dissolved phase of a stratified lake using the diffusive gradient in thin film technique. Environ. Pollut. **2009,** 157 (3), 987-993.

(17) Clarisse, O.; Hintelmann, H. Measurements of dissolved methylmercury in natural waters using diffusive gradients in thin film (DGT). J. Environ. Monit. **2006,** 8 (12), 1242-1247.

(18) Berg, T.; Sekkesaeter, S.; Steinnes, E.; Valdal, A. K.; Wibetoe, G. Springtime depletion of mercury in the European Arctic as observed at Svalbard. Sci. Total Environ. **2003,** 304 (1-3), 43-51.
(19) Sommar, J.; Wangberg, L.; Berg, T.; Gardfeldt, K.; Munthe, J.; Richter, A.; Urba, A.; Wittrock, F.; Schroeder, W. H. Circumpolar transport and air-surface exchange of atmospheric mercury at Ny-Â°lesund (79° N), Svalbard, spring 2002. Atmos. Chem. Phys. **2007,** 7 (1), 151-166.
(20) Ferrari, C. P.; Padova, C.; Faïn, X.; Gauchard, P.-A.; Dommergue, A.; Aspmo, K.; Berg, T.; Cairns, W.; Barbante, C.; Cescon, P.; Kaleschke, L.; Richter, A.; Wittrock, F.; Boutron, C. Atmospheric mercury depletion event study in Ny-Alesund (Svalbard) in spring 2005. Deposition and transformation of Hg in surface snow during springtime. Sci. Total Environ. **2008,** 397 (1-3), 167-177.
(21) Fain, X.; Ferrari, C. P.; Gauchard, P. A.; Magand, O.; Boutron, C. Fast depletion of gaseous elemental mercury in the Kongsvegen Glacier snowpack in Svalbard. Geophys. Res. Lett. **2006,** 33 (6), Doi 10.1029/2005gl025223.
(22) Sprovieri, F.; Pirrone, N.; Landis, M. S.; Stevens, R. K. Atmospheric mercury behavior at different altitudes at Ny Alesund during Spring 2003. Atmos. Environ. **2005,** 39 (39), 7646-7656.
(23) Bottenheim, J. W.; Gallant, A. G.; Brice, K. A. Measurements of NOy species and O3 at 82oN latitude. Geophys. Res. Lett. **1986,** 22, 599-602.
(24) Gauchard, P. A.; Aspmo, K.; Temme, C.; Steffen, A.; Ferrari, C.; Berg, T.; Strom, J.; Kaleschke, L.; Dommergue, A.; Bahlmann, E.; Magand, O.; Planchon, F.; Ebinghaus, R.; Banic, C.; Nagorski, S.; Baussand, P.; Boutron, C. Study of the origin of atmospheric mercury depletion events recorded in Ny-Alesund, Svalbard, spring 2003. Atmos. Environ. **2005,** 39 (39), 7620-7632.
(25) Lu, J. Y.; Schroeder, W. H.; Barrie, L. A.; Steffen, A.; Welch, H. E.; Martin, K.; Lockhart, L.; Hunt, R. V.; Boila, G.; Richter, A. Magnification of atmospheric mercury deposition to polar regions in springtime: the link to tropospheric ozone depletion chemistry. Geophys. Res. Lett. **2001,** 28 (17), 3219–3222.
(26) Johnson, K. P.; Blum, J. D.; Keeler, G. J.; Douglas, T. A. Investigation of the deposition and emission of mercury in arctic snow during an atmospheric mercury depletion event. J. Geophys. Res.-Atmos. **2008,** 113 (D17).
(27) Maron, L.; Dommergue, A.; Ferrari, C. P.; Delacour-Larose, M.; Faïn, X. How elementary mercury react in presence of halogen radicals and/or halogen anions: A DFT investigation. Chem.-Eur. J. **2008,** 14 (27), 8322-8329.
(28) Tackett, P. J.; Cavender, A. E.; Keil, A. D.; Shepson, P. B.; Bottenheim, J. W.; Morin, S.; Deary, J.; Steffen, A.; Doerge, C. A study of the vertical scale of halogen chemistry in the Arctic troposphere during Polar Sunrise at Barrow, Alaska. J. Geophys. Res.-Atmos. **2007,** 112 (D7), -.
(29) Lalonde, J. D.; Amyot, M.; Doyon, M. R.; Auclair, J. C. Photo–induced Hg(II) reduction in snow from the remote and temperate Experimental Lakes Area (Ontario, Canada). J. Geophys. Res. **2003,** 108 (D6).
(30) Dommergue, A.; Bahlmann, E.; Ebinghaus, R.; Ferrari, C.; Boutron, C. Laboratory simulation of Hg° emissions from a snowpack. Anal. Bioanal. Chem. **2007,** 388, 319-327.
(31) Bales, R. C.; Davis, R. E.; Williams, M. W. Tracer release in melting snow: diurnal and seasonal patterns. Hydrolog. Process. **1993,** 7, 389–401.
(32) Simoes, J. C.; Zagorodnov, V. S. The record of anthropogenic pollution in snow and ice in Svalbard, Norway. Atmos. Environ. **2001,** 35 (2), 403-413.
(33) Quinton, W. L.; Porneroy, J. W. Transformations of runoff chemistry in the Arctic tundra, Northwest Territories, Canada. Hydrolog. Process. **2006,** 20 (14), 2901-2919.
(34) Svendsen, H.; Beszczynska-Moller, A.; Hagen, J. O.; Lefauconnier, B.; Tverberg, V.; Gerland, S.; Orbaek, J. B.; Bischof, K.; Papucci, C.; Zajaczkowski, M.; Azzolini, R.; Bruland, O.; Wiencke, C.; Winther, J. G.; Dallmann, W. The physical environment of Kongsfjorden-Krossfjorden, an Arctic fjord system in Svalbard. Polar Res. **2002,** 21 (1), 133-166.
(35) St. Louis, V. L.; Sharp, M. J.; Steffen, A.; May, A.; Barker, J.; Kirk, J. L.; Kelly, D. J. A.; Arnott, S. E.; Keatley, B.; Smol, J. P. Some sources and sinks of monomethyl and inorganic mercury on Ellesmere island in the Canadian high arctic. Environ. Sci. Technol. **2005,** 39 (8), 2686–2701.

(36) Gardfeldt, K.; Munthe, J.; Stromberg, D.; Lindqvist, O. A kinetic study on the abiotic methylation of divalent mercury in the aqueous phase. Sci. Total Environ. **2003,** 304 (1-3), 127-136.
(37) Hammerschmidt, C. R.; Lamborg, C. H.; Fitzgerald, W. F. Aqueous phase methylation as a potential source of methylmercury in wet deposition. Atmos. Environ. **2007,** 41 (8), 1663-1668.
(38) Narcy, F.; Gasparini, S.; Falk-Petersen, S.; Mayzaud, P. Seasonal and individual variability of lipid reserves in Oithona similis (Cyclopoida) in an Arctic fjord. Polar Biol. **2009,** 32 (2), 233-242.
(39) Cossa, D.; Bernard, A.; Pirrone, N. The origin of methylmercury in open Mediterranean waters. Limnol. Oceanogr. **2009,** 54(3), 837-844.

Supporting Information

Deposition of mercury species in the Ny-Ålesund area (79°N) and their transfer during snowmelt

Aurélien Dommergue[1], Catherine Larose[1,2], Xavier Faïn[3], Olivier Clarisse[4,5], Delphine Foucher[4], Holger Hintelmann[4], Dominique Schneider[2] and Christophe P Ferrari[1]

[1] Université Joseph Fourier – Grenoble 1 / CNRS, LGGE
54 rue Molière BP56
38402 Saint Martin d'Hères – France

[2]Laboratoire Adaptation et Pathogénie des Micro-organismes, Université Joseph Fourier – Grenoble 1, BP 170, F-38042 Grenoble cedex – France

[3]Division of Atmospheric Sciences, Desert Research Institute, 2215 Raggio Parkway, Reno, NV, USA

[4]Department of Chemistry- Trent University
1600 West Bank Drive
Peterborough ON K9J 7B8 – Canada

[5]Now at Département de chimie et biochimie- Université de Moncton
Moncton, N.-B. E1A 3E9 – Canada

[6] CNRS UMR 5163

Content

Material and methods

Study site

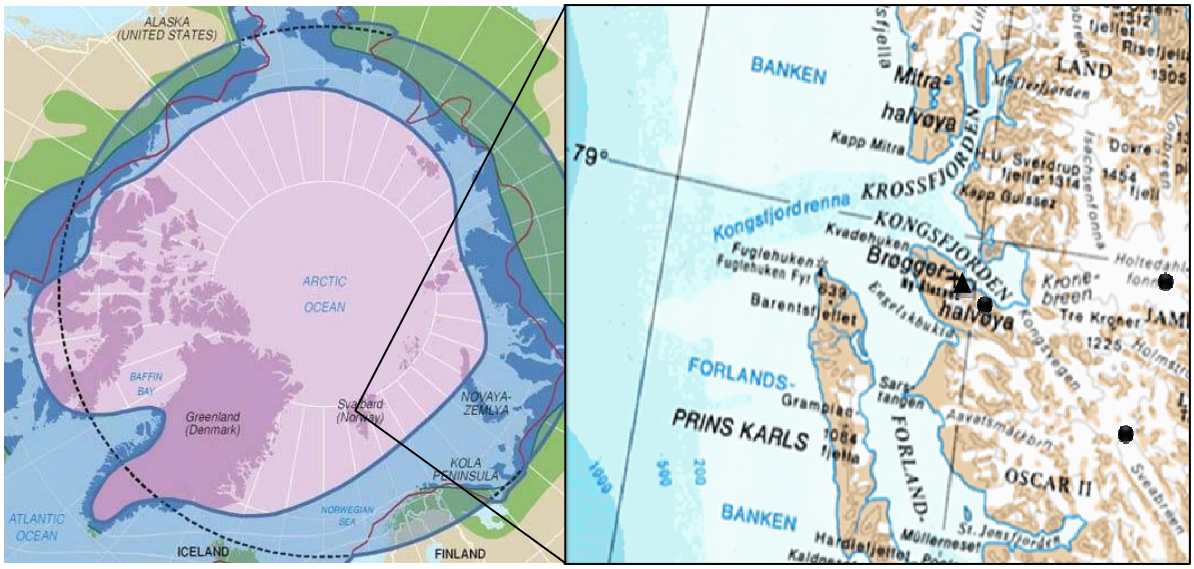

Figure S2: Location of the experiments. Left map **:** Circumpolar Arctic vegetation map (after (*1, 2*) (*3, 4*). Purple color indicates the High Arctic, Blue color the Low Arctic, Green color the Sub-arctic, dash line the arctic circle and redline, the 10°C July isotherm.
Right map shows the surroundings of Ny-Ålesund (black triangle), Svalbard (Norway). Sampling sites on the glaciers are shown with black spots.

Atmospheric Hg° measurements.

Atmospheric Hg° was measured two meters above snow surface using a Tekran model 2537A vapor-phase Hg analyzer. Briefly, ambient air is collected onto gold traps and Hg is detected using atomic fluorescence spectrometry following thermal desorption. Two parallel gold traps that alternatively collect and quantify provide a continuous determination of Hg° with a 5-minute interval. This instrument is calibrated every 25 hours with an internal permeation source.

The flux chamber covered an area of 29.5 x 8 cm². The chamber was 9 cm high, and pushed 5 cm into the snow so that a headspace of 4 cm was above the snowpack.

The chamber was made of Polycast SOLACRYL™ SUVT, which is characterized by high transmissivity for UVB (~80% at a wavelength of 270 nm). On one side, holes in the chamber wall enabled ambient air to enter the chamber (inlet) while on the other side we connected a Teflon line for air pumping (outlet). A switch unit connected to a Tekran 2537A analyzer controlled alternating sampling between two 1/4'' Teflon lines. The first line was directly connected to the outlet of the chamber. The second line enabled sampling air at the inlet of the chamber. Hg^0 fluxes were calculated using the following equation:

$$F = \frac{C_O - C_I}{A} \times Q$$

where F is the flux in $ng.m^{-2}.h^{-1}$, C^O and C^I are Hg^0 concentrations in ng m^{-3} at the outlet and inlet ports respectively, A the surface area of the chamber in m^2 (236 cm^2) and Q the airflow rate (1.5 $l.min^{-1}$).

Long-term exposure of the snow in the chamber may disturb perturb the physical and chemical properties of the snow, and thus the flux measurements. To avoid any artefact, the flux chamber was moved daily from April 26 to May 20, and twice a day (*i.e.* every morning and every evening) after May 20. Potential contamination from the chamber was investigated before field deployment, in laboratory (LGGE, France). After sealing the bottom of the chamber with a Polycast SOLACRYL™ SUVT plastic plate, Hg-free air was measured with a 2537A Tekran analyzer through the chamber. Hg^0 concentrations were measured constantly below d.l. (*i.e.* 0.000 $ng.m^{-3}$) during few hours. On the field, flux blanks of 0.13 ± 0.16 $ng.m^{-2}.h^{-1}$ were measured after connection of the chamber to the switch unit and the 2537A analyzer as described before.

Analytical Techniques

Total Mercury (THg) determination

Samples were oxidized to 0.5% v/v BrCl to preserve Hg^{2+} in solution and to digest strongly bounded complexes of Hg^{2+}. Excess BrCl was neutralized with pre-purified hydroxylamine hydrochloride. The sample is then automatically injected together with $SnCl_2$ to a reaction vessel, reducing Hg^{2+} to Hg°. Hg° is carried in an argon stream to two online gold traps. After thermal desorption, Hg° is detected by atomic fluorescence spectrometry. The Tekran Model 2600 was calibrated every day using standard prepared with the NIST SRM-3133 Hg standard. The limit of quantification calculated as 10 times the standard deviation of a set of 10 blanks was 0.3 $ng.L^{-1}$. The limit of detection (LOD) was re-evaluated every analytical run on a limited set of blanks (usually 3). During analytical session, 10 $ng.L^{-1}$ OPR (Ongoing Precision Recovery) were periodically analysed to check the reliability of the system. Procedure blanks were periodically realized and were all undetectable. All samples were analyzed in triplicate. THg concentrations reported in this paper are presented as mean ± 1 stdv.

Methylmercury determination using DGT (Diffusive Gradient in Thin Films)

Developed initially as a monitoring tool for MeHg in the water column (*5, 6*) or in sediment pore water (*7*) DGT technique was used for the first time in the snow and melting snow in order to assess the mobility of MeHg in this particular media.

In water, DGT principle is based on the diffusion of the dissolved species through a gel and their subsequent accumulation on an ion exchange resin. The well defined physical properties of the gel (thickness, area) itself and the deployment time of the DGT unit in the environment controls the preconcentration of the target species. According to the first Fick law of diffusion, a time average concentration could be calculated from the amount of the target species accumulated by the resin. In snow and melting snow, the DGT theory for MeHg is not fully established yet. MeHg preconcentration of MeHg by the DGT devices will depend on its transport in the polyacrylamide gel at subzero temperature, MeHg transportation in the snow itself and the presence of any local source of MeHg in this particular media. Consequently, MeHg DGT calculated concentrations are probably not absolute ones but they should reflect more likely the mobility of MeHg in the snow or melting snow during the deployment time period.

All DGT pistons units (DGT Research Ltd, Lancaster, UK) were loaded with a 0.4 mm thick resin gel (a thiol resin embedded in polyacrylamide gel), a 0.4 mm thick pure polyacrylamide diffusive gel and a 0.13 mm filter (0.45 mm pore size cellulose nitrate membrane). After deployement, DGT units were

rinsed with distilled water and kept in polyethylene bags for the transport to the laboratory. In the laboratory, DGT units were dismantled and the resin gel extracted. $Me^{201}Hg$ was spiked directly on the resin gel as an internal standard and the resin gels were eluted using a hydrochloric thiourea solution (1.3 M in 0.1 M HCl). MeHg in the eluate was ethylated and analysed by GC–ICP-MS. Details of DGT analyses and gel preparations have been outlined previously.

Other data

Ancillary meteorological data were kindly provided by the AWIPEV station. Atmospheric BrO distribution (*8*) were retrieved from data obtained by the SCIAMACHY instrument on ENVISAT (http://www.iup.uni-bremen.de/doas/). The back trajectories of air masses arriving at the Ny-Ålesund site were obtained via NOAA ARL (National Oceanic and Atmospheric Air Resources Laboratory). They were generated with the Real-time Environmental Applications and Display system (READY) and compiled by the HYSPLIT (HYbrid Single-Particle Lagrangian Integrated Trajectory) model, which uses the atmospheric pressure recorded at the wind origin point and meteorological model data (*9*). Sea ice map derived from the sea ice concentration archive calculated with the ARTISTSea Ice (ASI) algorithm (see www.seaice.de) using AMSR-E (Advanced Microwave Scanning Radiometer) data (*10*).

Table S1 : Methylmercury species (MeHg) measurements in surface snow and surface seawater using DGT with a 5-day integration time. The range of THg concentrations monitored on the same site on a daily basis is shown for comparison purposes.
(1)Two sets of 3 DGT were deployed at the same time
(2) THg is only available for surface seawater at the beginning of the DGT installation

Deployment date		[MeHg]	Range of [THg]
begin	end	$ng.L^{-1}$	$ng.L^{-1}$
DGT in surface snow			
04/19	04/24	0.074 ± 0.011	77,7 - 257,8
04/26	05/01	0.049 ± 0.012	86 - 157,4
05/01	05/06	0.053 ± 0.018	40,3 - 112
05/06	05/11	0.020 ± 0.003	4,4 - 68,7
05/10	05/15	0.121 ± 0.015	3 - 14,7
05/12	05/17	0.051 ± 0.001	1,2 - 3,5
05/14	05/19	0.060 ± 0.007	1,2 - 3,5
05/16	05/21	0.156 ± 0.036	0,5 - 2,9
05/18	05/23	0.157 ± 0.015	0,1 - 2,5
05/20	05/25	0.185 ± 0.010	0,1 - 1,9
05/22	05/27	0.060 ± 0.005	0,1 - 13,9
05/22	05/27	0.074 ± 0.015(1)	0,1 - 13,9
05/24	05/29	0.102 ± 0.013	0,4 - 237,7
05/26	05/31	0.162 ± 0.030	2,1 - 237,7
05/28	06/02	0.161 ± 0.015	1,7 - 237,7
05/30	06/04	0.040 ± 0.005	1,7 - 14,5
06/01	06/06	0.164 ± 0.030	1,7 - 3,8
06/03	06/08	0.259 ± 0.015	2,0 - 3,8
06/05	06/10	0.120 ± 0.016	2,9 - 4,6
06/07	06/12	0.104 ± 0.020	2,9 - 4,9
06/09	06/14	0.119 ± 0.008	3,3 - 7,2
06/11	06/16	0.021 ± 0.002	3,7 - 7,2
DGT in fjord surface seawater			
05/04	05/09	0.017 ± 0.003	NA
05/09	05/14	0.007 ± 0.002	NA
05/14	05/19	0.036 ± 0.003	NA
05/19	05/24	0.158 ± 0.030	1.7 ± 0.3(2)
05/24	05/29	0.025 ± 0.001	2.5 ± 0.1(2)
05/29	06/03	0.131 ± 0.012	2.9 ± 0.2(2)
06/03	06/08	0.093 ± 0.008	2.3 ± 0.1(2)
06/08	06/13	0.010 ± 0.001	1.6 ± 0.1(2)
DGT in meltwater river			
06/11	06/16	0.031 ± 0.003	2.4 - 4.4

Figure S2: 5-day back trajectories (HYSPLIT Dispersion model (*9*)) of air masses arriving at Ny-Ålesund on (a) April 18 (12 am and 12 pm) and April 19 (12 am and 12pm) and (b) on May 26 (12 am and 12 pm) and May 27 (12 am and 12pm). Sea-ice map (ARTIST Sea Ice (ASI) algorithm (*10*)) and BrO map (IUP Bremen, Andreas.Richter@iup.physik.uni-bremen.de) are also shown.

(a)

(b)

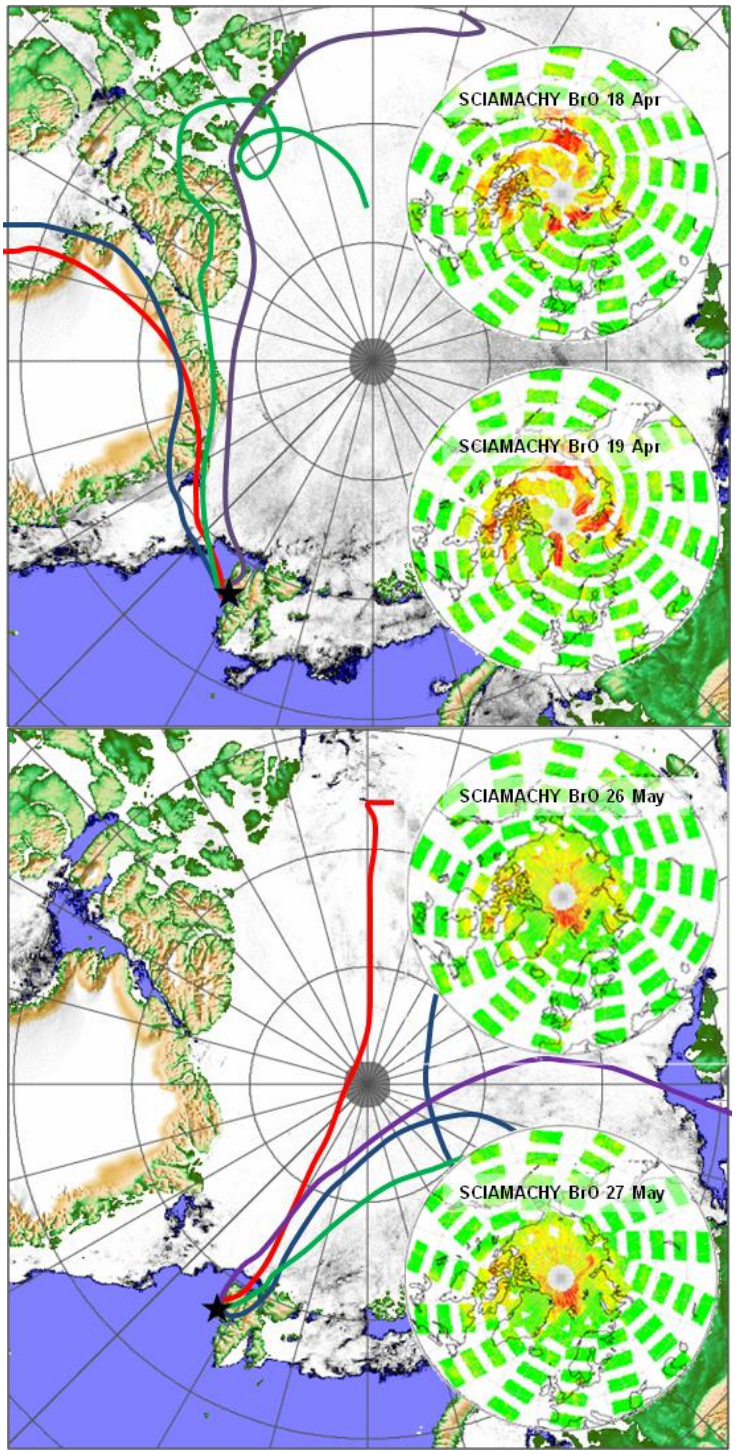

References

(1) AMAP Arctic Pollution Issues: A State of the Arctic **1997**.

(2) AMAP Assessment Report: Arctic Pollution Issues. **1998**.

(3) UNEP/GRID-Arendal Cartographe: Philippe Rekacewicz. Definitions of the Arctic. UNEP/GRID-Arendal Maps and Graphics Library. Available at: http://maps.grida.no/go/graphic/definitions_of_the_arctic. Accessed November 09, 2009. . **2005**.

(4) CAFF Arctic Flora and Fauna: Status and Conservation. **2001**.

(5) Clarisse, O.; Foucher, D.; Hintelmann, H. Methylmercury speciation in the dissolved phase of a stratified lake using the diffusive gradient in thin film technique. *Environ. Pollut.* **2009,** *157* (3), 987-993.

(6) Clarisse, O.; Hintelmann, H. Measurements of dissolved methylmercury in natural waters using diffusive gradients in thin film (DGT). *J. Environ. Monit.* **2006,** *8* (12), 1242-1247.

(7) Clarisse, O.; Dimock, B.; Hintelmann, H.; Best, E.; Fredrickson, H. Effect of mercury methylation, a biogeochemical process, on Diffusive Gradient in Thin film (DGT) measurements for methylmercury in sediment. *in preparation* **2009**.

(8) Richter, A.; Wittrock, F.; Eisinger, M.; Burrows, J. P. GOME observations of tropospheric BrO in northern hemispheric spring and summer 1997. *Geophys. Res. Lett.* **1998,** *25* (14), 2683-2686.

(9) Draxler, R. R.; Rolph, G. D. HYSPLIT (HYbrid Single-Particle Lagrangian Integrated Trajectory) Model access via NOAA ARL READY Website(http://www.arl.noaa.gov/ready/hysplit4.html). NOAA Air Resources Laboratory, Silver Spring, MD. **2003**.

(10) Kaleschke, L.; Lüpkes, L.; Vihma, T.; Haarpaintner, J.; Bochert, A.; Hartmann, J.; Heygster, G. SSM/I Sea Ice Remote Sensing for Mesoscale Ocean-Atmosphere Interaction Analysis. *Can. J. Rem. Sens.* **2001,** *27* (5), 526-537.

SECTION III

In Section II, we showed that the sequence diversity in Arctic snow and meltwater libraries is elevated and that common species exist among different cryosphere environments. This suggests that the snow can sustain a microbial community. In addition, the changes in phylotype abundance observed in the snow libraries collected at different times throughout the season suggest that certain members of the community may be active. This may have consequences on Hg transformations and cycling within the snowpack. As reported in Chapter 3 of Section II, MeHg concentrations increased in snowpacks. Since one of the main pathways for Hg methylation occurs within microbial cells, MeHg formation is dependent upon the bioavailable Hg (BioHg) fraction. Since BioHg cannot be measured using traditional analytical techniques, we recognized the need to develop a new tool, based on pre-existing luminescent biosensors that could easily be deployed in the field. In Chapter 4, we describe the construction of the *mer-lux* biosensor and BioHg measurement results obtained after its deployment during a two-month field campaign in Ny-Ålesund (Svalbard, Norway, 78°56'N, 11°52'E) in spring 2008. Our results revealed that the relative proportion of BioHg deposited during AMDEs is less significant than that observed during precipitation events.

Hg speciation is modified by the presence of other ligands such as organic molecules and inorganic ions. Therefore, we decided to explore the snowpack chemistry in more detail during the 2008 field campaign. In addition, based on the results presented in the second chapter of Section II, we altered our sampling protocol to include basal snow samples to improve our understanding of the dynamics of snowpack chemistry during melt. The results from this field study are presented in Chapter 5 of this section. Our approach highlighted the dynamic nature of the snowpack, since the snow chemistry evolved throughout the season, and also led us to develop a new model for mercury methylation involving BioHg and DMSP metabolism.

CHAPTER 4: BIOAVAILABILITY OF MERCURY DEPOSITED IN POLAR ENVIRONMENTS

Submitted for publication

Catherine Larose[1,2,3], Aurélien Dommergue[1], Nicolas Marusczak[1], Christophe P. Ferrari[1], and Dominique Schneider[2,3]

[1]Laboratoire de Glaciologie et Géophysique de l'Environnement, CNRS – Université Joseph Fourier Grenoble, 54 Rue Molière, 38400 St Martin d'Hères, France

[2]Laboratoire Adaptation et Pathogénie des Microorganismes, Université Joseph Fourier Grenoble 1, BP 170, F-38042 Grenoble cedex 9, France

[3] CNRS UMR 5163

Polar Regions are subject to contamination by mercury (Hg) transported from lower latitudes[1], severely impacting human and animal health. Once deposited, mercury can be transformed to methylmercury (MeHg), a highly toxic organo-metallic compound that accumulates in the food chain[2]. Of paramount importance, microbial uptake of mercury is a key step in both its methylation and bioaccumulation. Since their discovery in 1995[3], Atmospheric Mercury Depletion Events (AMDEs) have been considered as one of the major sources of mercury deposition in polar ecosystems. However, their impact, especially on the amount of bioavailable mercury (BioHg) deposited, has yet to be elucidated. Here we report the fraction of BioHg, *i.e.* mercury able to enter within living cells, over a two-month arctic field campaign that included AMDEs. We designed a highly sensitive biosensor as a molecular tool that we deployed in the field, which has rarely been performed. We demonstrated that snow fall events provided a higher proportion of BioHg deposited compared to AMDEs. Hence, AMDEs represented a potential source of 20 $t.y^{-1}$ of BioHg, while wet and dry deposition pathways provided 135-225 $t.y^{-1}$ of BioHg to Arctic surfaces. We believe that our study provides critical information about Hg cycling in polar environments in the context of climate change and predictions of increased precipitation for the Arctic.

Polar environments are vulnerable to contaminants transported from lower latitudes via long-range atmospheric processes[4]. The Arctic is especially sensitive to mercury (Hg) toxicity[5] and coastal sites are involved in Hg cycling[6]. Mercury is a persistent and toxic element that is found both naturally and as an anthropogenically-produced compound in the environment[7], leading to worldwide increases in Hg levels in soil, sediments and aquatic ecosystems[8]. In particular, high levels of Hg have been recorded in some northerner inhabitants of the Arctic following contamination of the food chain[9]. Transported to polar ecosystems mainly as gaseous elemental mercury (Hg°), Hg can undergo rapid oxidation and deposition during Atmospheric Mercury Depletion Events (AMDEs) in the spring[3]. These events occur via photochemically-initiated reactions believed to involve marine halogens[10] that transform Hg° to particulate mercury and reactive gaseous mercury species that may eventually be deposited onto the snow. Although AMDEs have been pointed as one of the major causes of mercury deposition in arctic regions[11], recent chemical studies challenged this hypothesis by suggesting large post-depositional fluxes of Hg° back to the atmosphere and the rapid loss of Total Hg (THg) from the snow surfaces[12,13]. However, uncertainties exist about both the fate of the Hg that remains within the snowpack, especially in terms of speciation, ecosystem transfer and contamination, and the availability of this Hg for methylation, considering the lack of knowledge on MeHg sources in arctic ecosystems.

MeHg is the only form of Hg that bioaccumulates in food webs and an important pathway for MeHg formation in temperate ecosystems is the microbial methylation of bioavailable mercury (BioHg)[14,15]. High microbial diversity has been detected in Polar Regions[16,17] and microorganisms impact different compartments of the Hg cycle in polar environments[5]. Although quantifying BioHg is essential to understand the fate of deposited Hg, it has rarely been performed in polar ecosystems, owing to technical limitations. Traditional instruments with high sensitivity and reproducibility are able to measure trace Hg levels in a variety of matrixes, but not BioHg. Molecular tools, such as luminescent biosensors, have been designed to quantify the fraction of BioHg[18,19]. In the single field study that

deployed biosensors in arctic environments, a relatively high proportion of BioHg deposited during AMDEs was reported[10,20]. However, BioHg was determined in only a limited amount of samples and for a limited time period and no biosensors have been used since in arctic mercury field studies, leading to critical gaps in knowledge.

Here, we report the longest time series of BioHg measures to date, obtained during a two-month arctic field campaign in Svalbard, Norway (79°N) in 2008. This period included several AMDEs during the 3rd week of April. In order to quantify BioHg, we designed a *mer-lux* biosensor (Fig. 1a), based on previous work[21]. We performed two types of control assays to ensure that the biosensor could specifically detect variable BioHg levels in a wide range of samples, from AMDEs up until snowmelt. First, we carried out a series of calibration curves with different known Hg concentrations that allowed us to establish a detection limit of 0.5 ng.L^{-1} for our biosensor, calculated as three times the standard deviation of 5 blank reactions without Hg, which provides us with a sensitive enough assay to quantify BioHg in arctic samples. Second, comparative assays with other metals revealed the very high specificity of the biosensor for Hg (Fig. 1b).

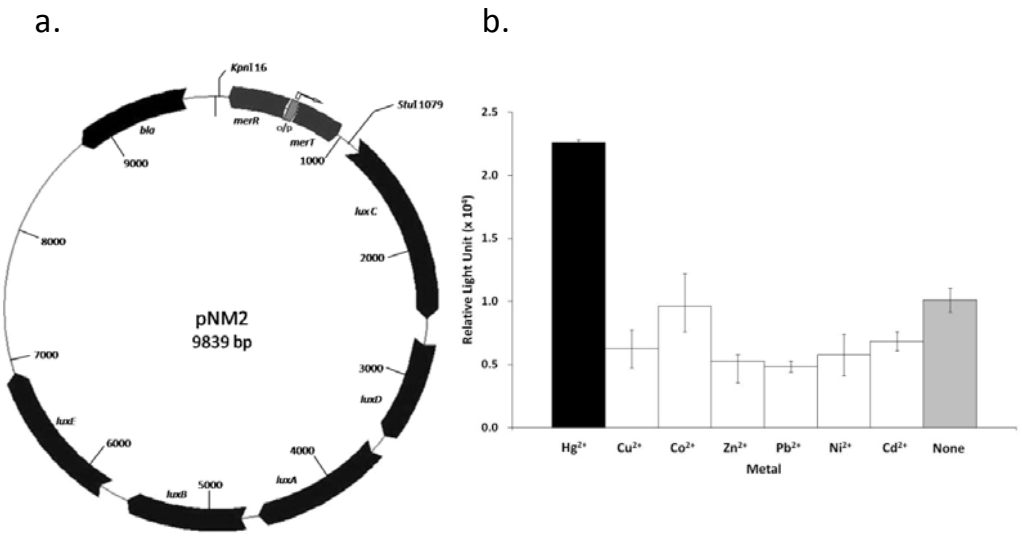

Figure 1 | Construction and specificity of the *mer-lux* biosensor. a, Schematic map of the *mer-lux* fusion plasmid pNM2 for the detection of BioHg (refer to Method Summary). This plasmid was introduced into *Escherichia coli* JM109, leading to the *mer-lux* biosensor. The following relevant informations are given on the map : *bla*, gene encoding β lactamase, conferring ampicillin resistance; *merR*, gene encoding the regulator of the *mer* operon; *merT*, gene encoding the mercury transport protein; o/p, *mer* promoter/operator locus**;** *luxABCDE* genes encoding luciferase from *Xenorhabdus luminescens*; *Kpn*I and *Stu*I are the restriction sites that were used to insert the *mer* genes into the pSBluc plasmid vector. Numbers indicate positions and size of the plasmid in base pairs. **b,** Response of the *mer-lux* biosensor to mercury and other metals. Hg^{2+} (black bar) was present as $HgCl_2$ to a final concentration of 50 $ng.L^{-1}$. Six additional metals were tested to a final concentration of 50 $ng.L^{-1}$, using the same protocol: zinc (CH_3COOZn), cobalt ($CoCl_2$), lead (CH_3COOPb), copper ($CuCl_2$), nickel ($NiCl_2$) and cadmium ($CdCl_2$). The grey bar figures the negative control measured without any metal in the medium. Vertical bars indicate the standard deviation of two separate assays of luminescence measurement. Luminescence is expressed in relative light units. The biosensor specificity was also checked with metal concentrations ranging from 0 to 500 $ng.L^{-1}$ and was demonstrated to be highly specific at all concentrations.

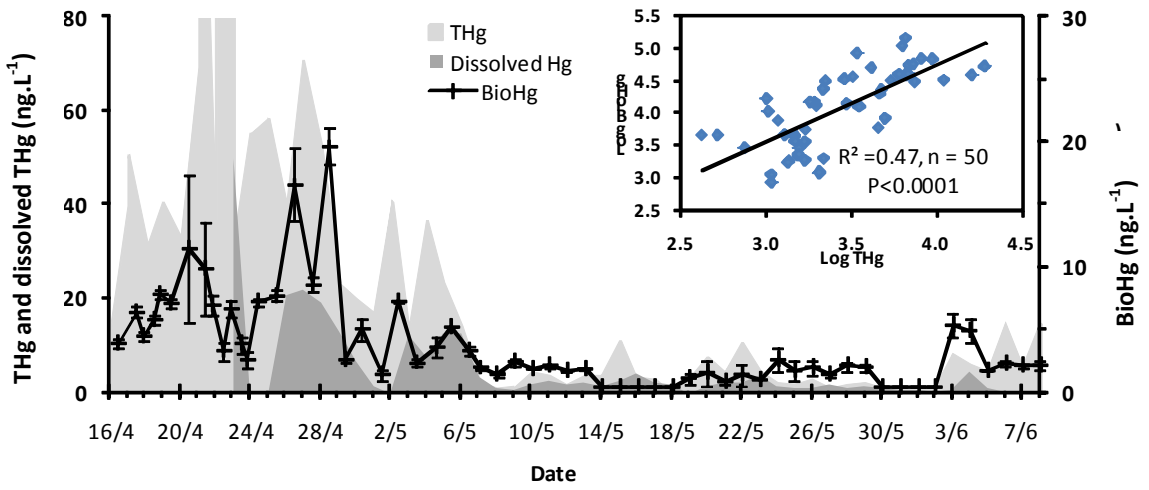

Figure 2 | Concentrations of mercury species in daily surface snow samples of an arctic snowpack. Total Hg (THg, light grey) and Dissolved Hg (after filtration on 0.45 µm filters, dark grey) are shown on the left axis. The error bars of THg and Dissolved Hg are typically less than 0.2 ng.L^{-1} and therefore cannot be represented here. Two THg concentration peaks (148.9 ng.L^{-1} and 110.6 ng.L^{-1} on April 21th and 22th respectively) are omitted on this graph for scaling clarity. Dissolved Hg measurements are not available from April 16th to April 23th. Bioavailable Hg (BioHg) is represented with a different scale on the right axis. BioHg is not available and set arbitrarily to 0 ng.L^{-1}) from both May 14th to May 18th and May 30th to June 2nd. In the upper right corner, we represent the linear relationship between THg and BioHg with log-transformed data. Significance levels were determined using the F-test.

Between the 16th of April and the 07th of June 2008, we measured THg and BioHg concentrations in surface snow samples collected daily, with AMDEs occurring between the 17th and 25th of April[22]. Two major trends emerged from these measurements (Fig. 2). First, a highly significant positive correlation ($p < 0.0001$) was detected between THg and BioHg levels measured in the surface snow samples. Second, the AMDEs period revealed high levels of both THg (up to 148.9 ng.L^{-1}) and BioHg (up to 16.2 ng.L^{-1}) deposition and these levels decreased as the season progressed. We simulated the inorganic speciation of mercury using a commercial chemical equilibrium program (Visual MINTEQ v2.61), with parameters such as chemical equilibrium, major ions, pH and some short chain organic compounds. It is however important to emphasize that Hg speciation is also modified by the presence of organic ligands such as dissolved organic carbon and humic acids that are neither integrated in the simulations nor determined in our snow samples. In the calculation, the speciation

of Hg is driven by the large chloride, and to a lesser extent bromide, contents and an acidic pH. Based on these simulations, most of our snow samples contained a large proportion of $HgCl_2$ complexes, followed by HgBrCl, $HgCl_{3^-}$ and $HgBr_2$, although a competition between chlorine and other ligands is most likely.

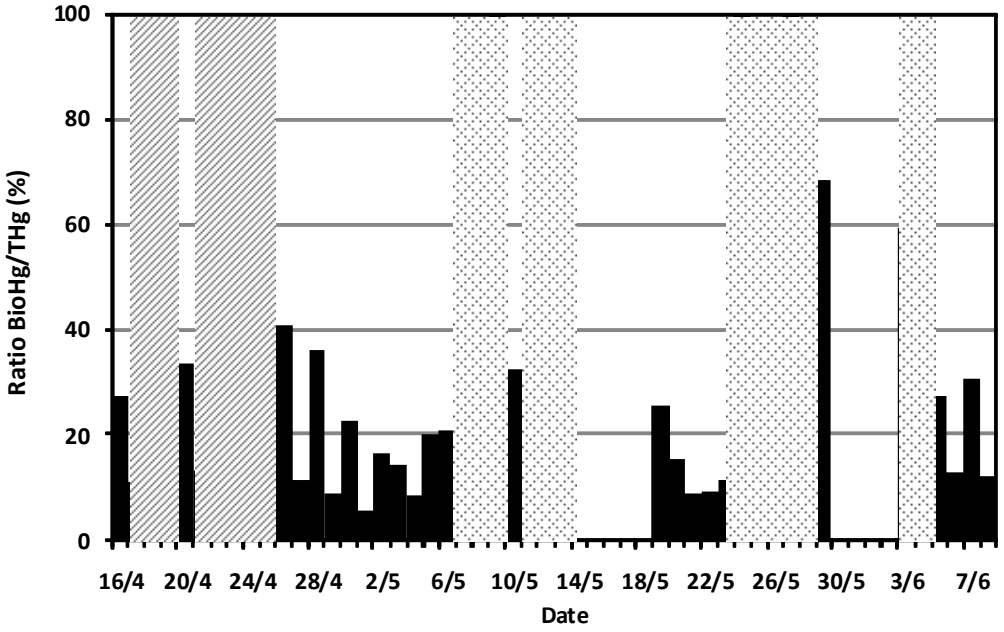

Figure 3 | Ratio of Bioavailable Hg over Total Hg. The ratio was calculated for surface snow samples collected daily over the two-month field campaign. Shaded areas with diagonal lines represent Atmospheric Mercury Depletion Events, while shaded areas with small dots represent freshly-fallen snow. Ratios are not available from both May 14th to May 18th and May 30th to June 2nd due to the absence of BioHg data.

Based on previous laboratory studies, these species are bioavailable and able to pass across biological membranes by passive diffusion[19,23]. We would therefore expect the entire fraction of Hg in our samples to be bioavailable. However, BioHg concentrations varied throughout the season and only rarely represented 100% of the THg fraction. Several explanations can be provided, all linked to post-depositional changes in Hg speciation and bioavailability. A portion is certainly photoreducible, which would account for the concomitant drop in both THg and BioHg concentrations following the AMDEs, consistent with high fluxes measured during the same period[22]. Another fraction of Hg in the

snow is bound to particles and probably not bioavailable due to large particle size (> 0.45 µm) relative to microbial cells. It is also likely that the high chloride concentrations in our samples limited bacterial uptake[19,23,24]. Finally, the drop in BioHg concentrations may be due to its rapid assimilation by microorganisms, although the reaction kinetics is unknown.

In order to determine the relative importance of AMDEs as a bioavailable Hg source to snowpacks, we compared the BioHg/THg ratio in surface samples during different events (AMDEs, wet deposition) throughout the two-month field season (Fig. 3). Higher percentages between the two AMDEs were associated with the occurrence of non Hg°-depleted air masses. While AMDEs were responsible for high levels of THg and BioHg deposited onto snowpacks, the relative amount deposited represented less than 20% of THg. In contrast, fresh snow events were always associated with an increase in the BioHg/THg ratio, which varied between 60 and 100%. A constant source of labile and bioavailable Hg was therefore scavenged from the atmosphere and its relative proportion strongly increased during wet deposition. Precipitation events occur all year long in the Arctic and we demonstrated here that they outweigh AMDEs as bioavailable Hg sources. Moreover, modeling estimates[11] have suggested that AMDEs deposit 100 $t.y^{-1}$ of Hg to the Arctic (north of 60°N), while wet and dry deposition represents 225 $t.y^{-1}$. Based on our data set, we conclude that AMDEs represent a potential source of only 20 $t.y^{-1}$ of BioHg (ratio BioHg/THg of 20%) to the Arctic. This contribution is low compared to wet and dry deposition pathways, which can potentially provide 135-225 $t.y^{-1}$ of BioHg (ratio 60-100 %) to environmental surfaces.

Our results also raise the question of the ecotoxicological relevance of AMDEs. These events are mainly recorded in early spring (March-April), yet mercury methylation is most likely to occur during periods of high productivity, *i.e.* during spring melt, which usually begins towards the end of May[12,25]. This suggests that the BioHg input from AMDEs occurs at a time of low productivity, during which methylation may be negligible. Finally, the results presented here will impact Hg mass-balance models for Polar Regions, especially in the context of the effects of climate change on contaminant

cycling, since predictions for the Arctic include increases in precipitation[26]. Based on our results, this could lead to a BioHg increase in arctic ecosystems.

Methods Summary

Surface snow mercury concentrations and speciation were monitored daily during a research campaign held between April 16th, 2008 and June 07th, 2008 at Ny-Ålesund, Svalbard, Norway (78°56'N, 11°52'E). The field site is located along the south coast of the Kongsfjorden, which is oriented east-west and open to the sea on the west side. Snow was sampled in acid-washed 250-mL glass bottles (Schott) using clean sampling techniques. Snow samples were left to melt at room temperature in the dark and aliquots were taken for total, dissolved and bioavailable Hg measurements. Total and dissolved Hg (determined after filtration on a 0.45 µm filter) were measured in triplicate with a Tekran model 2600 using USEPA method 1631 revision E. Bioavailable Hg was determined using a *mer-lux* biosensor[21]. Briefly, *Escherichia coli* JM 109 was transformed with plasmid pNM2 that we constructed by cloning the *merR* and *merT* genes with their operator/promoter region from *Cupriavidus metallidurans* CH34 upstream of the *luxABCDE* genes in plasmid pSBluc[27] (Fig.1a). Control assays for sensitivity and specificity of the biosensor were performed (Fig. 1b). Luminescence was measured using a luminometer (Modulus) with melted snow samples. Bioavailable Hg was analyzed in triplicate with three independent cultures.

References

1. Steffen, A. *et al.* A synthesis of atmospheric mercury depletion event chemistry in the atmosphere and snow. *Atmos. Chem. Phys.* **8**, 1445-1482 (2008)
2. Boudou, A. & Ribeyre, F. Experimental-Study of Trophic Contamination of Salmo-Gairdneri by 2 Mercury-Compounds - $HgCl_2$ and CH_3HgCl - Analysis at the Organism and Organ Levels. *Water Air Soil Pollut.* **26**, 137-148 (1985)
3. Schroeder, W. H. *et al.* Arctic springtime depletion of mercury. *Nature* **394**, 331–332 (1998)
4. AMAP. AMAP Assessment 2002: Human Health in the Arctic. Arctic Monitoring and Assesment Programme (AMAP). 137 (Oslo, Norway, 2003).
5. Barkay, T. & Poulain, A. J. Mercury (micro)biogeochemistry in polar environments. *FEMS Microbiol. Ecol.* **59**, 232-241 (2007)
6. Poulain, A. J. *et al.* Biological and chemical redox transformations of mercury in fresh and salt waters of the high arctic during spring and summer. *Environ. Sci. Technol.* **41**, 1883-1888 (2007)
7. Nriagu, J. O. & Pacyna, J. M. Quantitative Assessment of Worldwide Contamination of Air, Water and Soils by Trace-Metals. *Nature* **333**, 134-139 (1988)
8. Gray, J. E. & Hines, M. E. Mercury: Distribution, transport, and geochemical and microbial transformations from natural and anthropogenic sources - Preface. *Appl. Geochem.* **21**, 1819-1820 (2006)
9. Van Oostdam, J. *et al.* Human health implications of environmental contaminants in Arctic Canada: A review. *Sci. Total Environ.* **351**, 165-246 (2005)
10. Lindberg, S. E. *et al.* Dynamic Oxidation of Gaseous Mercury in the Arctic Troposphere at Polar Sunrise. *Environ. Sci. Technol.* **36**, 1245–1256 (2002)
11. Ariya, P. A. *et al.* The Arctic: a sink for mercury. *Tellus Series B* **56**, 397-403 (2004)
12. Dommergue, A. *et al.* Deposition of mercury species in the Ny-Ålesund area (79°N) and their transfer during snowmelt *Environ. Sci. Technol.* (accepted for publication)
13. Poulain, A. J. *et al.* Redox transformations of mercury in an Arctic snowpack at springtime. *Atmos. Environ.* **38**, 6763–6774 (2004)
14. Compeau, G. C. & Bartha, R. Sulfate-Reducing Bacteria - Principal Methylators of Mercury in Anoxic Estuarine Sediment. *Appl. Environ. Microbiol.* **50**, 498-502 (1985)
15. Fleming, E. J., Mack, E. E., Green, P. G. & Nelson, D. C. Mercury methylation from unexpected sources: Molybdate-inhibited freshwater sediments and an iron-reducing bacterium. *Appl. Environ. Microbiol.* **72**, 457-464 (2006)
16. Amato, P. *et al.* Bacterial characterization of the snow cover at Spitzberg, Svalbard. *FEMS Microbiol. Ecol.* **59**, 255-264 (2007)
17. Larose, C. *et al.* Microbial diversity in seasonal Arctic snow and meltwater from Svalbard, Norway *Extremophiles* (accepted for publication)
18. Selifonova, O., Burlage, R. & Barkay, T. Bioluminescent Sensors for Detection of Bioavailable Hg(II) in the Environment. *Appl. Environ. Microbiol.* **59**, 3083-3090 (1993)
19. Barkay, T., Gillman, M. & Turner, R. R. Effects of dissolved organic carbon and salinity on bioavailability of mercury. *Appl. Environ. Microbiol.* **63**, 4267-4271 (1997)
20. Scott, K. J. Bioavailable mercury in arctic snow determined by a light-emitting mer-lux bioreporter. *Arctic* **54**, 92-95 (2001)
21. Omura, T., Kiyono, M. & Pan-Hou, H. Development of a specific and sensitive bacteria sensor for detection of mercury at picomolar levels in environment. *J. Health Sci.* **50**, 379-383 (2004)
22. Steen, A. O. *et al.* Dynamic exchange of gaseous elemental mercury during polar night and day. *Atmos. Environ.* **43**, 5604-5610 (2009)
23. Gutknecht, J. Inorganic Mercury (Hg2+) Transport through Lipid Bilayer-Membranes. *J. Membr. Biol.* **61**, 61-66 (1981)

24. Compeau, G. C. & Bartha, R. Effect of Salinity on Mercury-Methylating Activity of Sulfate-Reducing Bacteria in Estuarine Sediments. *Appl. Environ. Microbiol.* **53**, 261-265 (1987)
25. Constant, P., Poissant, L., Villemur, R., Yumvihoze, E. & Lean, D. Fate of inorganic mercury and methyl mercury within the snow cover in the low arctic tundra on the shore of Hudson Bay (Quebec, Canada). *J. Geophys. Res.* **112**, D08309 (2007)
26. AMAP. AMAP Assessment 2009: Human Health in the Arctic. xiv+256 pp (Arctic Monitoring and Assessment Programme (AMAP), Oslo, Norway, 2009).
27. Lelong, C. *et al.* The Crl-RpoS regulon of Escherichia coli. *Mol. Cell. Proteomics* **6**, 648-659 (2007)

Supplementary Information: Methods

Construction of the *mer-lux* biosensor. The construction of the biosensor was based on the one developed by Omura *et al.*[21], which was reported to detect bioavailable Hg at the picomolar range. The bacteria *Escherichia coli* JM 109 was transformed with plasmid pNM2, which contains the DNA locus from *Cupriavidus metallidurans* CH34 that carries the *merR* and *merT* genes together with their operator/promoter region driving the transcription of the reporter *lux* genes in the pSBluc vector[26]. The *mer* locus was cloned as a *Kpn*I-*Stu*I fragment within pSBluc (Fig. 1b). The *mer-lux* biosensor (*E. coli* JM109::pNM2) was stored at -80°C in 20% glycerol until further use.

The biosensor was tested in the laboratory in order to determine optimal conditions. We tested for cell density, growth phase, specificity and detection limit. All tests were carried out at 37°C in LB culture medium supplemented with 100 $\mu g.mL^{-1}$ ampicillin. Bacterial cells were harvested at different time points (early and mid-exponential phase, stationary phase), diluted and exposed to different concentrations of Hg (added in a v/v ratio, with a final volume of 100 µL) in order to verify the linearity of the biosensor's response and its detection limit. After two hours of incubation at 37°C, luminescence was measured in each sample using a luminometer (Modulus). Once the optimal growth phase and cell density was determined, we used the same protocol to test for specificity using different metals such as zinc (CH_3COOZn), cobalt ($CoCl_2$), lead (CH_3COOPb), copper ($CuCl_2$), nickel ($NiCl_2$) and cadmium ($CdCl_2$).

Field assays were carried out to determine the robustness of the biosensor. The biosensor responded in a dose-dependent manner to Hg stress even in sub-optimal growth conditions (the field site lacked agitators for the incubator) and was convenient to handle in the field without the need for substrate addition. With a detection limit of 0.5 $ng.L^{-1}$ of Hg, it was sensitive enough to measure bioavailable Hg throughout the entire spring season.

Field measurements. Surface snow samples were collected daily during a spring research campaign held between April 16th, 2008 and June 07th, 2008 at Ny-Ålesund, Svalbard, Norway (78°56'N,

11°52'E). Samples were left to melt at room temperature in the dark and aliquots were collected for total, dissolved (after filtration on a 0.45 µm membrane) and bioavailable Hg. Total and dissolved Hg were measured in triplicate with a Tekran model 2600 using USEPA method 1631 revision E. Bioavailable Hg was measured using the *mer-lux* biosensor that was cultured overnight in LB medium containing 100 $\mu g.mL^{-1}$ ampicillin at 37°C without agitation. The culture was resuspended in LB media and experiments were carried out using cells in mid-exponential growth phase (OD_{600} = 0.4). Cells were exposed to either a series of Hg dilutions (0.5 to 30 $ng.L^{-1}$) in order to obtain a standard curve or to melted snow samples with unknown bioavailable Hg concentrations in a v/v ratio, and incubated for two hours at 37°C without agitation. The Hg standards were prepared from serial dilutions of a mono-elemental Hg^{2+} solution (NIST SRM-3133 Hg standard). Samples were analyzed in triplicate (using three independent cultures) and light emission was recorded using a luminometer (Modulus). Luminescence was expressed as relative light units (RLU) and normalized for optical density (measured with a spectrophotometer).

Acknowledgements This work was funded by INSU/CNRS (EC2CO and LEFE-CHAT 32), Université Joseph Fourier – Grenoble (pôle TUNES 2007) and CNRS. Logistical support was provided by the French Polar Institute IPEV (program CHIMERPOL). We acknowledge Alan Le Tressoler, Nicolas Soumis and AWIPEV for field support. We are grateful to Jacques Coves (IBS) for providing us with the *Cupriavidus metallidurans* CH34 strain. CL would like to acknowledge the FQRNT (Le Fonds Québécois de la Recherche sur la Nature et les Technologies) for a PhD research fellowship. CF thanks the Institut Universitaire de France (IUF) for its financial support.

CHAPTER 5: SEASONAL CHANGES IN SNOW CHEMISTRY LEAD TO NEW INSIGHTS INTO MERCURY METHYLATION IN THE ARCTIC

Manuscript in preparation for submission

Catherine Larose[1,2,3], Aurélien Dommergue[1], Martine De Angelis[1], Daniel Cossa[4], Bernard Averty[5], Nicolas Marusczak[1], Nicolas Soumis[1], Dominique Schneider[2,3], Christophe Ferrari[1].

[1] Université Joseph Fourier – Grenoble 1 / CNRS, LGGE

54 rue Molière BP56

38402 Saint Martin d'Hères – France

[2]Laboratoire Adaptation et Pathogénie des Microorganismes, Université Joseph Fourier Grenoble 1, BP 170,

F-38042 Grenoble cedex 9, France

[3] CNRS UMR 5163

[4] Ifremer, Centre de Méditerranée, La Seyne sur mer, France

[5]Ifremer, Centre de Nantes, Nantes, France

Abstract

Seasonal snow is an active media and an important climate factor that governs nutrient transfer in Arctic ecosystems. Since the snow stores and transforms nutrients and contaminants, it is of crucial importance to gain a better understanding of the dynamics of contaminant cycling within the snowpack and its subsequent release to catchments via meltwater. Over the course of a two-month field campaign in the spring of 2008, we collected snow and meltwater samples from a seasonal snow pack in Ny-Ålesund, Norway (78°56'N, 11°52'E), which were analyzed for inorganic and organic chemical species, as well as total, dissolved, bioavailable (THg, DHg, BioHg, respectively) and methylmercury (MeHg) species. We observe a seasonal gradient for ion concentrations, with surface samples becoming less concentrated as the season progressed. A significant negative correlation between bioavailable Hg and MeHg (r^2=0.26, p=0.0044, n=26) was observed in the snowpack. MeHg was positively and significantly correlated to methylsulfonic acid concentrations (r^2=0.45, p=0.0022, n=18). Based on these results, we propose a new model for aerobic methylation of mercury involving dimethylsulphoniopropionate.

Introduction

For High Arctic ecosystems, snow is one of the most important climatic factors. Snow is an active media that transfers particulates and gases between the atmosphere and landscape (Jones 1999), is highly photochemically active with snowpack impurities photolyzed to release reactive trace gases

into the boundary layer (Grannas et al. 2007a), and with its high albedo, fresh snow reflects as much as 90% of incoming radiation (Hinkler et al. 2008). Snow affects both the length of the growing season and primary plant production by acting as a soil insulator and also as a water and nutrient reservoir (Kuhn 2001; Edwards et al. 2007). Atmospheric scavenging and condensation largely condition snowpack chemistry and snowpacks accumulate particles, solutes and pollutants over winter and spring (Tranter et al. 1986; Loseto et al. 2004). Once deposited, they are subject to redistribution via different processes such as melt–freeze events during the winter season (Johannessen 1978), the geometry of the pore space, vapor pressure gradients and wind pressure, in addition to snow metamorphism and the physical-chemical properties of the particles themselves (Colbeck 1989; Kuhn 2001).

The Arctic is exposed to mercury (Hg), a toxic metal that can be transformed to methylmercury (MeHg), a potent neurotoxin that bioaccumulates in food webs see review by (Fitzgerald et al. 2007). Although there are no direct anthropogenic Hg sources in the Arctic, high levels have been found in the livers and tissues of marine mammals and birds (Wagemann et al. 1998; Campbell et al. 2005) leading to increased exposure for Native Communities that depend on these resources (AMAP 2009). The discovery of atmospheric mercury depletion events (AMDEs) in the Arctic (Schroeder et al. 1998) led to the hypothesis that these were the major sources of Hg to Arctic ecosystems. During AMDEs, atmospheric elemental mercury is oxidized to divalent mercury through reactions with halogens such as bromine radicals (Lindberg et al. 2001; Ariya et al. 2002) and then deposited onto snow surfaces at levels 400-800 fold higher within the space of hours (Lu et al. 2001; Dommergue et al. 2009). Recent reports suggest that some of this newly deposited Hg is bioavailable, i.e. able to cross biological membranes (Scott 2001; Lindberg et al. 2002; Larose et al. Submitted), but its post-depositional fate remains unclear. Field experiments have shown that Hg can be both oxidized and reduced in the snowpack (Lalonde et al. 2002; Dommergue et al. 2003; Poulain et al. 2004) and there is an increasing consensus that most of the deposited mercury is photo-reduced and reemitted back to the atmosphere (Poulain et al. 2004; Kirk et al. 2006).

In addition to the uncertainty regarding Hg sources to the Arctic, the mechanisms that produce MeHg in these cold environments are to date unresolved, although several pathways have been proposed. Methylation can occur both biotically and abiotically; biotic Hg methylation depends on microbial activity and the concentration of bioavailable mercury (BioHg) (Barkay et al. 1997), while abiotic methylation depends on the presence of methyl donors such as small organic molecules (i.e. methyl iodide and dimethylsulfide or acetate (Hammerschmidt et al. 2007) and larger organic components of dissolved organic matter such as fulvic and humic acids (Weber 1993; Siciliano et al.

2005). The chemistry of the snowpack therefore influences both Hg speciation and its transformation.

Since the snow stores and transforms atmospherically derived pollutants (Colbeck 1981; Daly and Wania 2004; Lei and Wania 2004), a better understanding of the dynamics of contaminant cycling within the snowpack, and its subsequent release to catchments via meltwater would help evaluate ecotoxicological impacts. The timing and magnitude of a pulse exposure is especially important for aquatic ecosystems during spring when biological activity is beginning (Loseto et al. 2004). The chemical concentrations at the initial stages of melt have been shown to be many times higher (3-7 fold) than averages for the entire snowpack in field and laboratory experiments, a phenomenon referred to as ionic pulse (Johannessen 1978; Colbeck 1981; reviewed by Kuhn 2001). As the snow begins to melt, soluble ions are removed by the first stages of percolation (e.g. Tranter et al. 1986), followed by the preferential elution of some ions before others (Eichler 2001). Species such as non-polar organic molecules are also found in meltwater, but are less easily entrained by percolating water due to their weak solubility (Meyer et al. 2006). Insoluble particulate material can also be removed by percolation, but usually remains in the snow until the final stages of melting (Hodgkins 1998; Lyons 2003; Meyer et al. 2006). During melt in the spring, these soluble and insoluble impurities are released to the environment in a few weeks and can impact the chemistry of snowmelt-fed ecosystems (Williams et al. 2009).

Here we present the chemical data from a seasonal Arctic snowpack sampled over a two-month period in the spring of 2008 in Ny-Ålesund, Norway. The focus of this research is the storage, transfer and subsequent release of solutes and mercury from the snowpack to snowmelt-fed ecosystems. We also explore possible interactions among the different chemical parameters that could potentially be involved in mercury methylation.

Material and methods

Field site:

The spring research campaign was held between April 16th, 2008 and June 8th, 2008 at Ny-Ålesund in the Spitsbergen Island of Svalbard, Norway (78°56'N, 11°52'E). The field site, a 50 m^2 perimeter with restricted access (to reduce contamination from human sources), is located along the south coast of the Kongsfjorden, which is oriented SE-NW and open to the sea on the west side. The Kongsfjorden was free of sea ice throughout the campaign.

Sampling:

Surface snow samples were collected daily for Hg speciation. Twice a week, a shallow pit was dug and both surface and basal samples were collected for ion and mercury analyzes. Samples for ion measurements were collected in sterile polycarbonate vials (acuvettes®) and stored at -20°C until analysis. For Hg analyzes, snow was collected in acid-washed 250 mL glass Schott bottles (see cleaning protocol outlined in (Ferrari et al. 2000) for more details) and subsampled for dissolved and BioHg. Samples for MeHg were collected in 125 mL acid-washed Teflon coated low-density polyethylene bottles and stored frozen until analysis. Meltwater was collected in acid-washed 250 mL glass Schott bottles from streams that formed the 1st of June, 2008.

In order to determine the spatial variability in mercury deposition, we sampled two snowpits integrating snow fall since the previous summer, the first on the Holtedahlfonna glacier (sample date 30/04/08, N79°08.17, E13°16.12, 1173 m, 40 km from the fjord) and the second on the Kongsvegen glacier (sample date 19/05/08, N78°45.29, E13°20.20, 670 m, 40 km from the fjord). The Holtedahlfonna pit, with a depth of 1.80 m, was sampled at 20 cm intervals, while the Konsvegen pit, with a depth of 2.75 m, was sampled at 30 cm intervals.

Field blanks were collected, filled with ultrapure water in the laboratory, opened during sample collection and handled as samples. To avoid contamination, Tyvex® body suits and latex gloves were worn during sampling and gloves were worn during all subsequent handling of samples.

Chemical analyzes:

Total Hg & speciation

THg in snow samples was measured in the field with a Tekran model 2600 using USEPA method 1631 revision E. Samples were oxidized to 0.5% v/v BrCl to preserve divalent Hg (Hg^{2+}) in solution and to digest strongly bound Hg^{2+} complexes. Excess BrCl was neutralized with pre-purified hydroxylamine hydrochloride. The sample is then automatically injected together with $SnCl_2$ to a reaction vessel, reducing Hg^{2+} to gaseous elemental Hg (Hg°). Hg° is carried in an argon stream to two online gold traps. After thermal desorption, Hg° is detected by atomic fluorescence spectrometry. The Tekran Model 2600 was calibrated every day with the NIST SRM-3133 Hg standard. All samples were analyzed in triplicate. Dissolved total Hg (DHg) concentrations were determined in all samples by measuring Hg concentrations after filtration on a 0.45 µm filter. BioHg concentrations were determined using the biosensor described in Larose et al. (In preparation). BioHg is detected using a genetically modified bacterium containing mercury resistance and luminescence genes, such that photons are produced in a dose dependent manner upon Hg exposure. Briefly, the biosensor was

cultured overnight in LB medium containing 100 µg/ml ampicillin at 37°C without agitation. The culture was resuspended in LB media and experiments were carried using cells in mid-exponential growth phase (OD_{600} of 0.4). Cells were exposed to either a series of Hg dilutions in order to obtain a standard curve, or to melted snow samples with unknown bioavailable Hg concentrations in a v/v ratio and incubated for two hours at 37°C without agitation. The Hg standards were prepared from serial dilutions of a monoelemental Hg^{2+} solution (SRM-3133 Hg standard). Samples were analyzed in triplicate, with three independent cultures, and light emission was recorded using a Modulus luminometer. Luminescence was expressed as relative light units (RLU) and normalized for optical density.

The pH was monitored at 20°C in all samples (Heito pH meter, Paris). In order to examine possible interactions between Hg speciation and snow chemical composition, inorganic ions (NO_3^-, Cl^-, SO_4^{2-}, NH_4^+, Ca^{2+}, Na^+, K^+ and Mg^{2+}) and organic acid (methanesulfonic acid (MSA), glutaric acid (Glut), oxalic acid (Ox),acetyl-glycine (Ace.Glyc), formate (F) and fluoride (Fl)) concentrations were measured at the Laboratoire de Glaciologie et Géophysique de l'Environnement by conductivity-suppressed Ion Chromatography using a Dionex ICS 3000. Due to the proximity of the fjord, samples were diluted 10 fold for organic acids and 100-1000 for inorganic ions prior to analysis.

Methylmercury analysis

All Teflon bottles were hermetically sealed, double-wrapped in polyethylene bags, stored at -20°C and transported frozen to the laboratory in France. MeHg was measured on unfiltered samples as volatile methyl mercury hydride, by purge and cryo-trapping gas chromatography, and detected as elemental Hg vapor by atomic fluorescence spectrometry (Tekran, Model 2500). The mercury hydrides (from methyl and inorganic mercury) were formed with $NaBH_4$, purged from the sample with He, concentrated and then separated by cryogenic chromatography before being converted into Hg^0 in a furnace (800°C) and detected by the AFS detector. This protocol is derived from the hydride generation technique described by (Tseng et al. 1998) and improved by (Stoichev et al. 2004). The hydrides are formed within a glass reactor and the column used is a silanized glass tube filled with Chromosorb W/AW-DMCS impregnated with 15% OV-3. Analytical reproducibility varied with time between 6% and 15%. Calibration was performed using the dilutions of a 1 g L^{-1} stock MMHg solution in isopropanol. The dilutions of the stock solution were performed in an aqueous HCl (0.4% Suprapur, Merck) solution. In addition, we used certified reference material, the ERM-AE670 from the Institute for Reference Materials and Measurements (IRMM, European Commission), which is $CH_3{}^{202}HgCl$ in a 2 % ethanol/water solution. The recovery of the spikes in seawater samples of 0.05 and 0.1 pmol L^{-1}

of ERM-AE670 was 103 ± 2% and 99±2%, respectively. The MeHg measurements took place within two months of sampling.

In order to determine Hg speciation within the snowpack, Vimteq simulations (Visual MINTEQ) that include parameters such as chemical equilibrium, major ions, pH and some short chain organic compounds were carried out.

Statistics

All data were log-transformed prior to statistical analysis in order to obtain data with a normal distribution with the exception of pH values. Statistical data analysis was performed using JMP 5.1 software (SAS Institute, 2003) and R. Simple linear regression analysis was carried out to detect associations between the different chemicals. Principal component analysis (PCA) was performed to reduce the dimensionality of the data set using the ade4 data package for R (The R Project for Statistical Computing http://www.r-project.org). Samples were clustered using Ward's linkage for hierarchical cluster analysis, where the error sum of squares at each successive clustering step is minimized. Analysis of variance (ANOVA) and Tukey-Kramer HSD multiple comparison tests were then used to determine significant differences in chemical parameters among the different clusters in JMP 5.1. Statistical significance was set at a probability level $\alpha < 0.05$.

Results

Snowpack dynamics

The seasonal snowpack began to develop in October, 2007, but a rain event in January 2008 resulted in a decrease in snow depth and the formation of a relatively thick (~10cm) ice layer above the soil surface (A. Le Tressoler, personal communication). The snowpack reformed above the ice layer and had a thickness of about 40 cm at the beginning of the sampling period (16th of April) and had disappeared almost completely by the 8th of June. Snow melt began mid May (around the 20th) and meltwater rivers that flowed to the fjord formed on the 1st of June, 2008. A total of 7 snowfall events occurred throughout the campaign.

Snowpack and meltwater chemistry

The snowpack is influenced by marine aerosols due to the proximity of the fjord. The dominant cations in the snowpack were Na^+ (1861 µeq L^{-1}) followed by Mg^{2+} (426 µeq L^{-1}) and Ca^{2+} (110 µeq L^{-1}), while the dominant anions were Cl^- (2119 µeq L^{-1}) followed by SO_4^{2-} (159 µeq L^{-1}) and NO_3^- (5 µeq L^{-1}). In meltwater, the average concentrations for cations and anions were 433, 263 and 359

µeq L^{-1} for Na^{+}, Mg^{2+} Ca^{2+}, respectively, and 569 µeq L^{-1} for Cl^{-}, 90 µeq L^{-1} for SO_4^{2-} and 4µeq L^{-1} for NO_3^{-}. In the snowpack, pH ranged from acidic to circumneutral values (2.9 to 6.6) and was stable at a pH around 6.8 in meltwater.

Based on the Vimteq results, mercury chloride ($HgCl_2$) is the dominant form of Hg complexes in all our samples, followed by HgBrCl, $HgCl_3^{-}$, $HgBr_2$. The speciation of Hg is driven by the large concentrations of chloride, but remains uncertain due to the lack of knowledge on binding constants of mercury with organic matter and the lack of robust speciation data of organic matter in snow. The presence of Hg complexes bound to organic compounds could readily change the photoreactivity and bioavailability of these complexes.

In order to reduce the dimensionality of the data set, we performed PCA analysis and then clustered the samples using Ward's linkage. The clustering results are presented in table I and the PCA is presented in Figure 1.

Table I: Groups, corresponding samples and sample dates as derived from PCA analysis and Ward's linkage for hierarchical clustering analysis

Cluster name	Nature of the sample	date
Group 1	early season surface snow and most of basal snow samples	16/04/08 to 06/05/2008
Group 2	mid-season surface snow	09/05/2008 to 30/05/2008
Group 3	late-season surface snow	01/06/2008 to 8/06/2008
Group 4	meltwater samples	01/06/2008 to 08/06/2008
Group 5	an early surface sample and four basal samples	19/04/2008,23/04/2008, 29/04/2008,09/05/2008, 20/05/2008

A general season effect is apparent, since group 1 comprises early season surface samples and most of the basal samples, group 2 contains mid-season surface samples, group 3 contains late-season surface samples, and group 4 is composed of meltwater samples. Although precipitation events occurred at different time periods throughout the campaign, they had no effect on sample distribution within the PCA, since samples collected during snowfall events did not cluster together. In the graphical representation of the PCA analysis, the length of the arrow represents the relative importance of the associated parameter in determining the distribution of samples. Based on the PCA analysis carried out on our data, the most important parameters driving sample distribution are BioHg and THg (group 1), MeHg, MSA and Glut (group 2), inorganic ions (group 5) and certain organic acids (group 4). The clustering of samples in group 3 is driven by low concentrations in inorganic ions and organic acids.

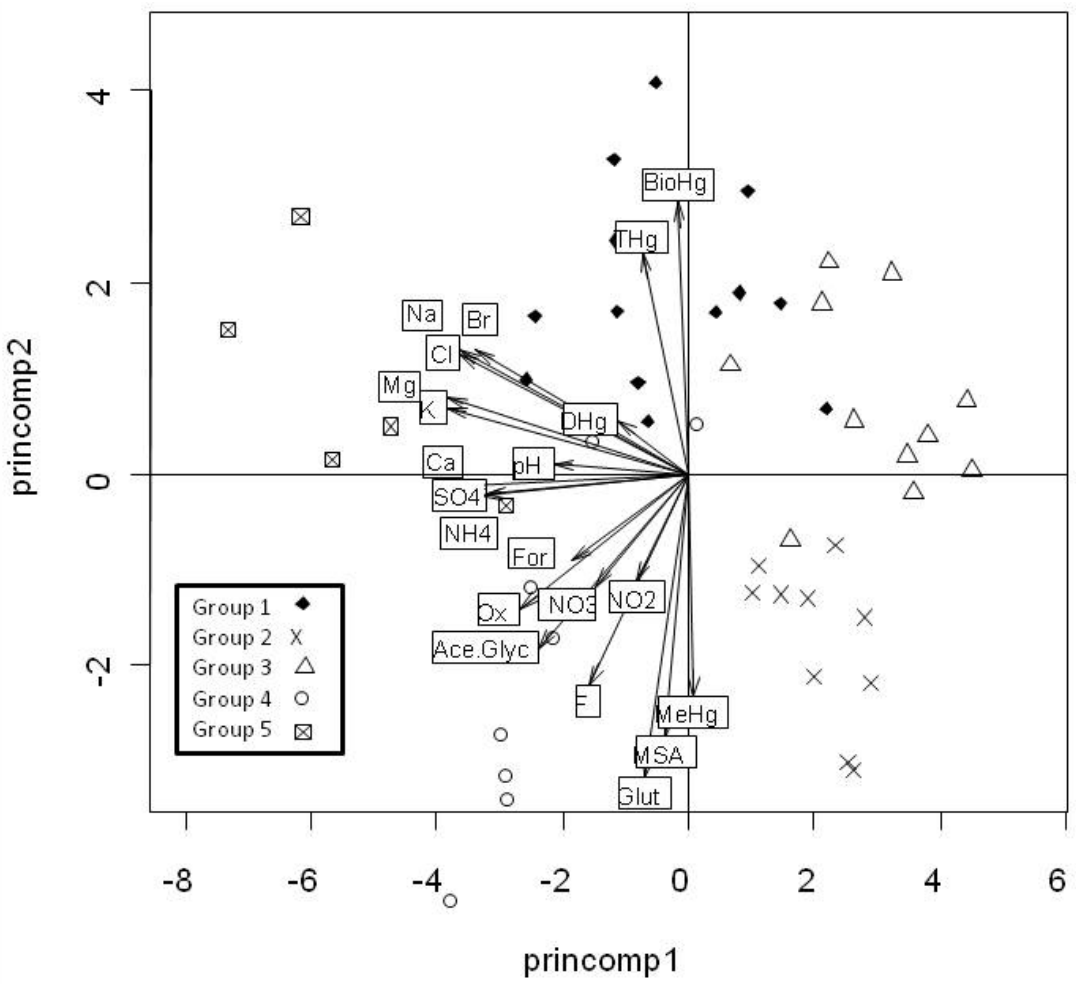

Figure 1: Principal component analysis for the sampling period. Chemical data (µeq.L^{-1} or ng.L^{-1} for Hg species) was log-transformed prior to analysis. The data set covers the entire sampling period (16th April- June 8th). Abbreviations: Glut=glutaric acid, MSA=methanesulfonic acid, Ox=oxalic acid, For=formate, F=fluoride, Ace.Glyc=acetyl-glycine, BioHg=bioavailable Hg, THg=total Hg, MeHg=methylmercury

ANOVA and multiple comparison tests were carried out in order to determine significant differences in chemical parameters among the 5 groups derived through PCA analysis and clustering using Ward's linkage. The results of these comparisons are presented in Table II. Chemical parameters varied significantly among groups, with the exception of THg, DHg and BioHg (data not shown) (Table II). There appears to be a seasonal gradient, with early season snow (group 1) that is generally more concentrated than snow sampled later in the season (groups 2 and 3). Meltwater (group 4) is enriched in ions relative to snow, with the exception of the five snow samples in group 5 that had the highest mean Na^+, NH_4, K^+, Mg^{2+}, Cl^-, SO_4^{2-} and Br concentrations. Group 5 and group 4 had the highest Ca^{2+} concentrations, and group 4 had the highest NO_2 levels and organics.

Table II: Mean and standard error of different chemical parameters among the 5 groups of samples. Concentrations are expressed in $\mu eq.L^{-1}$. Values with the same letter are not significantly different (Tukey-Kramer HSD, α=0.05). The statistics column contains the results and significance of the ANOVA comparisons.

Chemical parameter	statistics	1	2	3	4	5
pH	r^2=0.66, p<0.0001	5.2 [b] (3.5-6.5) n=13	4.2 [c] (2.9-5.1) n=11	5.4 [b] (4.6-6.6) n=11	6.8 [a] (6.4-7.1) n=9	5.8 [b] (5.1-6.4) n=5
Na	r^2=0.83, p<0.0001	647.3 [b] (141.8-1123.8) n=13	65.0 [c] (23.6-180.5) n=11	73.2 [c] (12.5-179.1) n=11	524.7 [b] (194.3-1258.2) n=9	13018.4 [a] (2185.7-31044.8) n=5
NH4	r^2=0.62, p<0.0001	11.3 [b] (1.3-26.0) n=13	9.5 [b] (3.6-19.9) n=11	2.1 [c] (1.3-3.7) n=11	10.2 [b] (8.0-15.7) n=9	46.1 [a] (15.6-100.5) n=5
K	r^2=0.86, p<0.0001	12.0 [c] (2.5-20.2) n=13	1.3 [d] (0.6-3.6) n=11	1.2 [d] (0.3-3.7) n=11	28.9 [b] (12.3-64.8) n=9	255.0 [a] (40.6-584.4) n=5
Mg	r^2=0.85, p<0.0001	147.5 [b] (32.0-259.8) n=13	18.1 [c] (5.5-50.0) n=11	16.6 [c] (3.5-44.6) n=11	264.6 [b] (133.9-505.9) n=9	2974.0 [a] (488.7-7074.8) n=5
Ca	r^2=0.63, p<0.0001	59.3 [b] (7.1-108.3) n=13	19.3 [c] (6.8-50.9) n=11	14.4 [c] (6.5-34.7) n=11	329.2 [a] (88.6-653.7) n=9	647.9 [a] (90.4-1748.6) n=5
Ox	r^2=0.65, p<0.0001	0.21 [b] (0-0.60) n=13	0.34 [b] (0.11-0.85) n=11	0.11 [b] (0-0.22) n=11	1.56 [a] (0-5.69) n=9	2.33 [a] (0.57-4.75) n=5
MSA	r^2=0.70, p<0.0001	0.05 [b] (0-0.24) n=13	1.81 [a] (1.01-3.07) n=11	0.09 [b] (0-0.40) n=11	2.15 [a] (0-9.55) n=9	0 (0-0) n=5
MeHg	r^2=0.37, p=0.0032	0.009 [b] (0.004-0.014) n=8	0.089 [a,b] (0.004-0.51) n=11	0.02 [a,b] (0.004-0.058) n=11	0.076 [a] (0.042-0.245) n=9	0.011 [a,b] (0.010-0.012) n=2
Cl	r^2=0.83, p<0.0001	768.9 [b] (156.1-1368.8) n=13	77.7 [c] (27.8-207.0) n=11	83.1 [c] (17.3-200.9) n=11	667.2 [b] (230.7-1456.7) n=9	14731.3 [a] (2435.5-35482.9) n=5
SO4	r^2=0.64, p<0.0001	44.8 [b] (10.1-94.4) n=13	21.6 [b] (9.6-41.4) n=11	3.8 [c] (0.1-19.1) n=11	88.6 [a,b] (23.6-126.0) n=9	1117.0 [a] (141.4-2179.3) n=5
NO3	r^2=0.35, p=0.0004	3.2 [b,c] (1.0-6.0) n=13	9.6 [a] (4.1-19.3) n=11	1.2 [c] (0-7.8) n=11	4.3 [b,c] (0-16.0) n=9	11.4 [a,b] (5.3-25.9) n=5
NO2	r^2=0.42, p=0.005	0.26 [a,b] (0-1.08) n=13	0.06 [b] (0-0.20) n=11	0.03 [b] (0-0.37) n=11	0.89 [a] (0-3.14) n=9	0 (0-0) n=5
Br	r^2=0.73, p<0.0001	1.51 [b] (0.25-4.56) n=13	0.15 [d] (0.07-0.36) n=11	0.24 [c,d] (0.05-1.06) n=11	0.88 [b,c] (0-3.97) n=9	30.8 [a] (5.45-76.6) n=5
Na:Cl	r^2=0.12, p=0.05	0.85 [a] (0.74-0.91) n=13	0.84 [a] (0.74-0.99) n=11	0.87 [a] (0.72-0.92) n=11	0.80 [a] (0.7-0.88) n=9	0.89 [a] 0.87-0.90) n=5
Br:Cl	r^2=0.09, p=0.36	0.0019 [a] (0.0005-0.0036) n=13	0.0023 [a] (0.0013-0.0042) n=11	0.0030 [a] (0.0013-0.013) n=11	0.0013 [a] (0-0.005) n=9	0.0020 [a] (0.0014-0.0022) n=5
SO4:Cl	r^2=0.35, p<0.0001	0.062 [b] (0.023-0.103) n=13	0.430 [a] (0.088-1.266) n=11	0.034 [b] (0.001-0.094) n=11	0.180 [b] (0.052-0.460) n=9	0.076 [b] (0.058-0.098) n=5
K:Cl	r^2=0.67, p<0.0001	0.016 [b] (0.012-0.019) n=13	0.019 [b] (0.013-0.034) n=11	0.015 [b] (0.006-0.027) n=11	0.052 [a] (0.016-0.087) n=9	0.017 [b] (0.016-0.018) n=5
Ca:Cl	r^2=0.40, p<0.0001	0.085 [b,c] (0.041-0.262) n=13	0.282 [a,b] (0.108-0.524) n=11	0.382 [a,b] (0.054-1.263) n=11	0.660 [a] (0.061-1.34) n=9	0.041 [c] (0.037-0.049) n=5
Mg:Cl	r^2=0.45, p<0.0001	0.195 [b] (0.165-0.227) n=13	0.235 [b] (0.147-0.355) n=11	0.247 [b] (0.064-0.619) n=11	0.474 [a] (0.190-0.775) n=9	0.204 [b] (0.199-0.215) n=5

Group 2 had the highest NO_3 concentrations while groups 2 and 4 had the highest MSA and glutaric acid levels. MSA and glutaric acid levels peaked in surface samples during May (Figure 2) and are significantly and positively correlated (r^2=0.62, p=0.0013, n=13).There are no significant differences among the groups in terms of Na:Cl and Br:Cl ratios, and the mean values of these ratios are close to those observed for seawater (Na:Cl=0,855 and Br:Cl=0,0015). The meltwater group has significantly higher K:Cl and Mg:Cl ratios (0.052 and 0.474, respectively) than the other groups, for whom the ratios resemble those found in seawater (K:Cl=0.0186 and Mg:Cl=0.193). Group 5 had the lowest Ca:Cl ratio, which is close to the seawater ratio (0.044), while the other groups had significantly higher values. The SO_4:Cl ratio was highest in group 2 at 0.430, and was closest to the seawater ratio (0.103) in groups 5 and 1.

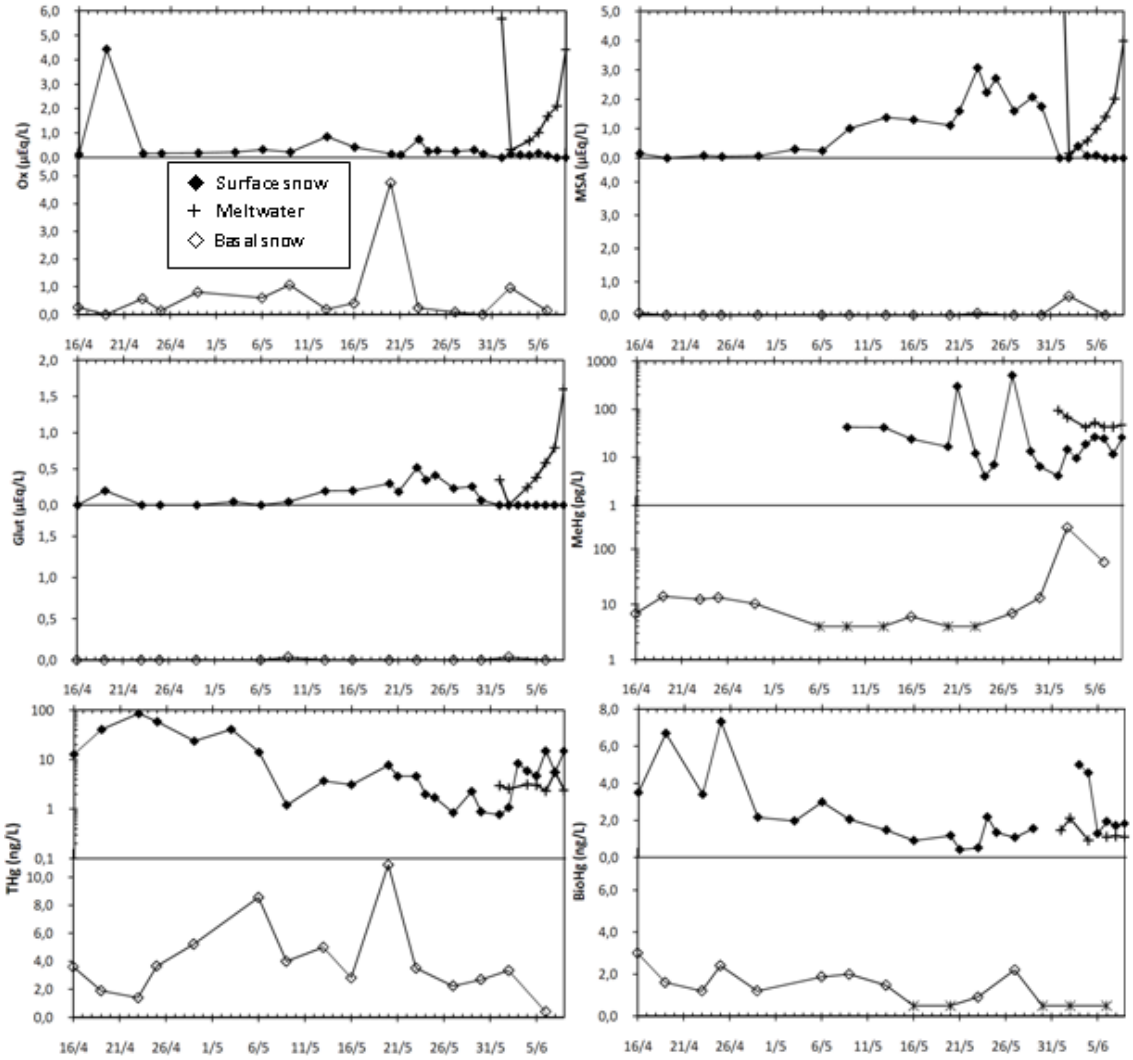

Figure 2: Chemical profiles over time for organics (MSA, glutaric acid, oxalic acid) and different mercury species. Organic concentrations are expressed in µeq.L^{-1}, while total mercury (THg) and bioavailable mercury (BioHg) are expressed in ng.L^{-1}. Methylmercury (MeHg) concentrations are expressed in pg.L^{-1}. Full squares represent surface samples, open squares represent basal samples and crosses are meltwater samples. Surface samples for MeHg and HgT are presented on a log-scale.

Meltwater samples were collected as of the 1st of June. The first sample collected had the highest Na^+, Cl^-, K^+, Mg^{2+}, SO_4^{2-} and MSA concentrations (Figure 3) and appears to correspond to the tail-end of the ionic pulse.

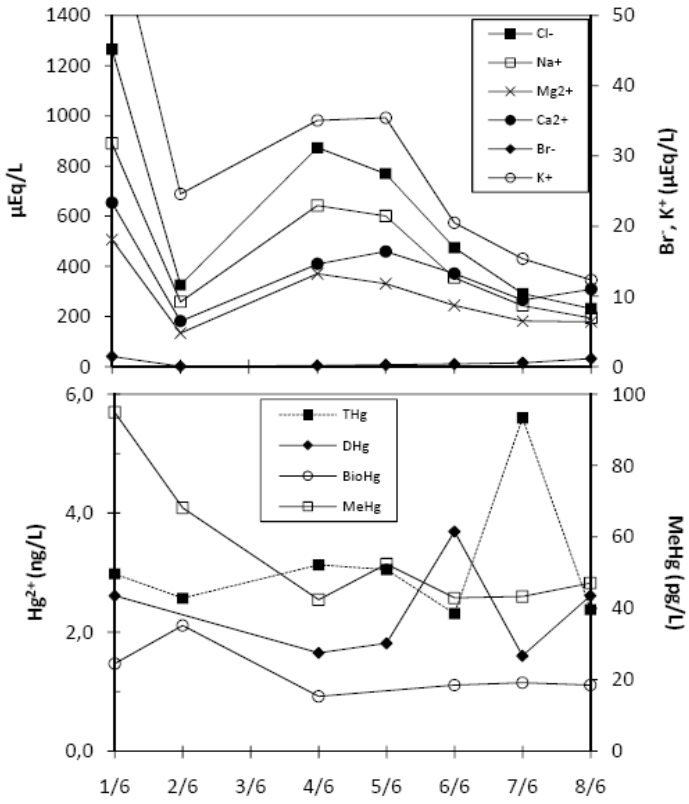

Figure 3: Meltwater elution curves for major ions and different mercury species over time. Ion concentrations are expressed in µeq.L^{-1}, while total (THg), dissolved total (DHg) and bioavailable (BioHg) mercury concentrations are expressed in ng.L^{-1}. Methylmercury (MeHg) concentrations are in pg.L^{-1}.

Glutaric acid, NO_3 and NO_2 concentrations increased as melting progressed and no peak in Br and NH_4 concentrations was observed. MeHg concentrations were highest in the first meltwater sample (1st of June), while concentrations for bioavailable Hg, dissolved Hg and total Hg peaked on the 2nd, 6th and 7th of June, respectively (Figure 3).

Hg dynamics

At the onset of sampling, surface snow had high THg concentrations, with levels reaching almost 90 ng.L^{-1}. These concentrations dropped to around 1 or 2 ng.L^{-1} by the 9th of May and increased again just prior to melt. THg concentrations in basal snow were relatively low at the beginning of the sampling period and increased gradually to levels above those of the surface around the 9th of May. THg concentrations in both basal and surface snow increased slightly from the 17th to the 23rd of May

(Figure 2). BioHg concentrations were higher in surface samples than basal samples and peaked at the beginning and end of the sampling period (Figure 2). No data was available for MeHg between the 16th of April and the 6th of May in surface samples since THg concentrations were too elevated to allow the detection of the MeHg peak with our analytical setup, but as of the 9th of May, concentrations were around 0.045 ng.L^{-1} and dropped progressively to around 0.010 ng.L^{-1} by the 25th of May. Two large MeHg peaks were measured in surface snow on the 21th and 27th of May with concentrations reaching 0.299 and 0.511 ng.L^{-1} respectively. Basal snow MeHg levels were measured throughout and concentrations were low, averaging 0.010 ng.L^{-1}, with the exception of a peak (0.245 ng.L^{-1}) on the 2nd of June (Figure 2).

Linear regression analysis was carried out to explore the relationship between different Hg species the major parameters influencing sample distribution as determined by PCA analysis. No significant linear correlations were obtained with MeHg and SO_4, NO_3 or Cl^- concentrations when samples were analyzed either together, by group or based on sampling depth. Total Hg concentrations were correlated to Cl concentrations in surface samples (r^2=0.31, p=0.0032, n=26) and basal samples (r^2=0.31, p=0.039, n=14). Based on PCA analysis, MeHg and MSA concentrations are correlated, and both are anti-correlated to bioavailable Hg concentrations. MSA, MeHg and glutaric acid also appear to be correlated (Figure 1). Linear regression analysis was carried out to determine the significance of these relationships and MeHg and MSA are significantly, positively correlated (r^2=0.45, p=0.0022, n=18), as are glutaric acid and MSA (r^2=0.62, p=0.0013, n=13), however there is no significant linear relationship between MeHg and glutaric acid (r^2=0.02, p=0.70, n=9). MeHg and bioavailable Hg are significantly, negatively correlated in the snowpack (r^2=0.26, p=0.0044, n=26), as are bioavailable Hg and MSA (r^2=0.52, p=0.0018, n=15), while no significant relationship exists between bioavailable Hg and glutaric acid (r^2=0.08, p=0.47, n=8).

THg and MeHg concentrations in glacier snowpits are presented in Figure 4.THg in both pits decreased rapidly with depth, with buried layers showing low or undetectable values. MeHg concentrations were highest in surface layers. Both pits exhibit similar MeHg patterns, with a drop in concentration in the lower layers, followed by a small increase or bump and a drop in concentrations.

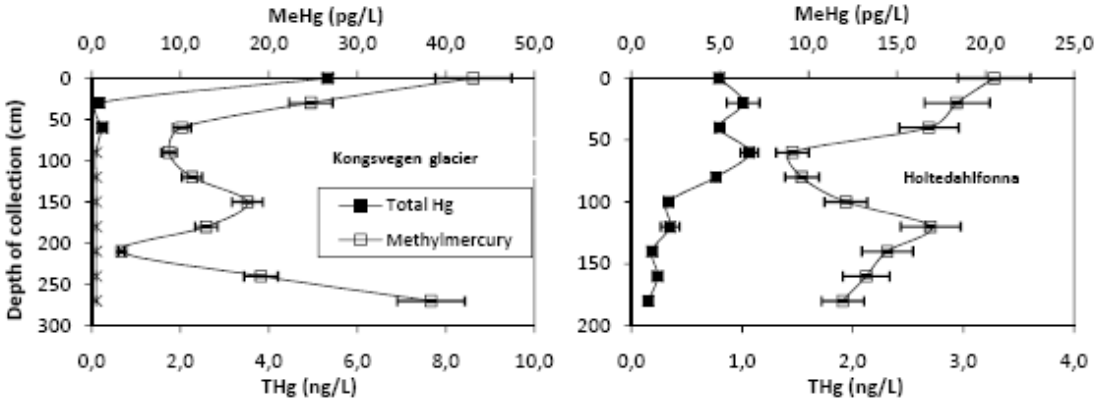

Figure 4: Snowpit total mercury (THg) and methylmercury (MeHg) profiles for Holtedahlfonna (sample date 30/04/2008) and Konsvegen (sample date 19/05/2008) glaciers.

In the Konsvegen pit, MeHg levels increased in the lowest layer (Figure 4), but not in the Holtedahlfonna pit. Organics (MSA, glutaric acid) could only be detected in surface and bottom layers whileSO_4:Cl, Na:Cl and Br:Cl ratios resembled those for seawater. Mg:Cl, K:Cl and Ca:Cl ratios were much higher than those of seawater. The detailed chemistry for both pits is given in Table III.

Table III: Values for chemical parameters at different depths for Holtedahlfonna (H) and Konsvegen (K) snow pits. Ion concentrations are expressed in µeq.L^{-1}

Snow sample	MSA	Cl	Br	NO3	Glut	SO_4	Na	NH4	K	Mg	Ca
H 0cm	0.12	5.56	0.00	1.27	0.03	5.38	5.39	1.64	0.13	1.79	1.81
H 20 cm	0.00	18.06	0.22	0.63	0.00	1.84	17.25	0.57	0.19	3.92	1.84
H 40 cm	0.00	62.37	0.52	3.06	0.00	8.40	56.82	2.16	0.89	16.26	4.79
H 60 cm	0.00	35.75	0.43	0.80	0.00	3.51	32.95	1.23	0.38	11.25	3.77
H 80 cm	0.00	46.21	0.43	0.69	0.00	4.70	37.83	1.08	0.37	12.63	2.68
H 100 cm	0.00	7.25	0.09	0.53	0.00	1.91	6.50	0.72	0.08	2.55	1.69
H 120 cm	0.00	21.98	0.22	0.70	0.00	2.03	19.43	1.30	0.29	6.45	1.97
H 140 cm	0.00	14.57	0.13	0.40	0.00	1.48	14.03	0.38	0.15	4.32	1.42
H 160 cm	0.00	0.89	0.00	0.37	0.00	0.57	0.77	0.50	0.03	0.35	0.91
H 180 cm	0.12	3.68	0.00	1.64	0.00	2.27	0.79	0.77	0.09	4.08	3.84
K 0 cm	1.66	13.53	0.22	3.10	0.07	16.10	12.01	4.68	0.11	5.98	4.72
K 30 cm	0.00	15.12	0.22	0.63	0.01	2.56	13.66	0.65	0.15	5.28	1.97
K 60 cm	0.00	38.97	0.30	2.00	0.00	5.69	38.43	1.03	0.35	11.72	3.34
K 90 cm	0.00	100.42	0.90	1.03	0.00	10.76	85.67	1.01	1.37	28.09	6.40
K 120 cm	0.00	34.18	0.34	1.13	0.00	3.21	34.74	0.43	0.40	10.28	2.13
K 150 cm	0.00	21.27	0.22	0.97	0.00	4.36	19.94	1.02	0.26	6.72	2.47
K 180 cm	0.00	46.40	0.47	0.51	0.00	5.29	40.47	1.34	0.45	17.00	3.31
K 210 cm	0.00	25.90	0.30	0.97	0.01	3.55	25.49	1.18	0.35	9.06	4.64
K 240 cm	0.10	11.98	0.13	0.51	0.03	3.61	12.16	0.97	0.17	5.69	3.33
K 270 cm	0.02	6.87	0.13	0.11	0.00	0.40	5.35	0.45	0.10	1.30	0.61

No significant correlations were observed between MeHg and Hg, or between Hg species and ion concentrations.

Discussion

Snowpack and meltwater chemical composition

The snowpack evolves chemically over time. We observe a seasonal gradient in ion concentrations in the snowpack, with the highest concentrations for most ions observed in early season surface and basal snow (group 1), and the lowest concentrations in samples collected in late spring, just prior to melt (Group 3). Since melting can occur at air temperatures below 0°C when solar radiation is sufficiently intense and penetrates into the snowpack (Kuhn 1987) causing the top snow layers to melt first, the surface layers gradually become less concentrated as the season progresses. The photochemical reactivity of surface layers also contributes to changes in ion concentrations, with snowpack impurities photolyzed to release reactive trace gases such as NO_2, HONO, CH_2O, BrO and Hg^0 to the boundary layer. These processes appear to be ubiquitous and the significance of their influence varies according to background concentrations of radicals (Grannas et al. 2007b).

Our results are consistent with those of Goto-Azuma et al. (1994), who observe higher ion concentrations at the base of an Arctic snowpack as a result of percolation and snowpack metamorphism (Goto-Azuma 1994). The surface and basal samples in group 5 had the highest ion concentrations among all groups, including the meltwater group. This is surprising since meltwater mobilizes solutes and contaminants within the snowpack, thus becoming enriched relative to the snow (Kuhn 2001; Meyer and Wania 2008). The samples in group 5 carry a strong marine salt signal, as determined by the different ion to Cl^- ratios (Table II). It is likely that the surface sample of this group (sample date 19/04/2009) contained sea-spray or was enriched by marine air masses. The signal of this event may have been retraced later in the basal samples following snowfall and elution. It is also possible that the highly concentrated basal samples may consist of older snow that had undergone similar deposition events from marine air masses.

Mid-season surface snow samples (group 2, May 9th to May 30th) had high levels of glutaric acid, MSA and NO_3^-, in addition to the highest SO_4^{2-} to Cl^- ratio among all groups. Glutaric acid, a C_5 dicarboxylic acid commonly found in aerosols and as cloud-condensation nuclei, is derived from a variety of sources including anthropogenic emissions such as motor exhaust, as well as biogenic emissions from the ocean (Kawamura and Ikushima 1993; Kawamura and Kasukabe 1996). Senescent marine phytoplankton cells release lipidic cell components (chlorophyll, chlorophyll phytyl chain, carotenoids, sterols, unsaturated fatty acids (e.g. oleic acid), alkenones and unsaturated alkenes) (Rontani 2001) that can be photooxidized to shorter diacids. Among the diacids, oxalic acid is generally the most abundant reported in aerosols, followed by succinic and malonic and glutaric acid

(Kawamura and Kasukabe 1996). This has been observed in diverse environments worldwide, including the Arctic. Another pathway involved in diacid production is the reaction of O_3 with cyclohexene, a symmetrical alkene molecule (Rontani 2001). The presence of diacids in the marine environment is therefore the result of two major processes: long-range transport from industrialized continents and in situ photochemical production. Legrand et al. (2007) reported seasonal differences in diacid concentrations for a coastal site, with high oxalic acid and low C_5 and C_4 concentrations in the winter. This was suggested to be the result of the ageing of air masses during transport that favored the production of short-chain diacids through the successive oxidation of C_5 and C_4 diacids (Legrand et al. 2007). This is consistent with our data, where the early season snow oxalic acid in the first sample of group 5 seems to result from older marine air masses having travelled over the Arctic Ocean (SCIAMACHY air mass trajectory model, data not shown). Glutaric acid was almost undetectable at the beginning of the season, but concentrations were high in samples from group 2, collected in surface snow during the month of May. In the summer, Legrand et al. (2007) reported peak concentrations of C_5 and C_4 acids in a mid-latitude marine atmosphere, which may be attributed to unsaturated fatty acid degradation. The fact that we observe high glutaric acid concentrations relative to oxalic acid suggest a close source of marine emissions accompanied by fatty acids, during which the succession of oxidations to shorter diacids did not have enough time to lead to total C_5 and C_4 depletion. Glutaric acid is also significantly positively correlated to MSA, which further supports a close marine source for organic acids. MSA is indeed a photo-oxidation product of DMS, which itself is a derivative of dimethylsulphoniopropionate (DMSP) produced by phytoplankton (Bentley and Chasteen 2004). DMSP is known as both an osmoprotectant and cryoprotectant for microorganisms, as well as a carbon and sulfur source. It is released from senescent or stressed cells (Kiene et al. 2000). MSA has been shown to exhibit a distinct seasonality that is linked to biological activity in Arctic waters and the importance of the phytoplankton bloom to DMS concentrations has also been reported (Leck and Persson 1996a). The most recent published data available on algae blooms in Svalbard were collected in 2007 and report that the bloom occurred in May (Narcy et al. 2009). Although the data for the 2008 period are unavailable, it is likely that the bloom occurred at the same time period.

The chemical changes of a snowpack and runoff are influenced by the chemical composition of the snow and wintertime refreezing processes of the meltwater (Colbeck 1981), (Davies 1982), (Bales et al. 1993). The first flush of meltwater is usually highly concentrated, with the preferential elution of certain solutes over others leading to a pulse ((Colbeck 1981),(Goto-Azuma 1994)). Meltwater samples had mean ion concentrations that were comparable to those reported for early seasonal snow (group 1), with the exception of K^+, Mg^{2+} and Ca^{2+} concentrations, which were much higher. In

addition, the Mg:Cl, K:Cl and Ca:Cl were also significantly higher than in the early season samples. These elevated ratios may reflect the contact between the meltwater and the soil, since meltwater can be modified by soil processes due to infiltration and leaching (Williams et al. 2009). Although concentrations in the first meltwater sample are high, it is likely that the pulse occurred before the formation of meltwater rivers and that we only measured the tail-end of the pulse, since we were unable to detect preferential elution. However, it appears that we did observe fractionation of mercury species. MeHg is preferentially eluted to BioHg, followed by the dissolved fraction. The remaining Hg, likely bound to insoluble particles, was eluted last.

Snowpack Hg dynamics

While AMDEs have been shown to lead to high deposition of Hg onto snow surfaces, the post-depositional fate of Hg has yet to be completely clarified. The consensus among researchers now is that a large portion is reemitted back to the atmosphere following an event (Poulain et al. 2004); and others. We recorded an AMDE at the beginning of the field season that led to high concentrations in the snowpack (max value 90 $ng.L^{-1}$) that then dropped rapidly. At the beginning of the field season, basal snow sample Hg concentrations were low, around 1-2 $ng.L^{-1}$, yet they increase almost 8 fold following the AMDE-induced peak in surface snow concentrations. The mechanisms responsible for this increase are unclear, but it is likely that Hg was transferred into deeper layers of the snowpack from the surface, possibly bound to particulate matter or percolated in a mobile chemical form (Daly and Wania 2004; Johnson et al. 2008). If the Hg levels in the basal layers of the snow result from AMDEs, then the quantity retained represents roughly 10% of the initial loading. These results suggest that although a large portion of Hg deposited by AMDEs returns to the atmosphere, a non-negligible quantity is trapped within the snowpack, from which it can then be transferred to other systems upon melting.

In a review on Hg microbiogeochemistry in polar environments, Barkay and Poulain (2007) outline possible methylmercury sources and methylation pathways in arctic ecosystems. These include atmospheric and aquatic sources with either abiotic or biotic methylation pathways (Barkay and Poulain 2007). In terms of snowpack MeHg concentrations, the most plausible sources are: 1) an atmospheric source of MeHg due to the photodegradation and deposition of plankton-derived dimethylmercury, 2) *in situ* methylation of BioHg in the snowpack (microbial), 3) biotic or abiotic methylation in the atmosphere, and 4) phytoplankton MeHg production.

Based on a positive correlation between MeHg and chloride in snow collected from Ellesmere Island, Nunavut, Canada, St. Louis et al. (2005) suggested that MeHg was bound to seasalt aerosols (i.e. source 1). Constant et al. (2007) also reported a similar correlation in subarctic snow. This led to the hypothesis that MeHg originated from gaseous dimethylmercury formed by phytoplankton in the water column (St. Louis et al. 2005; Constant et al. 2007), whose production has been reported in Arctic waters (Kirk et al., 2008). Since dimethylmercury is highly volatile, it can flux from the seawater and be oxidized to MeHg in the atmosphere by radical species such as OH and Cl (Niki et al. 1983a; Niki et al. 1983b) before being deposited onto nearby snow surfaces (St. Louis et al. 2005). However, no such correlation exists in our data set, even when the different snow types and groups are analyzed individually. This has also been previously reported in snow samples collected in Resolute Bay, Canada by St Louis et al. (2007), who attributed MeHg concentrations to dimethylmercury production and subsequent photodegradation based on the proximity of their sampling sites to the water despite the absence of correlation to Cl^- (St. Louis et al. 2007).

MeHg is significantly anti-correlated to BioHg in our snow samples, which suggests that a fraction of the BioHg is being transformed into MeHg. This supports the second hypothesis outlined by Barkay and Poulain (2007). Bacteria have been isolated from Arctic snowpacks (Amato et al. 2007) and microbial activity has been measured at temperatures down to -20°C (Christner 2002). Poulain et al. (2007) reported the presence of Hg resistance (*merA*) gene transcripts in Arctic biofilm samples; therefore it is likely that the microbial populations in Arctic environments are able to metabolize mercury (Poulain et al. 2007). Whether Hg methylation can occur in the snow remains uncertain. Constant et al. 2007, reported increases in the MeHg:THg ratio and positive correlations with bacterial colony counts and particles. These results led to the hypothesis that MeHg was being formed within the snowpack, despite the absence of correlation with sulfate-reducing bacteria (SRB), the principal methylators in anoxic environments (Constant et al. 2007). Since the snowpack is most likely oxygenated, this would suggest that other species able to methylate Hg aerobically may exist.

Hg methylation has been linked to sulfur and iron metabolism in bacteria (Fleming et al. 2006; Kerin et al. 2006). Early research into the mechanisms involved in Hg methylation is based on anoxic sediments (Compeau and Bartha 1985; Berman et al. 1990) and quickly focused on anaerobic, sulfate reducing bacteria. Choi et al. (1994) used radio-labeled ^{14}C incorporation and enzyme activity measurements to propose that methylation involves the tetrahydrofolate (THF) pathway in *Desulfovibrio desulfuricans*. In their model, the methyl group is transferred from CH_3-tetrahydrofolate via methylcobalamin with either serine or formate as the original methyl donors during the acetyl-CoA synthase pathway (Choi et al. 1994).

In our samples, MeHg is positively correlated to MSA, a by-product of DMSP and an important molecule in the marine microbial sulfur cycle (Kiene et al. 2000). DMSP can be metabolized via several different pathways in the water column (Figure 5), one involving enzymatic cleavage to produce DMS, but also by demethylation and demethiolation to produce methylsulfate in bacterial cells. Methylsulfate can then undergo thiol transmethylation to produce DMS (Bentley and Chasteen 2004). The initial demethylation (and a possible second demethylation) has recently been shown to be THF-dependent and catalyzed by an amino-methyltransferase enzyme in aerobic bacteria (Reisch et al. 2008). The similarities to anaerobic Hg methylation are striking, and it is not unlikely that BioHg, upon entering the cell, may undergo methylation by aerobic bacteria able to demethylate or metabolize DMSP. A total of four methyl transfer reactions occur at various stages of DMSP metabolism, and BioHg may serve as a methyl group acceptor at some point throughout. BioHg is also negatively correlated to MSA, which further suggests DMSP implication (or the implication of another product of DMSP metabolism) in the methylation of Hg. This is compounded by the fact that neither MeHg nor BioHg are significantly linearly correlated to glutaric acid, a biogenically produced dicarboxylic acid. Finally, this hypothesis is reinforced by the recent results evidencing Hg methylation in the oxic oceanic water column (Cossa et al. 2009; Sunderland et al. 2009).

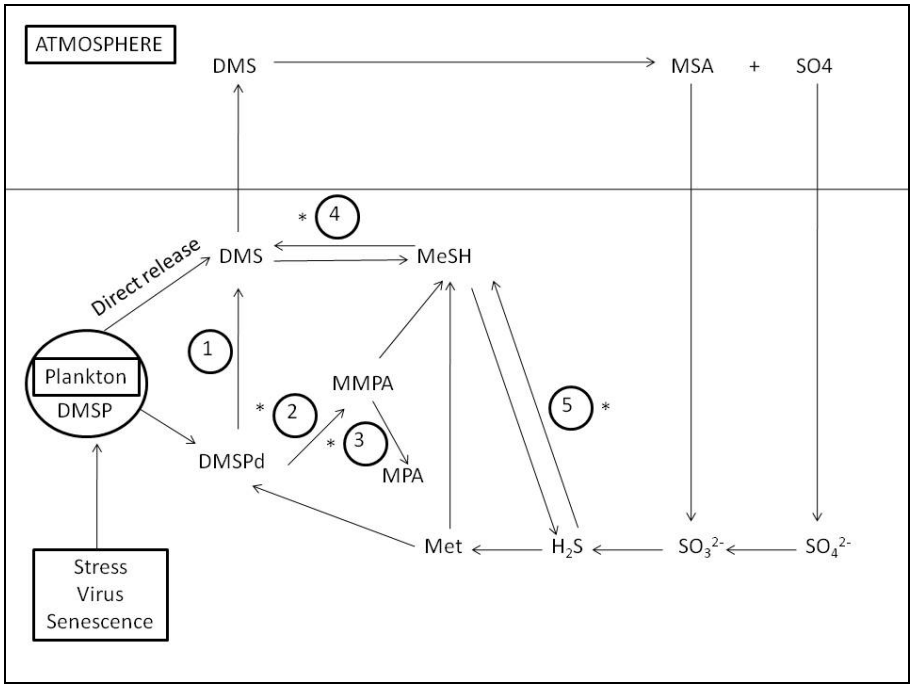

Figure 5: (modified from (Bentley and Chasteen 2004)): Sulfur cycle. The pathways represented here focus on biogenic transformations and the numbered pathways represent those discussed in the text. Other transformations occur, but are not addressed in this paper. The pathways are: 1) DMSP-lyase. 2) Demethylation. 3) MMPA demethylation. 4) Thiol transmethylation. 5) Thiol transmethylation. The star symbol represents reactions where BioHg could potentially be methylated.

Whether the methylation is occurring within the snowpack, in the water column or both simultaneously remains under debate, however, methylation appears to require a substrate involved in DMSP cycling. Therefore coastal sites may be especially at risk for MeHg contamination, since they are reported to contain higher Hg concentrations relative to inland sites (Douglas and Sturm 2004; Brooks et al. 2008) and are close to a DMSP source. In addition, the run-off during springtime melt may return concentrated water back to the aquatic ecosystem.

Although the case for biologically-produced MeHg is strong, the data from the snow pits sampled on April 30th and May 19th point to a combination of sources for MeHg in remote areas. Since the fjord is situated at a 40 km distance from both sampling sites, its effect on chemical composition is less important as reflected by the 1-3 order of magnitude lower Na^+ and Cl^- concentrations measured in our pit samples. MeHg profiles in the snowpits had concentrations that were generally higher than in the surface waters of the fjord (seasonal average 10.1±4.0 pg.L^{-1}, unpublished data) and higher than average MeHg levels in the seasonal snowpack excluding the peaks measured towards the end of May. In addition, BioHg and MSA concentrations were generally below detection limit in these samples, which would exclude the biotic methylation mechanism outlined above. THg levels were also low, and neither THg nor MeHg were significantly correlated to Cl^- concentrations. Taken together, these results suggest alternative sources for MeHg. It is possible that some form of abiotic methylation may be occurring in the atmosphere involving methyl donors such acetate and reactive mercury (not strongly bounded) in aqueous phase as proposed by Hammerschmidt et al. (Hammerschmidt et al. 2007). Kinetics obtained by Gardfelt (2003) suggest a reaction pathway where Hg^{2+} is bound to organic complexes. However, this does not exclude an oceanic source for MeHg, since the layers with marine organics also exhibit the highest MeHg concentrations. Finally, the elvated levels of MeHg in the Konsvegen basal layer may point to biotic methylation. Amato et al. (2007) found higher concentrations of bacteria in the summer layer in a pit dug on the same glacier and this may reflect microbial growth and metabolism. These potential sources may have been masked at the coastal site due to the influence of the fjord and it is likely that different pathways that lead to MeHg inputs are occurring simultaneously in Arctic environments.

Acknowledgements

This work is funded by EC2CO, LEFE-CHAT and by the French Polar Institute IPEV for logistical support. We acknowledge Alan Le Tressoler and AWIPEV for field support, as well as Emmanuel Prestat for advice on statistics. CL would like to acknowledge the FQRNT (le Fonds Québécois de la Recherche sur la Nature et les Technologies) for a PhD research fellowship.

References

AMAP (2009) AMAP Assessment 2009: Human Health in the Arctic. Arctic Monitoring and Assessment Programme (AMAP). In, Oslo, Norway

Amato P et al. (2007) Bacterial characterization of the snow cover at Spitzberg, Svalbard. Fems Microbiology Ecology 59:255-264

Ariya PA, Khalizov A, Gidas A (2002) Reactions of gaseous mercury with atomic and molecular halogens: Kinetics, product studies, and atmospheric implications. Journal of Physical Chemistry A 106:7310-7320

Bales RC, Davis RE, Williams MW (1993) Tracer release in melting snow: diurnal and seasonal patterns. Hydrological Processes 7:389–401

Barkay T, Gillman M, Turner RR (1997) Effects of dissolved organic carbon and salinity on bioavailability of mercury. Applied and Environmental Microbiology 63:4267-4271

Barkay T, Poulain AJ (2007) Mercury (micro)biogeochemistry in polar environments. FEMS Microbiology Ecology 59:232-241

Bentley R, Chasteen TG (2004) Environmental VOSCs--formation and degradation of dimethyl sulfide, methanethiol and related materials. Chemosphere 55:291-317

Berman M, Chase T, Jr., Bartha R (1990) Carbon Flow in Mercury Biomethylation by Desulfovibrio desulfuricans. Applied and Environmental Microbiology 56:298-300

Brooks S, Lindberg S, Southworth G, Arimoto R (2008) Springtime atmospheric mercury speciation in the McMurdo, Antarctica coastal region. Atmospheric Environment 42:2885-2893

Campbell LM, Norstrom RJ, Hobson KA, Muir DCG, Backus S, Fisk AT (2005) Mercury and other trace elements in a pelagic Arctic marine food web (Northwater Polynya, Baffin Bay). Science of the Total Environment 351:247-263

Choi SC, Chase Jr. T, Bartha R (1994) Enzymatic catalysis of mercury methylation by Desulfovibrio desulfuricans LS. . Applied and Environmental Microbiology 60 1342-1346

Christner BC (2002) Incorporation of DNA and protein precursors into macromolecules by bacteria at -15 degrees C. Applied and Environmental Microbiology 68:6435-6438

Colbeck SC (1981) A simulation of the enrichment of atmospheric pollutants in snow cover runoff. Water Resources Research 17 1383–1388

Colbeck SC (1989) Air movement in snow due to windpumping. Journal of Glaciology 35:209–213

Compeau GC, Bartha R (1985) Sulfate reducing bacteria: principal methylators of mercury in anoxic estuarine sediment. Applied and Environmental Microbiology 50:498–502

Constant P, Poissant L, Villemur R, Yumvihoze E, Lean D (2007) Fate of inorganic mercury and methyl mercury within the snow cover in the low arctic tundra on the shore of Hudson Bay (Québec, Canada). Journal of Geophysical Research 112

Cossa D, Averty B, Pirrone N (2009) The origin of methylmercury in open Mediterranean waters. Limnology and Oceanography 54:837–844

Daly GL, Wania F (2004) Simulating the Influence of Snow on the Fate of Organic Compounds. Environmental Science and Technology 38:4176-4186

Davies TD, Vincent, C.E., Brimblecombe, P. (1982) Preferential elution of strong acids from a Norwegian ice cap. Nature 300:161-163

Dommergue A, Ferrari CP, Poissant L, Gauchard PA, Boutron CF (2003) Diurnal cycles of gaseous mercury within the snowpack at Kuujjuarapik/Whapmagoostui, Quebec, Canada. Environmental Science and Technology 37:3289-3297

Dommergue A et al. A transfer study of mercury species to water systems in the Arctic: the case of Ny Alesund (79°N), april-june 2007. Accepted in Environmental Science and Technology

Douglas TA, Sturm M (2004) Arctic haze, mercury and the chemical composition of snow across northwestern Alaska. Atmospheric Environment 38:805-820

Edwards AC, Scalenghe R, Freppaz M (2007) Changes in the seasonal snow cover of alpine regions and its effect on soil processes: A review. Quaternary International 162–163 172–181

Eichler A, Schwikowski, M., Gäggeler, H.W., 2001. (2001) Meltwater induced relocation of chemical species in Alpine firn. Tellus 53B:192–203

Ferrari CP, Moreau AL, Boutron CF (2000) Clean conditions for the determination of ultra–low levels of mercury in ice and snow samples. Fresenius' Journal of Analytical Chemistry 366:433–437

Fitzgerald WF, Lamborg CH, Hammerschmidt CR (2007) Marine Biogeochemical Cycling of Mercury. Chemical Reviews 107:641-662

Fleming EJ, Mack EE, Green PG, Nelson DC (2006) Mercury Methylation from Unexpected Sources: Molybdate-Inhibited Freshwater Sediments and an Iron-Reducing Bacterium. Applied and Environmental Microbiology 72:457-464

Goto-Azuma K, Nakawo, M., Han, J., Watanabe,O., Azuma, N. (1994) Melt-induced relocation of ions in glaciers and in a seasonal snowpack IAHS Publication 223 287–298

Grannas AM, Bausch AR, Mahanna KM (2007a) Enhanced aqueous photochemical reaction rates after freezing. Journal of Physical Chemistry A 111:11043-11049

Grannas AM et al. (2007b) An overview of snow photochemistry: evidence, mechanisms and impacts. Atmospheric Chemistry and Physics 7: 4329-4373

Hammerschmidt CR, Lamborg CH, Fitzgerald WF (2007) Aqueous phase methylation as a potential source of methylmercury in wet deposition. Atmospheric Environment 41:1663-1668

Hinkler J, Hansen BU, Tamstorf MP, Sigsgaard C, Petersen D (2008) Snow and Snow-Cover in Central Northeast Greenland. Advances in Ecological Research 40:175-195

Hodgkins R, Tranter, M., and Dowdeswell, J. A. (1998) The hydrochemistry of runoff from a 'coldbased' glacier in the High Arctic (Scott Turnerbreen, Svalbard) Hydrological Processes 12:87–103

Johannessen M, Henriksen, A. (1978) Chemistry of snow melt water: changes in concentration during melting Water Resources Research 14:615-619

Johnson KP, Blum JD, Keeler GJ, Douglas TA (2008) Investigation of the deposition and emission of mercury in arctic snow during an atmospheric mercury depletion event. Journal of Geophysical Research 113: doi:10.1029/2008JD009893

Jones HG (1999) The ecology of snow-covered systems: a brief overview of nutrient cycling and life in the cold. Hydrological Processes 13:2135–2147

Kawamura K, Ikushima K (1993) Seasonal changes in the distribution of dicarboxylic acids in the urban atmosphere. Environmental Science and Technology 27:2227-2235

Kawamura K, Kasukabe H (1996) Sources and reaction pathways of dicarboxylic acids, ketoacids and dicarbonyls in Arctic aerosols: one year of observations. Atmospheric Environment 30:1709-1722

Kerin EJ, Gilmour CC, Roden E, Suzuki MT, Coates JD, Mason RP (2006) Mercury Methylation by Dissimilatory Iron-Reducing Bacteria. Applied and Environmental Microbiology 72:7919-7921

Kiene RP, Linn LJ, Bruton JA (2000) New and important roles for DMSP in marine microbial communities. Journal of Sea Research 43:209-224

Kirk JL, St. Louis VL, Sharp MJ (2006) Rapid Reduction and Reemission of Mercury Deposited into Snowpacks during Atmospheric Mercury Depletion Events at Churchill, Manitoba, Canada. Environmental Science and Technology 40:7590-7596

Kuhn M (1987) Micro-meteorological conditions for snow melt Journal of Glaciology 33:24-26

Kuhn M (2001) The nutrient cycle through snow and ice, a review. Aquatic Science 63:150-167

Lalonde JD, Poulain AJ, Amyot M (2002) The role of mercury redox reactions in snow on snow–to–air mercury transfer. Environmental Science and Technology 36:174–178

Larose C, Dommergue A, Marusczak N, Ferrari CP, Schneider D (Submitted) Bioavailability of mercury deposited in polar environments.

Leck C, Persson C (1996a) The central Arctic Ocean as a source of dimethyl sulfide - Seasonal variability in relation to biological activity Tellus 48B:156-177

Legrand M et al. (2007) Origin of C2–C5 dicarboxylic acids in the European atmosphere inferred from year-round aerosol study conducted at a west-east transect. Journal of Geophysical Research 112:D23S07, doi:10.1029/2006JD008019

Lei YDYD, Wania F (2004) Is rain or snow a more efficient scavenger of organic chemicals? Atmospheric Environment 38:3557-3571

Lindberg SE et al. (2001) Formation of Reactive Gaseous Mercury in the Arctic: Evidence of Oxidation of Hg° to Gas–Phase Hg–II Compounds after Arctic Sunrise. Water Air and Soil Pollution: Focus 1:295–302

Lindberg SE et al. (2002) Dynamic Oxidation of Gaseous Mercury in the Arctic Troposphere at Polar Sunrise. Environmental Science and Technology 36:1245–1256

Loseto LL, Lean DRS, Siciliano SD (2004) Snowmelt Sources of Methylmercury to High Arctic Ecosystems. Environmental Science and Technology 38:3004-3010

Lu JY et al. (2001) Magnification of atmospheric mercury deposition to polar regions in springtime: the link to tropospheric ozone depletion chemistry. Geophysical Research Letters 28:3219–3222

Lyons WB, Welch K. A., Fountain A. G., Dana G. L., Vaughn B. H., McKnight D. M. (2003) Surface glaciochemistry of Taylor Valley, southern Victoria Land, Antarctica, and its relation to stream chemistry. Hydrological Processes 17 115–130

Meyer T, Lei YD, Wania F (2006) Measuring the release of organic contaminants from melting snow under controlled conditions. Environmental Science and Technology 40:3320–3326

Meyer T, Wania F (2008) Organic contaminant amplification during snowmelt. Water Research 42:1847-1865

Narcy F, Gasparini S, Falk-Petersen S, Mayzaud P (2009) Seasonal and individual variability of lipid reserves in Oithona similis (Cyclopoida) in an Arctic fjord. Polar Biology 32:233-242

Niki H, Maker PD, Savage CM, Breitenbach LP (1983a) A long–path Fourier transform infrared study of the kinetics and mechanism for the hydroxyl radical–initiated oxidation of dimethylmercury. Journal of Physical Chemistry 87:4978 – 4981

Niki H, Maker PS, Savage CM, Breitenbach LP (1983b) A Fourier-transform infrared study of the kinetics and mechanism of the reaction of atomic chlorine with dimethylmercury. Journal of Physical Chemistry 87:3722-3724

Poulain AJ, Lalonde JD, Amyot M, Shead JA, Raofie F, Ariya PA (2004) Redox transformations of mercury in an Arctic snowpack at springtime. Atmospheric Environment 38:6763-6774

Poulain AJ et al. (2007) Potential for mercury reduction by microbes in the high arctic. Applied and Environmental Microbiology 73:2230-2238

Reisch CR, Moran MA, Whitman WB (2008) Dimethylsulfoniopropionate-dependent demethylase (DmdA) from Pelagibacter ubique and Silicibacter pomeroyi. The Journal of Bacteriology 190:8018-8024

Rontani J-F (2001) Visible light-dependent degradation of lipidic phytoplanktonic components during senescence: a review. Phytochemistry 58:187-202

Schroeder WH et al. (1998) Arctic springtime depletion of mercury. Nature 394:331–332

Scott KJ (2001) Bioavailable mercury in arctic snow determined by a light-emitting mer-lux bioreporter. Arctic 54:92-95

Siciliano SD, O'Driscoll NJ, Tordon R, Hill J, Beauchamp S, Lean DRS (2005) Abiotic production of methylmercury by solar radiation. Environmental Science and Technology 39:1071-1077

St. Louis VL et al. (2007) Methylated mercury species in Canadian high arctic marine surface waters and snowpacks. Environmental Science and Technology 41:6433-6441

St. Louis VL et al. (2005) Some sources and sinks of monomethyl and inorganic mercury on Ellesmere island in the Canadian high arctic. Environmental Science and Technology 39:2686–2701

Stoichev T, Rodriguez Martin-Doimeadios RC, Tessier E, Amouroux D, Donard OF (2004) Improvement of analytical performances for mercury speciation by on-line derivatization, cryofocussing and atomic fluorescence spectrometry. Talanta 62:433-438

Sunderland EM, Krabbenhoft DP, Moreau JW, Strode SA, Landing WM (2009) Mercury sources, distribution, and bioavailability in the North Pacific Ocean: Insights from data and models. Global Biogeochemical Cycles 23

Tranter M, Brimblecombe, P., Davies, T.D., Vincent, C.E., Abrahams,, P.W. B, I. (1986) A composition of snowfall, snowpack and meltwater in the Scottish Highlands—evidence for preferential elution Atmospheric Environment 20:517–525

Tseng CM, Garraud H, Amouroux D, Donard OF, de Diego A (1998) Open focused microwave-assisted sample preparation for rapid total and mercury species determination in environmental solid samples. Journal of Automatic Chemistry 20:99-108

Wagemann R, Trebacz E, Boila G, Lockhart WL (1998) Methylmercury and total mercury in tissues of arctic marine mammals. Science of the Total Environment 218:19-31

Weber JH (1993) Review of possible paths for abiotic methylation of mercury(II) in the aquatic environment. Chemosphere 26:2063-2077

Williams MW, Seibold C, Chowanski K (2009) Storage and release of solutes from a subalpine seasonal snowpack: soil and stream water response, Niwot Ridge, Colorado. Biogeochemistry 95:77-94

SECTION IV

In Section III we outlined the development of a molecular tool that allowed us to access new information on mercury speciation in Arctic snow. The results obtained with the biosensor led to a novel model for mercury methylation in oxic environments. Having determined that biotic methylation is probably occurring and that bacteria are present in the snow environment, we decided to explore the interactions between chemistry and microbial community structure and function in more detail.

In Chapter 6, we model the interactions between snow chemistry and community structure to elucidate potential relationships. To follow the dynamics of microbial community structure, we used a 16S microarray approach on snow and meltwater samples collected during a two-month field campaign in Ny-Ålesund (Svalbard, Norway, 78°56'N, 11°52'E) in spring 2008. We related these results to the chemical data presented in Chapter 5 of the previous section using co-inertia analysis. We then discuss the nature of these relationships and explore functional community changes due to mercury contamination of snowpacks. Based on our results, community structure and snow chemistry are linked and certain types of relationships are unidirectional, while some are interrelated. Mercury also affects community structure and function at concentrations lower than previously reported.

In Chapter 7, we present an overview of microbial community function based on results obtained by pyrosequencing.

CHAPTER 6: INTERACTIONS BETWEEN SNOW CHEMISTRY, MERCURY CONTAMINATION AND MICROBIAL POPULATION DYNAMICS IN AN ARCTIC SNOWPACK.

Manuscript in preparation for publication

Catherine Larose, Sebastien Cecillon, Emmanuel Prestat, Sibel Berger, Delina Lyon, Cédric Malandain, Aurélien Dommergue, Christophe Ferrari, Dominique Schneider and Timothy M. Vogel

Abstract

This study focuses on the interactions between microbial community structure, snowpack chemistry and mercury (Hg) contamination of Polar Regions. We used a 16S rRNA microarray to follow shifts in microbial community structure during a two-month field study in a high Arctic site, Svalbard, Norway (79°N). Snowpack chemistry (inorganic and organic ions), and more specifically mercury (Hg) speciation measurements, were determined in all samples. We linked changes in microbial community structure to snowpack and meltwater chemistry using co-inertia analysis (CIA) and explored changes in community function due to Hg contamination by Q-PCR quantification of Hg-resistance genes in metagenomic samples. Based on the CIA results, chemical and microbial data were linked (p=0.019) and bioavailable Hg and methylmercury (MeHg) both constituted important vectors in determining the ordination of samples. Mercury was shown to impact community function, with increases in *merA* gene copies.ngDNA^{-1} at MeHg concentrations above 30 pg.L^{-1}. Our results show that snowpacks can be considered as dynamic habitats whose components respond rapidly to environmental changes.

Introduction

The Arctic environment is undergoing change due to climate shifts, long-range transportation of contaminants and increased human activity. An important feature of the Arctic is seasonal snow-cover, which extends over a third of the Earth's land surface, covering up to 47 million km^2 (Hinkler et al. 2008), and can be considered as a dynamic habitat of limited duration (Jones 1999). Snow cover influences global energy and moisture budgets, thereby influencing climate (Hinkler et al. 2008), and is also a receptor surface and storage compartment for nutrients, soluble inorganic or organic matter and contaminants, such as mercury (Hg) that are delivered by wet and dry deposition (Kuhn 2001; Daly and Wania 2004). Hg is a toxic metal whose concentrations are increasing in the Arctic food chain (Muir et al. 1999) and can undergo transformations to form methylmercury (MeHg), a potent neurotoxin. Far from inert, seasonal Arctic snowpacks are chemically dynamic and interact with different environmental compartments such as the atmosphere, soil and meltwater-fed ecosystems.

Due to the cold conditions and the limited supply of liquid water, snow and ice have long been considered as no more than entrapment and storage systems for microorganisms that were thought to enter as vegetative and resting cells, transported by wind-blown particles, aerosols and ice crystals (Cowan 2004). However, this view has begun to change with the publication of a number of studies that examine the impact of microorganisms on the dynamics, composition and abundance of nutrients (Hodson et al. 2008), on their role in shifting surface albedo of snow and ice (Thomas and Duval 1995) and on hydrochemistry (Tranter et al. 2002). Microorganisms also impact the transformation of contaminants, such as Hg (Poulain et al. 2007) through detoxification processes that convert inorganic Hg to its volatile elemental form and methylation/demethylation processes that convert inorganic Hg to MeHg and vice versa (Barkay et al. 2003).

In turn, chemistry can impact the microbial community structure in different environments. Yergeau et al. (2007) recently reported the impact of soil vegetation cover on microbial communities in Antarctica and also showed that latitude has an effect on biodiversity, with increased latitude leading to decreased biodiversity. In field and laboratory studies, Duran et al. (2008) determined that Hg contributes to altering community structure and function with the enrichment of resistant populations and changes in contaminant metabolism in sediments (Duran et al. 2008). However, the dynamics of change in complex systems remain to be examined. A recent report on a seasonal Arctic snowpack showed that the chemical environment evolves rapidly along a seasonal gradient and that Hg transformations were occurring within (Larose et al. In preparation). If the chemistry of the snowpack is dynamic, then it is likely that the communities inhabiting this system are as well.

In order to gain insight into ecosystem functioning, it is essential to understand how the components that make up this system interact. While Arctic snowpack chemistry has been studied in detail (Dommergue et al. 2009; Larose et al. In preparation), knowledge about microbial community structure is lacking, despite the fact that microbial communities are key to understanding ecosystem-level processes (Schimel 1998). Here, we report the results of a two-month field study in a high Arctic site, Svalbard, Norway (79°N) where we used a 16S rRNA microarray to follow shifts in microbial community structure and link these changes to snowpack and meltwater chemistry by co-inertia analysis. We also explore changes in community function due to Hg contamination using Q-PCR to quantify resistance genes in metagenomic samples.

Methods

The spring research campaign was held between April 16th, 2008 and June 8th, 2008 at Ny-Ålesund in the Spitsbergen Island of Svalbard, Norway (78°56'N, 11°52'E). The field site, a 50 m^2 perimeter with

restricted access (to reduce contamination from human sources), is located along the south coast of the Kongsfjorden, which is oriented SE-NW and open to the sea on the west side. The Kongsfjorden was free of sea ice throughout the campaign.

Sampling

Twice a week, a shallow pit was dug and both surface (3 cm) and basal samples (10 cm above the ground) were collected for ion, mercury and microbial analyzes. A total of 38 samples were collected. Samples for ion measurements were collected in sterile acuvettes and stored at -20°C until analysis. For Hg analyzes, snow was collected in acid-washed 250 mL glass Schott bottles (see cleaning protocol outlined in Ferrari et al. 2000 for more details) and subsampled for dissolved and bioavailable Hg. Samples for MeHg were collected in 125 mL acid-washed Teflon coated low-density polyethylene bottles and stored frozen until analysis. Meltwater was collected in acid-washed 250 mL glass Schott bottles from streams that formed the 1st of June, 2008. Snow and meltwater chemistry is the subject of another report (Larose et al. In preparation) and sample handling and analysis is detailed therein. Samples for microbial analyzes were collected in three 3 L sterile sampling bags (a total of 3 L water equivalent) using a sterilized Teflon shovel. To avoid contamination, Tyvex® body suits and latex gloves were worn during sampling and gloves were worn during all subsequent handling of samples.

Microbial sample processing

Samples were processed immediately after collection in the field laboratory. Surface snow samples were left to melt (6 hours) at room temperature prior to being filtered onto sterile 0.22 µM 47 mm filters (Millipore) using a sterile filtration unit (Nalge Nunc International Corporation), while meltwater samples were filtered immediately. Filters were stored in sterile bead-beating tubes at -20°C until further analysis. Procedural blanks were carried out by filtering Nanopure water (Siemens) using the same procedure.

DNA extraction

DNA was extracted as previously described (David et al. 2009). Briefly, filters were chopped and placed in a Fastprep® bead-beating tube (Lysing matrix E, MP Biomedicals) to which 1 mL of DNA extraction buffer (David et al. 2009) and 20 mg ml^{-1} lysing enzyme (*Trichoderma harzianum*, Sigma L1412) were added. Tubes were left at room temperature for 1 hour and then frozen at -20°C overnight. The frozen tubes were incubated at 65°C for 30 minutes and placed in a Fastprep® bead-beater (MP Biomedicals) set at speed 5.5 for 30 seconds. DNA was extracted from the water phase with an equal volume of chloroform:isoamyl alcohol (24:1) and precipitated with isopropanol.

DNA taxonomic microarray analysis

The Agilent Sureprint Technologies microarray format was used, and consisted in 8 identical blocks of 15,000 spots each on a standard glass slide format 1" x 3" (25mm x 75mm). Each spot is formed by *in situ* synthesis of 20-mer oligoprobes that occur at least in triplicate within each block. A total of five slides were used for the hybridization of all samples. Probes were designed to target the *rrs* gene and to cover different taxonomic levels from a wide part of the *Bacteria* and *Archaea* phylogenic tree using the ARB software package. We chose to design 20mer long probes, with melting temperature range of 65±5°C and with a weighted mismatch less than 1.5.

The *rrs* genes were amplified by PCR from total DNA extracted from each sample, using universal primers pA (5' TAATACGACTCACTATAGAGAGTTTGATCCTGGCTCAG 3') and pH-T7 (5' AAGGAGGTGATCCAGCCGCA 3') (universal for most *Bacteria* and some *Archaea* can be amplified) and the illustra Hot Start Mix RTG (GE Healthcare) PCR kit. The 25 µL volume PCR reaction mix contained 0.6 µM of each primer, 2 µl DNA or 2 µl sterile water for the negative control. The PCR conditions used were 3 min at 94°C, followed by 35 cycles of 45 s of denaturation at 94°C, 45 s of annealing at 55°C, and 90 s of elongation at 72°C. After a final 5-min extension at 72°C, PCR products were separated by 1%-agarose gel electrophoresis, purified using the NucleoSpin® Extract II kit (Clonetech) and transcribed. *In vitro* transcription was carried out at 37°C during 4 hours in 20 µL reactions that contained 8 µL of the purified PCR product (50 ng.µL^{-1}) and 12 µL of the following mix: T7 RNA buffer (5X), DDT (100 mM), 10 mM of each of the four NTPs, RNasin (40 U.µL^{-1}), T7 RNA polymerase (1 µL) and UTP-Cy3 (5 mM). During transcription, Cy3-UTP (a fluorescent dye that emits light at 532nm) is incorporated to label RNA. RNA was purified using the Quiagene RNeasy mini Kit according to the manufacturer's instructions and quantified with a nanophotometer before undergoing chemical fragmentation by addition of 5.7 µL of a Tris Cl (1mM) and $ZnSO_4$ (100mM) mix. Samples were incubated for 30 minutes at 60°C and fragmentation was stopped by placing the tubes on ice. EDTA (500mM) was added to each tube (1.2 µL) followed by 1 µl RNAsin (40 U.µL^{-1}) after a minute incubation period at 25°C. The RNA solution was then diluted to 5 ng.µL^{-1} and a hybridization mix was prepared (v/v ratio) in a 50 µL reaction with 2x GeX Hyb Buffer (Agilent). A total of 100 ng of RNA were then placed on the slide and incubated at 60°C for 4 h in the Agilent Hybridization Oven.

Microarray scanning and data processing

An Innoscan 700 (Mapix) scanner was used for scanning microarray slides according to the manufacturer's instructions. Raw hybridization fluorescence signals for each spot were determined

based on the signal-to-noise ratio (SNR), which was calculated using the following formula: SNR = (signal intensity − background)/standard deviation of background.

Hybridization fluorescence signals for all probes including negative controls were log_2transformed. Since at least three replicates exist for all oligonucleotide probes, outliers were eliminated when any individual spot was greater than 2 standard deviations from the average of all replicates. Data was subsequently normalized by using the quantile approach.

Q-PCR screening for *merA* genes

Primer design

The primers were designed based on the alignments of known *merA* gene sequences. A total of 105 *merA* genes were retrieved from the NCBI data base (http://www.ncbi.nih.gov/blast) and aligned in Clustal X. Non-degenerate primers were designed for two branches covering a total of 30% of the known *merA* diversity, using Primer Select (DNASTAR, Inc., Madison, WI). Positive controls were constructed for both primer sets by a gene shuffling technique outlined in (David et al. 2008). Briefly, an initial PCR cycle was carried out with two long oligonucleotide primers but without the addition of any other DNA template. Hybridization of the primer complementary regions led the polymerase to synthesize double strands of DNA complementary to the whole targeted DNA region. The second step involved the amplification of the synthetic sequence using the first reaction products as DNA template in a conventional PCR reaction. The initial cycle was carried out in the presence of 50 ng of each of the two long oligonucleotide primers, 1X Titanium Taq PCR Buffer, 0.2 mM deoxynucleoside triphosphates, 1 µL Titanium Taq DNA polymerase (Clontech-Takara Bio Europe, Saint-Germain-en-Laye, France) and 1 µL of T4 gene 32 protein (Roche Diagnostics S.A.S., Meylan, France). The PCR amplification was performed as a single-tube reaction in a Thermal Cycler (Biometra T1 Labgene scientific instrument, Archamps, France) programmed as follows: 6 min at 96 °C, followed by 35 cycles of 95 °C for 1 min; 53 °C for 30 s; and 68 °C for 40 s, with a final extension at 68 °C for 6 min. The second reaction was performed using the same reaction mix as for the initial cycle, except that 50 ng of the first reaction product as DNA template and 0.5 µM of forward and reverse primers were used (David et al., 2008). The primer sets for *merA* amplification and gene shuffling are listed in Table I.

Table I: Short and long primers used for gene shuffling. The positive controls used for Q-PCR are also listed.

Primer type		**5' to 3'**
Short primers	MerA1F	ATCAGCGGATGTCTCCTACG
	MerA1R	CCGATAACCGAGTCCAGCTA
Long primers	1F	ATCAGCGGATGTCTCCTACGCCAAGGGCAGCGCCAAGCTCGCCATTGAGGTCGGC ACGTCACCCGACGCGCTGACG
	1R	CCGATAACCGAGTCCAGCTACAGCGGCCGTCAGCGCGTCGGGTGACGTGCCGACC TCAATGGCGAGCTTGGCGCTGCC
Positive control	MerA1	ATCAGCGGATGTCTCCTACGCCAAGGGCAGCGCCAAGCTCGCCATTGAGGTCGGC ACGTC ACCCGACGCGCTGACGGCCGCTGTAGCTGGACTCGGTTATCGG
Short primers	MerA2F	GAAGCGGGTGAACTGATCC
	MerA2R	TCGTCAGGTAGGGGAACAAC
Long primers	2F	GAAGCGGGTGAACTGATCCAGACGGCGGCTCTGGCCATTCGCAACCGCATGACGG TGCAGGAACTGGCCGAC
	2R	ATCGTCAGGTAGGGGAACAACTGGTCGGCCAGTTCCTGCACCGTCATGCGGTTGC GAATGGCCAGAGCCGCCG
Positive control	MerA2	GAAGCGGGTGAACTGATCCAGACGGCGGCTCTGGCCATTCGCAACCGCATGACGG TGCAG

Q-PCR

Q-PCR analyzes were carried out in triplicate in 20 µL reaction volumes containing 10 µL of Quantace SensiMix™ Plus SYBR® (Quantace), 0.5 µL of each primer (10 µM) and 2 µL of DNA (concentrations normalized to 3 ng.μL^{-1}) on a Rotor-Gene 3800 (Corbett Research, Sydney, Australia). The amplification protocol consisted of an initial denaturation phase (95°C for 10 min) followed by 45 cycles of denaturation (95°C for 15 s), annealing (57°C for 20 s) and elongation (72°C for 20 s). The integrity of Q-PCR products was confirmed by melting curve analyses, from 50°C to 99°C. Standard curves were calculated based on gene copies per µL using 10-fold increments and were adjusted from 10^8 to 10^1 gene copies μL^{-1}. Q-PCR amplicons were sequenced in order to verify the specificity of the primers.

Statistical analysis

Principal component analysis (PCA) was carried out on chemical and microbial data and results are plotted in two dimensions based on the scores of the first two principal components. Data were checked for normality and log-transformed. Co-inertia analysis (Dray et al. 2003), was used to study the relationships between microbial community structure and chemistry. The objective of co-inertia

analysis is to create a factorial plane deforming as little as possible the structure of each data set and enabling a simultaneous ordination of them. Coupling of correlation of snow/meltwater chemical characteristics and community structure data matrices produced new PC1 and PC2 co-inertia axes by projecting variables and sampling plots in a new factorial map. Co-inertia analysis is described in detail elsewhere (Dolédec and Chessel 1994; Thioulouse and Lobry 1995). A randomization test of 1000 permutations was carried out to verify the significance of the co-structure (Monte Carlo test). PCA, Monte Carlo and co-inertia tests were performed in R (The R Project for Statistical Computing http://www.r-project.org) using the ade4 software package (Thioulouse et al. 1997). Linear regression analysis was carried out in JMP-IN (SAS Institute, 2003) in order to explore relationships between specific probes and mercury species.

Results

Co-structure analysis between snow/meltwater chemistry and community structure

CIA analysis was carried out on snow/meltwater chemistry and community structure (Figure 1). The permutation test revealed a significant co-structure between the microbial community structure and snow/meltwater chemistry (p = 0.019, RV = 0.264). The RV-coefficient represents the correlation between both data sets and varies between 0 and 1: the closer the coefficient to 1, the stronger the correlation between the tables. The first two eigenvalues of the co-inertia analysis accounted for 51.8 and 19.4% of the explained variance, respectively, and both data sets were highly correlated (0.62 for the first axis and 0.69 for the second).

In the graphical representation presented in Figure 1A, the sample is identified in the box; the start of the arrow indicates the location of the sample in the chemical data set, while the tip of the arrow represents the location of the sample in the microbial data set. The length of the arrow indicates how well both data sets agree: a short arrow means that the data sets strongly agree, while a long arrow means that they strongly disagree. Variables are represented on correlation circles and correlations between the original data sets and the score or latent variable vectors are computed so that highly correlated variables cluster together in the resulting graphics. Therefore, interactions between two types of variables can be identified, in addition to identifying the relationship between variable clusters and associated sample clusters.

The chemical parameters that had the most influence on the co-structure as observed by the lengths of the vector arrows in Figure 1B (X canonical weights) formed five major axes: 1) BioHg; 2) THg; 3)

MeHg; 4) pH and organic acids; and 5) ions. There are less species in the Y canonical weights graph (Figure 1C) when BioHg and MeHg levels are elevated.

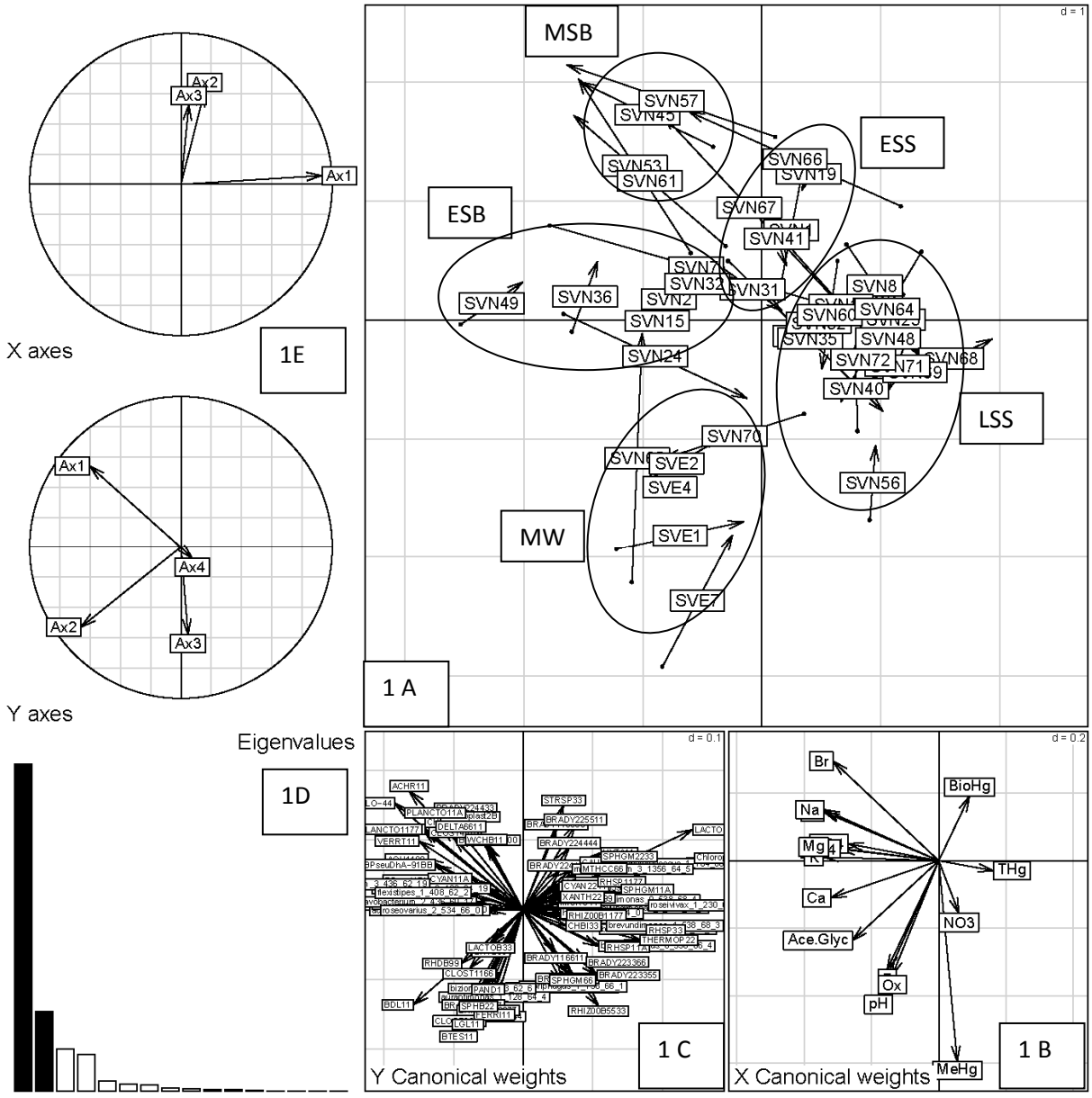

Figure 1: Co-structure analysis of the microbial and chemical data. (1A) Co-inertia output with sample names in the box. The tip of the arrow represents the ordination of the sample in the microbial data set, while the start of the arrow represents the position of the sample in the chemical data set. (1B) Main chemical vectors that affect sample ordination. (1C) Probes with the greatest influence. (1D) Co-inertia eigenvalues. (1E) Correlation circles showing the projections of the PCA axes from the chemical data (X axes) and microbial data (Y axes) onto the axes of the co-inertia analysis. These circles represent a view of the rotation needed to associate the two datasets. ESS, ESB, LSS, MSB and MW represent the early season surface, early season basal, late-season surface, mid-season basal and meltwater groups, respectively.

Based on the five major chemical axes described above, the samples can be clustered into 5 different groups (Table II): an early season surface group (ESS) with two late-season surface samples, an early

season basal (ESB) group, a late season surface group (LSS), a mid-season basal group (MSB), and finally a meltwater (MW) group. The oligonucleotide probes (positive hybridization of nucleotides representing different taxonomic levels on the microarray) that had the most effect on sample ordination as determined by CIA analysis were identified. The ordination of the ESS group was mainly influenced by the *Acidiphilum*, *Bacillus*, *Nocardiopsis* and *Streptomonospora* genera, while *Flavobacterium, Photobacterium* and *Vibrio* dominated in the ESB group. The ordination of the LSS group was dominated by *Nostoc*, *Moorella* and *Brevundimonas*. The ordination of the MSB group was most influenced by the *Nostoc*, *Desulfovibrio* and *Achromatium* genera and *Legionella* and *Dietza* dominated in the MW group.

Table II: Samples groups and their characteristics as determined by co-inertia analysis

Group name	Sample type	Sample dates
ESS	Early season surface samples and two late-season fresh snow samples	16/04/2008-09/05/2008 03/06/2008 & 04/06/2008
ESB	Early season basal samples	16/04/2008-09/05/2008
MSB	Mid-season basal samples	16/05/2008-30/05/2008,
LSS	Late-season surface samples	13/05/2008-08/06/2008
MW	3 basal samples and meltwater samples	02/06/2008,06/06/2008 01/06/2008-07/06/2008

Based on the CIA results, we identified probes that were correlated and anti-correlated to clusters in the chemical data set. Linear regression analysis was performed and examples of significant results are presented in Figure 2. For each of the main chemical vectors, certain probes increased with concentration, while others decreased. Probes that target *Flavobacteria* were significantly correlated to Cl concentrations (Flavobacterium1, $r^2 = 0.49$, $p < 0.0001$, n = 32, Flavobacterium2, $r^2 = 0.31$, $p = 0.0038$, n = 29), while probes targeting *Anabaena* and *Bradyrhizobium* were significantly negatively correlated to Cl concentrations ($r^2 = 0.22$, $p = 0.037$, n = 21 and $r^2 = 0.39$, $p = 0.0038$, n = 20, respectively) (Figure 2A). Significant positive correlations with pH include probes that target *Aurantimonas* ($r^2 = 0.76$, $p < 0.0001$, n = 22) and *Bizionia* ($r^2 = 0.33$, $p = 0.0082$, n = 20). Probes that targeted *Acidobacteria* were anti-correlated to pH ($r^2 = 0.45$, $p = 0.0033$, n = 21) (Figure 2B). Probes targeting *Rhizobiales* and *Pseudomonas* were significantly correlated to BioHg concentrations ($r^2 = 0.32$, $p = 0.0084$, n = 21 and $r^2 = 0.52$, $p = 0.0007$, n = 18, respectively) Probes targeting *Mesorhizobium* and *Caulobacteraceae* were significantly negatively correlated to BioHg concentrations ($r^2 = 0.53$, $p < 0.0001$, n = 27 and $r^2 = 0.59$, $p = 0.0005$, n = 16, respectively) (Figure 2C). Significant positive correlations with MeHg include probes that target an uncultured bacterium ($r^2 = 0.69$, $p < 0.0001$, n = 18) and *Clostridium* ($r^2 = 0.80$, $p = 0.0092$, n = 8). Probes that targeted *Caulobacteraceae* and *Mesorhizobium* were negatively correlated to MeHg ($r^2 = 0.39$, $p = 0.0092$, n = 16 and $r^2 = 0.48$, $p = 0.0012$, n = 12, respectively) (Figure 2D).

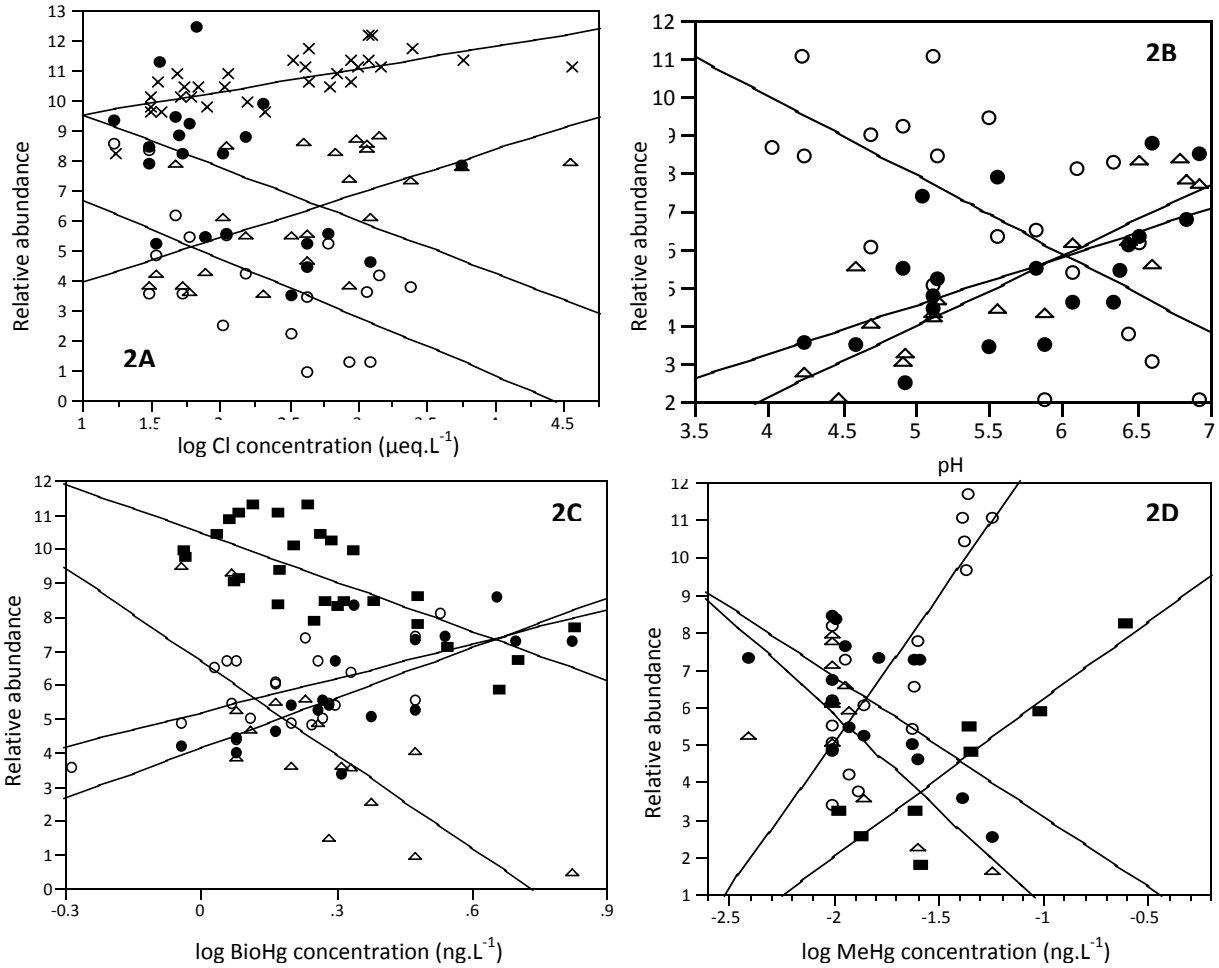

Figure 2: Positive and negative linear correlations between the relative abundance of probes and chemical parameters. Figure 2A: crosses are *Flavobacterium*1, open triangles are *Flavobacterium*2, open circles are *Anabaena* and closed circles are *Bradyrhizobium*. Figure 2B: open triangles are *Aurantimonas*, closed circles are *Bizionia* and open circles are *Acidobacteria*. Figure 2C: closed rectangles are *Mesorhizobium*, open triangles are *Caulobacteraceae*, open circles are *Rizobiales* and closed circles are *Pseudomonas*. Figure 2D: closed rectangles are *Clostridium*, open triangles are *Caulobacteraceae*, closed circles are *Mesorhizobium* and open circles are uncultured bacterium.

Presence of *merA* genes

Based on the observation that mercury has an influence on community structure, we performed Q-PCR analysis on all samples in order to determine whether *merA* genes were present and their amount. A significant linear correlation was detected between the gene copy number and the MeHg concentrations (r^2 = 0.46, p = 0.0014, n = 19) but neither to BioHg (r^2 = 0.03, p = 0.49, n = 19) nor THg (r^2 = 0.006, p = 0.76, n = 19). Both the relative abundance of probes targeting MeHg-resistant phylotypes and the *merA* gene copies.ng^{-1} of DNA were plotted against MeHg concentrations (Figure 5). The response curves of the resistant probes and *merA* gene copies.ng^{-1} of DNA were similar.

Probes that targeted non-resistant phylotypes were undetected in samples with MeHg concentrations above 30 pg.L^{-1}.

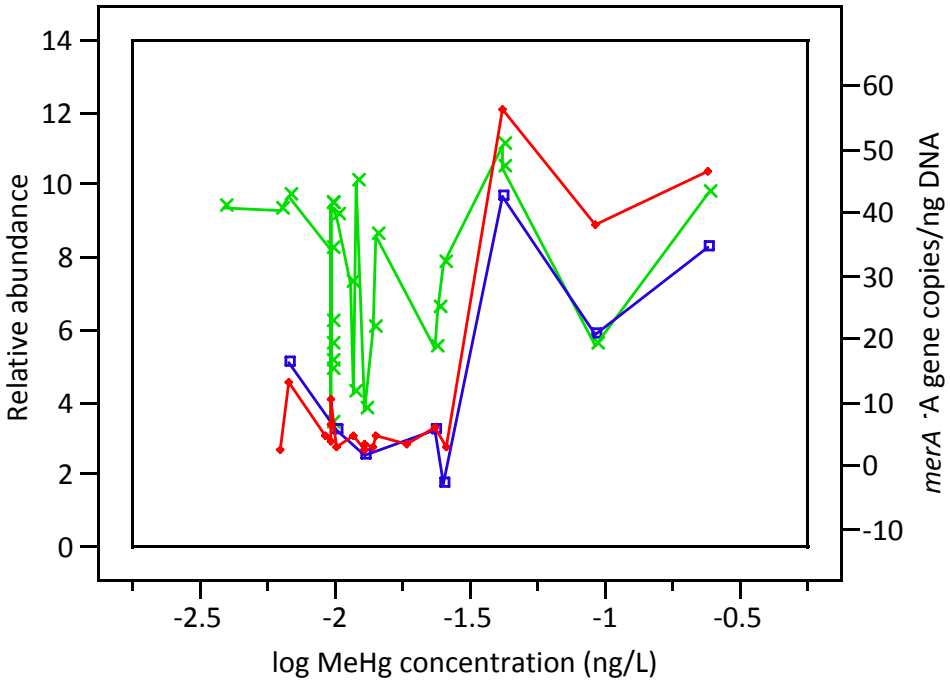

Figure 3: Relative abundance (left scale) and *merA* gene copies. ng^{-1} of DNA (right scale) plotted against log-transformed MeHg concentrations. The *merA* gene copy number is presented in red, and the relative abundance of two probes targeting either an uncultured bacterium or *Clostridium* is shown in green and blue, respectively. A MeHg concentration of -1.5 is equivalent to 30 pg.L^{-1}.

Discussion

Linking chemistry and microbial community structure

In order to elucidate the relationship between microbial community structure and snowpack/meltwater chemistry, co-inertia analysis was performed. This analysis revealed a significant co-structure as demonstrated by a Monte Carlo test with 1000 permutations (p =0.019). Therefore, chemistry and microbial community structure are linked. The dynamic nature of the snowpack in terms of both community structure and chemistry is revealed by the clusters that evolve along a seasonal gradient and surface and basal samples evolve differently over time. However, do microbial communities impact chemistry, or does chemistry drive population changes? Are these interactions unidirectional or bidirectional?

Microbial interactions with chemistry

In terms of identifying the nature of these interactions, co-inertia analysis determined the major chemical and microbial vectors that impacted the co-structure. Marine salts (inorganic ion axis) drove

the ordination of samples in the co-inertia analysis and the relative abundance of certain probes targeting specific phylotypes increased as a function of ion concentration (figure 2A). The genera that had the most influence on the ordination of the ESB group were *Flavobacterium*, *Vibrio* and *Photobacterium*. Members of these genera are commonly retrieved from polar marine environments and are known to be halotolerant (Farmer and Hickman-Brenner 2006; Murray and Grzymski 2007). Some strains of *Flavobacterium* isolated from Antarctic sea water even exhibited an absolute sea water requirement for growth (Bowman et al. 2003). The LSS group was anti-correlated to high ion concentrations and contains members that were negatively correlated to Cl (Figure 2) including *Anabaena,* a freshwater *Cyanobacteria*, and *Bradyrhizobium*, a nitrogen-fixing bacteria, commonly isolated from the cryosphere (Comte et al. 2007; Cooke et al. 2009). The effect of marine salts on microbial community structure is probably unidirectional, with species that are able to acclimate to osmotic stress via the accumulation of certain solutes (K+, glutamate, trehalose, proline and glycine betaine), at concentrations that are proportional to the osmolarity of the medium by upregulation of required proteins (Csonka 1989).

Organic acids and pH represented another important vector and were linked to the MW group. The organic acids measured are short-chained acids with 1 or 2 carbons, and their concentrations increased as the season progresses and the snowpack begins to melt. pH has been reported as one of the main factors in determining community structure in soils (Lauber et al. 2009), but, to the best of our knowledge, this is the first time that it has been reported as a driver of community structure in snow samples. For example, the relative abundance of *Bizionia* (*Flavobacteria* class) and *Aurantimonas* increased with pH, while that of *Acidobacteria* decreased. Members of both *Bizionia* and *Aurantimonas* have growth optima between pH 6 and 8 (Einen and Ovreas 2006; Anderson et al. 2009).

Based on co-inertia analysis, MeHg and BioHg constituted important vectors in determining sample ordination. Probe abundance along these axes was low, suggesting a negative effect on diversity even at pg. L^{-1} (MeHg) and ng.L^{-1} (BioHg) levels. Only very few probes were significantly and positively correlated to BioHg (less than 5% of the 140 most-influential probes) and among these were *Rhizobiales* and *Pseudomonas*. Some probes were only detected in the ESS samples that were collected at the beginning of the field campaign, and their relative abundance was negatively correlated to THg and BioHg concentrations (*Caulobacteraceae* and *Mesorhizobium*, for example, Figure 2C). At the beginning of the sampling period, we recorded several atmospheric depletion events or AMDEs that deposited high concentrations of both THg and BioHg onto snow surfaces (maximum values were 90 ng.L^{-1} THg and 16 ng.L^{-1} BioHg) (Larose et al. In preparation). This implies that although a large fraction of Hg is returned to the atmosphere following its deposition, AMDEs

still impact community structure through the rapid loss of non-resistant phylotypes. In a laboratory study with soil microcosms, Rasmussen and Sørensen (2001) also reported an immediate decrease in microbial diversity following the addition of 25 µg $Hg^{2+}.g^{-1}$ to the soil. Although diversity was recovered over time, this was due to a shift in community structure by enrichment of Hg-resistant members (Rasmussen and Sørensen 2001). Using protein-fingerprinting and automated ribosomal intergenic spacer analysis (ARISA), Maron et al. (2007) also demonstrated that Hg was able to induce changes in community functional and genetic structures. However, these results were obtained by adding 8 mg of $Hg.L^{-1}$ (Maron et al. 2007), far above the values found in natural environments that are typically in the $ng.L^{-1}$ range. This is to our knowledge the first time that environmentally-relevant concentrations of MeHg and BioHg have been shown to induce a shift in community structure.

While Hg appears to impact community structure, this relationship is bidirectional. Based on a significant anti-correlation between BioHg and MeHg, Larose et al. (in preparation) hypothesized that biotic methylation of Hg was occurring within the snowpack. Therefore, microorganisms can alter their chemical environment through the metabolism and transformation of elements or contaminants. In order to cope with the toxicity of Hg and MeHg, bacteria have developed specialized resistance mechanisms. For example, bacteria possessing the *mer* operon are able to detoxify Hg via MerA (Barkay et al. 2003). The genes that encode MerA have been isolated both from a variety of environments including soil (Oregaard and Sorensen 2007), Siberian permafrost (Mindlin et al. 2005) and Arctic biofilms (Poulain et al. 2007) and from bacteria (Barkay et al. 2003) and archaea (Schelert et al. 2004). Some bacteria are able to detoxify both BioHg and MeHg, while others are only able to transform inorganic mercury via the *mer* operon resistance pathway (Barkay et al. 2003).

Based on our Q-PCR results, low levels ($pg.L^{-1}$) of MeHg elicit a response in community function. The *merA* gene copy number was positively correlated to MeHg concentrations in the snowpack, but no correlation existed with other forms of Hg, such as BioHg. Probe abundance for *Clostridium* and an uncultured bacterium mirrored the increase in *merA* gene copy numbers, suggesting that these bacteria carry the resistance gene. At a putative level of 30 $pg.L^{-1}$ of MeHg, *merA* gene copy numbers increase, similar to the increase in abundance of the resistant phylotypes. In parallel, the relative abundance of probes targeting non-resistant MeHg phylotypes decreased at this concentration, suggesting that 30 $pg.L^{-1}$of MeHg may constitute a threshold level for toxicity in the snowpack (Figure 2D). Based on these results, it appears that bacteria are more sensitive to MeHg than inorganic Hg and that *mer* induction may be initiated by MeHg, possibly via MerB, at lower concentrations than for BioHg. This may explain the results reported by Poulain et al. 2007, who observed *merA*

transcripts in biofilms despite low Hg concentrations. Two competing phenomena likely carried out by different members of the same community were observed in the snowpack: some microorganisms were methylating Hg to MeHg, while others, possible in response to high MeHg levels, were demethylating MeHg via *merA*. Therefore, potential MeHg accumulation by organisms is dependent on the methylation/demethylation reaction rates (Schaefer et al. 2004).

Atmospheric effects

Although there was generally a good agreement for both data sets overall (p=0.019), certain samples had long arrows, showing disagreement among data. Based on arrow length, the chemical and microarray data in the MSB group were in poor agreement. The tips of these arrows seemed to converge while their starts were divergent. The location of these samples in the chemical data set is similar to that of the ESS group and yet in terms of community structure, both groups are different. It is likely that the MSB group was chemically enriched by early season surface snow due to meltwater percolation to the base of the snowpack, since melting had begun (melt began around the 20th of May, see Larose et al. (In preparation) for more details). Therefore, the presence of a larger quantity of water may have contributed to changes in community structure in this group with increased detection of *Achromatium*, *Nostoc* and *Desulfovibrio* genera. *Nostoc* is a genus of *Cyanobacteria* that has the ability to remain desiccated for months or years and fully recover metabolic activity within hours to days after re-hydration with liquid water (Walter et al. 1995). Moreover, the flooding of the basal layers of the snowpack may have reduced the oxygen content, which could explain the emergence of the genera *Achromatium*, sulfate reducers that are tolerant to anoxic conditions (Gray et al. 1997), and *Desulfovibrio*, which are anaerobes cabable of syntrophic metabolism (see review by McInerney et al. 2008).

Long arrows were also detected in the ESS group. Again, the sample positions in the microarray data set converged while their positions in the chemical set were different. During April, when the ESS samples were collected, several AMDEs occurred (19th and 25th of April), in addition to periods of strong winds and snowfall events (16th of April). Therefore, the poor agreement between microarray and chemical data are likely due to differences in chemistry arising from atmospheric processes (deposition from different air masses, precipitation) that either do not or need longer time periods to significantly alter the community structure. The ESS group also contains two late season surface samples. These samples correspond to fresh snowfall events that occurred on the 3rd and 4th of June. Fresh snow has been shown to deliver high levels of BioHg (Larose et al. Submitted), which would explain the ordination of these samples in the ESS group.

Conclusion

We have shown that snowpack/meltwater chemistry and microbial community structure are linked and that the snowpack is a dynamic habitat that undergoes rapid changes during the spring. In addition, mercury in its bioavailable and methylated forms impact microbial community structure, even at low doses. MeHg appears to induce a change in community response with an increase in *merA* gene copy numbers at concentrations above 30 $pg.L^{-1}$. Finally, linking a 16S rRNA microarray approach to chemical data allows us to gain access to information on interactions in complex ecosystems between bacteria and environmental parameters without the need for cultivation. While our results are specific to one particular field season and may not be extrapolated to other environments, they provide a basis for further studies on the interaction between chemistry and microbial community structure.

Acknowledgements

This work was funded by INSU/CNRS (EC2CO and LEFE-CHAT 32), Université Joseph Fourier – Grenoble (pôle TUNES 2007) and CNRS. Logistical support was provided by the French Polar Institute IPEV (program CHIMERPOL). We acknowledge Alan Le Tressoler, Nicolas Marusczak, Nicolas Soumis and AWIPEV for field support. CL would like to acknowledge the FQRNT (Le Fonds Québécois de la Recherche sur la Nature et les Technologies) for a PhD research fellowship. CF thanks the Institut Universitaire de France (IUF) for its financial support.

References

Anderson CR et al. (2009) *Aurantimonas manganoxydans*, sp. nov. and *Aurantimonas litoralis*, sp. nov.: Mn(II) oxidizing representatives of a globally distributed clade of *alpha-Proteobacteria* from the order *Rhizobiales*. Geomicrobiology Journal 26:189–198

Barkay T, Miller SM, Summers AO (2003) Bacterial mercury resistance from atoms to ecosystems. FEMS Microbiology Reviews 27:355-384

Bowman JP, Nichols CM, Gibson JAE (2003) *Algoriphagus ratkowskyi* gen. nov., sp. nov., *Brumimicrobium glaciale* gen. nov., sp. nov., *Cryomorpha ignava* gen. nov., sp. nov. and *Crocinitomix catalasitica* gen. nov., sp. nov., novel *flavobacteria* isolated from various polar habitats. International Journal of Systematic and Evolutionary Microbiology 53:1343-1355

Comte K, Sabacká M, Carré-Mlouka A, Elster J, Komárek J (2007) Relationships between the Arctic and the Antarctic *cyanobacteria*; three *Phormidium*-like strains evaluated by a polyphasic approach. FEMS Microbiology Ecology 59:366-376

Cooke MP et al. (2009) Bacteriohopanepolyol biomarker composition of organic matter exported to the Arctic Ocean by seven of the major Arctic rivers. Organic Geochemistry 40:1151-1159

Cowan DA, Tow, Lemese Ah (2004) Endangered Antacrctic Environments. Annual Reviews of Microbiology 58:649-690

Csonka LN (1989) Physiological and Genetic Responses of Bacteria to Osmotic Stress. American Society for Microbiology 53:121-147

Daly GL, Wania F (2004) Simulating the Influence of Snow on the Fate of Organic Compounds. Environmental Science and Technology 38:4176-4186

David MM, Mesle M, Malandain C, Cohen D, Vogel TM (2009) Molecular Biology-based strategy for site remediation. Environmental Science and Technology Submitted

David MM, Sapkota AR, Simonet P, Vogel TM (2008) A novel and rapid method for synthesizing positive controls and standards for quantitative PCR. Journal of Microbiological Methods 73:73-77

Dolédec S, Chessel D (1994) Co-inertia analysis: an alternative method for studying species-environment relationships. Freshwater Biology 31:277-294

Dommergue A et al. Deposition of mercury species in the Ny Ålesund area (79°N) and their transfer during snowmelt. Accepted in Environmental Science and Technology

Dray S, Chessel D, Thioulouse J (2003) CO-INERTIA ANALYSIS AND THE LINKING OF ECOLOGICAL DATA TABLES. Ecology 84:3078-3089

Duran R et al. (2008) Mercury methylation by a microbial community from sediments of the Adour Estuary (Bay of Biscay, France). Environmental Pollution 156:951-958

Einen J, Ovreas L (2006) *Flaviramulus basaltis* gen. nov., sp. nov., a novel member of the family Flavobacteriaceae isolated from seafloor basalt. International Journal of Systematic and Evolutionary Microbiology 56:2455-2461

Farmer J, Hickman-Brenner F (2006) The Genera *Vibrio* and *Photobacterium*. In: The Prokaryotes, pp 508-563

Ferrari CP, Moreau AL, Boutron CF (2000) Clean conditions for the determination of ultra–low levels of mercury in ice and snow samples. Fresenius' Journal of Analytical Chemistry 366:433–437

Gray ND, Pickup RW, Jones JG, Head IM (1997) Ecophysiological Evidence that Achromatium oxaliferum Is Responsible for the Oxidation of Reduced Sulfur Species to Sulfate in a Freshwater Sediment. Applied and Environmental Microbiology 63:1905–1910

Hinkler J, Hansen BU, Tamstorf MP, Sigsgaard C, Petersen D (2008) Snow and Snow-Cover in Central Northeast Greenland. Advances in Ecological Research 40:175-195

Hodson A et al. (2008) Glacial Ecosystems. Ecological Monographs 78:41-67

Jones HG (1999) The ecology of snow-covered systems: a brief overview of nutrient cycling and life in the cold. Hydrological Processes 13:2135–2147

Kuhn M (2001) The nutrient cycle through snow and ice, a review. Aquatic Science 63:150-167

Larose C et al. (In preparation) Seasonal changes in snow chemistry lead to new insights into mercury methylation in the Arctic.

Larose C, Dommergue A, Marusczak N, Ferrari CP, Schneider D (Submitted) Bioavailability of mercury deposited in polar environments.

Lauber CL, Hamady M, Knight R, Fierer N (2009) Soil pH as a predictor of soil bacterial community structure at the continental scale: a pyrosequencing-based assessment. Applied and Environmental Microbiology:AEM.00335-00309

Maron P-A, Mougel C, Siblot S, Abbas H, Lemanceau P, Ranjard L (2007) Protein Extraction and Fingerprinting Optimization of Bacterial Communities in Natural Environment. Microbial Ecology 53:426–434

McInerney MJ et al. (2008) Physiology, Ecology, Phylogeny, and Genomics of Microorganisms Capable of Syntrophic Metabolism. Annals of the New York Academy of Sciences 1125:58-72

Mindlin S et al. (2005) Present-day mercury resistance transposons are common in bacteria preserved in permafrost grounds since the Upper Pleistocene. Research in Microbiology 156:994-1004

Muir D et al. (1999) Spatial and temporal trends and effects of contaminants in the Canadian Arctic marine ecosystem: a review. The Science of the Total Environment 230:83-144

Murray AE, Grzymski JJ (2007) Diversity and genomics of Antarctic marine micro-organisms. Philosophical Transactions of the Royal Society B: Biological Sciences 362:2259–2271

Oregaard G, Sorensen SJ (2007) High diversity of bacterial mercuric reductase genes from surface and sub-surface floodplain soil (Oak Ridge, USA). Isme J 1:453-467

Poulain AJ et al. (2007) Potential for mercury reduction by microbes in the high arctic. Applied and Environmental Microbiology 73:2230-2238

Rasmussen LD, Sørensen SJ (2001) Effects of mercury contamination on the culturable heterotrophic, functional and genetic diversity of the bacterial community in soil. FEMS Microbiology Ecology 36:1-9

Schaefer JK et al. (2004) Role of the Bacterial Organomercury Lyase (MerB) in Controlling Methylmercury Accumulation in Mercury-Contaminated Natural Waters. Environmental Science & Technology 38:4304-4311

Schelert J, Dixit V, Hoang V, Simbahan J, Drozda M, Blum P (2004) Occurrence and Characterization of Mercury Resistance in the Hyperthermophilic Archaeon Sulfolobus solfataricus by Use of Gene Disruption. The Journal of Bacteriology 186:427-437

Schimel JP, Gulledge, J. (1998) Microbial community structure and global trace gases. Global Change Biology 4:745–758

Thioulouse J, Chessel D, Dolédec S, Olivier JM (1997) ADE-4: a multivariate analysis and graphical display software Statistics and Computing 7:75-83

Thioulouse J, Lobry JR (1995) Co-inertia analysis of amino-acid physico-chemical properties and protein composition with the ADE package. Comput Appl Biosci. 11:321-329

Thomas WH, Duval B (1995) Sierra Nevada, California, USA, snow algae: snow albedo changes, algal-bacterial interrelationships, and ultraviolet radiation effects. Arctic, Antarctic, and Alpine Research 27:389–399

Tranter M, Sharp MJ, Lamb HR, Brown GH, Hubbard BP, Willis IC (2002) Geochemical weathering at the bed of Haut Glacier d'Arolla, Switzerland—a new model. Hydrological Processes 16:959-993

Walter KD, Dolly AG, Dieter M (1995) THE ECOLOGY OF *NOSTOC*. Journal of Phycology 31:2-18

CHAPTER 7: A PYROSEQUENCING APPROACH TO EXPLORE COMMUNITY STRUCTURE AND FUNCTION IN ARCTIC SNOW

Introduction

The Arctic snowpack is chemically dynamic and interacts with different environmental compartments such as the atmosphere, the soil and meltwater. Each of these compartments probably supports unique ecosystems. Snowpacks store nutrients, soluble inorganic or organic matter and contaminants, such as mercury (Hg) that are delivered by wet and dry deposition (Kuhn 2001; Daly and Wania 2004) and are dynamic habitats able to sustain microorganisms (Jones 1999). Despite the cold conditions and limited water supply, microbial communities inhabiting the snow cover are dynamic and changes in community structure are linked to chemistry. In turn, microorganisms also have the potential to alter their chemical environment (Chapter 6). Microorganisms impact the dynamics, composition and abundance of nutrients (Hodson et al. 2008) and impact the transformation of contaminants, such as Hg (Poulain et al. 2007) through detoxification processes that convert inorganic Hg to its volatile elemental form and methylation/demethylation processes that convert inorganic Hg to methyl mercury (MeHg) and *vice versa* (Barkay et al. 2003, Chapter 6).

We used a pyrosequencing approach to uncover genes involved in microbial metabolism, nutrient cycling and contaminant transformation to provide insight into functional community structure in Arctic snow. Pyrosequencing also provided taxonomic data. An early spring season sample with low methyl mercury concentrations was compared to a late season sample with high methyl mercury concentrations in order to determine whether functional community properties varied. Here, we provide an overview of functional community structure within snowpacks and attempt to relate differences in functional community data to snow chemistry.

Methods

Samples were taken during a 2008 springtime field campaign in Ny-Ålesund (Svalbard, Norway, 78°56'N, 11°52'E). Samples were collected in three 3 L sterile sampling bags using a Teflon shovel sterilized for microbial analyzes from shallow pits (depth 35 cm) on the 19th of April and the 2nd of June. The samples will be hereafter referred to as ESS (early spring sample) for the sample collected on the 19th of April, and LSS (late spring sample) for the sample collected on the 2nd of June. To avoid contamination, Tyvex® body suits and latex gloves were worn during sampling and gloves were worn during all subsequent handling of samples. Snow chemistry was analysed in detail and is the subject of another paper (Larose et al. In preparation). However, a table with the major chemical parameters is presented as a basis for comparison between samples (Table 1).

Table I: Chemical parameters measured in each of the samples.

Parameter	ESS	LSS
date	19/04/2008	02/06/2008
pH	4.93	6.39
Total mercury (ng/L)	1.9	3.34
Methylmercury (ng/L)	0.014	0.245
Bioavailable mercury (ng/L)	1.6	<0.5
Formate µeq/L	0.05	0.22
Acetyl Glycine µeq/L	0.41	2.64
Propionate µeq/L	0.00	0.35
MSA µeq/L	0.00	0.57
Cl µeq/L	156.13	1456.69
NO_2 µeq/L	0.17	0.00
Br µeq/L	0.25	3.97
NO_3 µeq/L	2.16	1.88
Glutaric acid µeq/L	0.00	0.04
SO_4 µeq/L	11.61	76.41
Ox µeq/L	0.00	0.97
Na µeq/L	141.78	1258.22
NH_4 µeq/L	1.27	14.18
K µeq/L	2.52	24.03
Mg µeq/L	31.98	276.12
Ca µeq/L	7.15	88.64

Microbial sample processing

Samples were processed immediately after collection in the field laboratory. Samples were left to melt at room temperature prior to being filtered onto sterile 0.22 µM - 47 mm filters (Millipore) using a sterile filtration unit (Nalge Nunc International Corporation). Filters were stored in sterile bead-beating tubes at -20°C until further analysis. Procedural blanks were carried out by filtering Nanopure water (Siemens) using the same procedure.

DNA extraction

DNA was extracted as described previously (David et al. 2009). Briefly, filters were chopped and placed in a Fastprep® bead-beating tube (Lysing matrix E, MP Biomedicals). A mixture of 1 mL DNA extraction buffer and 20 $mg.ml^{-1}$ lysing enzyme (*Trichoderma harzianum*, Sigma L1412) was added. Tubes were left at room temperature for 1 hour and then frozen at -20°C overnight. The frozen tubes were incubated at 65°C for 30 minutes and placed in a Fastprep® bead-beater (MP Biomedicals) set at speed 5.5 for 30 seconds. DNA was extracted from the water phase with an equal volume of chloroform:isoamyl alcohol (24:1) and precipitated with isopropanol.

Pyrosequencing

The DNA (2µg/50µL) extracted from environmental samples was pyrosequenced by GATC (Constanz, Germany) using a Roche 454 Titanium pyrosequencer. For the ESS sample, 38,129 sequences of average 378 bp lengths were subsequently analyzed by the MG-RAST system (Meyer et al. 2008) and 36% of sequences were phylogenetically classified using the SEED database, while 29.2 % were classified into different microbial metabolic subsystems due to their similarity to known functional genes. For the LSS sample, 16,222 sequences of average 331 bp lengths were analyzed and 44% of the sequences were phylogenetically classified while 29.6 % were classified into metabolic subsystems. The *e*-value cutoff was set at 1e-5 for all analyzes and a minimum alignment length of 50 bp was used for phylogenetic assignment.

The relative number of sequences classified in different metabolic subsystems is shown as percentages of the total. In order to compare different samples, the normalized numbers of fragments in each subsystem are compared. In addition, the relative abundance of fragments in each subsystem was determined by adding the number of all fragments from all samples that are classified in a subsystem and dividing by the number of samples included in the comparison.

Results and Discussion

Microbial community structure in pyrosequence samples

The samples chosen for pyrosequencing analysis differ chemically (Section III, Chapter 5) and also in terms of community structure (Section IV, Chapter 6). The sequences in the ESS and LSS metagenomes covered four domains of which Bacteria dominated (> 90% for both metagenomes) and 17 different bacterial groups. In the ESS metagenome, the *Bacteriodetes/Chlorobi* (37%) and *Proteobacteria* (34%) groups dominated (Figure 1A), consistent with other studies in polar environments (Skidmore et al. 2005; Cheng and Foght 2007). In the *Bacteriodetes* group the most-represented class was *Flavobacteria* (70%), members of which are common in cold environments and are often cold-adapted (psychrophilic or psychrotolerant) (Bowman et al. 2003). In the LSS metagenome, *Proteobacteria* (70%) was the most-represented group, of which 93% were *Gammaproteobacteria* (Figure 1B). The predominance of *Gammaproteobacteria* has been reported in Everest snow samples (Liu et al. 2009) and Arctic sea ice (Brinkmeyer et al. 2003).

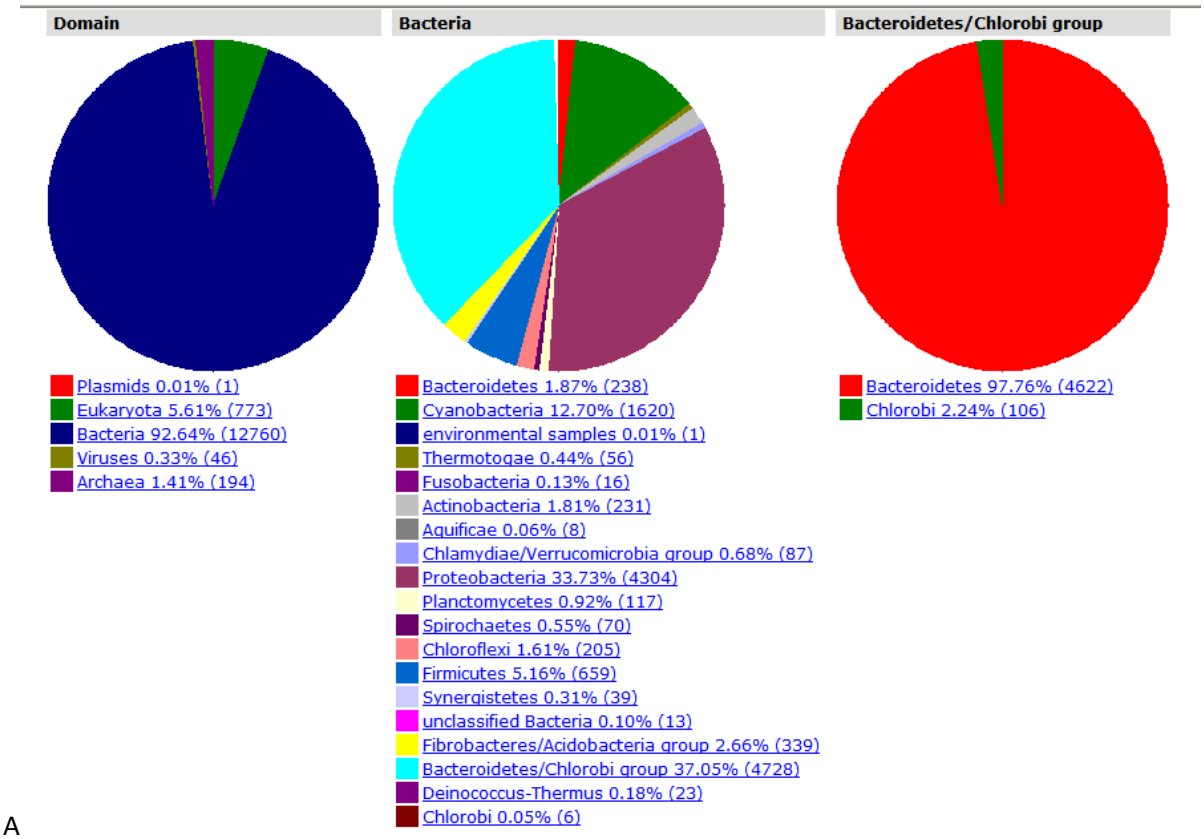

A

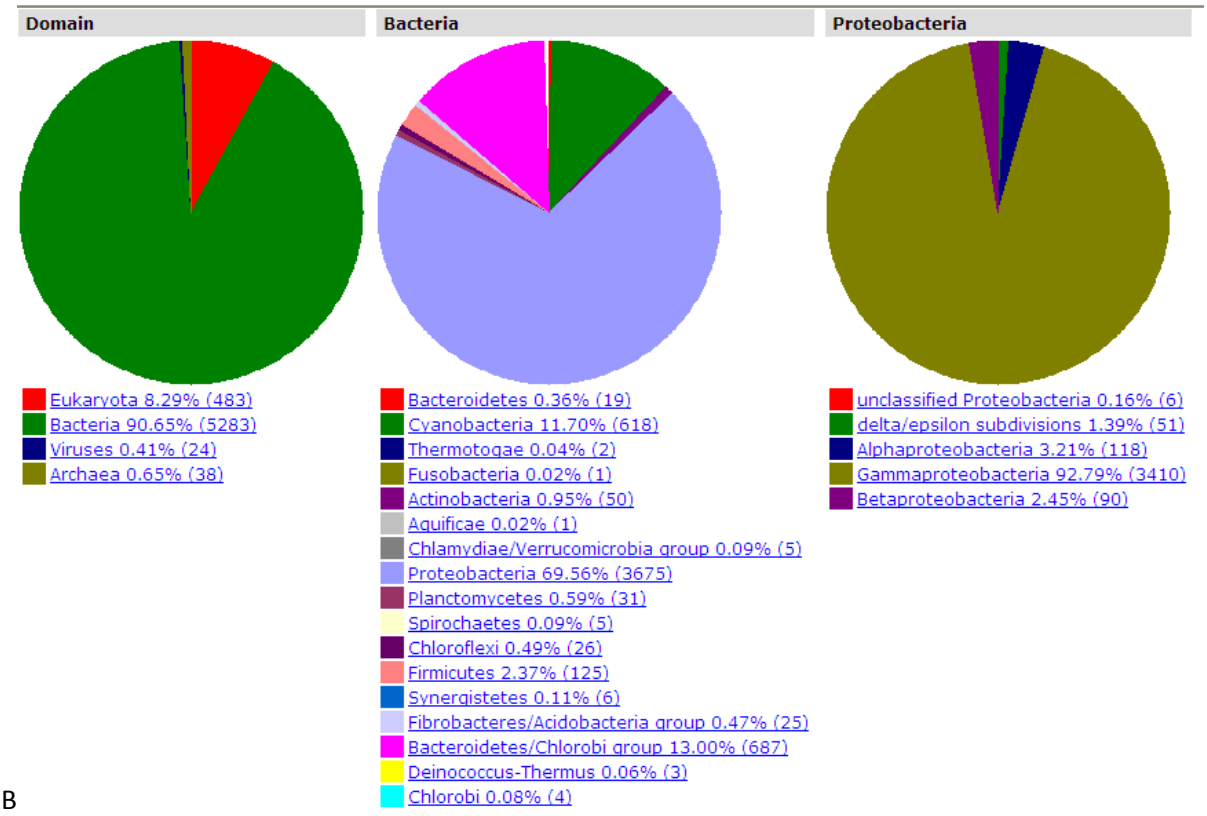

B

Figure 1: Taxonomic profiles for the ESS (A) and LSS (B) metagenomes. Sequences were classified using the SEED database in MG-RAST. The *e*-value cutoff was 1e-5 and a minimum alignment length of 50 bp was used.

The class distribution of both metagenomes was compared (Figure 2). In both samples, *Cyanobacteria* (*Nostocales*, *Chroococcales*) represented approximately 10% of the classes. The community structure differed, with higher percentages of *Gammaproteobacteria*, *Metazoa* and *Fungi* in the LSS metagenome, while *Acidobacteria* were detected only in ESS. Based on the SEED classification, the most common bacterium in the *Gammaproteobacteria* class was *Pseudoalteromonas haloplanktis* TAC125, a cold-adapted marine organism isolated from Antarctica (Giordano et al. 2007). The increased abundance of marine *Gammaproteobacteria* in the LSS sample may be linked to the higher salt concentrations. Among the *Fungi* species, *Neurospora crassa* was the most abundant. It is possible that this *Fungi* may contribute to the higher MeHg concentrations observed in the LSS sample, since it is able to methylate Hg in laboratory studies (Barkay et al. 2005). The lower pH in the ESS sample may explain why the *Acidobacteria* class was only observed in the ESS meteagenome.

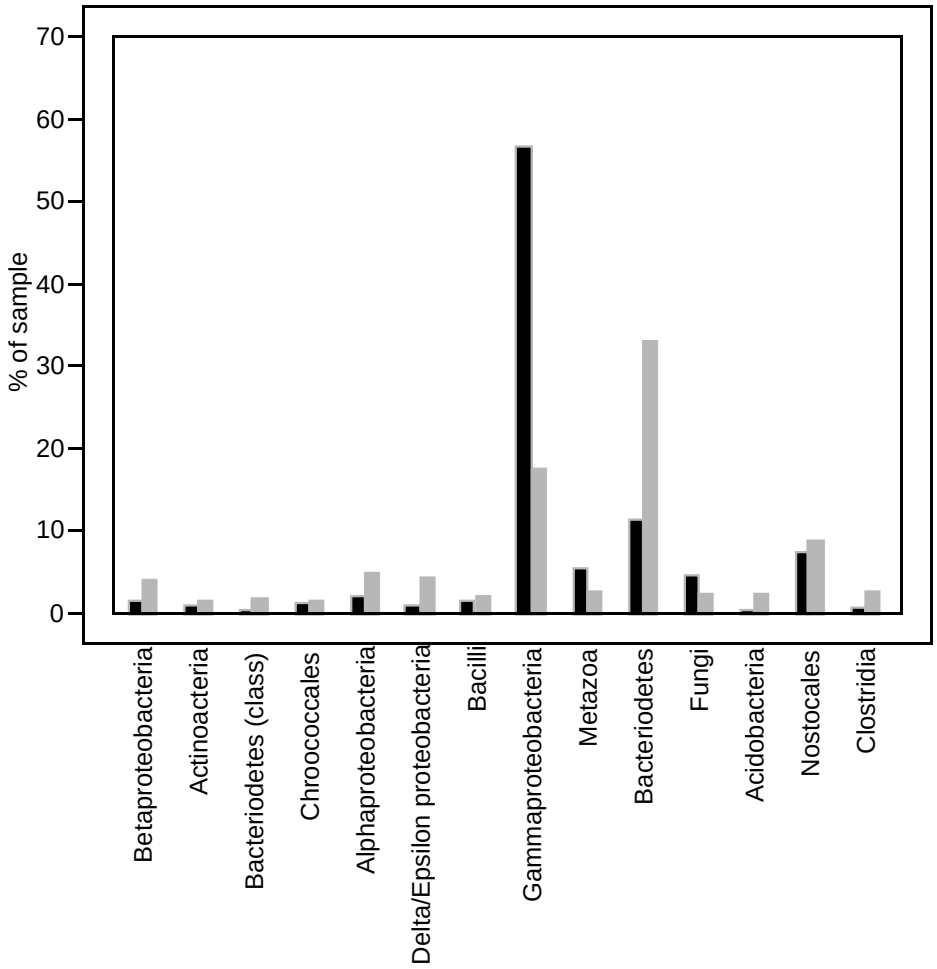

Figure 2: Taxonomic distribution in ESS and LSS metagenomes. A total of 17 bacterial classes are presented in addition to two members of the Eukarya domain (Metazoa and Fungi).The bars represent the percentage of each class in each library, with black and gray bars representing the LSS and ESS samples, respectively.

Community functional genes

Common functions

The pyrosequencing of snow samples allowed us to access a diverse set of functional genes. Genes common to both samples belong to a wide range of functional categories listed in Table II. Most fall into basic metabolic activities such as amino-acid and protein biosynthesis, membrane transport, respiration and DNA metabolism. Functional genes common to metagenomes from both samples also include genes encoding capsular and exopolysaccharides (EPS) (Table II). Both EPS production and increases in capsular wall thickness have been described as survival strategies to cold environments (Price and Sowers 2004). EPS production favors attachment (Junge 2004) and protects against freezing, dessiccation, viral and bacterial attacks (Mueller et al. 2005). Particle-associated bacteria producing EPS were shown to be more active than free-living cells as temperatures dropped (Junge 2004).

Table II: Metabolic functions common to both samples

Level 1	Level 2
Amino acids and derivatives	Arginine; urea cycle, polyamine metabolism
	Branched-chain amino acid biosynthesis
	Osmotic stress choline/betaine uptake and betaine biosynthesis
Carbohydrates	One-carbon metabolism serine/glyoxylate cycle
	Central carbohydrate metabolism
	CO_2 fixation (CO_2 uptake, carboxysome)
Cell Wall and capsule	Capsular and extracellular polysaccharides
	Gram-Negative cell wall components
Clustering-based subsystems	Purine metabolism
	DNA methylation
	Translation
Cofactors, Vitamins, Pigments	Biotin biosynthesis
	Tetrapyrrole (Heme/Siroheme, colbalamin, chlorophyll) biosynthesis
DNA metabolism	DNA replication
Fatty Acids and Lipids	Phospholipids
Membrane Transport	Membrane transport (potassium homosynthesis, zinc transport)
Motility and Chemotaxis	Flagellar motility in Prokaryota
Nitrogen metabolism	Nitrogen metabolism (nitrate, nitrite ammonification)
Protein metabolism	Protein degradation in Eukaryotes
Regulation and Cell signaling	Regulation and Cell signaling
Respiration	Electron accepting reactions (cytochrome C)
	Cytochrome C biogenesis
RNA metabolism	RNA processing and modification
Stress response	Stress response (copper, SigmaB response)
	Cold shock
Sulfur metabolism	Inorganic sulfur assimilation
Virulence	Resistance to antibiotics and toxic compounds (mercury)
	Iron scavenging mechanisms
	Ton and Tol transport systems

Common functions also include tetrapyrrole biosynthesis (Table II). Tetrapyrroles are ringed compounds that act as cofactors and vitamins (e.g. methyl cobalamin) and as pigments (e.g. chlorophyll). They are implicated in electron transfer, redox and a variety of metabolic reactions (Frankenberg et al. 2003). Due to the high irradiance of the snowpack, it is likely that increased pigment production could provide a protective mechanism for bacteria (Mueller et al. 2005).

Both samples contained genes involved in stress response and virulence. Among the stress response genes, cold shock and SigmaB response factor genes were identified. The SigmaB factor is required for the transcription of a subset of genes/operons that confer general stress resistance to the cell (Marles-Wright and Lewis 2007). The presence of stress resistance genes was not surprising considering the range of environmental stresses, including temperature, pH, osmolarity, radiation and the concentration of nutrients and contaminants to which bacteria are exposed in the snow. Among the virulence genes, genes encoding resistance to antibiotics and metals such as mercuric reductase were also identified (Figure 3).

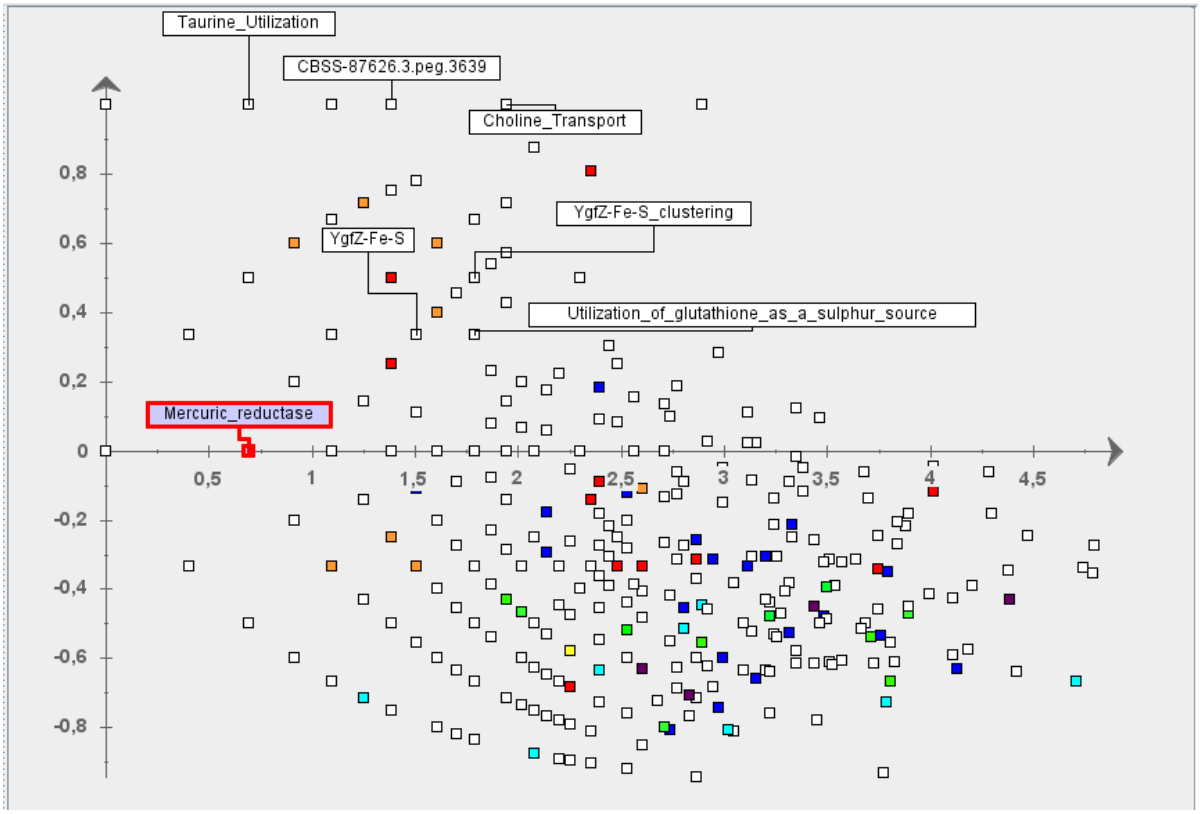

Figure 3: Differences in metabolic functions between the LSS and ESS samples. Squares in the upper part of the graph (positive values) represent genes identified more frequently in the LSS sample. Red squares represent stress response genes, orange squares represent ABC transporter genes, blue squares represent carbohydrate metabolism, yellow squares represent aromatic compound metabolism, green squares represent vitamin/cofactor metabolic genes, purple squares represent DNA repair and light blue squares represent protein biosynthesis.

Differences in community function

General metabolism

The metagenome from the ESS sample contained a higher proportion of genes involved in the biosynthesis of proteins (light blue squares, Figure 3) and vitamins/cofactors (green squares, Figure 3) than the LSS sample. In addition, genes involved in DNA repair (purple squares, Figure 3) were also more frequent in the ESS sample. Other differences include carbohydrate and aromatic compound metabolism, with a greater number of genes in the ESS sample. These metabolic differences may be due to differences in community structure, since the ESS sample contains a wider range of bacterial classes (Figure 2).

Sulfur metabolism

Sulfur assimilation varied between both samples, with inorganic sulfur pathways observed in the ESS sample and organic sulfur assimilation pathways observed in LSS. The LSS sample contained a higher proportion of genes involved in using glutathione and taurine as sulfur sources, which is indicative of sulfur starvation conditions (Viti et al. 2009). In addition, under sulfur starvation conditions, ABC transport systems have been shown to be up-regulated (Colin et al. 2007), which is also observed in the LSS metagenome (Figure 3). All living organisms require sulfur, which can be assimilated either from inorganic sources like sulfate and thiosulfate, or from organic ones like sulfate esters, sulfamates and sulfonates, for the synthesis of proteins and essential cofactors (Coppee et al. 2001). A major source of sulfur for bacteria in the marine environment is dimethylsulfoniopropionate (DMSP) (Howard et al. 2006). Larose et al. (Section III, Chapter 5) reported high methylsulfonic acid (MSA) concentrations in snow during the spring. Since MSA is a derivative of DMSP, the high concentrations observed suggest a close source for DMSP. DSMP can either undergo direct uptake by bacteria via specific transporters such as choline-betaine transporters (Kiene et al. 2000) or lysis by extra-cellular enzymes. Genes encoding choline transporters were only found in the LSS sample, suggesting that DMSP uptake is possibly occurring. Once inside the organism, DMSP is either retained (probably for osmo/cryoprotection), or metabolized for bioenergetic purposes (Kiene and Linn 2000) via two different pathways: the lyase pathway or the demethylation/demethiolation pathway (Bentley and Chasteen 2004). Unlike the lyase pathway, the demethylation/demethiolation pathway leads to sulfur assimilation (Kiene et al. 2000) and therefore, under sulfur-starvation conditions, this pathway should be favored.

The demethylation/demethiolation pathway involves an initial demethylation of DMSP to MMPA (3-methylmercaptoproprionate) and a methyl compound (Taylor and Gilchrist 1991). This reaction was

shown to occur in both aerobic and anaerobic cultures and involves methyltransferase activity (Bentley and Chasteen 2004). In the LSS sample, we observe the presence of aminomethyltransferase (CBSS-87626.3 peg. 3639), which was not present in the ESS sample (Figure 3). Recently, Reisch et al. (2008) demonstrated that aerobic demethylation of DMSP was THF-dependent (THF=tetrahydrofolate). The enzyme that catalyzes this reaction, DmdA, is in the aminomethyl transferase family (EC 2.1.2.10), which includes the T-protein of the glycine cleavage system (Reisch et al. 2008). Methyl-THF is an intermediate in the oxidative acetyl CoA/CO dehydrogenase pathway. Two clusters involved in THF synthesis (YgfZ-Fe-S) are more prominent in the LSS sample than in the ESS sample. YgfZ-Fe-S is an unclassified gene that clusters with dihydrofolate reductase, an enzyme that catalyzes the reduction of folate and 7,8-dihydrofolate (DHF) to 5,6,7,8-tetrahydrofolate (THF) (Elizabeth 2005). Taken together, these results suggest that demethylation reactions could potentially be carried out to a greater extent in the LSS sample than in the ESS sample.

Linking sulfur metabolism to mercury methylation

Early research into the mechanisms involved in mercury methylation was based on anoxic sediments (e.g. Compeau and Bartha 1985; Berman et al. 1990) and quickly focused on anaerobic, sulfate reducing bacteria. The isolation of mercury-methylating *Desulfovibrio desulfuricans* strains led to studies on the pathway of methylation and the potential methyl donors (Berman et al. 1990; Choi et al. 1994). Berman et al. (1990) suggested that the methyl donor in *D. desulfuricans* is likely closely related to or identical to methylcobalamin based on selective inhibition assays with propyl iodide. Choi et al. (1994) used radio-labeled ^{14}C incorporation and enzyme activity measurements to propose that methylation involves the tetrahydrofolate (THF) pathway. In their model, the methyl group is transferred from CH_3-tetrahydrofolate via methylcobalamin with either serine or formate as the original methyl donors via the acetyl-CoA synthase pathway (Choi et al., 1994). The parallels with DMSP demethylation are striking: both involve the THF and acetyl-CoA pathways and methyltransferases, except one occurs aerobically, while the other is anaerobic. Since these pathways are so similar, it is not farfetched to imagine that bioavailable Hg, upon entering the cell, may undergo methylation by aerobic bacteria able to demethylate or metabolize DMSP. Methyl transfer reactions occur at various stages of DMSP metabolism and many of the genes encoding the enzymes involved are present in the LSS, which is associated to high MeHg concentrations.

While these results are only preliminary, the LSS does appear to contain genes involved in methyltransfer and tetrahydrofolate metabolism that are not present in the ESS sample. In order to further explore the hypothesis that methylation is occurring, we have sent other samples for

pyrosequencing. The results from the future pyrosequencing should shed some light on metabolic pathways present in samples containing high levels of methylmercury.

References

Barkay T, Miller SM, Summers AO (2003) Bacterial mercury resistance from atoms to ecosystems. FEMS Microbiology Reviews 27:355-384

Barkay T, Wagner-Döbler I, Laskin AI, Bennett JW, M. GG (2005) Microbial Transformations of Mercury: Potentials, Challenges, and Achievements in Controlling Mercury Toxicity in the Environment. In: Advances in Applied Microbiology. Academic Press, pp 1-52

Bentley R, Chasteen TG (2004) Environmental VOSCs--formation and degradation of dimethyl sulfide, methanethiol and related materials. Chemosphere 55:291-317

Berman M, Chase T, Jr., Bartha R (1990) Carbon Flow in Mercury Biomethylation by Desulfovibrio desulfuricans. Applied and Environmental Microbiology 56:298-300

Bowman JP, Nichols CM, Gibson JAE (2003) *Algoriphagus ratkowskyi* gen. nov., sp. nov., *Brumimicrobium glaciale* gen. nov., sp. nov., *Cryomorpha ignava gen*. nov., sp. nov. and *Crocinitomix catalasitica* gen. nov., sp. nov., novel flavobacteria isolated from various polar habitats. International Journal of Systematic and Evolutionary Microbiology 53:1343-1355

Brinkmeyer R, Knittel K, Jurgens J, Weyland H, Amann R, Helmke E (2003) Diversity and structure of bacterial communities in Arctic versus Antarctic pack ice. Applied and Environmental Microbiology 69:6610-6619

Cheng SM, Foght JM (2007) Cultivation-independent and -dependent characterization of Bacteria resident beneath John Evans Glacier. FEMS Microbiology Ecology 59:318-330

Choi SC, Chase T, Jr., Bartha R (1994) Enzymatic catalysis of mercury methylation by *Desulfovibrio desulfuricans* LS. Applied and Environmental Microbiology 60:1342-1346

Colin S, Margaret EH, Christopher WC, Robyn JR, John GO, Tara DS (2007) A global response to sulfur starvation in *Pseudomonas putida* and its relationship to the expression of low-sulfur-content proteins. FEMS Microbiology Letters 267:184-193

Compeau GC, Bartha R (1985) Sulfate reducing bacteria: principal methylators of mercury in anoxic estuarine sediment. Applied and Environmental Microbiology 50:498–502

Coppee J-Y et al. (2001) Sulfur-limitation-regulated proteins in *Bacillus subtilis*: a two-dimensional gel electrophoresis study. Microbiology 147:1631-1640

Daly GL, Wania F (2004) Simulating the Influence of Snow on the Fate of Organic Compounds. Environmental Science and Technology 38:4176-4186

David MM, Mesle M, Malandain C, Cohen D, Vogel TM (2009) Molecular Biology-based strategy for site remediation. Environmental Science and Technology Submitted

Elizabeth EH (2005) Searching Sequence Space: Two Different Approaches to Dihydrofolate Reductase Catalysis. ChemBioChem 6:590-600

Frankenberg N, Moser J, Jahn D (2003) Bacterial heme biosynthesis and its biotechnological application. Applied Microbiology and Biotechnology 63:115-127

Giordano D et al. (2007) The truncated hemoglobins in the Antarctic psychrophilic bacterium Pseudoalteromonas haloplanktis TAC125. Gene 398:69-77

Hodson A et al. (2008) Glacial Ecosystems. Ecological Monographs 78:41-67

Howard EC et al. (2006) Bacterial Taxa That Limit Sulfur Flux from the Ocean. Science 314:649-652

Jones HG (1999) The ecology of snow-covered systems: a brief overview of nutrient cycling and life in the cold. Hydrol Process 13:2135–2147

Junge K, Eicken,Hajo, Deming, Jody W. (2004) Bacterial Activity at -2 to -20°C in Arctic Wintertime Sea Ice. Applied and Environmental Microbiology 70:550-557

Kiene RP, Linn LJ (2000) The fate of dissolved dimethylsulfoniopropionate (DMSP) in seawater: tracer studies using 35S-DMSP. Geochimica et Cosmochimica Acta 64:2797-2810

Kiene RP, Linn LJ, Bruton JA (2000) New and important roles for DMSP in marine microbial communities. Journal of Sea Research 43:209-224

Kuhn M (2001) The nutrient cycle through snow and ice, a review. Aquatic Science 63:150-167

Larose C et al. (In preparation) Seasonal changes in snow chemistry lead to new insights into mercury methylation in the Arctic.

Liu Y et al. (2009) Bacterial diversity in the snow over Tibetan Plateau Glaciers. Extremophiles 13:89-99

Marles-Wright J, Lewis RJ (2007) Stress responses of bacteria. Current Opinion in Structural Biology 17:755-760

Meyer F et al. (2008) The metagenomics RAST server - a public resource for the automatic phylogenetic and functional analysis of metagenomes. BMC Bioinformatics 9:386

Mueller DR, Vincent WF, Bonilla S, Laurion I (2005) Extremotrophs, extremophiles and broadband pigmentation strategies in a high arctic ice shelf ecosystem. FEMS Microbiology Ecology 53:73–87

Poulain AJ et al. (2007) Potential for mercury reduction by microbes in the high arctic. Applied and Environmental Microbiology 73:2230-2238

Price PB, Sowers T (2004) Temperature dependence of metabolic rates for microbial growth, survival and maintenance. Proc Natl Acad Sci USA 101 4631–4636

Reisch CR, Moran MA, Whitman WB (2008) Dimethylsulfoniopropionate-dependent demethylase (DmdA) from *Pelagibacter ubique* and *Silicibacter pomeroyi*. The Journal of Bacteriology 190:8018-8024

Skidmore M, Anderson SP, Sharp M, Foght J, Lanoil BD (2005) Comparison of microbial community compositions of two subglacial environments reveals a possible role for microbes in chemical weathering processes. Applied and Environmental Microbiology 71:6986-6997

Taylor BF, Gilchrist DC (1991) New Routes for Aerobic Biodegradation of Dimethylsulfoniopropionate. Applied and Environmental Microbiology 57:3581-3584

Viti C, Decorosi F, Mini A, Tatti E, Giovannetti L (2009) Involvement of the oscA gene in the sulphur starvation response and in Cr(VI) resistance in *Pseudomonas corrugata* 28. Microbiology 155:95-105

SECTION V: GENERAL CONCLUSION AND PERSPECTIVES

The Arctic climate is changing. A 20th century warming trend has been documented in the Arctic, with air temperatures over land areas increasing by as much as 5°C and increased temperatures over sea ice (AMAP 2009). In addition, precipitation has also increased. Other changes include a 2.9% per decade decrease in Arctic sea-ice extent (1978-1996), the thinning of sea-ice, an increase in melt days par summer, the warming of Atlantic water flowing into the Arctic Ocean, the thinning of the oceanic surface layer and the increase in ground temperatures and resulting permafrost melt (Anisimov O 2001). Decreases in snow and ice cover, increased plant growth, increased primary production of terrestrial algae in freshwater lakes, and the northward movement of the tree line in the most-warmed Arctic regions have also been reported (AMAP 2009). While it is unclear whether these changes are linked to natural cycles in climate or exclusively to global warming, human activities are clearly impacting the climate, with arctic (and polar) environments subjected to substantial warming and increases in precipitation over the 21st century.

Climate change is also expected to alter contaminant loading and transformations in the Arctic. The predicted warming of air temperatures at lower latitudes will have direct effects on contaminants through increased volatility, more rapid degradation and altered partitioning between phases (Macdonald et al. 2005), while increased precipitation could lead to more scavenging of contaminants by rain and snow, thereby augmenting inputs to aquatic and terrestrial ecosystems (AMAP 2009). Extended ice-free areas in the Arctic Ocean may favor both atmospheric scavenging by precipitation in addition to seawater partitioning (AMAP 2009) and certain contaminants might evade from surface seawater more rapidly (Macdonald et al. 2005).

While it appears that microbial life is well adapted to cold ecosystems, the response of these populations to changing environments is mostly unknown. Climate change may alter microbial functioning by increasing growth rates and substrate use due to increased temperature. This may lead to changes in process rates. Another impact could be the restructuring of microbial communities (Schimel 1998). Biodiversity may increase as the Arctic warms and population shifts occur as non-heat tolerant species disappear in favour of more heat tolerant ones. For example, a circumpolar shift was seen in the fossil remains of algae and invertebrates in the mid to late 19th century probably due to climate change. In order to predict how ecological processes will evolve as a function of global change, it is essential to identify which populations participate in each process, how they vary physiologically, and how the relative abundance, activity and community structure will change under altered environmental conditions (Schimel and Gulledge 1998).

This thesis sought to explore the relationships between chemical parameters in arctic snowpacks and the microbial communities inhabiting them. Chemistry and community structure were shown to be linked. Major results include the observation that precipitation may be a more important source for bioavailable mercury inputs to arctic snowpacks than previously expected. This may have far-reaching consequences in light of predicted changes due to global warming. Another important finding is a possible link between the marine sulphur cycle and the biotic production of methylmercury. Based on our results, biotic methylation occurs when the snowpack is melting, thus warmer, wetter snowpacks, coupled with more productive surface waters, may lead to increases in methylmercury. Both bioavailable mercury and methylmercury impact community structure at concentrations lower than previously reported. In turn, microbial communities are able to modify the chemical environment by transforming contaminants, and the rates of these reactions may determine ecosystem contamination levels. Therefore, the role of microorganisms in ecosystem functioning should not be neglected.

All the results presented here are derived from field studies. These data will now allow laboratory studies to a) improve our knowledge on mercury speciation, especially in terms of organics; b) verify the implication of DMSP in mercury methylation with the use of stable isotopes; and c) improve our understanding of the interactions between individual species and chemical parameters using pure cultures. Other future research directions should include functional gene analysis with pyrosequencing technologies and RNA analysis to elucidate which genes are being transcribed.

BIBLIOGRAPHY

Allard B, Arsenie I (1991) Abiotic reduction of mercury by humic substances in aquatic system — an important process for the mercury cycle. Water, Air and Soil Pollution 56:457–464

AMAP (1997) Arctic Pollution Issues: A State of the Arctic.

AMAP (1998) Assessment Report: Arctic Pollution Issues.

Amap (2003) AMAP Assessment 2002: Human Health in the Arctic. Arctic Monitoring and Assesment Programme (AMAP). In, Oslo, Norway, p 137

AMAP (2009) AMAP Assessment 2009: Human Health in the Arctic. Arctic Monitoring and Assessment Programme (AMAP). In, Oslo, Norway

AMAP/UNEP (2008) Technical Background Report to the Global Atmospheric Mercury Assessment. Arctic Monitoring and Assessment Programme/UNEP Chemicals Branch. In, Oslo, p 159

Amato P et al. (2007) Bacterial characterization of the snow cover at Spitzberg, Svalbard. Fems Microbiology Ecology 59:255-264

Amyot M, Gill GA, Morel FMM (1997) Production and Loss of Dissolved Gaseous Mercury in Coastal Seawater. Environmental Science and Technology 31:3606–3611

Ancora S, Rossi R, Di Simplicio P, Lusini L, Leonzio C (2002) In Vitro Study of Methylmercury in Blood of Bottlenose Dolphins (*Tursiops truncatus*). Archives of Environmental Contamination and Toxicology: 348-353

Anderson CR et al. (2009) *Aurantimonas manganoxydans*, sp. nov. and *Aurantimonas litoralis*, sp. nov.: Mn(II) oxidizing representatives of a globally distributed clade of *alpha-Proteobacteria* from the order *Rhizobiales*. Geomicrobiology Journal 26:189–198

Anisimov O FB (2001) Polar regions (Arctic and Antarctic) In: McCarthy JJ CO, Leary NA, Dokken DJ, White KS (eds) (ed) Intergovernmental Panel on Climate Change Climate Change 2001: Impacts, Adaptation, and Vulnerability. Cambridge University Press, Cambridge, pp 801-841

Ariya PA et al. (2004) The Arctic: a sink for mercury. Tellus Series B-Chemical and Physical Meteorology 56:397-403

Ariya PA, Khalizov A, Gidas A (2002) Reactions of gaseous mercury with atomic and molecular halogens: Kinetics, product studies, and atmospheric implications. Journal of Physical Chemistry A 106:7310-7320

Aspmo K et al. (2005) Measurements of atmospheric mercury species during an international study of mercury depletion events at Ny-Alesund, Svalbard, spring 2003. How reproducible are our present methods? Atmospheric Environment 39:7607-7619

Bales RC, Davis RE, Williams MW (1993) Tracer release in melting snow: diurnal and seasonal patterns. Hydrological Processes 7:389–401

Barkay T, Gillman M, Turner RR (1997) Effects of dissolved organic carbon and salinity on bioavailability of mercury. Applied and Environmental Microbiology 63:4267-4271

Barkay T, Miller SM, Summers AO (2003) Bacterial mercury resistance from atoms to ecosystems. FEMS Microbiology Reviews 27:355-384

Barkay T, Poulain AJ (2007) Mercury (micro)biogeochemistry in polar environments. FEMS Microbiology Ecology 59:232-241

Barkay T, Wagner-Döbler I, Laskin AI, Bennett JW, M. GG (2005) Microbial Transformations of Mercury: Potentials, Challenges, and Achievements in Controlling Mercury Toxicity in the Environment. In: Advances in Applied Microbiology. Academic Press, pp 1-52

Barrie LA, Bottenheim JW, Schnell RC, Crutzen PJ, Rasmussen RA (1988) Ozone destruction and photochemical reactions at polar sunrise in the lower Arctic atmosphere. Nature 334:138–141

Bellion M, Courbot M, Jacob C, Blaudez D, Chalot M (2006) Extracellular and cellular mechanisms sustaining metal tolerance in ectomycorrhizal fungi. FEMS Microbiology Letters 254:173–181

Bentley R, Chasteen TG (2004) Environmental VOSCs--formation and degradation of dimethyl sulfide, methanethiol and related materials. Chemosphere 55:291-317

Berg T, Sekkesaeter S, Steinnes E, Valdal AK, Wibetoe G (2003) Springtime depletion of mercury in the European Arctic as observed at Svalbard. Science of the Total Environment 304:43-51

Berman M, Chase T, Jr., Bartha R (1990) Carbon Flow in Mercury Biomethylation by Desulfovibrio desulfuricans. Applied and Environmental Microbiology 56:298-300

Berntssen MHG, Aatland A, Handy RD (2003) Chronic dietary mercury exposure causes oxidative stress, brain lesions, and altered behaviour in Atlantic salmon (*Salmo salar*) paar Aquatic Toxicology 65:55-72

Bottenheim JW, Gallant AG, Brice KA (1986) Measurements of NOx species and O_3 at 82°N latitude. Geophysical Research Letters 22:599-602

Boudou A, Delnomdedieu M, Georgescauld D, Ribeyre F, Saouter E (1991) Fundamental roles of biological barriers in mercury accumulation and transfer in freshwater ecosystems (analysis at organism, organ, cell and molecular levels). Water, Air, and Soil Pollution 56 807-821

Bowman JP, Nichols CM, Gibson JAE (2003) *Algoriphagus ratkowskyi* gen. nov., sp. nov., *Brumimicrobium glaciale* gen. nov., sp. nov., *Cryomorpha ignava* gen. nov., sp. nov. and *Crocinitomix catalasitica* gen. nov., sp. nov., novel *flavobacteria* isolated from various polar habitats. International Journal of Systematic and Evolutionary Microbiology 53:1343-1355

Brimblecombe P, Tranter, M., Tsiouris, S., Davies, T. D. and Vincent, C. E. (1986) The chemical evolution of snow and meltwater. Modelling Snowmelt-Induced Processes (Proceedings of the Budapest Symposium July 1986) IAHS Publ 155:283-295

Brinkmeyer R, Knittel K, Jurgens J, Weyland H, Amann R, Helmke E (2003) Diversity and structure of bacterial communities in Arctic versus Antarctic pack ice. Applied and Environmental Microbiology 69:6610-6619

Brooks S, Lindberg S, Southworth G, Arimoto R (2008) Springtime atmospheric mercury speciation in the McMurdo, Antarctica coastal region. Atmospheric Environment 42:2885-2893

Brunker RL (1976) Mercurial Toxicity in Yeast: Evidence for Catabolic Pathway Inhibition. Applied and Environmental Microbiology 32:498-504

Buffle J, Wilkinson KJ, van Leeuwen HP (2009) Chemodynamics and Bioavailability in Natural Waters. Environmental Science and Technology 43:7170-7174

CAFF (2001) Arctic Flora and Fauna: Status and Conservation.

Campbell LM, Norstrom RJ, Hobson KA, Muir DCG, Backus S, Fisk AT (2005) Mercury and other trace elements in a pelagic Arctic marine food web (Northwater Polynya, Baffin Bay). Science of the Total Environment 351:247-263

Carpenter EJ, Lin S, Capone DG (2000) Bacterial activity in South Pole snow. Applied and Environmental Microbiology 66:4514-4517

Castoldi AF, Coccini, Teresa, Ceccatelli, Sandra, Manzo, Luigi (2001) Neurotoxicity and molecular effects of methylmercury Brain Research Bulletin 55:197-203

Celo V, Lean DR, Scott SL (2006) Abiotic methylation of mercury in the aquatic environment. Science of the Total Environment 368:126-137

Champier L, Duarte V, Michaud-Soret I, Coves J (2004) Characterization of the MerD protein from *Ralstonia metallidurans* CH34: a possible role in bacterial mercury resistance by switching off the induction of the *mer* operon. Molecular Microbiology 52:1475-1485

Chao A (1984) Non-parametric estimation of the number of classes in a population. Scandinavian Journal of Statistics 11:265-270

Chauhan S, Shivaji S (1994) Growth and pigmentation in *Sphingobacterium antarcticus*, a psychrotrophic bacterium from Antarctica. Polar Biology 14:31-36

Chen J, Pehkonen SO, Lin C-J (2003) Degradation of monomethylmercury chloride by hydroxyl radicals in simulated natural waters. Water Research 37:2496-2504

Cheng SM, Foght JM (2007) Cultivation-independent and -dependent characterization of Bacteria resident beneath John Evans Glacier. FEMS Microbiology Ecology 59:318-330

Choi SC, Chase Jr. T, Bartha R (1994a) Enzymatic catalysis of mercury methylation by *Desulfovibrio desulfuricans* LS . Applied and Environmental Microbiology 60 1342-1346
Christner BC (2002) Incorporation of DNA and protein precursors into macromolecules by bacteria at -15 degrees C. Applied and Environmental Microbiology 68:6435-6438
Christner BC, Morris CE, Foreman CM, Cai R, Sands DC (2008) Ubiquity of biological ice nucleators in snowfall. Science 319:1214
Christner BC, Mosley-Thompson E, Thompson LG, Reeve JN (2001) Isolation of bacteria and 16S rDNAs from Lake Vostok accretion ice. Environmental Microbiology 3:570-577
Christner BC, Mosley-Thompson E, Thompson LG, Zagorodnov VS, Sandman K, Reeve JN (2000) Recovery and Identification of Viable Bacteria Immured in Glacial Ice. Icarus 144:479-485
Clarisse O, Foucher D, Hintelmann H (2009) Methylmercury speciation in the dissolved phase of a stratified lake using the diffusive gradient in thin film technique. Environmental Pollution 157:987-993
Clarisse O, Hintelmann H (2006) Measurements of dissolved methylmercury in natural waters using diffusive gradients in thin film (DGT). Journal of Environmental Monitoring 8:1242-1247
Colbeck SC (1978) The physical aspects of water flow through snow. Advances in Hydrosciences 11:165-206
Colbeck SC (1981) A simulation of the enrichment of atmospheric pollutants in snow cover runoff. Water Resources Research 17 1383–1388
Colbeck SC (1989) Air movement in snow due to windpumping. Journal of Glaciology 35:209–213
Colbeck SC (1991) The layered character of snow covers. Reviews of Geophysics 29:81-96
Cole JR et al. (2003) The Ribosomal Database Project (RDP-II): previewing a new autoaligner that allows regular updates and the new prokaryotic taxonomy. Nucleic Acids Res 31:442-443
Cole JR et al. (2009) The Ribosomal Database Project: improved alignments and new tools for rRNA analysis. Nucleic Acids Research 37, :Database Issue D141–D145 doi:110.1093/nar/gkn1879
Colin S, Margaret EH, Christopher WC, Robyn JR, John GO, Tara DS (2007) A global response to sulfur starvation in *Pseudomonas putida* and its relationship to the expression of low-sulfur-content proteins. FEMS Microbiology Letters 267:184-193
Compeau GC, Bartha R (1985) Sulfate reducing bacteria: principal methylators of mercury in anoxic estuarine sediment. Applied and Environmental Microbiology 50:498–502
Compeau GC, Bartha R (1987) Effect of salinity on mercury-methylating activity of sulfate-reducing bacteria in estuarine sediments. Applied and Environmental Microbiology 53:261–265
Comte K, Sabacká M, Carré-Mlouka A, Elster J, Komárek J (2007) Relationships between the Arctic and the Antarctic cyanobacteria; three *Phormidium*-like strains evaluated by a polyphasic approach. FEMS Microbiology Ecology 59:366-376
Constant P, Poissant L, Villemur R, Yumvihoze E, Lean D (2007) Fate of inorganic mercury and methyl mercury within the snow cover in the low arctic tundra on the shore of Hudson Bay (Québec, Canada). Journal of Geophysical Research 112
Cooke MP et al. (2009) Bacteriohopanepolyol biomarker composition of organic matter exported to the Arctic Ocean by seven of the major Arctic rivers. Organic Geochemistry 40:1151-1159
Coppee J-Y et al. (2001) Sulfur-limitation-regulated proteins in *Bacillus subtilis*: a two-dimensional gel electrophoresis study. Microbiology 147:1631-1640
Cossa D, Bernard A, Pirrone N (2009) The origin of methylmercury in open Mediterranean waters. Limnology and Oceanography 54(3):837-844
Costa M, Liss PS (1999) Photoreduction of mercury in sea water and its possible implications for Hg 0 air–sea fluxes. Marine Chemistry 68:87–95
Cowan DA, Tow, Lemese Ah (2004) Endangered Antacrctic Environments. Annual Reviews of Microbiology 58:649-690
Craig PJ (1986) Organometallic compounds in the environment. Longman, London
Csonka LN (1989) Physiological and Genetic Responses of Bacteria to Osmotic Stress. American Society for Microbiology 53:121-147

Daly GL, Wania F (2004) Simulating the Influence of Snow on the Fate of Organic Compounds. Environmental Science and Technology 38:4176-4186

Daré E, Li, W., Zhivotovsky, B., Yuan, X., Ceccatelli, S. (2001) Methylmercury and H_2O_2 provoke lysosomal damage in human astrocytoma D384 cells followed by apoptosis Free Radical Biology & Medicine 30:1347-1356

David MM, Mesle M, Malandain C, Cohen D, Vogel TM (2009) Molecular Biology-based strategy for site remediation. Environmental Science and Technology Submitted

David MM, Sapkota AR, Simonet P, Vogel TM (2008) A novel and rapid method for synthesizing positive controls and standards for quantitative PCR. Journal of Microbiological Methods 73:73-77

Davies TD, Vincent, C.E., Brimblecombe, P. (1982) Preferential elution of strong acids from a Norwegian ice cap. Nature 300:161-163

Davis RE (1991) Links between snowpack physics and snowpack chemistry. In: T.D. Davies MT, H.G. Jones (ed) Seasonal Snowpacks NATO ASI Series G. Springer-Verlag, Berlin, pp 115-138

Davis RE, Petersen, C.E., Bales, R.C. (1995) Ion flux through a shallow snowpack: effects of initial conditions and melt sequences. IAHS Publication 228:115–126

Dietz R, Outridge PM, Hobson KA (2009) Anthropogenic contributions to mercury levels in present-day Arctic animals--A review. Science of the Total Environment 407:6120-6131

Dietz R et al. (2006) Trends in mercury in hair of greenlandic polar bears (Ursus maritimus) during 1892-2001. Environmental Science and Technology 40:1120-1125

Dolédec S, Chessel D (1994) Co-inertia analysis: an alternative method for studying species-environment relationships. Freshwater Biology 31:277-294

Dommergue A, Bahlmann E, Ebinghaus R, Ferrari C, Boutron C (2007) Laboratory simulation of Hg0 emissions from a snowpack. Analytical and Bioanalytical Chemistry 388:319-327

Dommergue A, Ferrari CP, Poissant L, Gauchard PA, Boutron CF (2003) Diurnal cycles of gaseous mercury within the snowpack at Kuujjuarapik/Whapmagoostui, Quebec, Canada. Environmental Science and Technology 37:3289-3297

Dommergue A et al. (accepted for publication) Deposition of mercury species in the Ny-Ålesund area (79°N) and their transfer during snowmelt. Environmental Science and Technology

Douglas TA, Sturm M (2004) Arctic haze, mercury and the chemical composition of snow across northwestern Alaska. Atmospheric Environment 38:805-820

Douglas TA, Sturm M, Simpson WR, Brooks S, Lindberg SE, Perovich DK (2005) Elevated mercury measured in snow and frost flowers near Arctic sea ice leads. Geophysical Research Letters 32:-

Draxler RR, Rolph GD (2003) HYSPLIT (HYbrid Single-Particle Lagrangian Integrated Trajectory) Model access via NOAA ARL READY Website(http://www.arl.noaa.gov/ready/hysplit4.html). NOAA Air Resources Laboratory, Silver Spring, MD.

Dray S, Chessel D, Thioulouse J (2003) CO-INERTIA ANALYSIS AND THE LINKING OF ECOLOGICAL DATA TABLES. Ecology 84:3078-3089

Duran R et al. (2008) Mercury methylation by a microbial community from sediments of the Adour Estuary (Bay of Biscay, France). Environmental Pollution 156:951-958

Ebinghaus R et al. (2002) Antarctic Springtime Depletion of Atmospheric Mercury. Environmental Science and Technology 36:1238 –1244

Edwards AC, Scalenghe R, Freppaz M (2007) Changes in the seasonal snow cover of alpine regions and its effect on soil processes: A review. Quaternary International 162–163 172–181

Eichler A, Schwikowski, M., Gäggeler, H.W., 2001. (2001) Meltwater induced relocation of chemical species in Alpine firn. Tellus 53B:192–203

Einen J, Ovreas L (2006) *Flaviramulus basaltis* gen. nov., sp. nov., a novel member of the family *Flavobacteriaceae* isolated from seafloor basalt. International Journal of Systematic and Evolutionary Microbiology 56:2455-2461

Elizabeth EH (2005) Searching Sequence Space: Two Different Approaches to Dihydrofolate Reductase Catalysis. ChemBioChem 6:590-600

Fain X (2007) Soixante années d'évolution des concentrations atmosphériques en mercure élémentaire gazeux reconstruites grâce aux archives glaciaires du groenland. Université Joseph Fourier, http://www-lgge.ujf-grenoble.fr/doctorat/these-fain.pdf

Faïn X et al. (2009) Polar firn air reveals large-scale impact of anthropogenic mercury emissions during the 1970s. Proceedings of the National Academy of Sciences of the United States of America:10.1073/pnas.0905117106

Fain X, Ferrari CP, Gauchard PA, Magand O, Boutron C (2006) Fast depletion of gaseous elemental mercury in the Kongsvegen Glacier snowpack in Svalbard. Geophysical Research Letters 33:Doi 10.1029/2005gl025223

Falter R, Wilken R-D (1998) Isotope experiments for the determination of the abiotic mercury methylation potential of a River Rhine sediment. Vom Wasser 90:217-231

Farmer J, Hickman-Brenner F (2006) The Genera *Vibrio* and *Photobacterium*. In: The Prokaryotes, pp 508-563

Ferrari C et al. (2005) Snow-to-air exchanges of mercury in an Arctic seasonal snow pack in Ny-Alesund, Svalbard. Atmospheric Environment 39:7633-7645

Ferrari CP, Moreau AL, Boutron CF (2000) Clean conditions for the determination of ultra–low levels of mercury in ice and snow samples. Fresenius' Journal of Analytical Chemistry 366:433–437

Ferrari CP et al. (2008) Atmospheric mercury depletion event study in Ny-Alesund (Svalbard) in spring 2005. Deposition and transformation of Hg in surface snow during springtime. Science of the Total Environment 397:167-177

Fitzgerald WF, Engstrom, D. R., Mason, R. P., Nater, E. A. (1998) The case for atmospheric mercury contamination in remote areas Environmental Science and Technology 32:1-7

Fitzgerald WF, Lamborg CH, Hammerschmidt CR (2007) Marine Biogeochemical Cycling of Mercury. Chemical Reviews 107:641-662

Fleming EJ, Mack EE, Green PG, Nelson DC (2006a) Mercury Methylation from Unexpected Sources: Molybdate-Inhibited Freshwater Sediments and an Iron-Reducing Bacterium. Applied and Environmental Microbiology 72:457-464

Fleming EJ, Mack EE, Green PG, Nelson DC (2006b) Mercury methylation from unexpected sources: Molybdate-inhibited freshwater sediments and an iron-reducing bacterium. Applied and Environmental Microbiology 72:457-464

Frankenberg N, Moser J, Jahn D (2003) Bacterial heme biosynthesis and its biotechnological application. Applied Microbiology and Biotechnology 63:115-127

Gardfeldt K, Munthe J, Stromberg D, Lindqvist O (2003) A kinetic study on the abiotic methylation of divalent mercury in the aqueous phase. Science of the Total Environment 304:127-136

Gauchard PA et al. (2005) Study of the origin of atmospheric mercury depletion events recorded in Ny-Alesund, Svalbard, spring 2003. Atmospheric Environment 39:7620-7632

Giordano D et al. (2007) The truncated hemoglobins in the Antarctic psychrophilic bacterium Pseudoalteromonas haloplanktis TAC125. Gene 398:69-77

Golding GR, Kelly CA, Sparling R, Loewen PC, Barkay T (2007) Evaluation of mercury toxicity as a predictor of mercury bioavailability. Environmental Science and Technology 41:5685-5692

Golding GR, Kelly CA, Sparling R, Loewen PC, Rudd JWM, Barkay T (2002) Evidence for facilitated uptake of Hg(II) by Vibrio anguillarum and Escherichia coli under anaerobic and aerobic conditions. Limnology and Oceanography 47:967–975

Good IL (1953) The population frequencies of species and the estimation of population parameters. Biometrika 40:237-264

Goto-Azuma K, Nakawo, M, Han, J, Watanabe,O, Azuma, N (1994) Melt-induced relocation of ions in glaciers and in a seasonal snowpack IAHS Publication 223 287–298

Grannas AM, Bausch AR, Mahanna KM (2007a) Enhanced aqueous photochemical reaction rates after freezing. Journal of Physical Chemistry A 111:11043-11049

Grannas AM et al. (2007b) An overview of snow photochemistry: evidence, mechanisms and impacts. Atmospheric Chemistry and Physics 7: 4329-4373

Gray JE, Hines, M. E. (2006) Mercury: Distribution, Transport, and Geochemical and Microbial Transformations from Natural and Anthropogenic Sources. Applied Geochemistry 21:1819-1820

Gray ND, Pickup RW, Jones JG, Head IM (1997) Ecophysiological Evidence that *Achromatium oxaliferum* Is Responsible for the Oxidation of Reduced Sulfur Species to Sulfate in a Freshwater Sediment. Applied and Environmental Microbiology 63:1905–1910

Gueldry O et al. (2003) Ycf1p-dependent Hg(II) detoxification in *Saccharomyces cerecisiae*. European Journal of Biochemistry 270:2486-2496

Gutknecht J (1981) Inorganic mercury (Hg^{2+}) transport through lipid bilayer membranes. Journal of Membrane Biology 61:61–66

Hamlett NV, Landale EC, Davis BH, Summers AO (1992) Roles of the Tn21 merT, merP, and merC gene products in mercury resistance and mercury binding. Journal of Bacteriology 174:6377-6385

Hammerschmidt CR, Lamborg CH, Fitzgerald WF (2007) Aqueous phase methylation as a potential source of methylmercury in wet deposition. Atmospheric Environment 41:1663-1668

Harada M (1995) Minamata disease: methylmercury poisoning in Japan caused by environmental pollution. Critical Reviews in Toxicology 25:1-24

Hinkler J, Hansen BU, Tamstorf MP, Sigsgaard C, Petersen D (2008) Snow and Snow-Cover in Central Northeast Greenland. Advances in Ecological Research 40:175-195

Hodgkins R, Tranter, M., and Dowdeswell, J. A. (1998) The hydrochemistry of runoff from a 'coldbased' glacier in the High Arctic (Scott Turnerbreen, Svalbard) Hydrological Processes 12:87–103

Hodson A et al. (2008) Glacial Ecosystems. Ecological Monographs 78:41-67

Hoham RW (1975) Optimal temperatures and temperature ranges for growth of snow algae. Arct. Alp. Res. 7:13-24

Hoham RW, Duval B (2001) Microbial ecology of snow and freshwater ice with emphasis on snow algae In: Jones HG, Pomeroy JW, Walker DA, Hoham RW (eds) Snow ecology: an interdisciplinary examination of snow-covered ecosystems. Cambridge University Press, Cambridge, pp 168–228

Howard EC et al. (2006) Bacterial Taxa That Limit Sulfur Flux from the Ocean. Science 314:649-652

Hughes JB, Hellmann JJ, Ricketts TH, Bohannan BJM (2001) Counting the uncountable: statistical approaches to estimating microbial diversity. Applied and Environmental Microbiology 67:4399–4406

Iwahori K, Takeuchi F, Kamimura K, Sugio T (2000) Ferrous Iron-Dependent Volatilization of Mercury by the Plasma Membrane of *Thiobacillus ferrooxidans*. Applied and Environmental Microbiology 66:3823-3827

Johannessen M, Dale, T., Gjessing, E.T., Henriksen, A., Wright, R.F. (1977) Acid precipitation in Norway: the regional distribution of contaminants in snow and the chemical concentration processes during snow melt. IAHS Publication 118:116–120

Johannessen M, Henriksen, A. (1978) Chemistry of snow melt water: changes in concentration during melting Water Resources Research 14:615-619

Johansen P, Mulvad G, Pedersen HS, Hansen JC, Riget F (2007) Human accumulation of mercury in Greenland. Science of the Total Environment 377:173-178

Johnson KP, Blum JD, Keeler GJ, Douglas TA (2008a) Investigation of the deposition and emission of mercury in arctic snow during an atmospheric mercury depletion event. Journal of Geophysical Research-Atmospheres 113

Johnson KP, Blum JD, Keeler GJ, Douglas TA (2008b) Investigation of the deposition and emission of mercury in arctic snow during an atmospheric mercury depletion event. Journal of Geophysical Research 113: doi:10.1029/2008JD009893

Jones HG (1999) The ecology of snow-covered systems: a brief overview of nutrient cycling and life in the cold. Hydrological Processes 13:2135–2147

Jones HG, Pomeroy, J. W., Walker, D. A., Hoham, R. W. (ed) (2001) Snow Ecology. Cambridge University Press, Cambridge, UK

Jones RT, Robeson MS, Lauber CL, Hamady M, Knight R, Fierer N (2009) A comprehensive survey of soil acidobacterial diversity using pyrosequencing and clone library analyses. Isme J 3:442-453

Jordan RE, Albert, M.R., Brun, E. (2008) Physical Processes within Snow and Their Parameterization. In: Armstrong RL, Brun, E. (ed) Snow and Climate. Cambridge University Press, Cambridge, pp 12-69

Jukes TH, Cantor CR (1969) Evolution of protein molecules. In: Munro HN (ed) Mammalian protein metabolism. Academic Press, New York, pp 21-132

Junge K, Eicken,Hajo, Deming, Jody W. (2004) Bacterial Activity at -2 to -20°C in Arctic Wintertime Sea Ice. Applied and Environmental Microbiology 70:550-557

Kaleschke L et al. (2001) SSM/I Sea Ice Remote Sensing for Mesoscale Ocean-Atmosphere Interaction Analysis. Canadian Journal of Remote Sensing 27:526-537

Kawamura K, Ikushima K (1993) Seasonal changes in the distribution of dicarboxylic acids in the urban atmosphere. Environmental Science and Technology 27:2227-2235

Kawamura K, Kasukabe H (1996) Sources and reaction pathways of dicarboxylic acids, ketoacids and dicarbonyls in Arctic aerosols: one year of observations. Atmospheric Environment 30:1709-1722

Kemp PF, Aller JY (2004) Bacterial diversity in aquatic and other environments: what 16S rDNA libraries can tell us. FEMS Microbiology Ecology 47:161-177

Kerin EJ, Gilmour CC, Roden E, Suzuki MT, Coates JD, Mason RP (2006) Mercury Methylation by Dissimilatory Iron-Reducing Bacteria. Applied and Environmental Microbiology 72:7919-7921

Kiene RP, Linn LJ (2000) The fate of dissolved dimethylsulfoniopropionate (DMSP) in seawater: tracer studies using 35S-DMSP. Geochimica et Cosmochimica Acta 64:2797-2810

Kiene RP, Linn LJ, Bruton JA (2000) New and important roles for DMSP in marine microbial communities. Journal of Sea Research 43:209-224

Kirk JL, St. Louis VL, Sharp MJ (2006) Rapid Reduction and Reemission of Mercury Deposited into Snowpacks during Atmospheric Mercury Depletion Events at Churchill, Manitoba, Canada. Environmental Science and Technology 40:7590-7596

Kiyono M, Sone Y, Nakamura R, Pan-Hou H, Sakabe K (2009) The MerE protein encoded by transposon Tn21 is a broad mercury transporter in Escherichia coli. FEBS Letters 583:1127-1131

Kong IC, Bitton G, Koopman B, Jung KH (1995) Heavy metal toxicity testing in environmental samples Reviews of Environmental Contamination & Toxicology 142:119−147

Kritee K, Blum JD, Barkay T (2008) Mercury stable isotope fractionation during reduction of Hg(II) by different microbial pathways. Environmental Science and Technology 42:9171-9177

Kuhn M (1987) Micro-meteorological conditions for snow melt. Journal of Glaciology 33:24-26

Kuhn M (2001) The nutrient cycle through snow and ice, a review. Aquatic Science 63:150-167

Lakowicz JR, Anderson CJ (1980) Permeability of lipid bilayers to methylmercuric chloride: Quantification by fluorescence quenching of a carbazole-labeled phospholipid. Chemico-Biological Interactions 30:309-323

Lalonde JD, Amyot M, Doyon MR, Auclair JC (2003) Photo–induced Hg(II) reduction in snow from the remote and temperate Experimental Lakes Area (Ontario, Canada). Journal of Geophysical Research 108

Lalonde JD, Amyot M, Kraepiel AML, Morel FMM (2001) Photooxidation of Hg(0) in artificial and natural waters. Environmental Science and Technology 35:1367–1372

Lalonde JD, Poulain AJ, Amyot M (2002) The role of mercury redox reactions in snow on snow–to–air mercury transfer. Environmental Science and Technology 36:174–178

Lamborg CH, Fitzgerald, W.F., O'Donnell, J., Torgersen,T. (2002) A non-steady-state compartmental model of global-scale mercury biogeochemistry with interhemispheric atmospheric gradients Geochimica et Cosmochimica Acta 66:1105-1118

Larose C et al. (accepted for publication) Microbial diversity in seasonal Arctic snow and meltwater from Svalbard, Norway Extremophiles

Larose C et al. (In preparation) Seasonal changes in snow chemistry lead to new insights into mercury methylation in the Arctic.

Larose C, Dommergue A, Marusczak N, Ferrari CP, Schneider D (Submitted) Bioavailability of mercury deposited in polar environments.

Larsen KS, Grogan, Paul, Jonasson, Sven, Michelsen, Anders (2007) Respiration and Microbial Dynamics in Two Subarctic Ecosystems during Winter and Spring Thaw: Effects of Increased Snow Depth Arctic, Antarctic, and Alpine Research 39:268-276

Lauber CL, Hamady M, Knight R, Fierer N (2009) Soil pH as a predictor of soil bacterial community structure at the continental scale: a pyrosequencing-based assessment. Applied and Environmental Microbiology:AEM.00335-00309

Leck C, Persson C (1996a) The central Arctic Ocean as a source of dimethyl sulfide - Seasonal variability in relation to biological activity Tellus 48B:156-177

Ledwidge R et al. (2005) NmerA, the metal binding domain of mercuric ion reductase, removes Hg^{2+} from proteins, delivers it to the catalytic core, and protects cells under glutathione-depleted conditions. Biochemistry 44:11402–11416

Legrand M et al. (2007) Origin of C2–C5 dicarboxylic acids in the European atmosphere inferred from year-round aerosol study conducted at a west-east transect. Journal of Geophysical Research 112:D23S07, doi:10.1029/2006JD008019

Lei YD, Wania F (2004) Is rain or snow a more efficient scavenger of organic chemicals? Atmospheric Environment 38:3557-3571

Lelong C et al. (2007) The Crl-RpoS regulon of Escherichia coli. Molecular & Cellular Proteomics 6:648-659

Libbrecht KG (2005) The physics of snow crystals. Reports on Progress in Physics 68:855-895

Lindberg SE et al. (2007) A synthesis of progress and uncertainties in attributing the sources of mercury in deposition. Ambio 36:19-32

Lindberg SE et al. (2001) Formation of Reactive Gaseous Mercury in the Arctic: Evidence of Oxidation of Hg° to Gas–Phase Hg–II Compounds after Arctic Sunrise. Water Air and Soil Pollution: Focus 1:295–302

Lindberg SE et al. (2002) Dynamic Oxidation of Gaseous Mercury in the Arctic Troposphere at Polar Sunrise. Environmental Science and Technology 36:1245–1256

Liu Y et al. (2009) Bacterial diversity in the snow over Tibetan Plateau Glaciers. Extremophiles 13:89-99

Liu Y, Yao T, Jiao N, Kang S, Zeng Y, Huang S (2006) Microbial community structure in moraine lakes and glacial meltwaters, Mount Everest. FEMS Microbiology Letters 265:98-105

Loseto LL, Lean DRS, Siciliano SD (2004) Snowmelt Sources of Methylmercury to High Arctic Ecosystems. Environmental Science and Technology 38:3004-3010

Lu JY et al. (2001) Magnification of atmospheric mercury deposition to polar regions in springtime: the link to tropospheric ozone depletion chemistry. Geophysical Research Letters 28:3219–3222

Lund PA, Brown NL (1987) Role of the merT and merP gene products of transposon Tn501 in the induction and expression of resistance to mercuric ions. Gene 52:207-214

Lyons WB, Welch K. A., Fountain A. G., Dana G. L., Vaughn B. H., McKnight D. M. (2003) Surface glaciochemistry of Taylor Valley, southern Victoria Land, Antarctica, and its relation to stream chemistry. Hydrological Processes 17 115–130

Macdonald RW, Harner T, Fyfe J (2005) Recent climate change in the Arctic and its impact on contaminant pathways and interpretation of temporal trend data. Science of the Total Environment 342:5-86

Magurran AE (1988) Ecological diversity and its measurement. Princeton University Press, Princeton, N.J.

Marles-Wright J, Lewis RJ (2007) Stress responses of bacteria. Current Opinion in Structural Biology 17:755-760

Maron L, Dommergue A, Ferrari C, Delacour-Larose M, Fain X (2008) How elementary mercury reacts in the presence of halogen radicals and/or halogen anions: a DFT investigation. Chemistry 14:8322-8329

Maron P-A, Mougel C, Siblot S, Abbas H, Lemanceau P, Ranjard L (2007) Protein Extraction and Fingerprinting Optimization of Bacterial Communities in Natural Environment. Microbial Ecology 53:426–434

Mason RP, Fitzgerald, W. F., Morel, F.M.M. (1994) The biogeochemistry of elemental mercury−anthropogenic influences. Geochimica et Cosmochimica Acta 58:3191-3198

McInerney MJ et al. (2008) Physiology, Ecology, Phylogeny, and Genomics of Microorganisms Capable of Syntrophic Metabolism. Annals of the New York Academy of Sciences 1125:58-72

Meyer F et al. (2008a) The metagenomics RAST server - a public resource for the automatic phylogenetic and functional analysis of metagenomes. BMC Bioinformatics 9:386

Meyer T, Lei YD, Muradi I, Wania F (2008b) Organic Contaminant Release from Melting Snow. 2. Influence of Snow Pack and Melt Characteristics. Environmental Science & Technology 43:663-668

Meyer T, Lei YD, Wania F (2006) Measuring the release of organic contaminants from melting snow under controlled conditions. Environmental Science and Technology 40:3320–3326

Meyer T, Wania F (2008) Organic contaminant amplification during snowmelt. Water Research 42:1847-1865

Mindlin S et al. (2005) Present-day mercury resistance transposons are common in bacteria preserved in permafrost grounds since the Upper Pleistocene. Research in Microbiology 156:994-1004

Miteva V (2008) Bacteria in Snow and Glacier Ice. In: Margesin Rea (ed) Psychrophiles: from Biodiversity to Biotechnology Springer-Verlag, Berlin Heidelberg, pp 31-47

Miwa T (1975) Clostridia in soil of the Antarctica. Japanese Journal of Medical Science & Biology 28:201-213

Mueller DR, Vincent WF, Bonilla S, Laurion I (2005) Extremotrophs, extremophiles and broadband pigmentation strategies in a high arctic ice shelf ecosystem. FEMS Microbiology Ecology 53:73–87

Muir D et al. (1999) Spatial and temporal trends and effects of contaminants in the Canadian Arctic marine ecosystem: a review. The Science of the Total Environment 230:83-144

Munthe J (1992) The aqueous oxidation of elemental mercury by ozone. Atmospheric Environment 26A:1461–1468

Murray AE, Grzymski JJ (2007) Diversity and genomics of Antarctic marine micro-organisms. Philosophical Transactions of the Royal Society B: Biological Sciences 362:2259–2271

Najera I, Lin CC, Kohbodi GA, Jay JA (2005) Effect of chemical speciation on toxicity of mercury of Escherichia coli biofilms and planktonic cells. Environmental Science and Technology 39:3116−3120

Narcy F, Gasparini S, Falk-Petersen S, Mayzaud P (2009) Seasonal and individual variability of lipid reserves in *Oithona similis* (*Cyclopoida*) in an Arctic fjord. Polar Biology 32:233-242

Nigro M, Leonzio,C. (1996) Intracellular storage of mercury and selenium in different marine vertebrates. Marine Ecology Progress Series 135:137-143

Niki H, Maker PD, Savage CM, Breitenbach LP (1983a) A long–path Fourier transform infrared study of the kinetics and mechanism for the hydroxyl radical–initiated oxidation of dimethylmercury. Journal of Physical Chemistry 87:4978 – 4981

Niki H, Maker PS, Savage CM, Breitenbach LP (1983b) A Fourier-transform infrared study of the kinetics and mechanism of the reaction of atomic chlorine with dimethylmercury. Journal of Physical Chemistry 87:3722-3724

Nriagu JO (1989) A global assessment of natural sources of atmospheric trace metals. Nature 338:47–49

Nriagu JO (1994) Mechanistic steps in the photoreduction of mercury in natural waters. Science of the Total Environment 154:1-8

Nriagu JO, Pacyna, J.M. (1988) Quantitative assessment of worldwide contamination of air, water and soils with trace metals. Nature 333:134-139

Omura T, Kiyono M, Pan-Hou H (2004) Development of a specific and sensitive bacteria sensor for detection of mercury at picomolar levels in environment. Journal of Health Science 50:379-383

Onnis-Hayden A et al. (2009) Prokaryotic real-time gene expression profiling for toxicity assessment. Environmental Science and Technology 43:4574-4581

Oregaard G, Sorensen SJ (2007) High diversity of bacterial mercuric reductase genes from surface and sub-surface floodplain soil (Oak Ridge, USA). Isme J 1:453-467

Oremland RS, Culbertson CW, Winfrey MR (1991) Methylmercury Decomposition in Sediments and Bacterial Cultures: Involvement of Methanogens and Sulfate Reducers in Oxidative Demethylation. Applied and Environmental Microbiology 57:130-137

Outridge PM, Macdonald RW, Wang F, Stern GA, Dastoor AP (2008) A mass balance inventory of mercury in the Arctic Ocean. Environmental Chemistry 5:89-111

Pacyna EG, Pacyna JM, Steenhuisen F, Wilson S (2006) Global anthropogenic mercury emission inventory for 2000. Atmospheric Environment 40:4048-4063

Passou H, Rothstein A (1960) The binding of mercury by the yeast cell in relation to changes in permeability. The Journal of General Physiology 43:621-633

Peng C, Chuan H (2004) A General Strategy to Convert the MerR Family Proteins into Highly Sensitive and Selective Fluorescent Biosensors for Metal Ions. Journal of the American Chemical Society 126:728-729

Perrière G, Gouy M (1996) WWW-Query: An on-line retrieval system for biological sequence banks. Biochimie 78:364-369

Pettitt AN (1982) Cramér-von Mises statistic. In: Kotz S, Johnson NL, Read CB (eds) Encyclopedia of statistical sciences. Wiley, New York, pp 220-221

Pomeroy JW, Brun, E. (2001) Physical properties of snow. In: H.G. Jones JWP, D.A. Walker and R.W. Hoham (ed) Snow Ecology. An Interdisciplinary Examination of Snow-Covered Ecosystems. Cambridge University Press, Cambridge, pp 45–126

Poulain AJ, Garcia E, Amyot M, Campbell PGC, Raofie F, Ariya PA (2007a) Biological and chemical redox transformations of mercury in fresh and salt waters of the high arctic during spring and summer. Environmental Science and Technology 41:1883-1888

Poulain AJ, Lalonde JD, Amyot M, Shead JA, Raofie F, Ariya PA (2004) Redox transformations of mercury in an Arctic snowpack at springtime. Atmospheric Environment 38:6763–6774

Poulain AJ et al. (2007) Potential for mercury reduction by microbes in the high arctic. Applied and Environmental Microbiology 73:2230-2238

Price PB, Sowers T (2004) Temperature dependence of metabolic rates for microbial growth, survival and maintenance. Proc Natl Acad Sci USA 101 4631–4636

Priscu JC, Christner BC (2004) Earth's icy biosphere. In: Bull AT (ed) Microbial Diversity and Bioprospecting. American Society for Microbiology, Washington, D.C., pp 130-145

Qiu Y, Vishnivetskaya TA, Lubman DM (2009) Proteomic Insights: Cryoadaptation of Permafrost Bacteria. In: Permafrost Soils, pp 169-181

Quinton WL, Porneroy JW (2006) Transformations of runoff chemistry in the Arctic tundra, Northwest Territories, Canada. Hydrological Processes 20:2901-2919

Rasmussen LD, Sørensen SJ (2001) Effects of mercury contamination on the culturable heterotrophic, functional and genetic diversity of the bacterial community in soil. FEMS Microbiology Ecology 36:1-9

Reisch CR, Moran MA, Whitman WB (2008) Dimethylsulfoniopropionate-dependent demethylase (DmdA) from Pelagibacter ubique and Silicibacter pomeroyi. The Journal of Bacteriology 190:8018-8024

Richter A, Wittrock F, Eisinger M, Burrows JP (1998) GOME observations of tropospheric BrO in northern hemispheric spring and summer 1997. Geophysical Research Letters 25:2683-2686

Rontani J-F (2001) Visible light-dependent degradation of lipidic phytoplanktonic components during senescence: a review. Phytochemistry 58:187-202

Rowland IR, Davies MJ, Grasso P (1977) Volatilization of methylmercuric chloride by hydrogen sulphide. Nature 265 718-719

Saitou N, Nei M (1987) The neighbor-joining method: a new method for reconstructing phylogenetic trees. Molecular Biology and Evolution 4:406-425

Sasaki Y, Minakawa T, Miyazaki A, Silver S, Kusano T (2005) Functional dissection of a mercuric ion transporter Mer C from *Acidithiobacillus ferrooxidans* Bioscience, Biotechnology, and Biochemistry 69:1394–1402

Sattler B, Puxbaum H, Psenner R (2001) Bacterial growth in super cooled cloud droplets Geophysical Research Letters 28:239–242

Schaefer JK et al. (2004) Role of the Bacterial Organomercury Lyase (MerB) in Controlling Methylmercury Accumulation in Mercury-Contaminated Natural Waters. Environmental Science and Technology 38:4304-4311

Schelert J, Dixit V, Hoang V, Simbahan J, Drozda M, Blum P (2004) Occurrence and Characterization of Mercury Resistance in the Hyperthermophilic Archaeon *Sulfolobus solfataricus* by Use of Gene Disruption. The Journal of Bacteriology 186:427-437

Schiering N, Kabsch W, Moore MJ, Distefano MD, Walsh CT, Pai EF (1991) Structure of the detoxification catalyst mercuric ion reductase from *Bacillus* sp. strain RC607. Nature 352:168-172

Schimel JP, Gulledge, J. (1998) Microbial community structure and global trace gases. Global Change Biology 4:745–758

Schindler DW, Smol JP (2006) Cumulative Effects of Climate Warming and Other Human Activities on Freshwaters of Arctic and Subarctic North America. AMBIO: A Journal of the Human Environment 35:160-168

Schloss PD, Handelsman J (2005) Introducing DOTUR, a computer program for defining operational taxonomic units and estimating species richness. Applied and Environmental Microbiology 71:1501-1506

Schloss PD, Larget BR, Handelsman J (2004) Integration of microbial ecology and statistics: a test to compare gene libraries. Applied and Environmental Microbiology 70:5485-5492

Schroeder WH et al. (1998) Arctic springtime depletion of mercury. Nature 394:331–332

Schue M, Dover LG, Besra GS, Parkhill J, Brown NL (2009) Sequence and analysis of a plasmid-encoded mercury resistance operon from *Mycobacterium marinum* identifies MerH, a new mercuric ion transporter. The Journal of Bacteriology 191:439-444

Schultz IR, Newman, M. C. (1997) Methyl mercury toxicokinetics in channel catfish (*Ictalurus punctatus*) and largemouth bass (*Micropterus salmoides*) after intravascular administration. Environmental Toxicology and Chemistry 16:990-996

Scott KJ (2001) Bioavailable mercury in arctic snow determined by a light-emitting *mer-lux* bioreporter. Arctic 54:92-95

Scott KJ (2003) Development and Use of a mer-lux Bioreporter for the Measurement and Characterization of Bioavailable Hg(II) in Defined Media and Aquatic Environmental Samples. In: Department of Microbiology. University of Manitoba, Winnepeg, p 172

Segawa T, Miyamoto K, Ushida K, Agata K, Okada N, Kohshima S (2005) Seasonal change in bacterial flora and biomass in mountain snow from the Tateyama Mountains, Japan, analyzed by 16S rRNA gene sequencing and real-time PCR. Applied and Environmental Microbiology 71:123-130

Seigneur C, Wrobel J, Constantinou E (1994) A chemical kinetic mechanism for atmospheric inorganic mercury. Environmental Science and Technology 28:1589–1597

Selifonova O, Burlage R, Barkay T (1993) Bioluminescent sensors for detection of bioavailable Hg(II) in the environment. Applied and Environmental Microbiology 59:3083-3090

Sellers P, Kelly CA, Rudd JWM, MacHutchon AR (1996) Photodegradation of methylmercury in lakes. Nature 380:694-697

Siciliano SD, Lean DR (2002) Methyltransferase: an enzyme assay for microbial methylmercury formation in acidic soils and sediments. Environmental Toxicology and Chemistry 21:1184-1190

Siciliano SD, O'Driscoll NJ, Tordon R, Hill J, Beauchamp S, Lean DRS (2005) Abiotic production of methylmercury by solar radiation. Environmental Science and Technology 39:1071-1077

Simoes JC, Zagorodnov VS (2001) The record of anthropogenic pollution in snow and ice in Svalbard, Norway. Atmospheric Environment 35:403-413

Skidmore M, Anderson SP, Sharp M, Foght J, Lanoil BD (2005) Comparison of microbial community compositions of two subglacial environments reveals a possible role for microbes in chemical weathering processes. Applied and Environmental Microbiology 71:6986-6997

Skidmore ML, Foght JM, Sharp MJ (2000) Microbial life beneath a high arctic glacier. Applied and Environmental Microbiology 66:3214-3220

Skogerboe RK, Wilson SA (1981) Reduction of ionic species by fulvic acid Analytical Chemistry 53:228–232

Skov H et al. (2004) Fate of elemental mercury in the arctic during atmospheric mercury depletion episodes and the load of atmospheric mercury to the arctic. Environmental Science and Technology 38:2373-2382

Slaveykova VI, Wilkinson KJ (2005) Predicting the bioavailability of metals and metal complexes: critical review of the biotic ligand model. Environmental Chemistry 2 9–24

Slemr F et al. (2003) Worldwide trend of atmospheric mercury since 1977. Geophysical Research Letters 30

Smith T, Pitts K, McGarvey JA, Summers AO (1998) Bacterial Oxidation of Mercury Metal Vapor, Hg(0). Applied and Environmental Microbiology 64:1328-1332

Sommar J et al. (2007) Circumpolar transport and air-surface exchange of atmospheric mercury at Ny-A°lesund (79° N), Svalbard, spring 2002. Atmospheric Chemistry and Physics 7:151-166

Sørensen SJ, de Lipthay JR, K. MA, T B, Hansen LH, Rasmussen LD (eds) (2002) Molecular methods for assessing and manipulating the diversity of microbial populations and processes Marcel Dekker Inc., New York

Spring S, Merkhoffer B, Weiss N, Kroppenstedt RM, Hippe H, Stackebrandt E (2003) Characterization of novel psychrophilic clostridia from an Antarctic microbial mat: description of *Clostridium frigoris* sp. nov., *Clostridium lacusfryxellense* sp. nov., *Clostridium bowmanii* sp. nov. and *Clostridium psychrophilum* sp. nov. and reclassification of *Clostridium laramiense* as *Clostridium estertheticum subsp. laramiense subsp. nov*. International Journal of Systematic and Evolutionary Microbiology 53:1019-1029

Sprovieri F, Pirrone N, Landis MS, Stevens RK (2005) Atmospheric mercury behavior at different altitudes at Ny Alesund during Spring 2003. Atmospheric Environment 39:7646-7656

St. Louis VL et al. (2007) Methylated mercury species in Canadian high arctic marine surface waters and snowpacks. Environmental Science and Technology 41:6433-6441

St. Louis VL et al. (2005) Some sources and sinks of monomethyl and inorganic mercury on Ellesmere island in the Canadian high arctic. Environmental Science and Technology 39:2686–2701

Stackebrandt E, Brambilla E, Cousin S, Dirks W, Pukall R (2004) Culture-independent analysis of bacterial species from an anaerobic mat from Lake Fryxell, Antarctica: prokaryotic diversity revisited. Cellular and Molecular Biology (Noisy-le-grand) 50:517-524

Steen AO, Berg T, Dastoor AP, Durnford DA, Hole LR, Pfaffhuber KA (2009) Dynamic exchange of gaseous elemental mercury during polar night and day. Atmospheric Environment 43:5604-5610

Steffen A et al. (2008) A synthesis of atmospheric mercury depletion event chemistry in the atmosphere and snow. Atmospheric Chemistry and Physics 8:1445-1482

Stibal M, Elster J, Sabacka M, Kastovska K (2007) Seasonal and diel changes in photosynthetic activity of the snow alga *Chlamydomonas nivalis* (*Chlorophyceae*) from Svalbard determined by pulse amplitude modulation fluorometry. FEMS Microbiology Ecology 59:265-273

Stoichev T, Rodriguez Martin-Doimeadios RC, Tessier E, Amouroux D, Donard OF (2004) Improvement of analytical performances for mercury speciation by on-line derivatization, cryofocussing and atomic fluorescence spectrometry. Talanta 62:433-438

Suda I, Suda M, Hirayama K (1993) Degradation of methyl and ethyl mercury by singlet oxygen generated from sea water exposed to sunlight or ultraviolet light. Archives of Toxicology 67:365-368

Sugio T, Fujii M, Takeuchi F, Negishi A, Maeda T, Kamimura K (2003) Volatilization of mercury by an iron oxidation enzyme system in a highly mercury-resistant *Acidithiobacillus ferrooxidans* strain MON-1. Bioscience, Biotechnology, and Biochemistry 67:1537-1544

Sugio T, Iwahori K, Takeuchi F, Negishi A, Maeda T, Kamimura K (2001) Cytochrome c oxidase purified from mercury-resistant strain of *Acidithiobacillus ferroxidans* volatilizes mercury. Journal of Bioscience and Bioengineering 92:44-49

Sunderland EM, Krabbenhoft DP, Moreau JW, Strode SA, Landing WM (2009) Mercury sources, distribution, and bioavailability in the North Pacific Ocean: Insights from data and models. Global Biogeochemical Cycles 23

Svendsen H et al. (2002) The physical environment of Kongsfjorden-Krossfjorden, an Arctic fjord system in Svalbard. Polar Research 21:133-166

Tackett PJ et al. (2007) A study of the vertical scale of halogen chemistry in the Arctic troposphere during Polar Sunrise at Barrow, Alaska. Journal of Geophysical Research-Atmospheres 112:-

Taylor BF, Gilchrist DC (1991) New Routes for Aerobic Biodegradation of Dimethylsulfoniopropionate. Applied and Environmental Microbiology 57:3581-3584

Thioulouse J, Chessel D, Dolédec S, Olivier JM (1997) ADE-4: a multivariate analysis and graphical display software Statistics and Computing 7:75-83

Thioulouse J, Lobry JR (1995) Co-inertia analysis of amino-acid physico-chemical properties and protein composition with the ADE package. Computer Applications in the Biosciences 11:321-329

Thomas WH, Duval B (1995) Sierra Nevada, California, USA, snow algae: snow albedo changes, algal-bacterial interrelationships, and ultraviolet radiation effects. Arctic, Antarctic, and Alpine Research 27:389–399

Thoming J, Kliem BK, Ottosen LM (2000) Electrochemically enhanced oxidation reactions in sandy soil polluted with mercury. Science of the Total Environment 261:137-147

Thompson DR (1990) Metal levels in marine vertebrates. In: Furness RW, Rainbow, P. S. (ed) Heavy metals in the marine environment. CRC Press, Boca Raton

Thompson JD, Gibson TJ, Plewniak F, Jeanmougin F, Higgins DG (1997) The ClustalX windows interface: flexible strategies for multiple sequence alignment aided by quality analysis tools. Nucleic Acids Research 24:4876-4882

Tranter M, Brimblecombe, P., Davies, T.D., Vincent, C.E., Abrahams,, P.W. B, I. (1986) A composition of snowfall, snowpack and meltwater in the Scottish Highlands—evidence for preferential elution Atmospheric Environment 20:517–525

Tranter M, Sharp MJ, Lamb HR, Brown GH, Hubbard BP, Willis IC (2002) Geochemical weathering at the bed of Haut Glacier d'Arolla, Switzerland—a new model. Hydrological Processes 16:959-993

Tseng CM, Garraud H, Amouroux D, Donard OF, de Diego A (1998) Open focused microwave-assisted sample preparation for rapid total and mercury species determination in environmental solid samples. Journal of Automatic Chemistry 20:99-108

Ullrich SM, Tanton, T.W., Abdrashitova, S.A. (2001) Mercury in the aquatic environment: a review of factors affecting methylation. Critical Reviews in Environmental Science and Technology 31:241-293

UNEP/GRID-Arendal (2005) Cartographe: Philippe Rekacewicz. Definitions of the Arctic. UNEP/GRID-Arendal Maps and Graphics Library. Available at: http://maps.grida.no/go/graphic/definitions_of_the_arctic. Accessed November 09, 2009.

Vincent WF (2000) Evolutionary origins of Antarctic microbiota: invasion, selection and endemism Antarctic Science 12:374-385

Viti C, Decorosi F, Mini A, Tatti E, Giovannetti L (2009) Involvement of the oscA gene in the sulphur starvation response and in Cr(VI) resistance in Pseudomonas corrugata 28. Microbiology 155:95-105

Wagemann R, Trebacz E, Boila G, Lockhart WL (1998) Methylmercury and total mercury in tissues of arctic marine mammals. Science of the Total Environment 218:19-31

Walker JB et al. (2006) Maternal and umbilical cord blood levels of mercury, lead, cadmium, and essential trace elements in Arctic Canada. Environmental Research 100:295-318

Walter KD, Dolly AG, Dieter M (1995) THE ECOLOGY OF *NOSTOC*. Journal of Phycology 31:2-18

Wania F, Semkin R, Hoff JT, Mackay D (1999) Modelling the fate of non-polar organic chemicals during the melting of an Arctic snowpack. Hydrological Processes 13:2245-2256

Ward DM, Weller R, Bateson MM (1990) 16S rRNA sequences reveal numerous uncultured microorganisms in a natural community. Nature 345:63-65

Weber JH (1993) Review of possible paths for abiotic methylation of mercury(II) in the aquatic environment. Chemosphere 26:2063-2077

Wiatrowski HA, Ward PM, Barkay T (2006) Novel reduction of mercury (II) by mercury-sensitive dissimilatory metal reducing bacteria. Environmental Science and Technology 40:6690-6696

Williams MW, Seibold C, Chowanski K (2009) Storage and release of solutes from a subalpine seasonal snowpack: soil and stream water response, Niwot Ridge, Colorado. Biogeochemistry 95:77-94

Worms I, Simon, D. F., Hassler,C.S., Wilkinson,K.J. (2006) Bioavailability of trace metals to aquatic microorganisms: importance of chemical, biological and physical processes on biouptake. Biochimie 88:1721-1731

Yao TD, Xiang SR, Zhang XJ, Wang NL, Wang YQ (2006) Microorganisms in the Malan ice core and their relation to climatic and environmental changes. Global Biogeochem Cycles 20:GB1004. doi:1010.1029/2004GB002424

Yee S, Choi, B. H. (1994) Methylmercury Poisoning Induces Oxidative Stress in the Mouse Brain. Experimental and Molecular Pathology 60:188-196

Yergeau E, Newsham KK, Pearce DA, Kowalchuk GA (2007) Patterns of bacterial diversity across a range of Antarctic terrestrial habitats. Environmental Microbiology 9:2670-2682

Yokoo EM, Valente, J. G., Grattan, L., Schmidt, S. L., Platt, I., Silbergeld, E. K. (2003) Low level methylmercury exposure affects neurophysiological function in adults. Environmental Health, A Global Access Science Source 2:8

Zhang H, Lindberg SE (2001) Sunlight and iron(III)–induced photochemical production of dissolved gaseous mercury in freshwater. Environmental Science and Technology 35:928–935

Zhang T (2005) Influence of the seasonal snow cover on the ground thermal regime: An overview Reviews of Geophysics 43:RG4002, doi:4010.1029/2004RG000157